Zwitterionic Late Transition Metal Alkene Polymerisation Catalysts containing Aminofulvene-aldiminate (AFA) Ligands

Mohammed Mahmudur Rahman

A Thesis Submitted for the Degree of

Doctor of Philosophy

The University of Edinburgh

October 2010

Declaration

I hereby declare that this thesis has been entirely composed by myself and that the work described herein is my own except where clearly mentioned either in acknowledgement, reference or text. It has not been submitted in whole or in part, for any other degree, diploma or other qualification.

Mohammed Mahmudur Rahman
October 2010

Acknowledgements

First and foremost, I would like to thank my supervisor Dr. Philip J. Bailey for his guidance and support during my doctoral study at the School of Chemisty, the University of Edinburgh. I would also like to thank School of Chemistry and EaStCHEM for financial support.

I thank Prof. Simon Parsons and his co-workers Dr. Fraser J. White and Dr. Anna Collins for their help with the crystallography.

I also thank Prof. Polly Arnold (Head of Research) and Dr. Jason Love and their research groups for their encouragement and support during my work in the lab.

Many thanks to Dr. Juraj Bella, John Smith and Dr. Marika Cremoux for helping me with NMR analysis, Alan Taylor for the Mass Spec and Sylvia Williamson (University of St. Andrews) for CHN analysis.

I also thank to Professor P. Mountford of University of Oxford for giving me some innovative ideas to achieve the goal of this work. I had a nice discussion with him at a conference in Oxford.

Thanks to all the Bailey group members especially Filipa Cavaco and Nicola Bell, and all the project students who worked with me: Peter Haack, Damian Smith, Muhammed Azhar and Alan Pedgrift.

Thanks to Dr. H. C. L. Abbenhuis of Eindhoven University of Technology, the Netherlands who always encourages and supports me to be a successful person in academia. I met him several times in conferences even though I left TU/e in 2006.

Finally, I am grateful to my parents and my wife Poly and all my family members for their support and encouragement during my laboratory work and writing period.

Abstract

Over recent years significant progress has been made in the design and development of late transition metal cationic catalysts for olefin polymerisation. Never-the-less, the activation of catalyst precursors and generation of active species still remains a challenge. In this respect, zwitterionic catalysts could offer a range of advantages over the traditional two component catalytic systems. For example, stable zwitterions are well-defined, single component catalysts which do not require Lewis acid co-catalysts for activation. Therefore, this eliminates the possibility of anions coordinating to the active site and could provide highly active catalysts. Moreover, this could reduce the production costs. In this thesis the 6-aminofulvene-2-aldiminate (AFA) ligand system has been employed to develop zwitterionic, charge-neutral complexes, analogues of Brookhart-type cationic alkene polymerisation catalyst containing 1,2-diimine ligand.

Chapter 1 of the thesis provides a comprehensive literature review of the late transition metal (Group 10) α-diimine catalytic systems and the zwitterionic early and late transition metal alkene polymerisation catalysts.

Chapter 2 describes the synthesis and characterisation of some novel zwitterionic complexes [(Ph_2AFA)Pd(Me)(DMAP)], [(Ph_2AFA)(N,N-dimethylbenzylamine-2-C,N)-Pd(II)] and [(Ph_2AFA)Ni(η^3-C_3H_5)] and their possible application as catalyst precursors in alkene polymerisation. In principle, upon activation these complexes should exhibit higher catalytic activity.

The ideal catalyst precursor for a highly active palladium based system would be a halide-bridged dimer of the form [(Ph_2AFA)Pd(μ-X)]$_2$. Chapter 2 describes several efforts towards the synthesis of such complexes using a range of R_2AFA ligands. Even with the introduction of bulky N-substituents such as cyclohexyl or tert-butyl, the halide-bridged dimers could not be synthesised. Instead, the reaction between the deprotonated

ligand and $[PdCl_2(NCPh)_2]$ provides bis-chelated complexes $[(R_2AFA)_2Pd]$. In order to introduce more steric bulk into the AFAH ligand which might lead to a halide-bridged dimer, two more ligands N,N'-bis(2,6-diisopropyl)phenyl-6-aminofulvene-2-aldimine and N,N'-di-(2,4,6-trimethyl)phenyl-6-aminofulvene-2-aldimine have been synthesised and characterised. It has been found that the presence of the 2,6-diisopropylphenyl substituents in N,N'-bis(2,6-diisopropyl)phenyl-6-aminofulvene-2-aldimine not only prevents the coordination of two ligands to the same metal, but precludes complexation all together. Chapter 2 also describes several efforts to develop a hemi-labile complex for alkene polymerisation.

Chapter 3 describes the synthesis of metalloligands of aminofulvene-aldimine (AFA) and corresponding bimetallic complexes. The AFA ligand affords transition metal complexes via both η^5- as well as κ^2-coordination modes.

A new synthetic methodology has been developed to synthesise metalloligands $[Cp^*Ru^{II}(Ph_2AFA)H][BF_4]$, $[Cp^*Rh^{III}(Cy_2AFA)H][BF_4]_2$ and $[Cp^*Rh^{III}(Cy_2AFA)][BF_4]$. The basicity of the monocationic Rh metalloligand is found to be significantly lower than that of its Ru analogues. This is significant as it opens a potentially easy synthetic route to bimetallic complexes. The bimetallic complex $[Cp^*Rh^{III}(Cy_2AFAPdCl_2)][BF_4]$ has been developed for alkene polymerisation in an attempt to investigate the charge effect in alkene polymerisation catalysis. Upon activation this monocationic Rh/Pd bimetallic complex would provide a dicationic active species which would in principle be a more highly active catalyst than the Brookhart mono cationic diimine catalysts.

Chapter 4 describes all the experimental procedure and polymerisation tests in this thesis.

Abbreviations

DMF	dimethylformamide
DMS	dimethyl sulfate
DMAP	4-dimethylaminopyridine
PPh_3	triphenylphosphine
PMe_3	trimethylphosphine
NaCp	sodium cyclopentadienide
Cp*	pentamethylcyclopentadienyl
Cp	cyclopentadienyl
º	degree
ºC	degree centigrade
Å	angstrom
J	spin-spin coupling constant
Ar	aryl
AFA	6-aminofulvene-2-aldiminate
AFAH	6-aminofulvene-2-aldimine
ca.	circa
COD	cyclooctadiene
Cy	cyclohexyl
Ph	phenyl
MAO	methylaluminoxane
MeCN	acetonitrile
EIMS	electron impact mass spectrometry
FABMS	fast atom bombardment mass spectrometry
i-Pr	iso-propyl
Me	methyl
ppm	parts per million

LTM	Late transition metal
ETM	Early transition metal
br	broad
d	doublet
dd	doublet of doublet
dt	doublet of triplet
t	triplet
s	singlet
NMR	Nuclear Magnetic Resonance

Table of Contents

Chapter 1 Introduction & Literature Review

1.1 Introduction

The commercial production of polyolefins has developed into a giant industry after Ziegler's discovery of the polymerisation of ethylene with $TiCl_4$-$AlClEt_2$ catalysts[1] and Natta's discovery of the stereoselective polymerisation of propylene.[2, 3] Polyolefins have wide and various applications such as in rigid and flexible packaging (film, bottles, food storage), pipe, tubing, wire and cable insulation, fibers, automotive applications etc. due to their high melting points (up to 135 ºC for polyethylene, 160 ºC for polypropylene) as well as low weight, transparency, corrosion resistance, rigidity, shock resistance and ability to be modified. In the year 2007, 65 million tons of polyethylene and 50 million tons of polypropylene were produced, mainly by Ziegler-Natta and Phillips catalysts[4] (chromium oxide supported on an amorphous material such as silica, CrO_x/SiO_2) based on early transition metals.[5] Phillips catalysts are responsible for the commercial production of more than one-third of the PE sold worldwide.[6] The production of polyethylene and polypropylene is increasing 3% – 7% annually.[7]

Classical Ziegler-Natta catalysts are heterogeneous in nature where the polymerisation takes place on dislocations and edges of $TiCl_3$ crystals. As a result, there are many different types of active sites and the resulting polymer has a typically broad molecular weight distribution.[8] Although Ziegler-Natta catalysts are active at 25 ºC and 1 bar, the non uniformity of the active sites in these heterogeneous catalysts renders mechanistic study and rational design of modified catalysts extremely difficult. In addition, polymer structure can be influenced only to a limited degree with these catalytic systems. A further impact in this area happened when Wilkinson and coworkers first synthesised Group 4 metallocenes.[9] The 1st homogeneous metallocene catalyst for ethylene polymerisation was discovered independently by Natta[10] and Breslow[11] at the Hercules Research Center by reacting

Wilkinson's titanocene dichloride, Cp_2TiCl_2 with an alkylating agent, diethylaluminium chloride (Et_2AlCl) (Fig. 1.1).

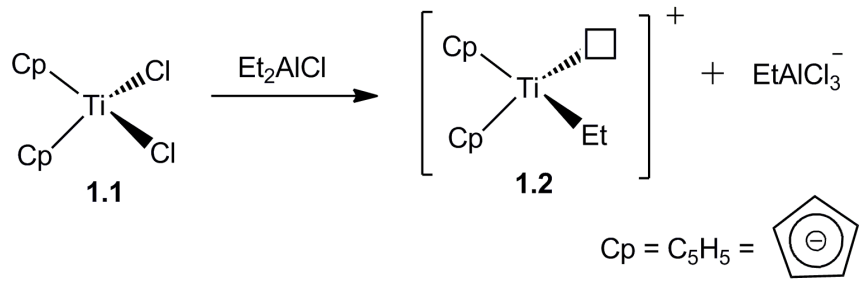

Figure 1.1. The first homogeneous metallocene catalyst for ethylene polymerisation.

However, this soluble metallocene catalyst was only able to polymerise ethylene with a very low activity, and not any of its higher homologues like propylene. Propylene leads to dimerisation only with this catalytic system. The difference in behavior between ethylene and propylene has been explained by the presence of a hydrogen atom at a tertiary carbon that is formed during chain growth using propylene, which undergoes β–hydride elimination. Later in 1975, Breslow[12] also found that the addition of small amounts of water to the alkylaluminum chloride co-catalysts increases ethylene polymerisation activity one to two fold.

A breakthrough happened in 1980 when Kaminsky[13, 14] reported an extremely fast homogeneous catalyst for ethylene polymerisation by the reaction of $Cp_2Zr(CH_3)_2$ and methylaluminoxane (MAO) (Fig. 1.3). MAO is the product of the partial hydrolysis of trimethylaluminium (Fig. 1.2).

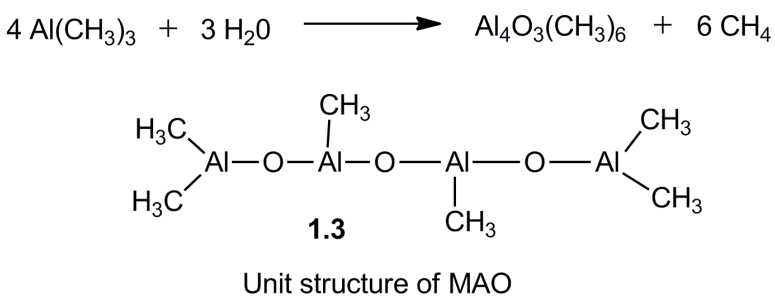

Figure 1.2. Synthesis of methylaluminoxane (MAO) and its unit structure.

Due to the discovery of MAO, about 4 million tons of polyolefins such as linear low density polyethylene (LLDPE), ethylene/propylene (EP) elastomers and polypropylene are produced annually by metallocene catalysts.[5] MAO is the most widely used co-catalyst in olefin polymerisation. MAO has two structure elements; cyclic and linear structure and they are at equilibrium with each other. For this reason, it is not possible to obtain single crystals of MAO for X-ray analysis. The bulky structure of MAO is responsible for the high activity of metallocene catalyst. However, there is still a large interest to find cheaper co-catalysts other than MAO or perfluorophenylborates.[5]

Thus there are three classes of olefin polymerisation catalysts. These are:

(i) Ziegler-Natta catalysts

(ii) Phillips type catalysts

(iii) Homogeneous single-site catalysts or supported homogeneous catalysts, like metallocene catalysts

Heterogeneous Ti-based Ziegler-Natta systems are still not able to provide fine control of the polymer microstructure.[15] On the other hand, soluble homogeneous catalysts offer several advantages over their heterogeneous counterparts.[16] For example:

1. Homogeneous catalysts are single site catalysts, i.e. only one type of a coordinatively unsaturated complex is involved in the migratory insertion of the olefinic monomer. Polyolefins thus obtained are usually uniform and have narrow molecular weight distribution ($M_w/M_n \approx 2$).

2. Homogeneous catalysts have the potential to polymerise prochiral olefins, such as propylene, to give stereospecific polymers (isotactic, syndiotactic polypropylene). This variety opens the door to polyolefin elastomers.

3. Homogeneous catalysts allow one to establish relationships between the

molecular structure of the precatalysts and the material properties of the polymers obtained. Design and improvement of ligands can provide higher catalytic performance. It is possible to tailor the microstructure of the polymers by tuning the ligands.

4. Metallocenes immobilised on solid support materials can provide new application - oriented polymer materials and simplify the process engineering required.

5. Structurally well defined homogeneous catalysts enable mechanistic studies on a molecular scale.

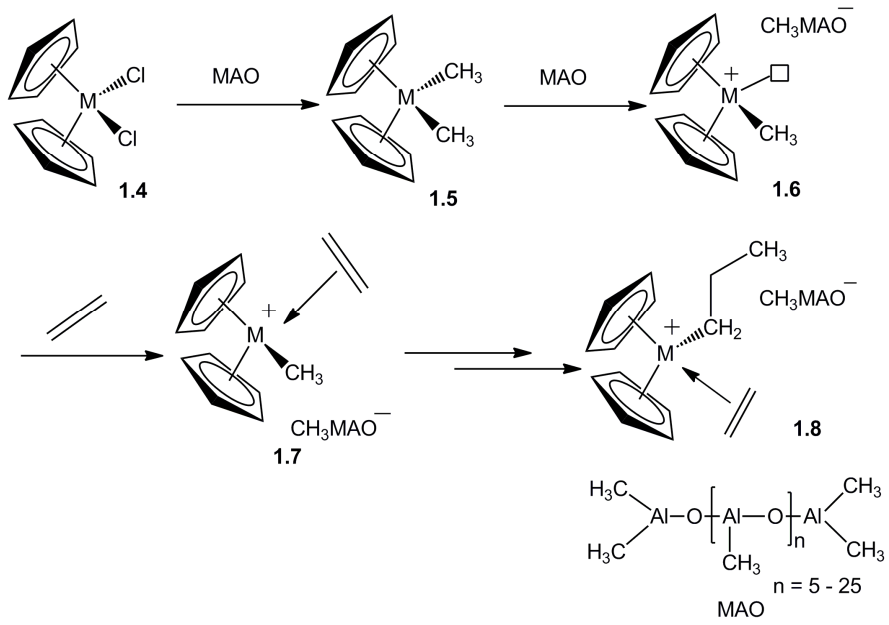

Figure 1.3. Traditional homogeneous metallocene olefin polymerisation.

However, there are major drawbacks of homogeneous metallocene catalysts. These include: (i) unavoidable use of a large excess of costly Lewis acid activating reagents makes the process more expensive; (ii) precatalysts with complicated ligands need tedious multistep syntheses; (iii) early transition metal (Ti, Zr, or Cr; usually active in high oxidation states) metallocene or Ziegler catalysts are highly sensitive to polar comonomer (Lewis base) due to their strong Lewis acid character. The high oxophilicity (the tendency to react irreversibly with oxygen-containing molecules) of early transition metal catalysts causes them to be poisoned by most functionalised

olefins, particularly polar comonomers such as methyl (meth) acrylate, (meth) acrylic acid, and vinyl acetate. Therefore, copolymers of ethylene with functionalised polar monomers cannot be made with these early transition metal catalysts. Copolymerisation with polar monomers can only be possible if the polar functional groups are protected.[17, 18] Copolymers of ethylene with polar monomers such as acrylate and vinyl acetate are still produced commercially by free-radical polymerisation.[19, 20] Free radical processes result in branched (co-)polymers and relatively broad molecular weights and have no control over polymer architecture (tacticity or crystallinity). Free radical processes also require extreme pressures and thus suffer from high manufacturing costs. In this respect, the lower oxophilicity and presumed greater functional-group tolerance of late transition metals (Fe, Co, Ni and Pd; active in low oxidation states) compared to early transition metals make them attractive targets for catalysts development for the copolymerisation of ethylene with polar comonomers. However, late transition metal catalysts exhibit reduced activities for olefin insertion relative to the early transition metal catalysts and β-hydride elimination typically competes with chain growth, resulting in the formation of oligomers or dimers. Exploiting this property Keim and coworkers[21] developed the Shell Higher Olefin Process (SHOP) catalyst to produce linear ethylene oligomers in the C_6 to C_{18} range, which are converted to detergents, plasticisers, lubricants, and a variety of fine chemicals (Fig. 1.4).[22, 23]

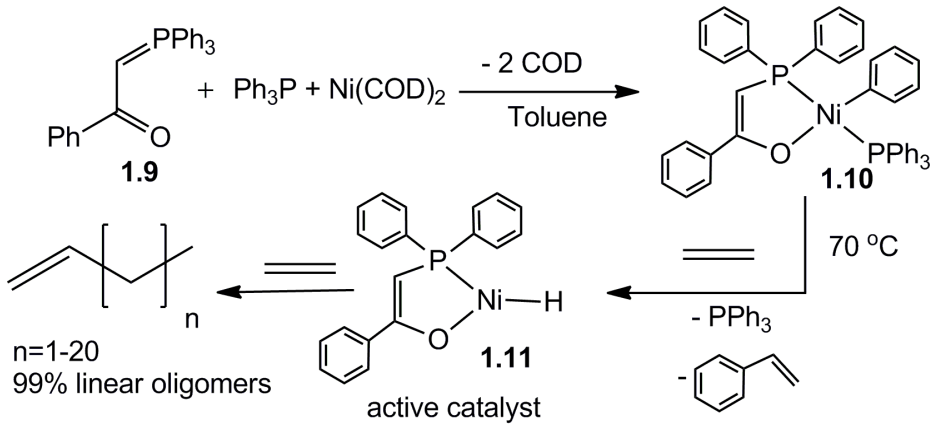

Figure 1.4. Keim catalyst for Shell Higher Olefin Process (SHOP).

SHOP-type oligomerisation catalyst can also make polyethylene with molecular weight over 100000 under certain conditions.[21, 24, 25] The key step to the conversion of this SHOP oligomerisation catalyst to polymerisation catalyst is the removal of the PPh_3 ligand with phosphine scavengers such as $[Ni(COD)_2]$ (COD = 1,5-cyclooctadiene), or the use of more labile groups as ligand such as pyridine or ylides. These SHOP catalysts are also found to be active for the copolymerisation of ethylene with higher α-olefins.[26]

Since 1970s, the late transition metal (Fe and Co) alkyl complexes with bipyridine ligands have been known for their ability in the insertion polymerisation of acrylonitrile (Fig. 1.5).[7, 27]

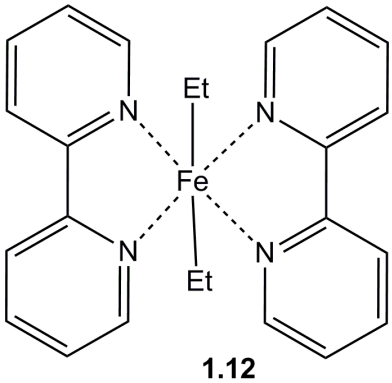

1.12

Figure 1.5. Bipyridine-coordinated iron alkyl complex for the polymerisation of acrylonitrile.

Unfortunately, these diethylbis(bipyridine)iron(II) and related cobalt complexes[27] showed low activity for monomer conversion. These complexes suffered from a weak coordination between iron and the bipyridine ligands. This facilitates β-H elimination and reductive elimination of the growing polymer chain leading to fast deactivation of the catalytically active species.[28]

In 1967, Yamamoto[29] also reported a diethyldipyridylnickel complex for polymerisation of acrylonitrile (Fig. 1.6). It was assumed that acrylonitrile is first coordinated to the nickel atom through the vinyl group, and the interaction causes the "weakening" of the ethyl-nickel bonds. The weakening may lead to the scission of

the ethyl-nickel bonds and the initiation of the polymerisation by a coordinated mechanism.

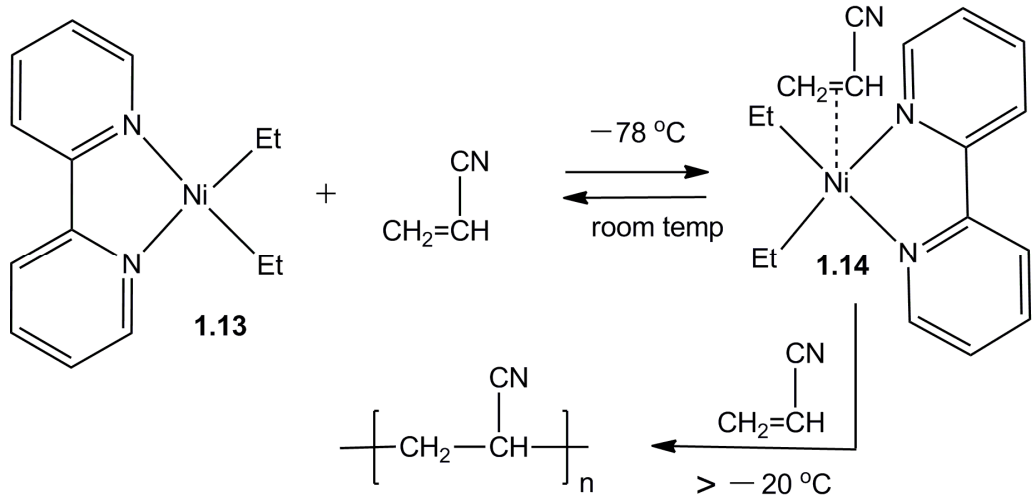

Figure 1.6. Polymerisation of acrylonitrile by diethyldipyridylnickel complex.

Later in the 1980s pioneeing work in the field of Ni and Pd based polymerisation catalysts was done by Keim[30] and Fink[31]. Keim and coworkers[30] synthesised nickel and palladium complexes containing a bis(trimethylsilyl)aminobis-(trimethylsilylimino)phosphorane as chelate ligand (Fig. 1.7).

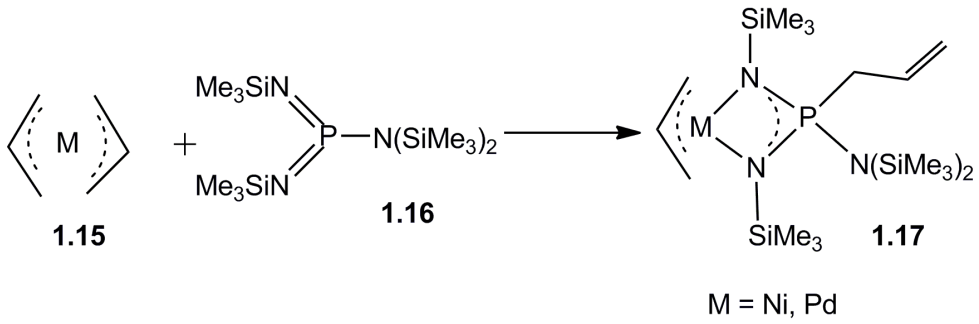

Figure 1.7. Ni/Pd complex of aminobis(imino)phosphorane ligand.

The reaction bis-(η^3-allyl)nickel with the bis(trimethylsilyl)aminobis-(trimethylsilylimino)phosphorane in toluene yields a catalyst which polymerises ethylene to polyethylene at 70 ºC and 50 bar. They achieved activities of 1000 mol

ethylene per mol of nickel and it is a short-chain, branched polymer. However, the palladium complex of the aminobis(imino)phosphorane ligand could not catalyse the polymerisation of ethylene. A few years later in 1985 Fink[31] was successful in polymerising α-olefins using the nickel(0)compound/ aminobis(imino)phosphorane ligand catalytic system. This system can also produce copolymers of ethylene with other α-olefins.

Following this pioneering work, Maurice Brookhart and coworkers[20, 32] in 1995 made a major breakthrough in the research on late transition metal polymerisation catalysts. They discovered that cationic nickel(II) and palladium(II) complexes of bulky substituted neutral diimine ligands are unique in polymerising ethylene to highly branched, high molecular weight homopolymers. The α-diimine nickel catalysts exhibit extremely high activities when activated with MAO (11000 kg of PE mol^{-1} of Ni h^{-1}) which are comparable to those of metallocene catalysts. Polyethylene with molecular weights of up to 10^6 can be obtained by varying the temperature, pressure and the structure of the ligand. This discovery by Brookhart's group emerges as an alternative to traditional heterogeneous and homogeneous Ziegler-Natta catalysts for the polymerisation of α-olefins to high molecular weight polymers. This catalyst also has the ability to produce copolymers of ethylene with various functionalised vinyl monomers. Further development in the field of late transition metal polymerisation catalysis was achieved by Grubbs[33, 34] and Mecking[35] and others.

Thus the supporting ligands play an important role in the development of alkene polymerisation catalysts. Their roles include:[25, 36]

1. To control metal coordination number.
2. To control metal coordination geometry.
3. To control formal oxidation sate of the metal.
4. To provide steric protection of the active site and influence over (stereo)selectivity.
5. Upon activation, the complex should have two cis-coordination sites: one for monomer entry and the other for polymer growth.

Present research in ethylene polymerisation has the following objectives:[37]

1. High activity to produce high molecular weight polyethylene.
2. Living polymerisation to control molecular weights.
3. High or controllable incorporation of comonomers in copolymerisation.
4. Formation of polyethylene with regulated branching.

For gaseous monomers such as ethylene and propylene, the catalyst activities are generally expressed in the units $g_{(polymer)}\ mmol_{(catalyst)}^{-1}\ h^{-1}\ bar_{(monomer)}^{-1}$ and for liquid α-olefins such as 1-hexene, the unit is: $g\ mmol^{-1}\ h^{-1}$. The catalyst activities are classified as:[25, 38]

1. Very high (>1,000)
2. High (1,000-100)
3. Moderate (100-10)
4. Low (10-1)
5. Very low (<1)

1.2 Late transition metal (Group 10) catalysts for olefin polymerisation

1.2.1 Nickel and palladium based α-diimine catalysts

As mentioned earlier, Brookhart and co-workers[32] added momentum to the search for LTM polymerisation catalysts with the discovery of the highly active cationic nickel(II) and palladium(II) diimine catalysts for polymerisation of ethylene and α-olefins. The steric bulk of the aryl-substituted α-diimine ligands are responsible for the ability of these late transition-metal catalysts to provide polymer rather than oligomers.

There are three key features of α-diimine catalysts.[20] These are:

1. Highly electrophilic, cationic Ni and Pd metal centers.
2. Use of sterically bulky α-diimine (1,4-diazadiene, R-DAB (also called, DAD)) ligand to block axial sites (R = aryl).
3. Use of noncoordinating counterions.

Brookhart's α-diimine ligands[17, 39] (Fig. 1.8) can be synthesised by a simple acid-catalysed condensation reaction of α,β-diketones with commercially available 2,6-diisopropylaniline.[40-42] The bis(imino)acenaphthenes (R-BIAN, R = aryl) are also synthesised in a similar manner of condensation reaction between acenaphthenequinone and 2,6-diisopropylaniline. The α-diimine (DAB) ligands are very versatile.[36, 43, 44] The versatility is due to:

1. Flexibility of the N=C-C=N backbone.
2. Strong σ-donor and π-acceptor properties. R-DAB ligand uses its 4e in the σ,σ-N,N' coordination mode. The π and π* orbitals of the N=C-C=N backbone are sufficiently low in energy to be used for interaction with metal d orbitals.
3. Possibility of changing both the R substituents by which both the electronic and steric properties can be influenced.

However, the R-BIAN ligands are rigid and they exhibit a limited range of bonding modes and thus the resulting metal complexes are very robust. The R substituents of R-BIAN ligands are also tuneable to influence electronic and steric properties.[44]

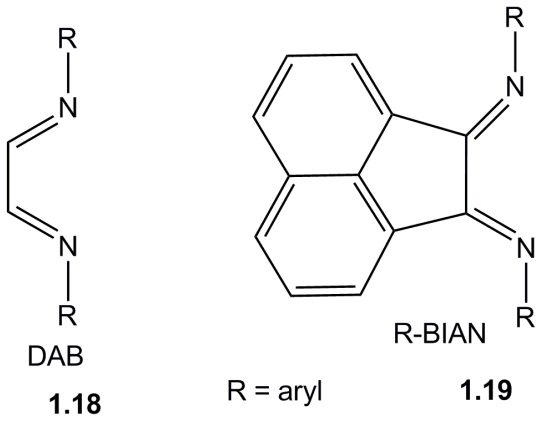

Figure 1.8. α-diimine ligand.

The Ar-BIAN ligands have been known for many years, Elsevier[41] brought attention to these ligands for their possible application in catalysis by synthesing both neutral [Pd(R)X(Ar-BIAN)] (Fig. 1.9) and cationic [Pd(R)(MeCN)(Ar-BIAN)]SO_3CF_3 complexes of this rigid bidentate nitrogen ligand, bis(arylimino)acenaphthene. They also found that rigidly chelating Ar-BIAN ligands have an activating effect on the insertion of CO and alkenes in palladium-carbon bonds as compared to other (bidentate) phosphorus and nitrogen ligands, and a stabilizing effect on the Pd-acyl and Pd-alkyl complexes.

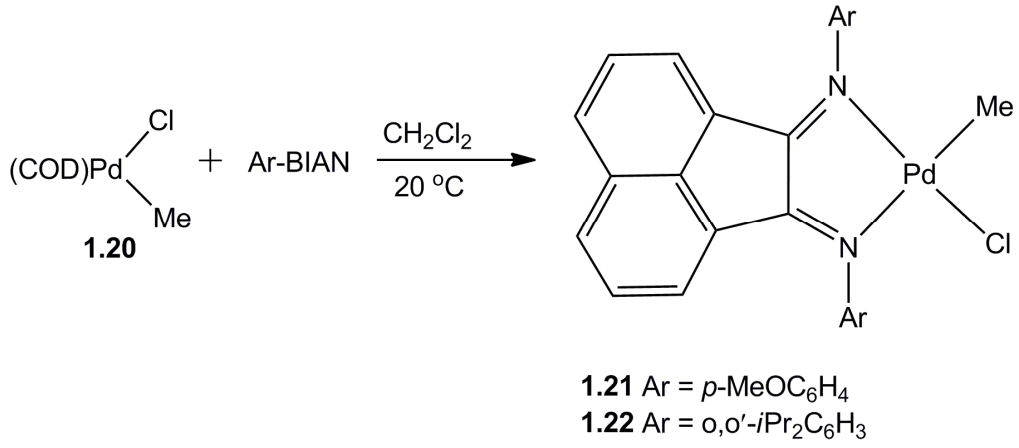

Figure 1.9. Neutral [Pd(R)X(Ar-BIAN)] complex by Elsevier.

Later Brookhart synthesised highly active cationic nickel(II) and palladium(II) catalyst employing these aryl-substituted α-diimine ligands containing bulky N-substituents. The nickel catalyst precursor, a neutral dibromo complex (α-diimine)$NiBr_2$ is easily prepared by reacting α-diimine ligand with (DME)$NiBr_2$ (DME = 1,2 -dimethoxyethane) by ligand substitution (Fig. 1.10).

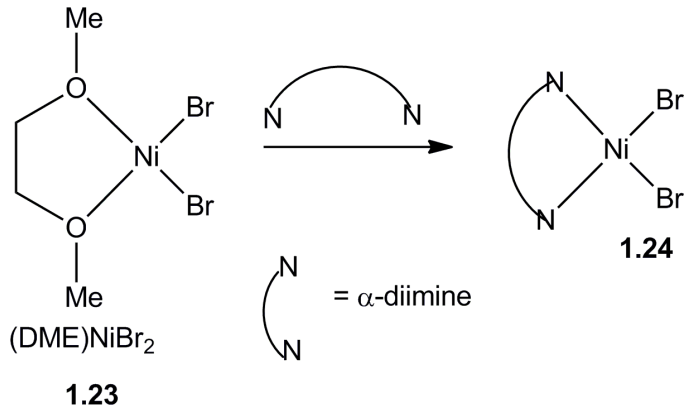

Figure 1.10. Synthesis of (α-diimine)$NiBr_2$ complex.

The (α-diimine)$NiBr_2$ complex, **1.24** can be converted into (α-diimine)$Ni(alkyl)_2$ by reacting with an alkylating agent, MeMgX.[39] An alternative route for the synthesis of (α-diimine)$NiMe_2$ is the reaction of an α-diimine ligand with $Ni(acac)_2$ (acac = acetylacetonate) in ether and subsequent alkylation with Me_2Mg.[32] Similarly, the palladium precatalyst, (α-diimine)Pd(Me)Cl, **1.25** can be conveniently synthesised via the displacement of weakly coordinating ligands, such as COD from (COD)Pd(Me)Cl (COD = 1,5 -cyclooctadiene) (Fig. 1.11).

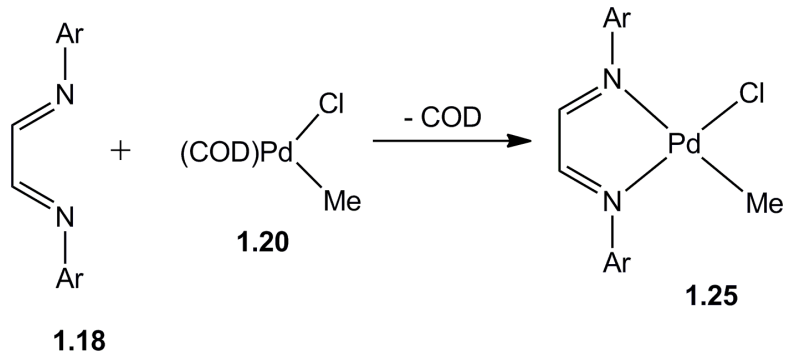

Figure 1.11. Synthesis of (α-diimine)Pd(Me)Cl.

The (α-diimine)Pd(Me)Cl, **1.25** can also be formed by reacting the α-diimine ligand with [$(PhCN)_2Pd(Me)Cl$],[45] generated *in situ* by reaction of $(PhCN)_2PdCl_2$ with tetramethyltin ($SnMe_4$) at low temperature (-40 ºC) under an argon atmosphere. The precatalyst of the type (α-diimine)$PdMe_2$, is generated by reacting (α-diimine)Pd(Me)Cl with Me_2Mg.[32] The (COD)$PdMe_2$ precursor can also be converted into (α-diimine)$PdMe_2$.[46, 47] Elsevier and coworkers[47] reported the synthesis of (α-diimine)$PdMe_2$ through in situ generation of (COD)$PdMe_2$ by reacting 1 equivalent of MeLi with (COD)PdMeCl in THF at low temperature to form (COD)$PdMe_2$, and subsequent reaction with α-diimine produces the (α-diimine)$PdMe_2$ complex (Fig. 1.12).

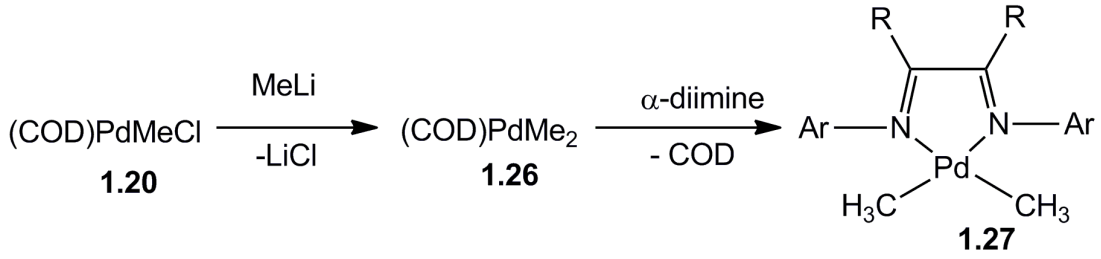

Figure 1.12. Synthetic procedure of (α-diimine)$PdMe_2$ complex by Elsevier.

The aryl rings of all these square-planar α-diimine complexes lie roughly perpendicular to the square plane and the ortho substituents are then positioned above and below the plane. The bulky ortho substituents (for example, 2,6-(i-$Pr)_2C_6H_3$) of the aryl ring block axial approach of monomer and thus retard the rate of chain transfer relative to chain propagation leading to the formation of polymer.[32] The active cationic species which are responsible for olefin polymerisation are generated *in situ* by activation of the above mentioned neutral α-diimine Ni and Pd complexes. In the case of α-diimine Ni catalysts, the active catalyst is obtained by treatment of the (α-diimine)$NiBr_2$, **1.24** with methylaluminoxane (MAO) (Fig. 1.13).[32] This activation process is similar to the methods used in the activation of early transition metal systems.[48] In this process, transmetallation occurs with aluminum, doubly alkylating the precatalyst and this is followed by mono-dealkylation of the metal center by the Lewis acidic Al centres in MAO to provide a vacant coordination site so that ethylene monomer can bind. The diamagnetic

complex [(α-diimine)Ni(acac)]$^+$[X]$^-$ (acac = acetylacetonato, X = [B(C_6F_5)$_4$]$^-$) is an important second generation precursor that can afford active catalysts upon treatment with trialkylaluminum (R_3Al) (Fig. 1.13).[17, 49, 50] The complex [(α-diimine)Ni(acac)]$^+$[X]$^-$ can be synthesied by abstracting one acac ligand from Ni(acac)$_2$ with a trityl salt, [CPh_3][B(C_6F_5)$_4$], or [CPh_3][$SbCl_6$], in the presence of an α-diimine ligand in DCM solvent. Moreover, the one-pot *in situ* activation of Ni(acac)$_2$ with MAO in the presence of an α-diimine ligand can catalyse polymerisation of ethylene.[51] Here, MAO causes the acac ligand to be replaced by α-diimine, finally resulting in the active Ni(II) species coordinated with α-diimine. The combination of Ni(COD)$_2$, α-diimine and $H^+BAr'_4^-$ (Ar' = 3,5-$C_6H_3(CF_3)_2$) also catalyses ethylene polymerisation.[46] In this one-pot catalytic system, activation occurs with an initial replacement of COD with α-diimine followed by protonation with $H^+BAr'_4^-$ .This system eliminates the preparation of the precatalyst-Ni(II) complexes with α-diimine. For mechanistic study or small scale work, active polymerisation catalysts can be prepared by protonolysis of (α-diimine)$NiMe_2$ complexes with one equivalent of the Brønsted acid[32], [$H^+(OEt_2)_2BAF^-$] where BAF^- = [B(3,5-$(CF_3)_2C_6H_3)_4$]$^-$. The sodium salt of the anion tetrakis(3,5-bis(trifluoromethyl)phenyl)borate, (Na^+BAF^-, BAF^- = [B(3,5-$(CF_3)_2C_6H_3)_4$]$^-$) is commonly used to abstract halide from metal precatalysts to generate active species. The trityl salt [CPh_3][B(C_6F_5)$_4$] is also used to obtain active catalysts. These bulky and weakly-coordinating fluorinated tetraarylborate counter anions such as BAF^- and B(C_6F_5)$_4^-$ are necessary to obtain high catalytic activity.

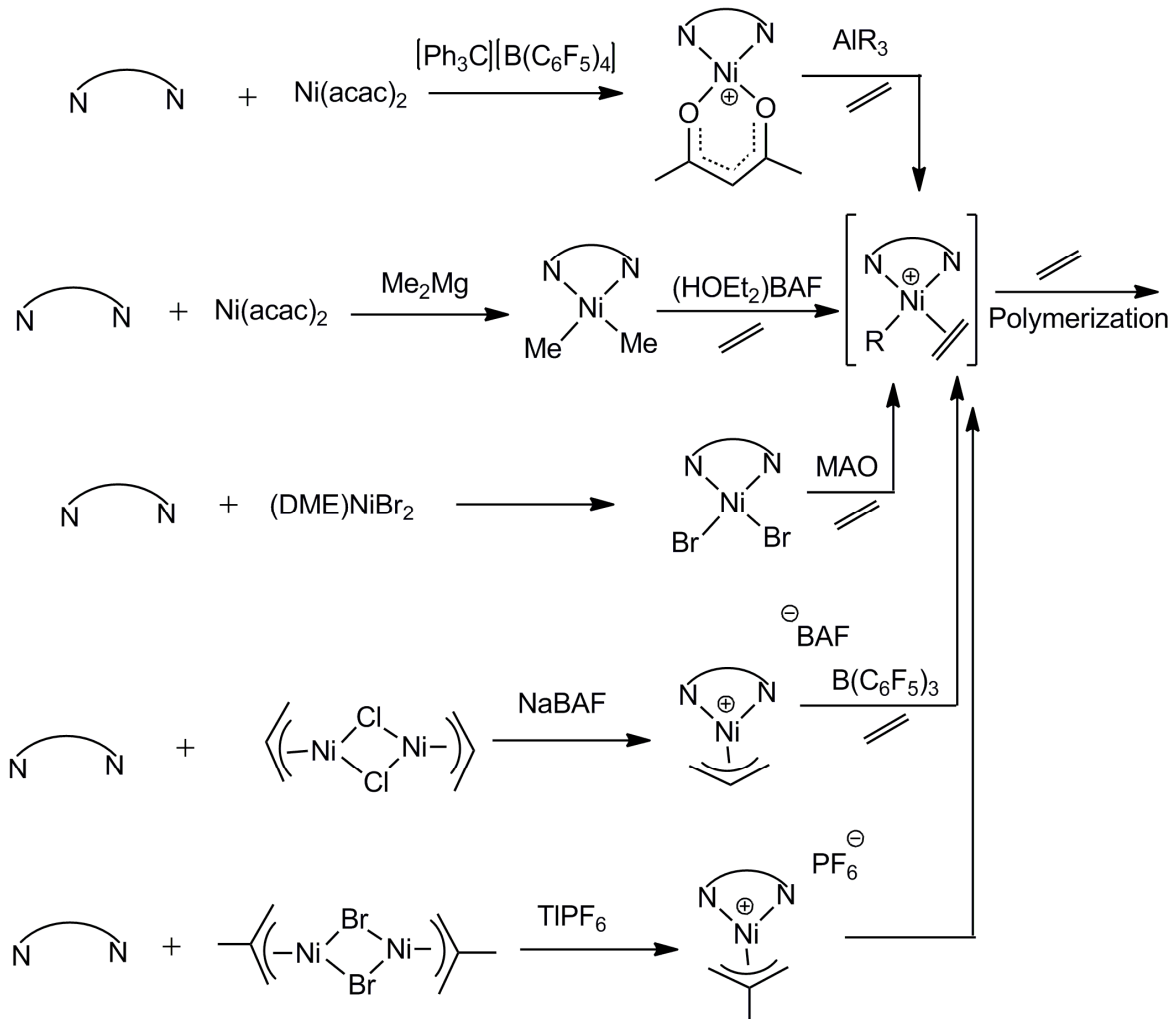

Figure 1.13. A summary of the preparation and activation procedures of (α-diimine)Ni polymerisation catalysts.

In contrast to Ni, (α-diimine)palladium precursors can be prepared easily and isolated due to their greater stability. The precatalyst (α-diimine)Pd(Me)Cl can be cleanly activated for ethylene polymerisation with NaBAF or a silver (I) salt by abstracting the chloride ligand. The highly electrophilic acetonitrile adduct [(α-diimine)PdMe(NCMe)]$^{+}$[BAr'$_4$] (**1.29**) (where Ar' = 3,5-$C_6H_3(CF_3)_2$ and α-diimine = ortho *tert*-butyl-substituted α-diimine, 2-C_6H_4(*t*-Bu)N=C(Me)C(Me)=N-2-C_6H_4(*t*-Bu)) can be prepared by addition of NaBAr'$_4$ to (COD)PdMeCl at low temperature in a mixture of CH_2Cl_2 and acetonitrile to form a salt [(COD)PdMe(NCMe)][BAr'$_4$], followed by addition of the α-diimine ligand (Fig. 1.14).[46, 52] The salt

[(COD)PdMe(NCMe)][BAr'$_4$] can be isolated at -30 ºC and is stable for an extended period.

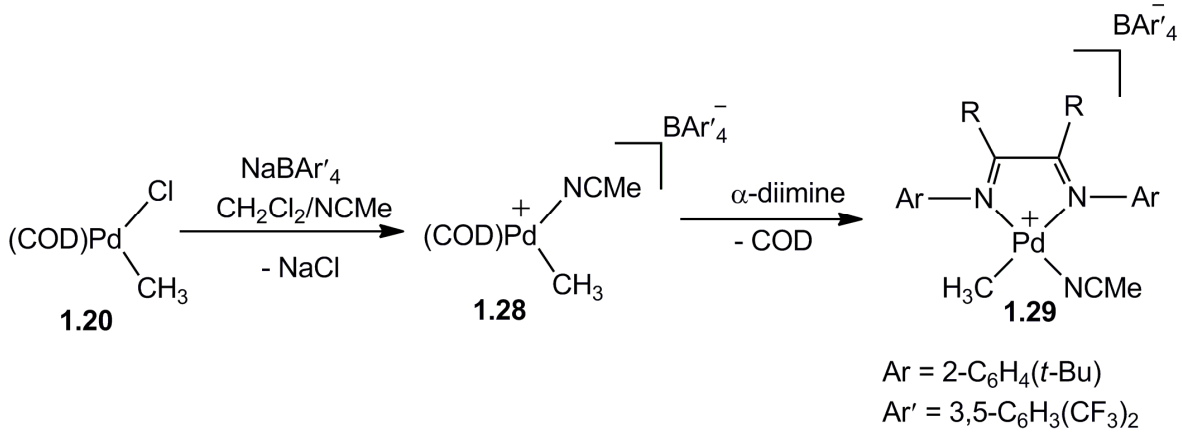

Figure 1.14. Synthesis of [(α-diimine)PdMe(NCMe)][BAr'$_4$].

The six-membered ester chelate complex [(diimine)Pd(CH$_2$)$_3$COOMe] (**1.30**) is also a useful catalyst precursor.[53] This stable chelate complex can be prepared easily by adding 1.1 equivalent of methyl acrylate (CH$_2$=CH-COOMe) to a mixture of 1 equivalent of [(α-diimine)Pd(Me)Cl] and 1 equivalent of NaBAr'$_4$ in ether. As shown in Figure 1.15 the methyl acrylate inserts into the Pd-C bond in a 2,1-migratory insertion fashion leading to four membered chelate **1.30a**. The intermediate **1.30a** does not insert olefin but isomerises at –60 °C to the five membered chelate complex **1.30b** which rearranges at –20 °C to the six-membered chelate complex **1.30**. Reversible opening of **1.30** allows for coordination and insertion of ethylene monomer.

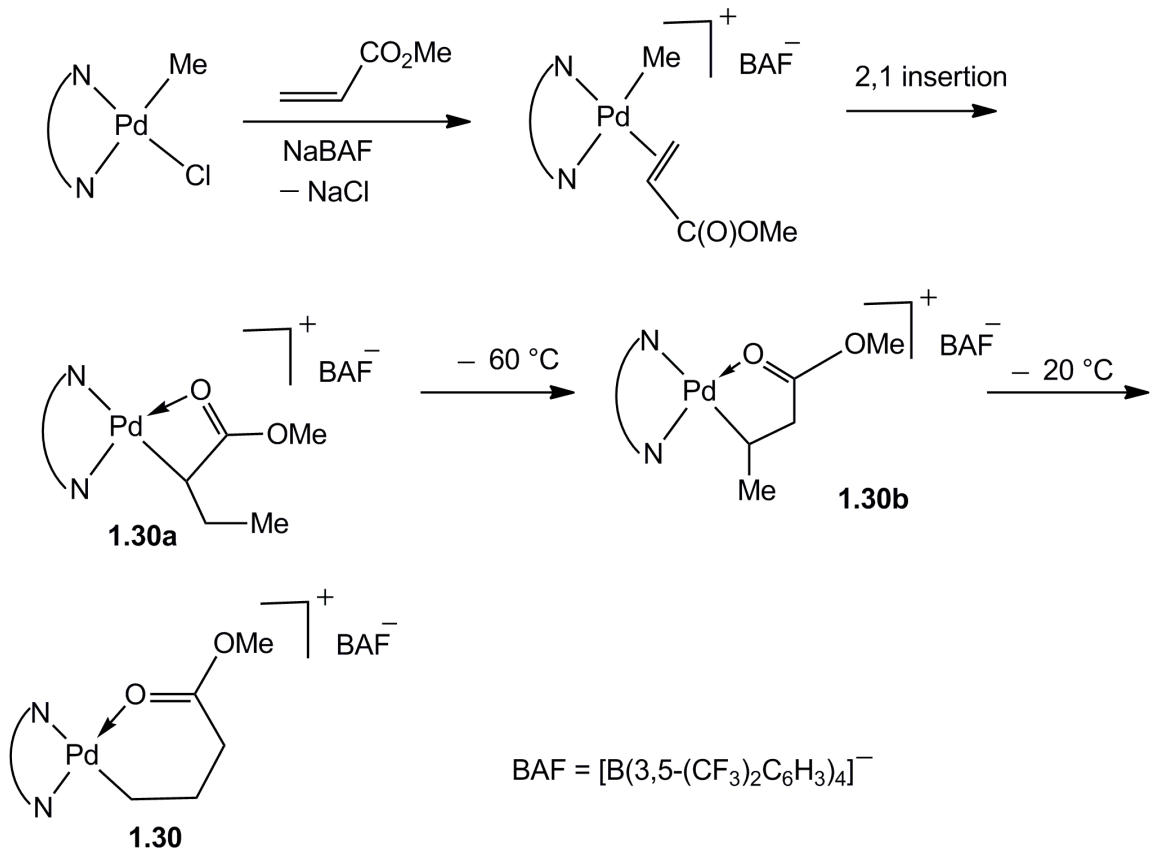

Figure 1.15. Synthesis of chelate complex [(α-diimine)Pd$(CH_2)_3$COOMe].

The ether adduct [(α-diimine)PdMe(OEt_2)]$^+$[BAr'$_4$]$^-$ (**1.31**) is synthesised through the addition of oxonium acid,[54] [H$(OEt_2)_2$]$^+$[BAr'$_4$]$^-$ to the [(α-diimine)PdMe$_2$] complex (Fig. 1.16).[32, 52] In this process the oxonium acid protonates the complex [(α-diimine)PdMe$_2$] with the loss of methane and thus creates a vacant coordination site which the solvent molecule diethyl ether occupies. Due to the high lability of ether, this adduct complex is ideal for low-temperature NMR mechanistic studies. Exposure of the palladium or nickel ether adducts to ethylene, propylene or 1-hexene results in the formation of high molecular weight polymers.

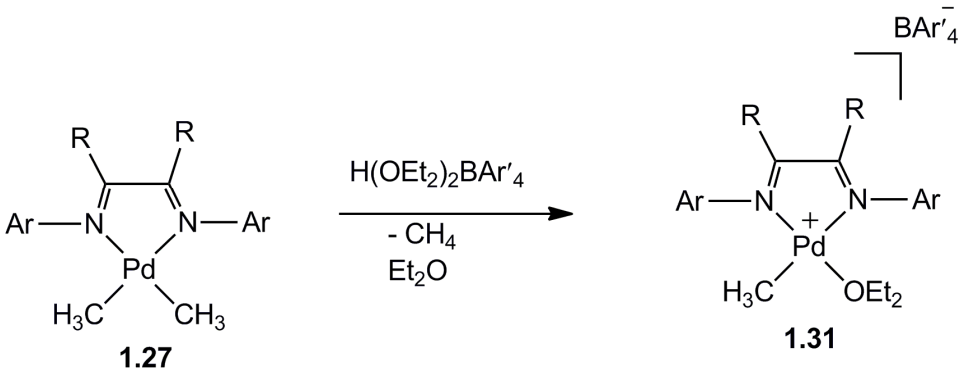

Figure 1.16. Synthesis of ether adduct [(α-diimine)PdMe(OEt$_2$)][BAr'$_4$].

A summary of the preparation and activation procedures of (α-diimine)Pd polymerisation catalysts is shown in Figure 1.17.

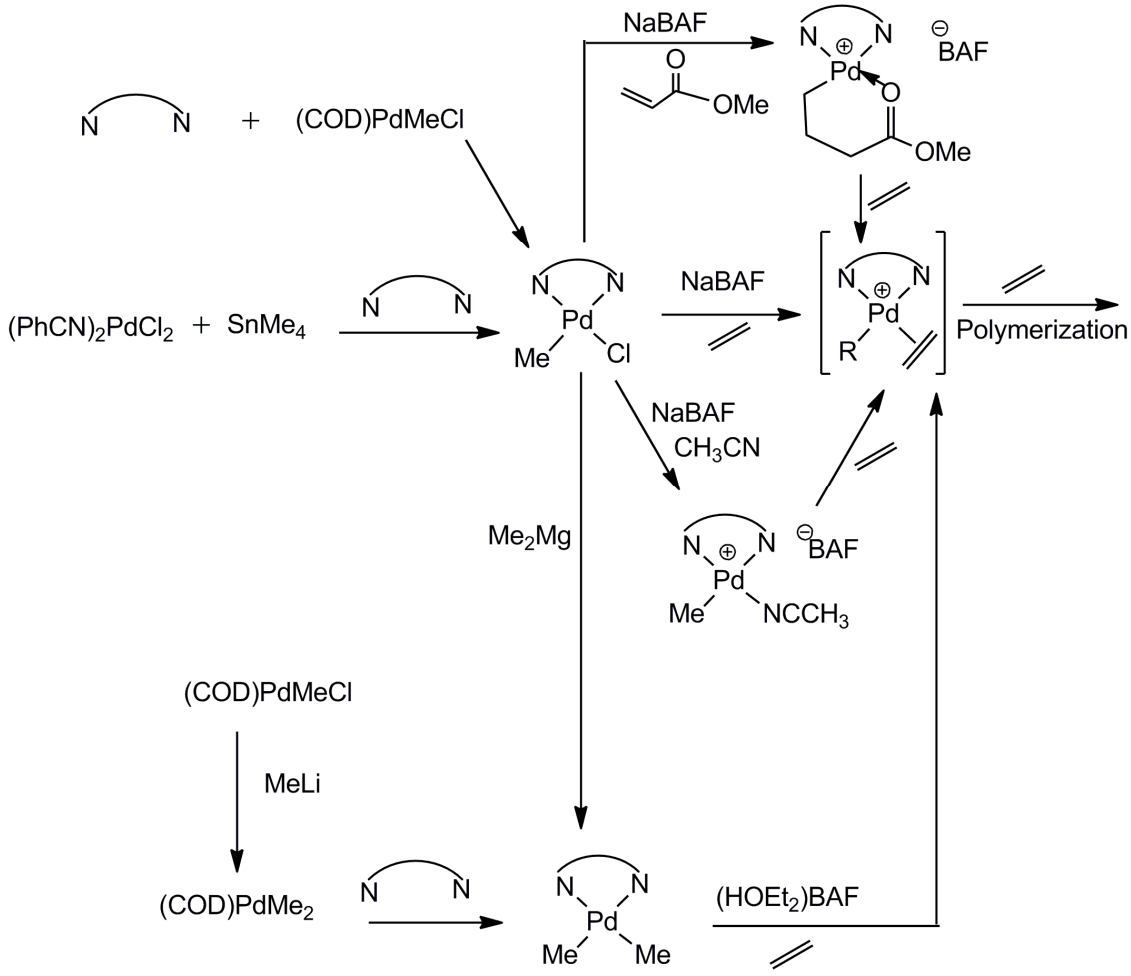

Figure 1.17. A summary of the preparation and activation procedures of (α-diimine)Pd polymerisation catalysts.

All these cataionic complexes only require addition of olefin to initiate polymerisation.

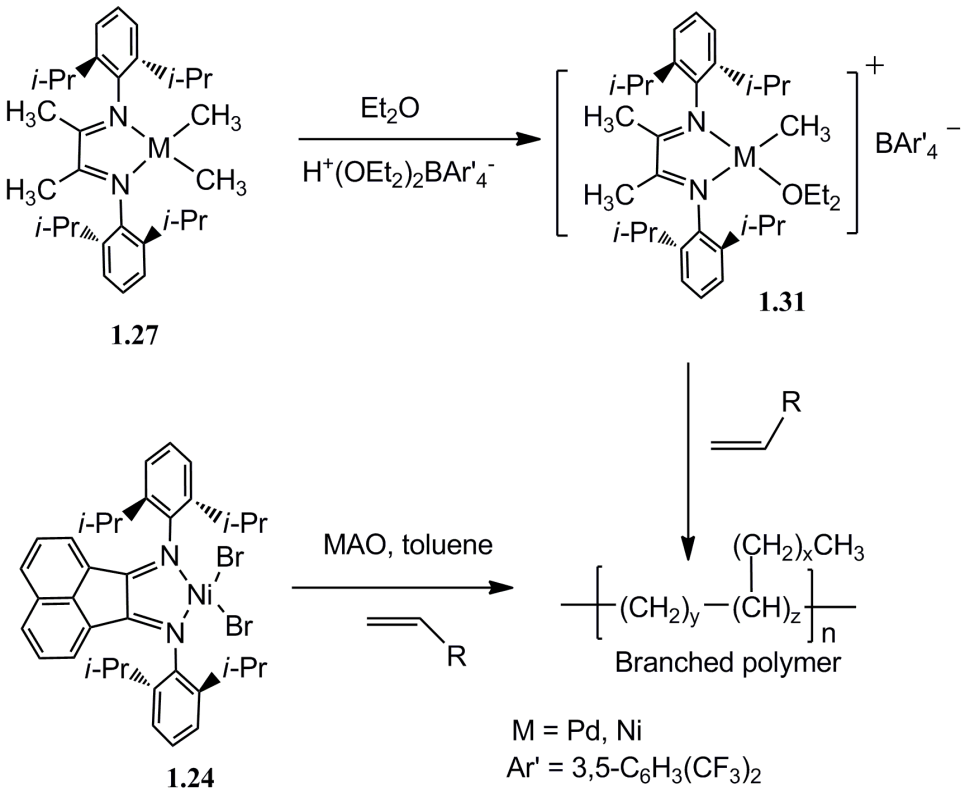

Figure 1.18. Brookhart nickel(II) and palladium(II) diimine catalysts for polymerisation of ethylene and α-olefins.

Brookhart catalysts are capable of producing polyethylene at one bar of pressure at 25 ºC (Fig. 1.18). Catalysts bearing ortho isopropyl substituents on the diimine aryl ring give higher molecular weight polymer than the corresponding less bulky methyl-substituted catalysts. The produced polyethylene is highly branched and amorphous containing mainly methyl branches (103 branches per 1000 carbon atoms). The branches result from metal migration along the polymer chain via β-hydride elimination/reinsertion reactions without undergoing chain transfer. The β-hydride elimination is less favorable in the Ni(II) catalysts compared to the Pd(II) catalysts. For this reason, Ni(II) systems afford polymer with low to moderate density of short-chain branches, mostly methyl groups. The extent of branching depends on

temperature, ethylene pressure and catalyst structure.[55] The branching decreases with the increase of ethylene pressure and increases with increasing temperature. Introduction of less bulky ortho-methyl groups in place of the ortho-isopropyl groups in the diimine ligand results in a less branched, more linear polymer.

However, as shown in Figure 1.19, the Ni(II) diimine catalysts lacking bulky aryl ortho substituents are found to produce a Schulz-Flory distribution of ethylene oligomers. By eliminating the steric bulk of the ortho-substituents, rates of associative chain transfer is substantially increased which results in oligomerisation rather than polymerisation reactions.[56]

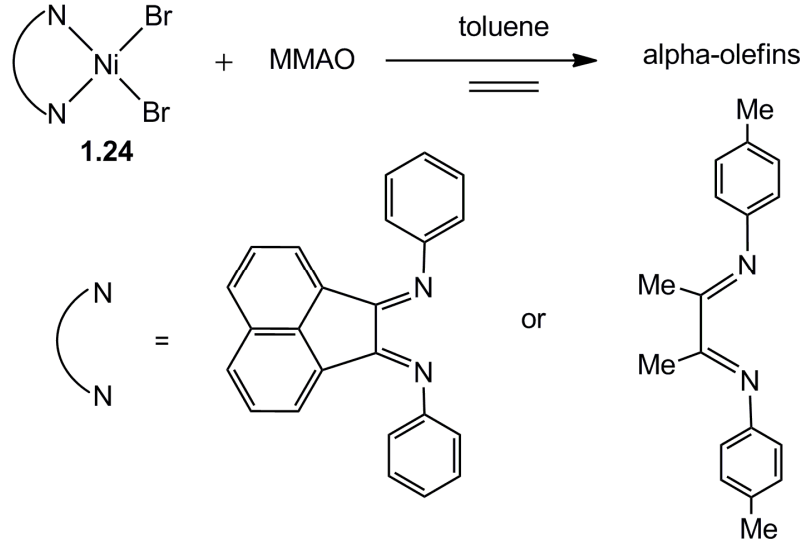

Figure 1.19. Ni(II) diimine catalysts lacking bulky aryl ortho substituents which produce ethylene oligomers.

The sterically unhindered (α-diimine)-nickel(II) catalysts also dimerise propylene (Fig. 1.20).[57] Treatment of precatalysts **1.24a-1.24e** with modified MAO (MMAO) or Et_2AlCl in toluene generates active catalysts which dimerise propylene at 0 ºC and propylene pressures above 2 bar.

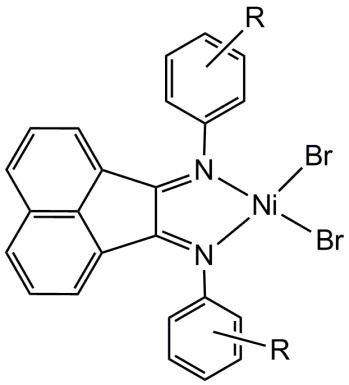

1.24a R = 4-CF_3
1.24b R = 4-H
1.24c R = 4-Me
1.24d R = 4-OMe
1.24e R = 2-Me

Figure 1.20. Sterically unhindered (α-diimine)-nickel(II) catalysts for propylene dimerisation.

1.2.2 Mechanism of ethylene polymerisation by Ni and Pd based diimine catalysts

Brookhart and coworkers extensively investigated the polymerisation mechanism of the late transition metal α-diimine catalysts.[20, 52, 58] It has been revealed that polymerisation occurs by the generally accepted Cossee mechanism[48, 59] by repeated migratory insertion of olefin into the cis-oriented metal-carbon bond. But it has an additional feature called chain walking.

Beyond initiation, the mechanism of ethylene polymerisation consists of three main processes:
(1) chain propagation
(2) metal migration along the polymer chain ("chain walking") and
(3) chain transfer

The chain propagation and chain transfer processes are common to all ethylene polymerisation and oligomerisation catalysts. In the chain initiation step after activating the precatalyst by a co-catalyst, olefin coordinates to the vacant site of the square-planar metal center and inserts into the metal-alkyl bond. Low temperature NMR studies of ethylene polymerisation have shown that the resting state of the Ni and Pd based diimine catalysts is the ethylene-metal-alkyl complex and not the metal-alkyl complex as is the case for the early transition metal catalysts. For early transition metal catalysts, the alkene complex intermediates are never observed. Thus the migratory insertion is the rate-determining step (the so-called "turnover limiting step") and the reaction rate is independent of the ethylene concentration. In the absence of excess olefin, the cationic metal intermediate that is formed after insertion is a highly dynamic β-agostic alkyl complex.[52, 58]

The chain propagation occurs by coordination of free olefins and successive insertion into the M-R bond (R = growing chain). As mentioned before, a remarkable feature of the Ni or Pd based diimine catalyst is its "chain-walking" behavior which is responsible for the branching in the polymer. In a chain-walking catalyst, the catalytic site (i.e. active growing site) isomerises or walks along the polymer chain during propagation so that the next monomer unit can be assembled onto any part of the polymer backbone instead of at the end, resulting in the formation of branching in the polymer backbone. In the early transition metal Ziegler-Natta and metallocene catalysts, the chain-walking rate is usually very small compared to the insertion rate, and the chain growth is linear. However, late transition metal catalysts are usually very good at catalysing alkene isomerisation.[31, 60]

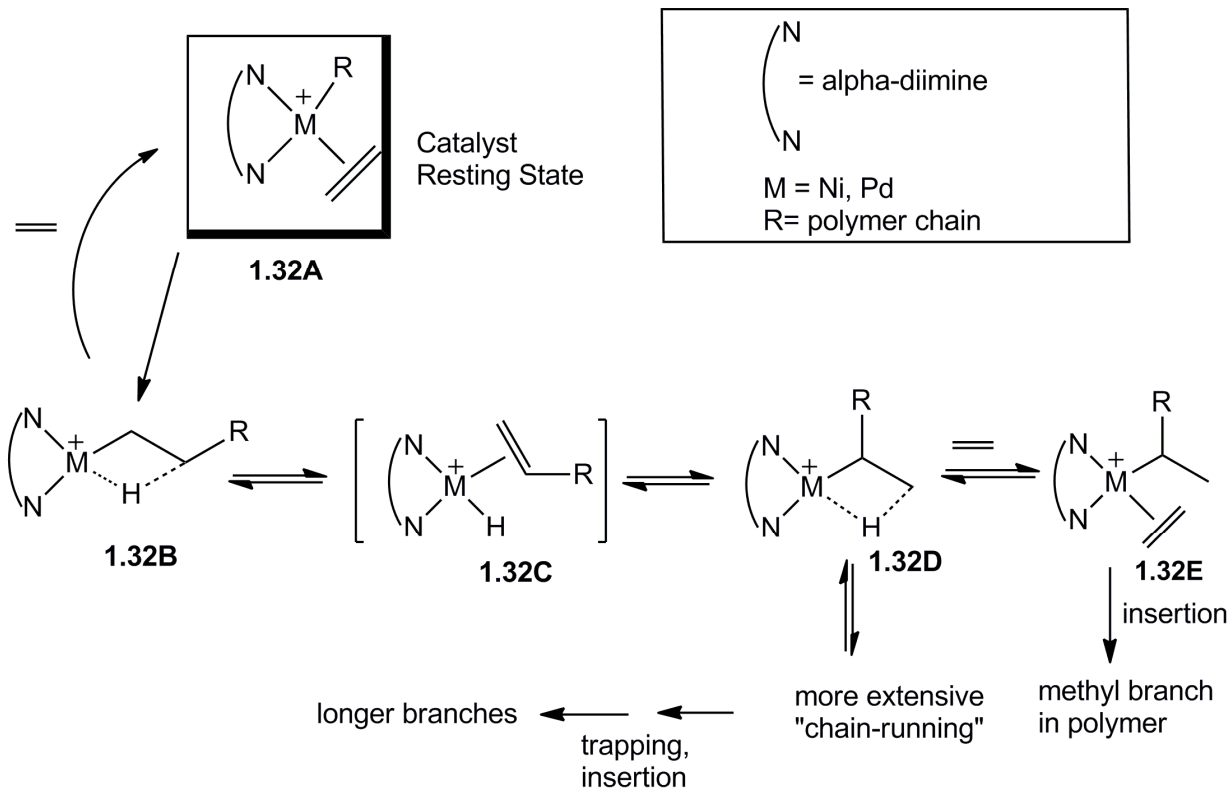

Scheme 1.1. Mechanism of ethylene polymerisation with Ni and Pd diimine catalysts.

As depicted in Scheme 1.1, the catalyst resting state is indicated by alkyl olefin complex **1.32A**. Migratory insertion of ethylene results in the linear coordinatively unsaturated $14e^-$ alkyl agostic complex **1.32B**. Rapid association of ethylene (trapping) in **1.32B** may lead back to resting state **1.32A**. Successive trapping of ethylene in **1.32A** followed by insertion may result in chain growth without the introduction of a branch in the polymer. Alternatively, prior to trapping and insertion, **1.32B** can also undergo β-hydride elimination to yield an olefin hydride species **1.32C**. Then **1.32C** can undergo hydride reinsertion with opposite regiochemistry, which introduces a methyl branched β-agostic species **1.32D**. The branched alkyl cation **1.32D** can continue to "chain run" by β-hydride elimination and hydride reinsertion with opposite regiochemistry, producing longer branches. Alternatively, **1.32D** can be trapped with ethylene, and insertion produces a polymer chain containing a methyl branch along the backbone. This phenomenon of running of the metal along the polymer chain is called chain-walking. Longer chain-walks introduce

longer branches.[52] During the isomerisation process palladium can even cross tertiary carbon atoms, since "branches on branches" are also obtained.

The Pd(II)-α-diimine catalysts produce more heavily branched polymer with longer branch lengths and more branch-on-branch than the corresponding Ni(II) catalysts. This is because chain-walking is very facile in the Pd(II) catalyst as compared to migratory insertion. The strong tendency of Pd to undergo rapid and reversible β-hydride elimination and reinsertion leads to the extensive chain-walking. On the other hand, the Ni(II)-α-diimine catalyst promote rapid migratory insertion and high polymerisation activity, making these catalysts attractive for industrial applications.[36]

In terms of chain-transfer, two possible mechanisms have been proposed. These are:
(i) Associative displacement from the olefin hydride intermediate
(ii) Direct β-hydride transfer to monomer from the alkyl-olefin resting state

(i) Associative displacement from the olefin hydride intermediate

As shown in Scheme 1.2, a free monomer can initiate an associative displacement of the bound unsaturated polymer chain from the olefin hydride intermediate. However, the rate of displacement is very slow (as high molecular weight polymer is produced) relative to chain propagation due to the presence of bulky ortho-substituents in the diimine catalysts which block axial approach of monomer. The rate of associative chain-transfer increases with the reduction of the steric bulk of the ortho-substituents which results in the formation of oligomers rather than polymers.[20]

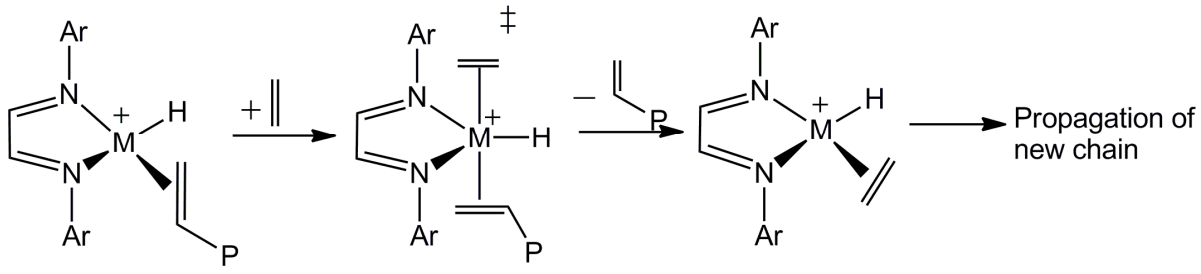

Scheme 1.2. Associative displacement from the olefin hydride intermediate.

(ii) Direct β-hydride transfer to monomer from the alkyl-olefin resting state

This mechanism (Scheme 1.3) has been proposed on the basis of theoretical calculations by Ziegler and coworkers.[61] According to this proposal, chain transfer occurs from the alkyl olefin resting state by direct β-hydride transfer to monomer.

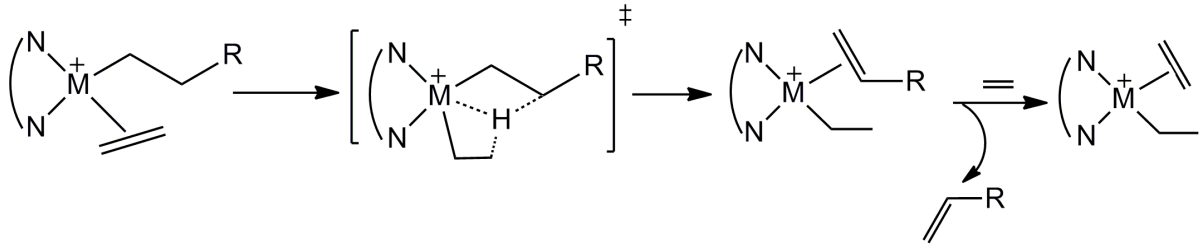

Scheme 1.3. Direct β-hydride transfer to monomer from the alkyl-olefin resting state.

Zielger[61, 62] and Morokuma[63] found that inclusion of bulky Ar susbtituents in the diimine Ni and Pd complex destabilises the alkyl olefin complex and reduces the migratory insertion barrier and insertion rate increases as steric bulk increases. In the case of Pd(II), replacing an ortho-methyl group with a more bulky ortho-isopropyl substituents result in a 0.6 kcal/mol decrease in the migratory insertion barrier[52] while in the Ni(II) system the decrease is 0.5 kcal/mol.[64] Low temperature NMR studies also showed that the barriers to migratory insertions in the nickel complexes are substantially lower and in the range of 13-14 kcal/mol, whereas the barriers for the insertions in palladium systems lie in the range of 17-18 kcal/mol. The barrier differences of ca. 4-5 kcal/mol account for the much higher catalytic activities of the nickel complexes. Thus ethylene polymerisation by Ni(II) α-diimine catalysts is over 1000 times more active than that of the analogous Pd(II) catalysts. This is also in line with expectations of differences between first-row and second-row insertion barriers.[20]

In recent years electrospray ionisation mass spectrometry (ESI-MS) has become an important technique for mechanistic studies of homogeneously catalysed reactions[65] and high-throughput screening of homogeneous catalysts.[66] For example, Chen and

coworkers[67] reported a high-throughput screening method for Brookhart-type Pd(II) olefin polymerisation catalysts using electrospray ionisation mass spectrometry (ESI-MS). Among different aryl substituted α-diimine Pd complexes, they have found that the 2,6-diisopropylphenyl substituted α-diimine Pd(II) complex is the most active catalyst. This result is also in agreement with the experimental result of Brookhart.[32, 53] They have also found that an unsubstituted backbone for the 1,2-diimine ligand produces low molecular weight polymer. This means that isopropyl groups on the arene have little effect when the backbone of the 1,2-diimine ligand is unsubstituted. This feature is also in agreement with Brookhart's result.[32, 53] Later, J. O. Metzger[68] developed an on-line monitoring system of Brookhart polymerisation by ESI-MS to study the reaction mechanism of Brookhart polymerisation. In this technique, a microreactor where the polymerisation reaction takes place is coupled to the ion source and detects the positive ion on-line by ESI-MS. The reaction of [(α-diimine)Pd(Me)Cl] with AgOTf (or MAO) in CH_2Cl_2 and MeCN showed the most abundant ion is the adduct $[(\alpha\text{-diimine})Pd(CH_3)(MeCN)]^+$ of m/z 566. The ion $[(\alpha\text{-diimine})Pd(CH_3)]^+$ of m/z 525 was also observed and increasing the cone voltage increases the signal intensity of ion $[(\alpha\text{-diimine})Pd(CH_3)]^+$ and decreases the intensity of the adduct ion $[(\alpha\text{-diimine})Pd(CH_3)(MeCN)]^+$. This gives evidence that $[(\alpha\text{-diimine})Pd(CH_3)]^+$ ion is formed by in-source decay of $[(\alpha\text{-diimine})Pd(CH_3)(MeCN)]^+$. On the basis of this result they proposed that the $[(\alpha\text{-diimine})Pd(CH_3)]^+$ ion is the active species in ethylene polymerisation.

1.2.3 Chain-walking property and electronic effect of α-diimine catalysts

The success of Brookhart inspired other research groups to explore these catalytic systems. Z. Guan and coworkers exploited the chain walking property of the Pd(II) α-diimine catalyst to control polymer topology (Fig. 1.21).[60, 69, 70] Guan found pressure plays an important role on polymer topology. Linear polyethylene is formed at high pressure and dendritic polyethylene at low pressures. At high pressure, ethylene has high concentration in the polymerisation solution and hence insertion

becomes relatively fast leading to linear polyethylene. At lower ethylene pressure, chain-walking becomes increasingly competitive with the insertion. So, the catalyst can walk extensively along the polymer chain between two consecutive insertions which leads to dendritic polymer. This is a remarkable achievement as this offers a simple one-pot process to tune polymer topologies ranging from linear to hyperbranched to dendritic starting with simple existing monomers such as ethylene. Currently, hyperbranched polymers are made from condensation polymerisation of specially designed monomer where branching is introduced by the structure of the monomer.

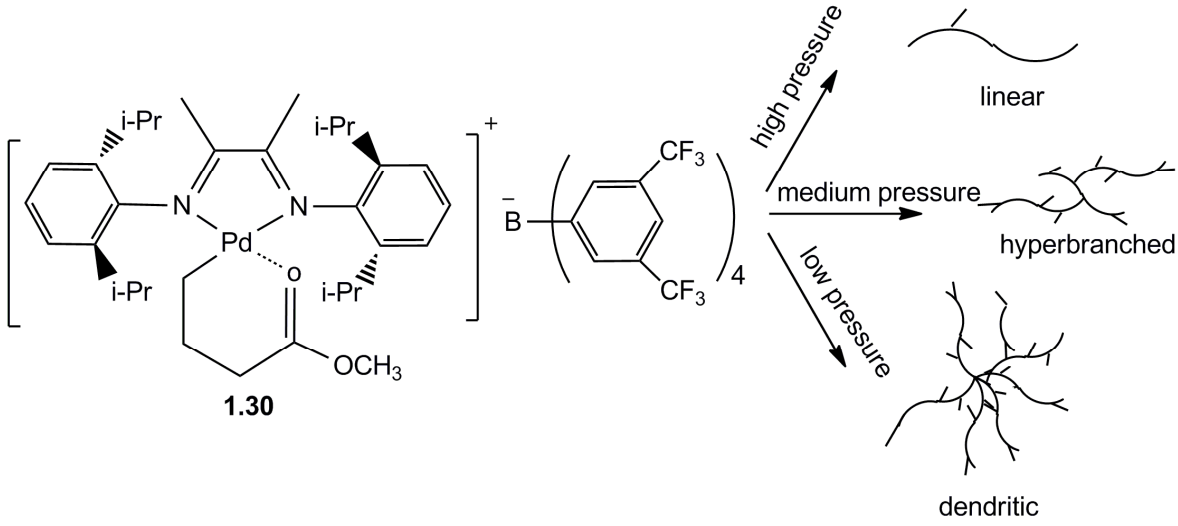

Figure 1.21. Control of polyethylene topology by exploiting the chain walking property of α-diimine catalysts.

The ligand electronic effect is known to play an important role in many catalytic systems. Brookhart α-diimine catalyst could also have influence on ligand electronic effect. However, research on α-diimine catalyst was mainly on the ligand steric tuning and not ligand electronics. Z. Guan and coworkers[71, 72] systematically studied ligand electronic effects in Brookhart α-diimine catalysts while not changing steric effect at the metal center (Fig. 1.22). Guan group introduce a range of electron donating and –withdrawing susbtituents in the *para*-aryl position on the α-diimine ligands to influence the donating ability of the ligand.

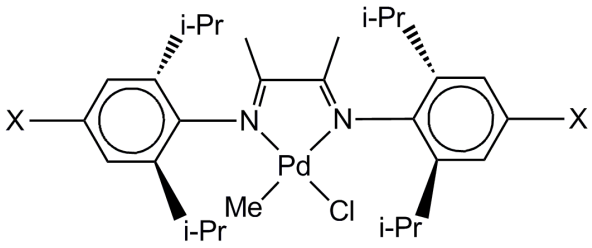

1.25a X = NO_2 **1.25e** X = Me
1.25b X = CF_3 **1.25f** X = OMe
1.25c X = Cl **1.25g** X = NMe_2
1.25d X = H

Figure 1.22. Electronic effect of Brookhart α-diimine catalyst.

These functionalised Pd(II) α-diimine catalysts have been tested for both ethylene homopolymerisation and the copolymerisation of ethylene with methyl acrylate. The following general results have been observed from this study:

1. For ethylene polymerisation, higher molecular weight is obtained with catalysts bearing more strongly electron-donating ligands.
2. The ligand electronic structure of the catalysts has showed significant effect on topology of the polyethylene. More dendritic polyethylene is formed with the catalysts bearing more strongly electron-withdrawing ligands. This means more electron-deficient catalysts are more dendritic than those made by the electron-rich catalysts. This provides another approach to control polymer branching topology.
3. For the copolymerisation of ethylene with methyl acrylate, catalysts bearing strongly electron-donating ligands are more tolerant to polar comonomers and afforded copolymers with higher incorporation of the polar comonomers. The more electron rich catalysts showed higher catalytic activity with the production of higher MW copolymer.

It is assumed that the stronger electron-donating character of the ligand in these catalysts stabilises the alkyl agnostic intermediate and inhibits β-hydride elimination and subsequent chain transfer.

1.2.4 Living polymerisation by α-diimine catalysts

Living polymerisation techniques are an important tool in the synthesis of polymers with precisely controlled molecular weight, narrow molecular weight distribution, end-functionalised polymers and well-defined block copolymers.[73-75] Living polymerisation methods allow the creation of limitless types of new materials from cheap available monomers. The term 'living polymerisation' was first introduced by Szwarc[76, 77] in 1956 because the chain ends remain active until killed and living ends are able to grow further if an additional amount of monomer is available.'*Ideally, living polymers propagate while their termination or chain-transfer are rigorously prevented'*. This is an ideal concept and can never be reached. Szwarc[78] proposed that 'living polymers *are the polymers that retain their ability to propagate for a long time and grow to a desired maximum size while their degree of termination chain transfer is still negligible'*. In other words, living polymerisation means chain-growth polymerisation that enable consecutive enchainment of monomer units without termination. In living polymerisation catalytic system each catalyst only forms one chain, whereas common alkene polymerisation catalysts can produce thousands of chains each as a result of periodic chain transfer or termination. There are seven generally accepted criteria for a living polymerisation.[74] These are: 1) polymerisation proceeds to complete monomer conversion and chain growth continues upon further monomer addition; 2) number average molecular weight (M_n) of the polymer increases linearly as a function of conversion; 3) the number of active centers remains constant for the duration of the polymerisation; 4) molecular weight can be precisely controlled through stoichiometry; 5) polymers display narrow molecular weight distributions ($M_w/M_n = 1$); 6) block copolymers can be prepared by sequential monomer addition; 7) end-functionalised polymers can be synthesised. In 1964 Bier[79] synthesised the first living polymers of α-olefins with Ziegler catalysts. Bier found that polymerisation can be interrupted for several hours after removal or consumption of monomer without diminishing the activity of the catalyst on renewed addition of monomer. Kaminsky and coworkers[80] showed living polymers of ethylene with high yield with a Ziegler catalytic system consisting of bis(cyclopentadienyl)zirconium complex, $(C_5H_5)_2Zr(CH_3)_2$ and methylaluminoxane (MAO). In 1979 Doi and coworkers[81] reported the first catalytic olefin

polymerisation system that satisfied all the requirements for a living polymerisation. The catalytic system [$V(acac)_3$] with Et_2AlCl produced partially syndiotactic polypropylenes with extremely narrow molecular weight distributions (M_w/M_n = 1.05-1.20) with M_n = 100,000 g mol^{-1}. This catalytic system exhibits living character only at very low temperature (-78 ºC).

Although a large number of living olefin polymerisation catalysts have been reported in the literature to produce living polymers of narrow molecular weight distribution at low temperature,[74] until very recently there existed a comparative lack of living olefin polymerisation systems that can produce living polymers at near ambient temperature. This is because alkene polymerisation catalysts often undergo irreversible chain transfer to metal alkyls and β-elimination reactions that result in the initiation of new polymer chains by the catalyst. Only recently Brookhart reported the first true living polymerisation catalyst based on nickel and palladium α-diimine that can produce high molecular weight polymer of ethylene and α-olefins with very narrow molar mass distributions at near ambient temperature (0 to -10 ºC) (Fig. 1.23).[82-86] For example, propylene polymerisation with the nickel catalyst, [ArN=C(R)-C(R)=NAr]$NiBr_2$ (Ar = 2,6-(*i*-Pr)$_2C_6H_3$), **(1.24f, 1.24g)** activated by MMAO (MMAO = modified methylaluminoxane containing 25% isobutyl aluminoxane) at -10 ºC at a pressure of 1bar produces polypropylene (Mn = 161000) with Mw/Mn = 1.13 (Fig. 1.24). The polymerisation of 1-hexene (0.8M) by the same catalytic system at -10 ºC yields poly(1-hexene) (Mn = 44000) with Mw/Mn = 1.09. The narrow molecular weight distribution indicates the living polymerisation feature of this system.

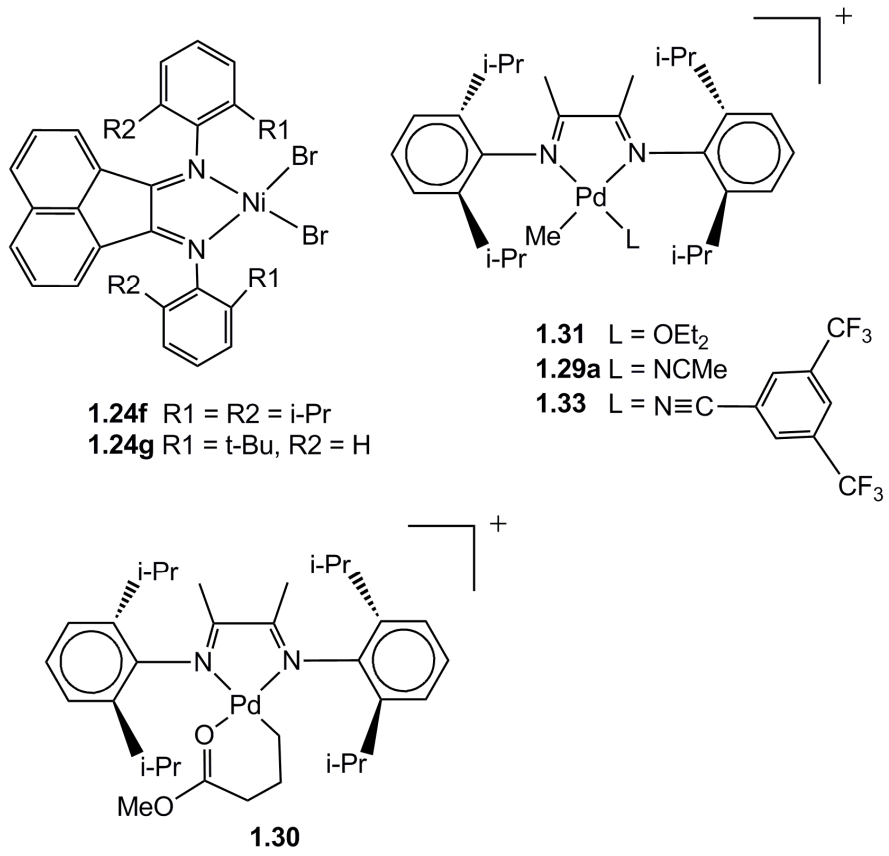

Figure 1.23. Ni and Pd α-diimine catalysts for living polymerisation.

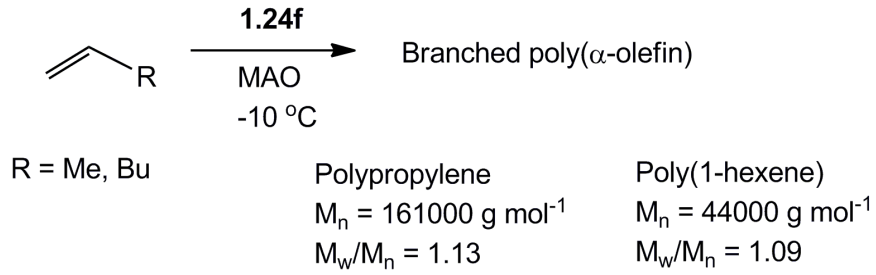

Figure 1.24. Living polymerisation of α-olefins with a nickel diimine catalyst system.

Palladium diimine catalyst **1.30** (Fig. 1.23) shows living ethylene polymerisation at 5 ºC and 27 bar of ethylene. The narrow molecular weight distribution (Mw/Mn < 1.08) and linear increase in Mn with polymerisation time shows the proof of the living system. This system produces amorphous polyethylene. The acetonitrile adduct of Pd, **1.29a** polymerises 1-hexene (0.8M) at 0 ºC in a living polymerisation manner to produce poly(1-hexene) with narrow molecular weight distribution. However, the acetonitrile ligated catalysts **1.29a and 1.33** (Fig. 1.23) produce low molecular weight poly(1-hexene), 30000 and 14000 respectively. The lower molecular weight of the polymer made by nitrile catalysts is believed to be due to the ability of the nitrile to compete with 1-hexene for coordination at palladium active site.

Living features of active olefin polymerisation catalysts depend on temperature. At higher temperature, living features of active olefin polymerisation catalysts are usually lost due to increase chain transfer. It is highly desirable to develop more robust living polymerisation catalysts that can operate at higher temperature. Zhibin Guan[87] recently has developed the first late transition metal catalysed living polymerisation of propylene and hexene at elevated temperature (25 to 50 ºC) using cyclophane-based nickel catalyst activated by methylaluminoxane (MMAO) (Fig. 1.25). In the case of propylene polymerisation, this catalyst produced polypropylene with molecular weight distributions (MWD = Mw/Mn) in the range of 1.06-1.16. The narrow molecular weight distribution suggests living polymerisation features at elevated temperature. There are very few examples of living polymerisation of ethylene or α-olefin above room temperature by early transition metal catalysts.[88, 89]

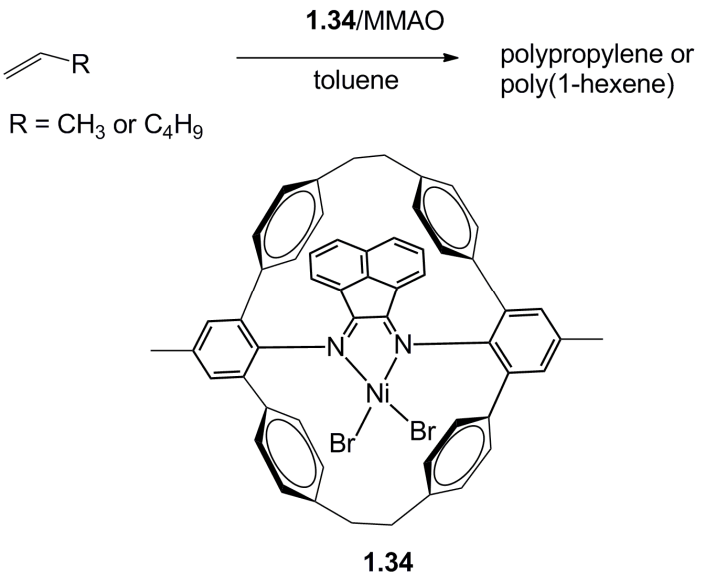

Figure 1.25. Cyclophane-based nickel catalyst for living polymerisation of propylene and 1-hexene.

1.2.5 Allyl-nickel-diimine catalysts

The allyl-transition metal complexes are interesting for homogeneous catalysis. The π-allylnickel halide, $(\pi\text{-}C_3H_5NiX)_2$ (X = Cl, Br) is a dimeric complex and acts as a catalyst precursor for propylene dimerisation in presence of alkylaluminum dihalide or aluminium trihalide in a polar solvent like DCM or chlorobenzene at low temperature (-30 to -40 ºC) to produce dimers consisting of 80% 2-methylpentenes and 20% n-hexenes. The π-allylnickel halide also polymerises butadiene to polybutadiene when activated with Lewis acids.[90] The allyl ligand-based alternative Brookhart type catalyst, the $[\eta^3$-methallyl-nickel-diimine$]PF_6$ complex (Fig. 1.26) has been shown to be active for ethylene polymerisation using diethylaluminium chloride (DEAC) as a cocatalyst under mild reaction conditions with temperatures between -10 ºC and 25 ºC and a pressure from 1 to 15 bar.[91, 92]

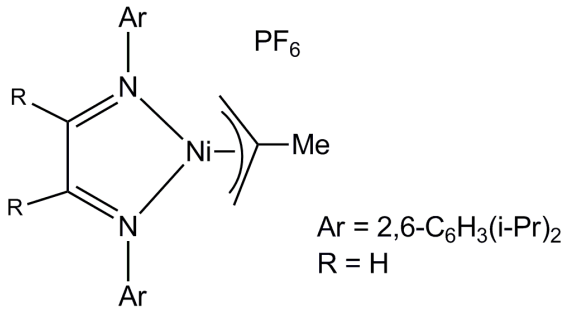

1.35

Figure 1.26. The η^3-methallyl-nickel-diimine complex as catalyst precursor for ethylene polymerisation.

This catalytic system replaces expensive MAO co-catalyst and expensive counter anions such as $[B(3,5\text{-}(CF_3)_2C_6H_3)_4]^-$ (BAF). The solvent has important effects on the polymerisation activity. Higher activity of the catalyst is obtained by changing the solvent from nonpolar (toluene) to polar (chlorobenzene) solvent. The higher yield of polymer in chlorobenzene is probably due to higher solubility of polymer in this solvent which prevents encapsulation of the catalytic active sites. The activity of the catalyst is also found to be affected by temperature. The activity increases from 27.8 kg of polymer/(mol Ni. h) (at -10 ºC) up to 278 kg of polymer/(mol Ni. h) (at 20 ºC). However, the catalyst is deactivated above 30 ºC. The [η^3-methallyl-nickel-diimine]PF_6 complex has been synthesised by reacting bis[η^3-2-methallyl-nickel bromide] with diimine ligand and $TlPF_6$.[91]

Alex S. Ionkin and coworkers[93] have synthesised the *para*- and *meta*-trimethylsilylphenyl *ortho*-substituted N,N-phenyl α-diimine ligand based η^3-allylNi complex for ethylene polymerisation (Fig. 1.27). The trimethylsilyl group has been introduced to provide steric bulk in the axial sites of the square-planar nickel complex and thus retard the rate of chain transfer. The η^3-allyl(α-diimine)Ni complex has been made by reacting π-allylnickel chloride dimer, α-diimine ligand and sodium tetrakis[3,5-bis(trifluoromethyl)phenyl]borate (NaBAF) or silver hexafluoro-antimonate ($AgSbF_6$). The corresponding complex could not be achieved by reacting this bulky ligand with $(DME)NiBr_2$. The η^3-allyl(α-diimine)Ni complex is active in ethylene polymerisation when activated with $B(C_6F_5)_3$ in the presence of ethylene.

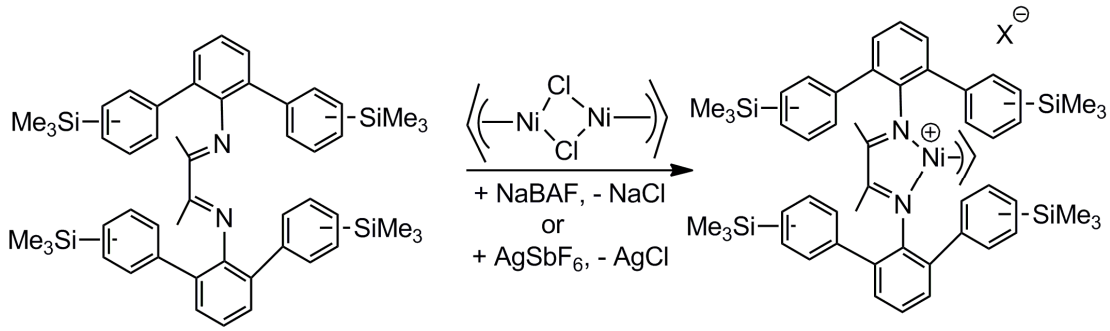

1.36a R = 4-Me_3Si
1.36b R = 3-Me_3Si

1.37a R = 4-Me_3Si, X = BAF
1.37b R = 4-Me_3Si, X = SbF_6
1.37c R = 3-Me_3Si, X = BAF
1.37d R = 3-Me_3Si, X = SbF_6

Figure 1.27. η^3-allyl(α-diimine)nickel(II) complex bearing trimethylsilyl groups for ethylene polymerisation.

1.2.6 Deactivation of α-diimine catalysts

Brookhart cationic Ni(II) and Pd(II) α-diimine catalysts are prone to deactivate under comparatively mild conditions. These catalysts suffer from relatively low thermal stability. The catalysts decompose rapidly and molecular weight reduces drastically above 50 ºC. The cationic ether adducts are found to undergo decomposition via C-H activation of the ortho aryl substituents to give a six-membered palladacycle and methane (Fig. 1.28). This intramolecular C-H activation requires one of the ligand aryl rings to rotate into the square plane of the complex. By increasing the steric bulk of the ligand is therefore expected to make this intramolecular C-H activation process less favorable. The C-H activation process should become more facile upon decreasing the steric bulk of the ligand.[52]

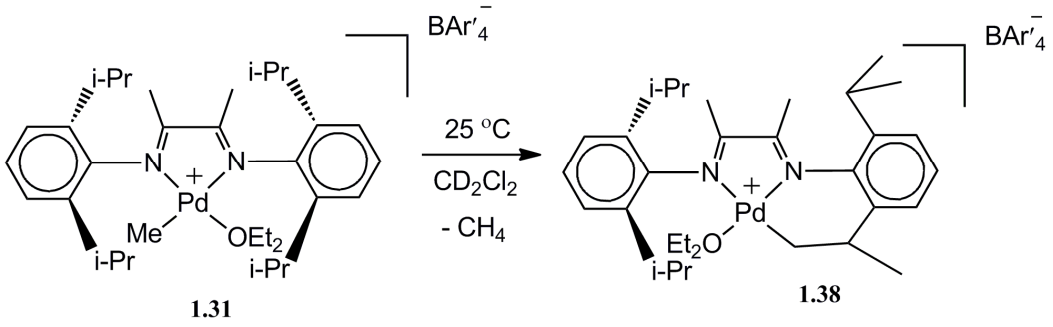

1.31 1.38

Figure 1.28. Decomposition of Brookhart cationic ether adducts via C-H activation.

1.2.7 Nickel and palladium based salicylaldimine catalysts

As mentioned before, Grubbs[33, 34] and Mecking[35] further developed the field of late transition metal polymerisation catalysts. Grubbs and coworkers[33, 34] synthesised neutral nickel(II) complexes using salicylaldimine ligand systems which allowed the investigation of steric effects on the metal centre (Fig. 1.29). The activity of this catalyst is strongly related to the steric bulk of the substituents on the aryl ring. The salicylaldimine ligands, **1.40a-g** can be prepared by condensation of the corresponding salicylaldehydes, **1.39** and 2,6-diisopropylaniline (Fig. 1.29). The deprotonation of the salicylaldimine ligands by NaH in THF results in the sodium salt **1.41a-g**. Reaction of the sodium salts **1.41a-g** with *trans*-[NiCl(Ph)(PPh_3)$_2$] provides the correspondoing salicylaldimine Ni(II) complexes **1.42a-g.** These complexes are active ethylene polymerisation catalysts under mild conditions in the presence of a phosphine scavenger such as Ni(COD)$_2$ or B(C_6F_5)$_3$. The phosphine scavengers bind PPh_3 more strongly than the Ni(II) catalysts and thus effectively remove phosphine and create a vacant site for alkene to coordinate. The introduction of bulky substituents in the 3-position of the salicylaldiminato ring was found to enhance the activity of the catalyst and also produce higher molecular weight polyethylene with Mn values of 11 400 to 54 000. The salicylaldimine Ni(II) complexes produces linear, low-branched polyethylene contrasting with the highly branched materials obtained with the Brookhart cationic Ni(II) and Pd(II) catalysts. Introduction of the electron-withdrawing substituent in the para position of the oxygen-donor in neutral salicylaldimine nickel(II) complex increases catalytic

activity substantially.[33] The electron deficient system such as **1.42g** is the most active catalyst, whereas the catalytic activity diminishes for electron-rich complexes such as **1.42f** (Fig. 1.29).

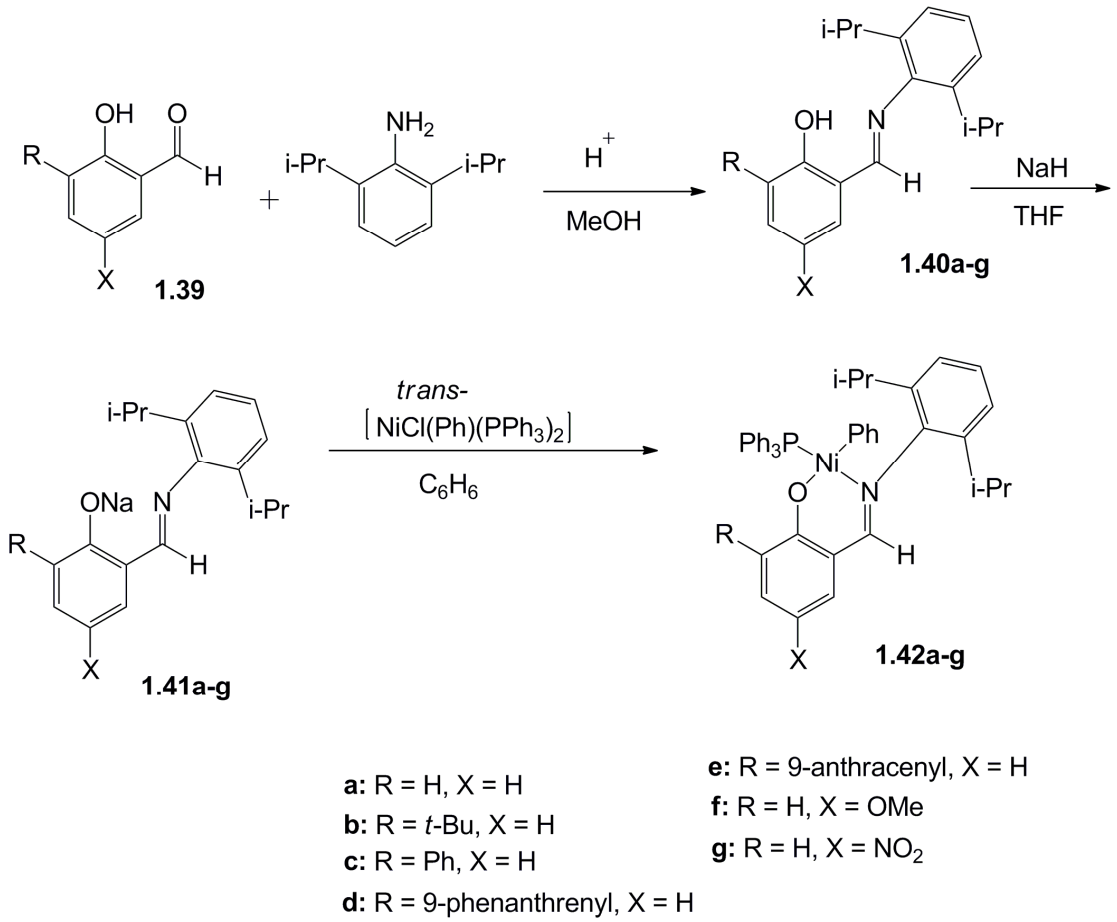

Figure 1.29. Synthesis of Grubbs Ni(II) salicylaldimine catalyst.

Recently it has been found that ligand size has influence on catalyst stability and the ligand framework must be sufficiently bulky to allow formation of a catalytically active mono-ligated complex.[94]

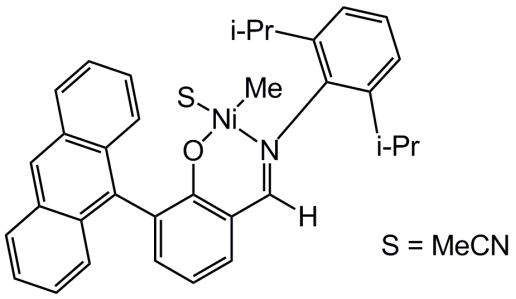

1.43

Figure 1.30. Grubbs phosphine-free highly active polyethylene catalyst.

Grubbs synthesised a phosphine-free highly active mono-ligated Ni complex (**1.43**) by introducing two different bulky groups in one ligand (Fig. 1.30). This hinders the coordination of two chelating ligands on the same metal center. This highly active catalyst can produce polyethylene up to 6 x 10^3 Kg PE mol^{-1} h^{-1} (10 ºC, 17 bar of ethylene).[94]

Mecking and coworkers[35] studied electronic effects in the neutral salicylaldimine Ni(II) complexes by introducing electron-withdrawing substituents in the aryl ring (Fig. 1.31). It has been found that substituents R, R' have dramatic effects on branching, and thus crystallinity, and on polymer molecular weight. Using CF_3 in both R and R' positions, a semicrystaline, stiff polymer of 50% crystallinity is obtained. On the other hand complexes **1.44b** and **1.44c** afford polyethylene with a high degree of branching and low crystallinity. Mostly, amorphous materials are obtained with **1.44d** and **1.44e** substituted complexes (Fig. 1.31).

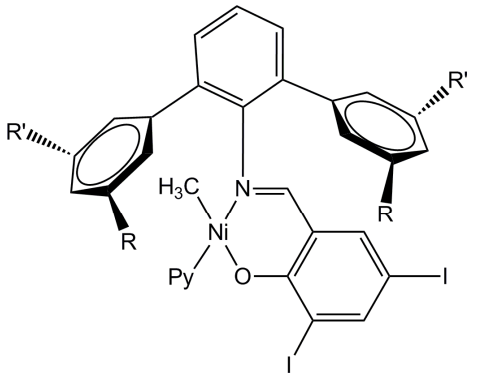

	R	R'
a:	CF_3	CF_3
b:	NO_2	H
c:	H	H
d:	CH_3	CH_3
e:	OCH_3	OCH_3

1.44a-e

Figure 1.31. Mecking's neutral Ni(II) salicylaldimine catalysts.

1.2.8 Copolymerisation of olefins and polar monomers by late transition metal α-diimine catalysts

It has been mentioned earlier that the the highly oxophilic nature of early transition metal-based catalysts make them incompatible in the copolymerisation of ethylene with polar monomers and as a consequence, ethylene-acrylate or ethylene-vinyl acetate copolymers are produced commercially by free radical polymerisation at a high pressure. Coordination copolymerisation of olefins with polar monomers remains a challenging and industrially important goal. Incorporation of polar groups into the hydrocarbon polymers (such as polyethylene, polypropylene and polystyrene) is important not only because it provides new properties in the polymer but also polar groups control other important properties such as toughness, adhesion and surface properties (paintability, printability, etc.). Polar groups also influence material properties of the polymer (such as solvent resistance, miscibility with other polymers and rheological properties) and also product performance (such as hardness, gloss etc.).[95] As the late transition metals are less oxophilic and more tolerant of the oxygen functionalities in the monomer, late transition metals in recent years have attracted attention for the copolymerisation of hydrocarbon monomers with readily available polar monomers such as acrylates, vinyl ethers and vinyl acetate. Due to higher electronegativity and low oxidation state, late transition metals form covalent bond with soft ligands (polarisable ligands, such as P and S donors).

Brookhart reported the first metal-catalysed copolymerisation of ethylene with acrylate monomer (methyl acrylate, *tert*-butyl acrylate) which yields high molecular weight polymers.[53, 96] The copolymerisation catalyst is a cationic palladium complex with bulky substituted α-diimine ligands. The palladium ether adduct **1.31** or palladium chelate complex **1.30** catalyses copolymerisation of ethylene or propylene with methyl acrylate (MA) at a pressure of 1-6 bar and 25 – 35 ºC (Fig. 1.32).

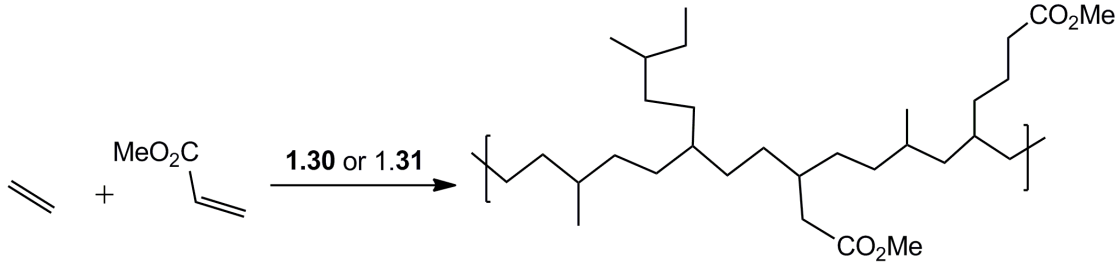

Figure 1.32. Copolymerisation of ethylene with methyl acrylate catalysed by palladium ether adduct 1.31 or palladium chelate complex 1.30.

The high molecular weight random copolymers produced are amorphous, highly branched with 100 branches/1000 carbon atoms with ester groups at the end of the branches. The T_g values of these polymers are in the range of -67 to -77 ºC. In Pd α-diimine catalysed copolymerisation of ethylene and methyl acrylate (MA), the MA incorporation ratio increased with increasing concentration of MA in the reaction mixture.

During the copolymerisation, migratory insertion of acrylate into the Pd-alkyl bond occurs regioselectively in a 2,1-insertion mode and rearrangement leads to the formation of a stable six-membered chelate complex (Fig. 1.33). This chelate complex is the catalyst resting state. Further chain growth occurs with the coordination and insertion of ethylene. The migratory insertion of the electron deficient methyl acrylate (MA) into the Pd-carbon bond occurs more rapidly than the insertion of the nonpolar olefins (ethylene). However, the electron deficient MA binds more weakly to the electrophilic metal center than ethylene. This results in

predominant incorporation of ethylene into the copolymers at equal molar concentrations of the comonomers in the copolymerisation reaction.

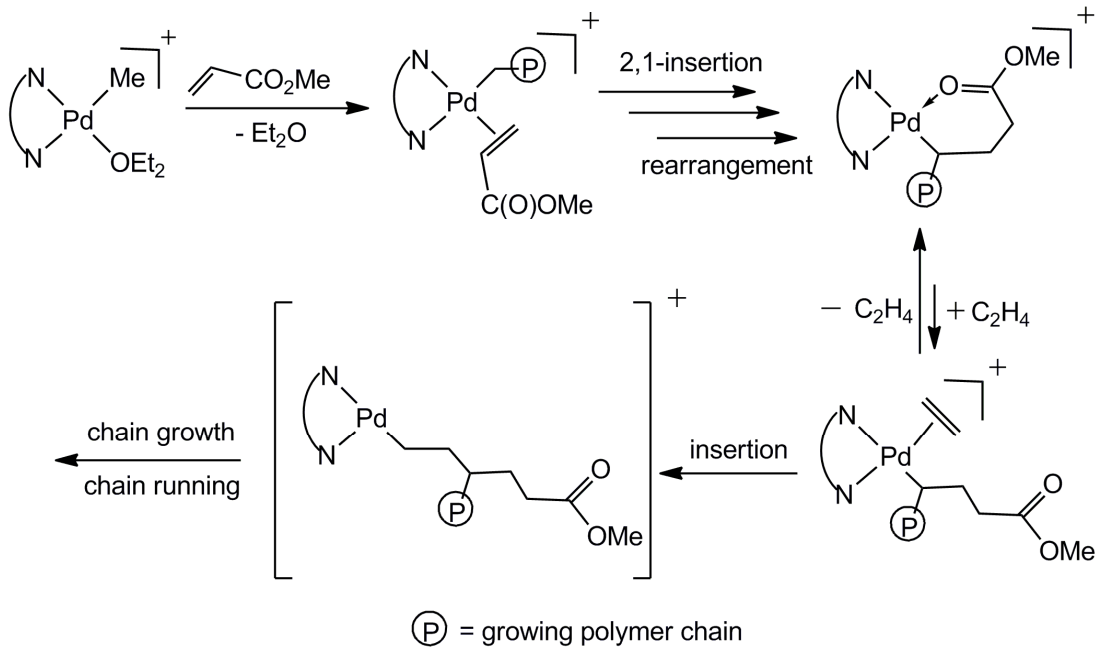

Figure 1.33. Mechanism of copolymerisation of ethylene with functionalised vinyl monomers.

Brookhart diimine catalysts are also effective in the copolymerisation of α-olefins such as propylene and 1-hexene with methyl acrylate (MA). However, the α-olefin-acrylate copolymerisation rate is lower compared to the ethylene-acrylate copolymerisation rate, due to the displacement of the chelating carbonyl group being less effective with α-olefins. Moreover, the lower rate of migratory insertion of α-olefins in comparison to ethylene results in a lower polymerisation activity. Surprisingly, Pd α-diimine catalysts are inactive to the homopolymerisation of methyl acrylate (MA). The Pd α-diimine catalyst decomposes in the presence of an excess amount of MA in the absence of nonpolar olefins.

Johnson and coworkers[97, 98] reported a (α-diimine)Ni allyl catalyst for the copolymerisation of ethylene with MA (Fig. 1.34). Although the copolymerisation can be carried out without the addition of cocatalyst, the addition of a Lewis acid

such as $B(C_6F_5)_3$ increases productivity. This catalyst required elevated temperature (80 ºC and above) and pressure (34 bar and above) for its high activity. The copolymer obtained with this catalyst is moderately linear (30 methyl per 1000 carbons) to highly branched with predominantly in-chain acrylate incorporation. The obtained polymer is low molecular weight with low incorporation of polar monomers (<1.4 mol %).

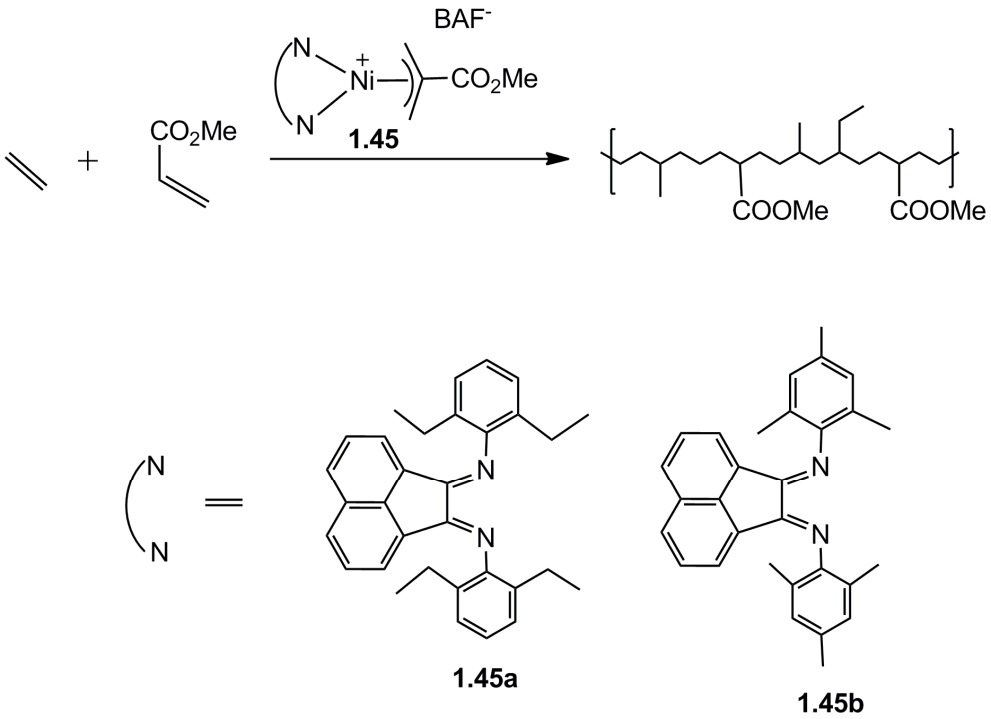

Figure 1.34. Copolymerisation of ethylene with MA by Ni α-diimine catalyst.

Guan and coworkers[99] have found that a cyclic cyclophane-based Pd(II) catalyst is much more efficient in incorporating polar comonomers (acrylate) in copolymers with ethylene than its acyclic α-diimine Pd(II) analogue (Fig. 1.35).

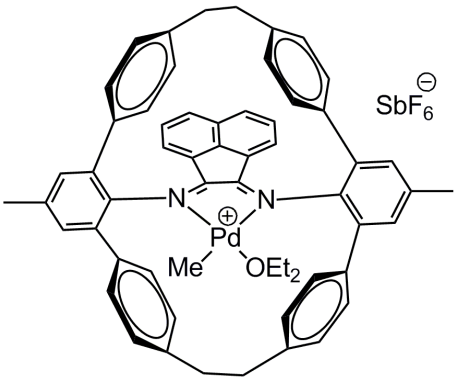

1.46

Figure 1.35. Cyclic cyclophane-based Pd(II) catalyst for copolymerisation of ethylene with functionalised vinyl monomers (acrylate).

The structure of the cyclophane ligand, especially its ability to shield the axial binding sites, significantly reduces the rate of comonomer exchange and thereby suppresses the catalyst's ability to discriminate between monomers for binding and thus enhances the incorporation for the polar olefins. The cyclophane-based Pd(II) catalyst afforded copolymer of over 20% MA, whereas α-diimine Pd(II) catalyst analogue incorporate only 4% MA.

1.2.9 Heterogenisation of α-diimine system

Effective immobilisation of homogeneous catalysts on a support material is an essential prerequisite for their large-scale industrial polyolefin production in the existing slurry or gas-phase polymerisation processes. Without heterogenisation of homogeneous catalysts new polyolefins produced by homogeneous catalysts could not be produced at all on an industrial scale.[100, 101]

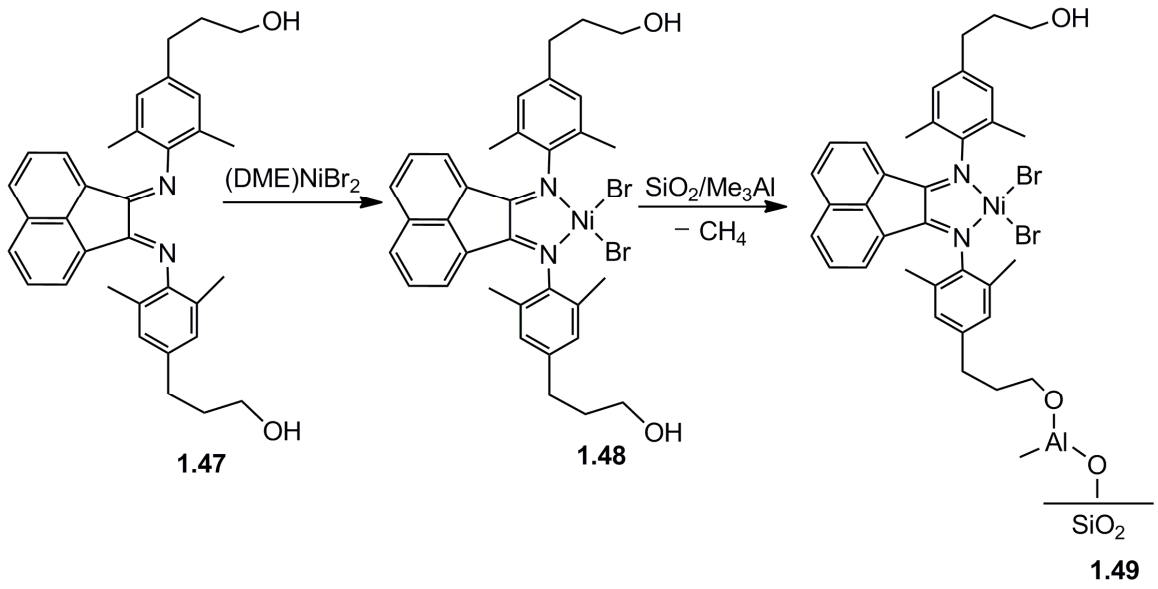

1.47 **1.48** **1.49**

Figure 1.36. Immobilisation of Ni(II) diimine catalysts.

Supported Ni(II) α-diimine catalysts have shown high activity in ethylene polymerisation.[102, 103] When amino or hydroxy functionalised α-diimine Ni(II) complexes are reacted with trimethylaluminum (TMA)-treated silica, Ni(II) α-diimine complexes become covalently attached to the silica through the functional groups of the ligand backbone (Fig. 1.36). Upon activation of these precatalysts in a slurry phase polymerisation with an inexpensive cocatalyst such as an alkylaluminum halide, this system afforded up to 820 kg of PE/g of Ni in 2h at 60 ºC and 10 bar of ethylene, equivalent to an activity of around 2330 kg/mol. bar. h. The narrow polydispersity (around 3.5) indicates that the single-site characteristics of the catalysts are unaffected by immobilisation on the support. Immobilised catalysts show nearly the same productivity per gram of nickel as in the homogeneous system (Fig. 1.37).

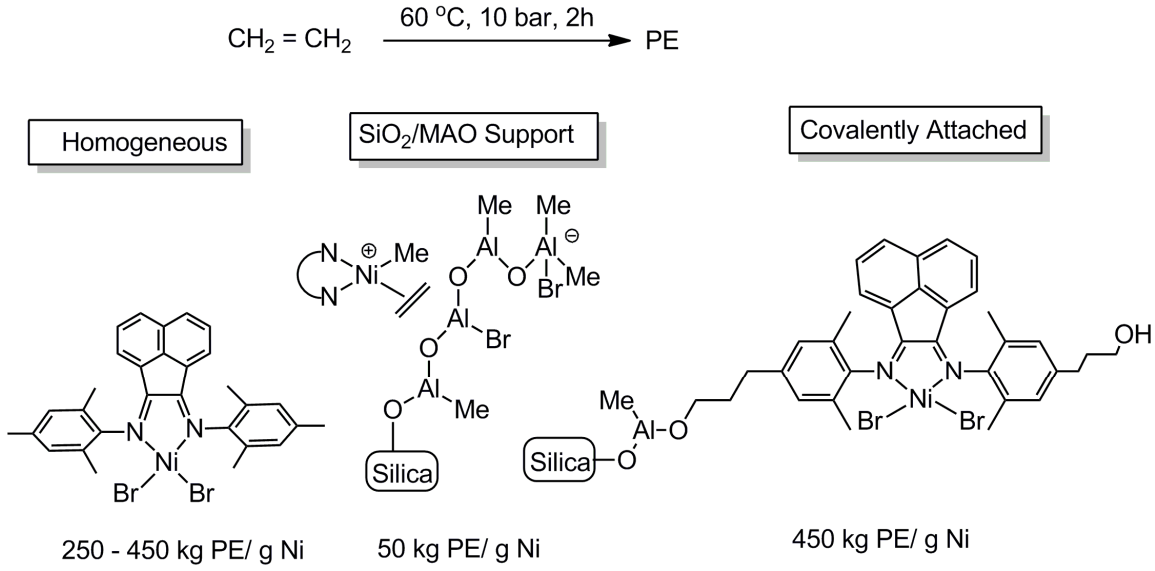

Figure 1.37. Comparison of homogeneous vs. heterogenised diimine nickel(II) catalyst.

Chadwick and coworkers[104] discovered a simple and effective support, $MgCl_2/AlR_n(OEt)_{3-n}$, for the immobilisation and activation of Ni(II) α-diimine complexes which do not require any functionalisation of the ligands for immobilisation. They carried out immobilisation by mixing the support with a toluene solution of the Ni(II) diimine complexes and reacting at 50 ºC for 4 hours. Activation of the precursor catalyst by Al-$^{i}Bu_3$ in light petroleum at 50 ºC and 5 bar of ethylene pressure afforded a highly active catalyst with activity 11416 kg/mol. bar. h. The obtained polymers are free-flowing powders. All these achievements suggest the possibility of commercial production of polyethylene with Brookhart Ni(II) diimine catalysts.

1.3 Zwitterionic catalytic systems for olefin polymerisation

Traditional homogeneous olefin polymerisation catalyst consists of two components. These are a neutral metallocene precursor (metallocene dichloride or dimethyl derivatives e.g. $Cp_2M(CH_3)_2$) and an activator such as methylaluminoxane (MAO), Brønsted acid ($R_3NH^+BAr_4^-$), Lewis acid ($B(C_6F_5)_3$), or other suitable alkyl group

activator such as triphenylcarbenium salt ($Ph_3C^+BAr_4^-$). The reaction of these two components generates ion-pairs, [$Cp_2MCH_3^+/CH_3MAO^-$] and weak coordination of the counter anion to the active site can not be ruled out.[105-107] For example, anions such as BPh_4^- and $B(C_6H_4F)_4^-$ are found to coordinate to cationic d^0 metal centers and compete with olefin substrate for coordination site required for olefin to coordinate.[105] This will eventually lower the catalytic activity.

This ion pairing drawback of traditional homogeneous Ziegler-Natta olefin polymerisation catalyst can be overcome by either using 'noncoordinating' counter anions (BF_4^-, PF_6^-) while maintaining a stable catalyst species or with zwitterionic[108-122] catalytic systems where the counter ion is affixed covalently to the ancillary or reactive ligand structure of the molecule, and this will provide an overall neutral molecule which will not require any cocatalyst for activation. The zwitterionic catalytic system seems to be more promising than the other concept because the classic 'noncoordinating' anions (BF_4^-, PF_6^-) are more prone to be degraded by the metallocene cation.[108, 123]

Zwitterionic catalysts offer a range of advantages over the traditional two-component catalytic systems. For example:
(i) stable zwitterions are pre-activated, well-defined single component catalysts which do not require Lewis acid co-catalysts for activation;
(ii) eliminates the possibility of anions coordinating to the active site;
(iii) zwitterionic complexes should exhibit higher solubilities in the non-polar solvents in which olefin polymerisation processes are performed;
(iv) due to the less oxophilic nature of LTM, ethylene co-polymerisation with polar co-monomers could be performed using late transition metal zwitterionic catalysts.

Zwitterionic catalysts can not only produce olefin polymers but also produce olefin dimers selectively. Shell developed the zwitterionic zirconocene alkyl complex **1.51**(Fig. 1.38) which can act as a single component catalyst for 1-pentene dimerisation to produce 2-propyl-1-heptene with >99% selectivity.[124]

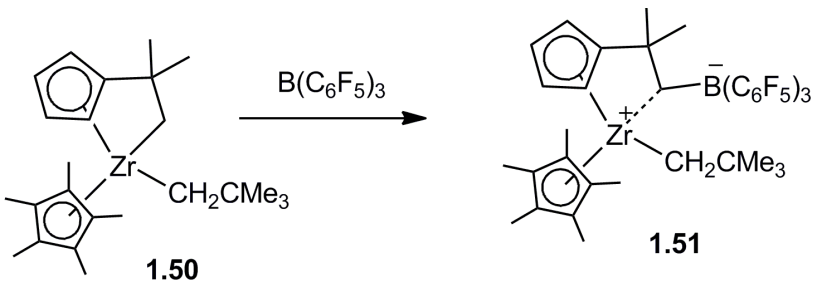

Figure 1.38. Zwitterionic zirconocene alkyl complex 1.51 for selective olefin dimerisation.

As depicted in Figure 1.39, in a zwitterionic system the active cationic metal center [L_nM^+] can be connected with a suitable anion component [-X-] by means of a hydrocarbon chain. In its open form, this system will act as a single component Ziegler-Natta catalyst system. Coordination of an alkene to the metal centre and subsequent insertion into the metal-carbon bond will eventually form the polymer. In the absence of an alkene, given sufficient flexibility in the link an internal ion pair will be formed which will protect the active catalyst in an equilibrium situation.[115]

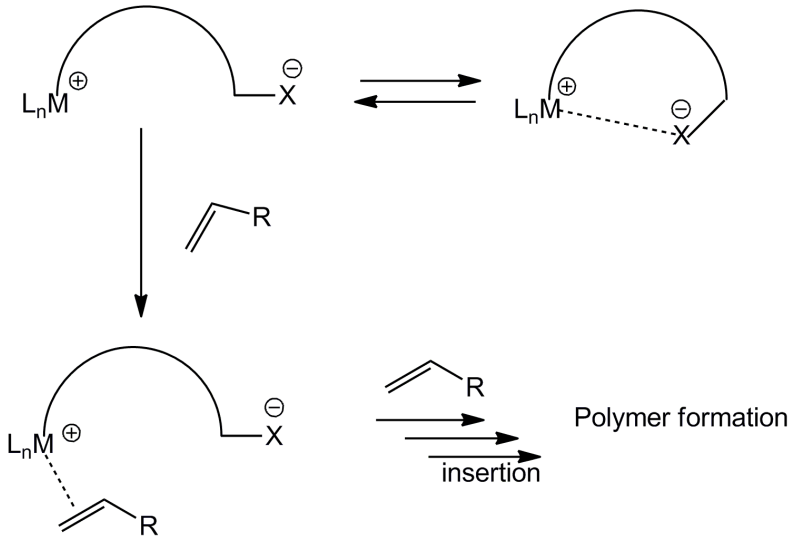

Figure 1.39. Zwitterionic polymerisation.

Both early and late transition metal based zwitterionic catalysts are known for ethylene polymerisation.

1.3.1 Zwitterionic catalysts by early transition metals

On the basis of the location of the counter ions in the molecular structure, zwitterionic metallocene catalysts can be classified as three types (Fig. 1.40). These are:

1. girdle zwitterions: counterion is attached to the alkyl group in the reactive girdle;
2. ring zwitterions: counterion is attached to the cyclopentadienyl ring;
3. bridge zwitterions: counterion is attached into the backbone linker of an ansa-metallocene.

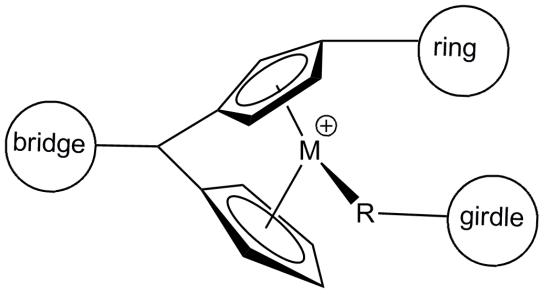

Figure 1.40. Three types of zwitterionic metallocene catalysts.

1. Girdle zwitterions

The first zwitterionic metallocence catalyst, Cp^*_2Zr-(+)-(m-C_6H_4)-B(-)Ph_3 was of the girdle type discovered by Hlatky and Turner (Fig. 1.41).[108] The reaction between $Cp^*_2ZrMe_2$ (where, Cp* = C_5Me_5) and [n-Bu_3NH][BPh_4] first produces a non-zwitterionic mono-methyl cation which subsequently reacts with the tetraphenylborate anion to form the girdle zwitterions Cp^*_2Zr-(+)-(m-C_6H_4)-B(-)Ph_3. The driving force for the formation of this zwitterion is not only the formation of stronger Zr-C(phenyl) bond, but also extra stabilization provided by an ortho C-H agostic interaction. This complex acts as an active catalyst which produce linear polyethylene under mild condition (6 bar ethylene and 80 ºC) with an activity of 375 g PE/mmol Zr. h. atm).[108]

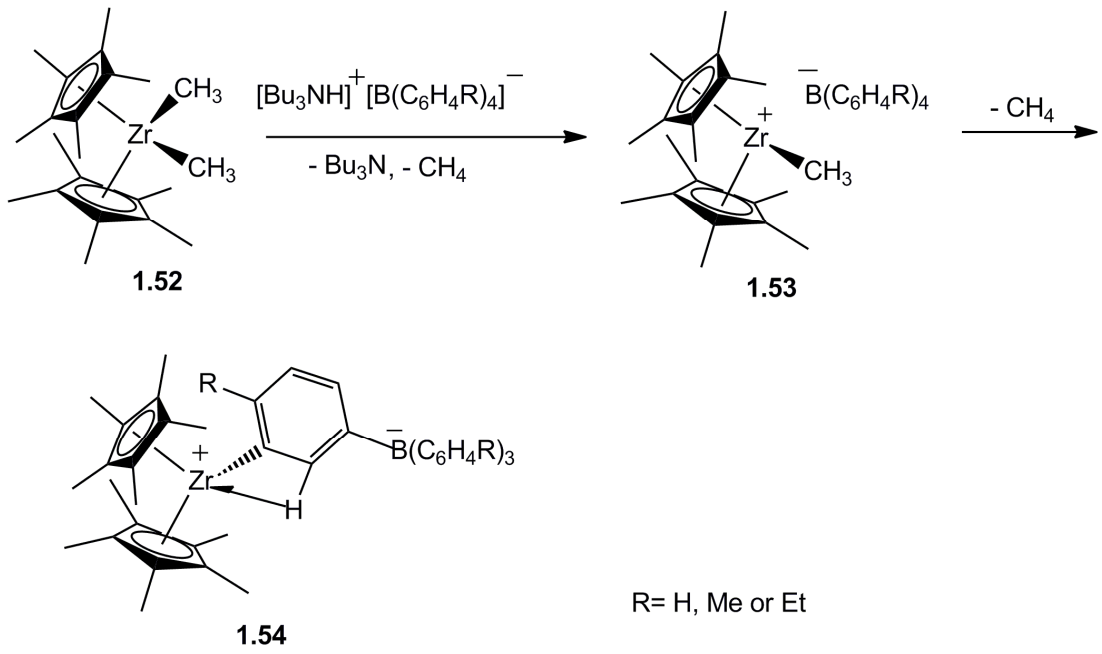

Figure 1.41. Hlatky's first zwitterionic polymerisation catalyst.

Marks and co-workers[125] synthesised another girdle-type zwitterionic complex, $Cp_2ZrMe(\mu\text{-}Me)B(C_6F_5)_3$ by reacting zirconocene dimethyls with $B(C_6F_5)_3$ (where, Cp = η^5-C_5H_5, η^5-1,2-$(CH_3)_2C_5H_3$, η^5-$(CH_3)_5C_5$) (Fig. 1.42).

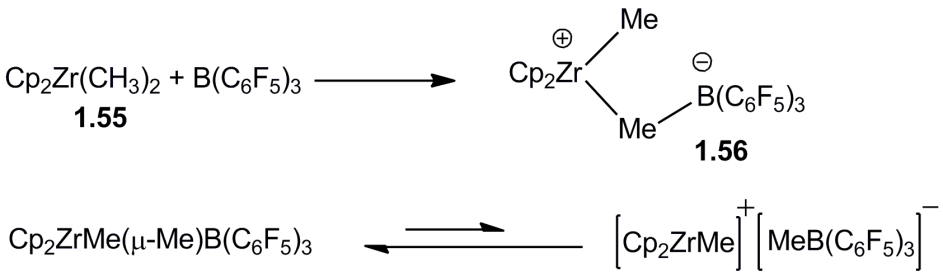

Figure 1.42. Marks' girdle type zwitterions.

In this system, the dissociation equilibrium must be established before alkene polymerisation can take place and the equilibrium is prone to shift to the left hand side. The anion, $[MeB(C_6F_5)_3]^-$ acts as a strongly coordinating anion.[106, 125] Polyethylene produced from their complex is highly linear with molecular weight (Mw = 124000, Mn = 61200) with an activity of 4.5 x 10^6 g of polyethylene (mol of Zr)$^{-1}$ h^{-1} atm^{-1} at a temperature of 25 ºC and 1 bar pressure.

Erker and co-workers[126-128] further developed the concept of girdle-type zwitterionic catalysts by synthesizing a metallocene-borate-betaine system where the cationic and anionic parts are combined into a neutral molecule retaining the catalytic reactivity of the essential alkylmetallocene cation deriving from [$Cp_2Zr(\eta^4$-butadiene)] (**1.57**) and $B(C_6F_5)_3$ (Fig. 1.43). The reaction between (butadiene)zirconocene and tris(pentafluorophenyl)-borane first produces a cationic distorted π-allyl product. The allyl product is stabilised due to the weak coordination of an ortho-fluoro substituent to the zirconium. Under the polymerisation conditions (20 ºC) the fluoride bridge is easily opened which results in a betaine species that contains a very electrophilic zirconium center, and eventually it can readily coordinate and insert α-olefin. The anionic group is thus located at the end of the growing polymer chain. The activity of this catalyst is 135 g polyethylene per mmol [Zr] per hour at 20 ºC in toluene. This complex also polymerises propylene. Unfortunately, the girdle-type zwitterions are short lived under catalytic conditions. After several insertions termination occurs due to β-hydrogen elimination leading to a conventional, non-zwitterionic active site.

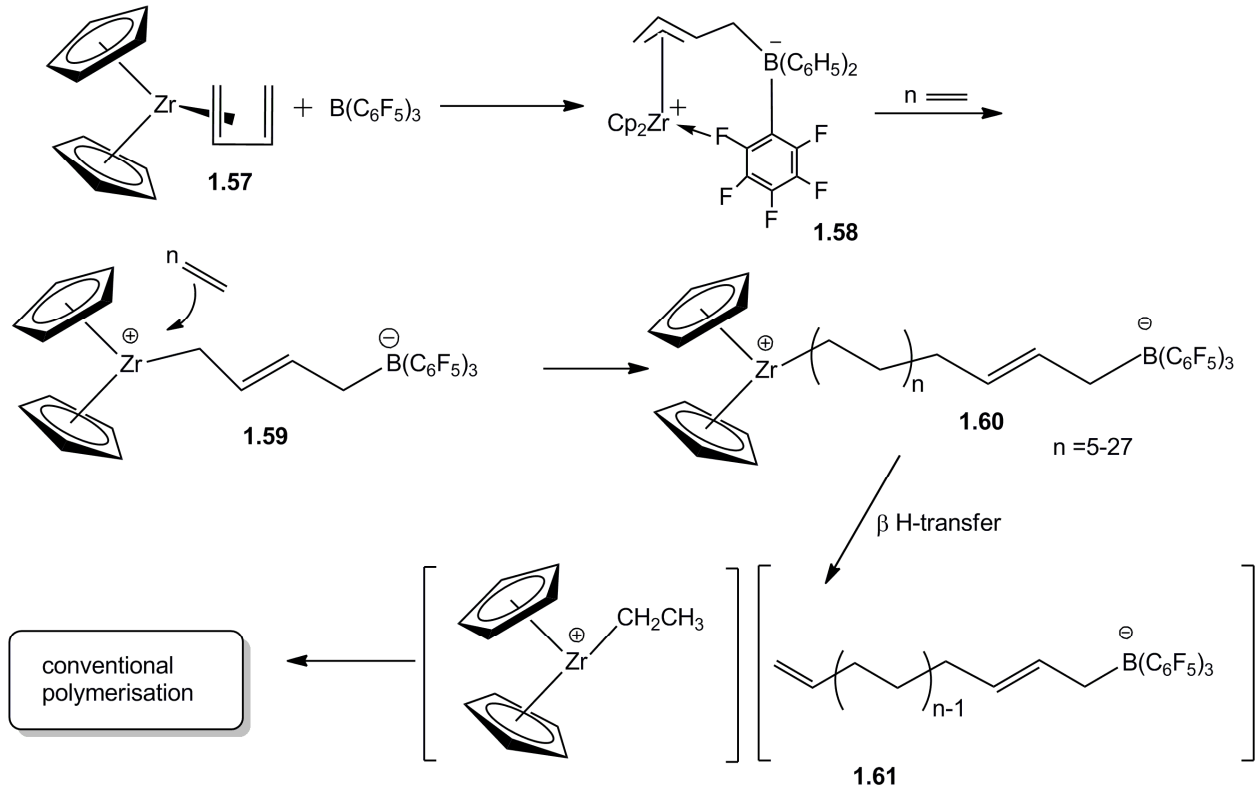

Figure 1.43. Erker's girdle type zwitterionic catalyst.

2. Ring zwitterions

Ring-type zwitterions are much more promising than girdle-type zwitterions as the zwitterionic property of the catalysts remain throughout the polymerisation process. Bochmann and coworkers[119] synthesised a ring zwitterion precatalyst in which a cyclopentadienyl ligand carries an anionic tris(pentafluorophenyl)borato substituent (Fig. 1.45). The anionic substituent does not coordinate to the metal.

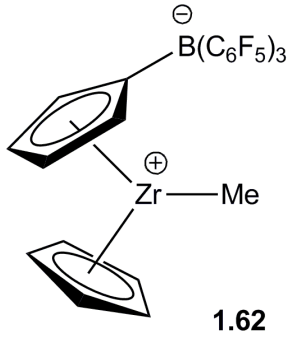

1.62

Figure 1.44. Ring zwitterionic catalyst.

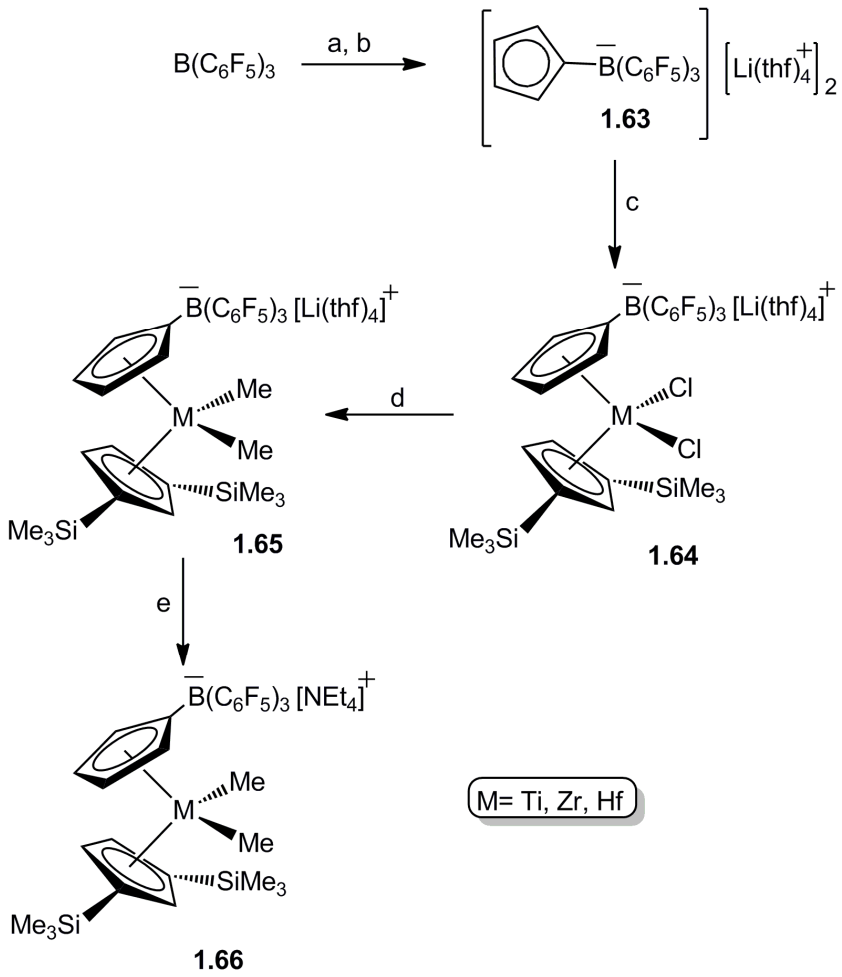

Figure 1.45. Synthesis of Bochmann's ring zwitterionic catalyst. a) C_5H_5Li in THF; b) BuLi; c) [{$C_5H_3(SiMe_3)_2$}MCl_3]; d) 2 MeLi; e) [NEt_4][BF_4].

Later Bochmann[113] and Piers[114] independently discovered another approach to generate ring-type zwitterionic single-component alkene polymerisation catalysts. In this system, reaction between tuck-in zirconocene complex [Cp*($C_5Me_4CH_2$)ZrPh] and $B(C_6F_5)_3$ in toluene produces the zwitterionic system where the anionic $B(C_6F_5)_3$ substituent is separated from the cyclopentadienyl ring by a CH_2 spacer (Fig. 1.46). The reaction proceeds selectively with the attack on the fulvene-CH_2 group to form the zwitterionic complex. In the presence of ethylene under 1 bar pressure and a wide range of temperatures (from 20 ºC to -78 ºC) this system can produce polyethylene with molecular weight up to M_w = 861,000 with an activity up to 3 x 10^6 g PE [(mol Zr).bar. h]$^{-1}$.[111]

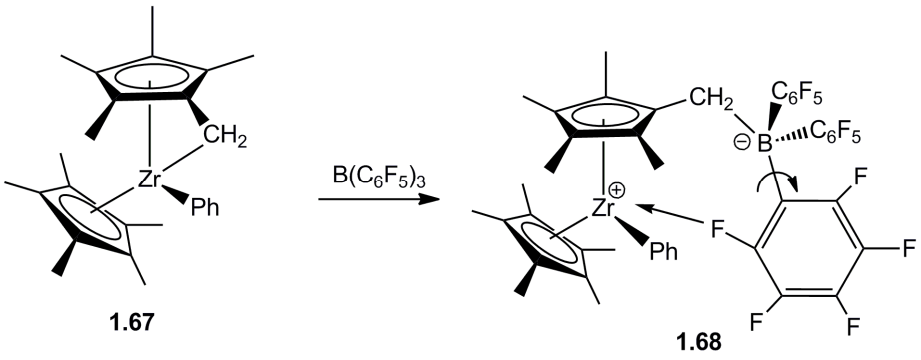

Figure 1.46. Zwitterionic catalyst derived from tuck-in zirconocene precursor.

3. Bridge zwitterions

Although in the literature there are no specific examples of bridge type zwitterionic catalyst, recent developments in the synthetic methodologies suggest that they should be accessible.

Borate-free zwitterions:

Recently a borate-free zwitterionic polymerisation catalyst has been developed by Mountford and coworkers[120] using a tris(pyrazolyl)methane ligand, as exemplified by $HC(Me_2pz)_3$ (Fig. 1.47).

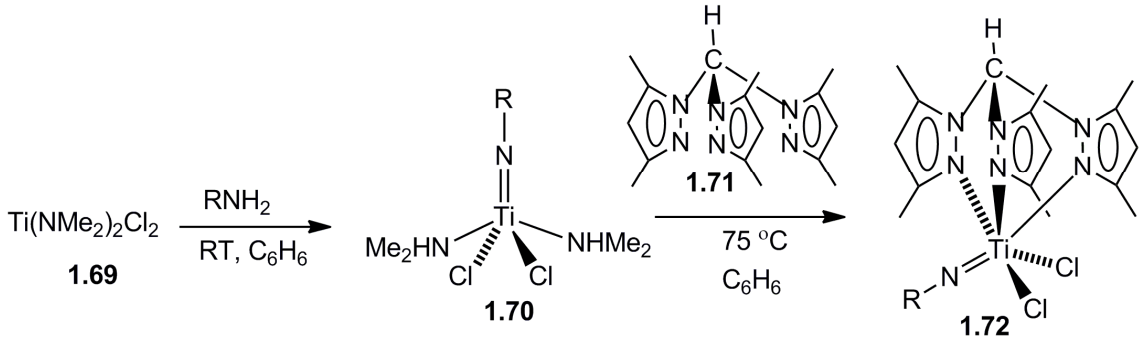

Figure 1.47. Synthesis of tris(pyrazolyl)methane-supported titanium imido compound.

The reaction of the tris(pyrazolyl)methane-supported titanium imido compound with

MeLi produces the zwitterionic complex (Fig. 1.48).

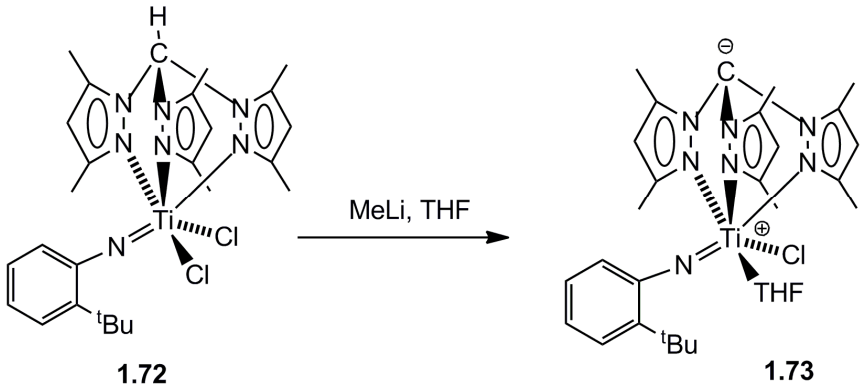

1.72 1.73

Figure 1.48. Synthesis of borate free zwitterionic precatalyst.

Upon activation of this zwitterionic precatalyst with MAO (Al/Ti = 3200) the system can produce polyethylene with activity of 131 000 kg PE mol^{-1} h^{-1} bar^{-1}. Activation of this zwitterionic complex with $Al^{i}Bu_3$ (Al/Ti = 3200) can give an even higher activity of 146700 kg PE mol^{-1} h^{-1} bar^{-1} (M_w = 409 000, PDI = 2.5). The Lewis acidic $Al^{i}Bu_3$ activator shows high activity because it acts both as an alkylating and THF abstracting agent. The catalytically active species in this system is believed to be a charge-neutral, zwitterionic alkyl cation of the type [Ti(N-2-$C_6H_4{}^{t}Bu$){$C(Me_2pz)_3$}R] (R = growing polymer chain).

1.3.2 Zwitterionic catalysts by late transition metals

It is known that the use of very weakly coordinating anions is a prerequisite for high polymerisation activity. In this regard, incorporation of the counter anion into the ligand framework may prevent the close association of the anion with the active metal site. On the basis of this concept several zwitterionic systems have been developed with the early transition metals which have been discussed already in the preceding sections. This activation method also has been successfully applied in the late transition metal based zwitterionic catalyst. For example, Erker and coworkers[116] have applied the metal/butadiene/borane activation method on Brookhart cationic

diimine late transition metal catalysts to generate its zwitterionic counter part. The reaction of [DADNiBr$_2$] with the butadienemagnesium (MgC_4H_6.2THF) produces a (η^4-butadiene)nickel complex (**1.74**) (Fig. 1.49).[129] The addition of $B(C_6F_5)_3$ to this complex forms the butadienenickel-based zwitterionic catalyst (Fig. 1.50). This zwitterionic complex does not require any additional activation and is therefore a true single component catalyst. In this system branched polymer is produced at a temperature of 25 ºC and 2 bar pressure with an activity of 159 kg (PE) mol (Ni)$^{-1}$ h^{-1} bar (ethylene)$^{-1}$.

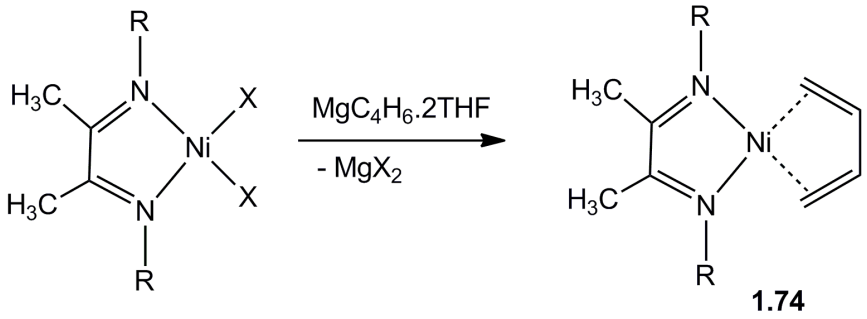

1.74

Figure 1.49. (η^4-butadiene)nickel diimine complex.

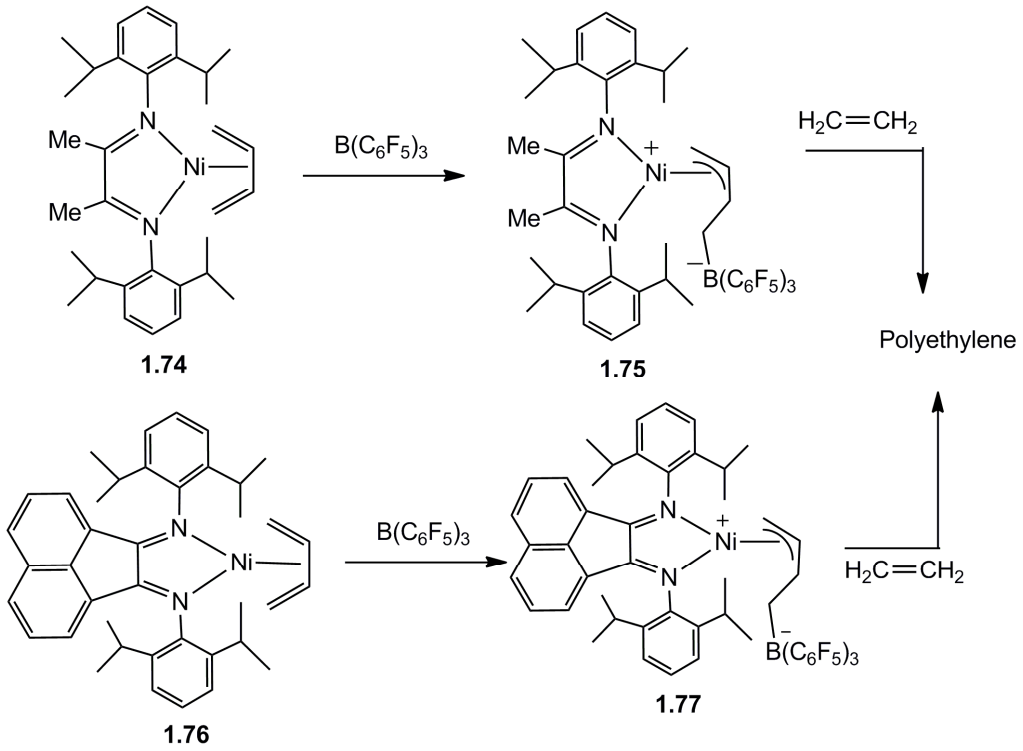

Figure 1.50. Butadienenickel-based zwitterionic single-componet ethylene polymerisation catalyst.

As depicted in Figure 1.51 Bazan and coworkers[130] synthesised series of α-iminocarboxamide Ni complexes by varying the substituents on nitrogen of the ligand.

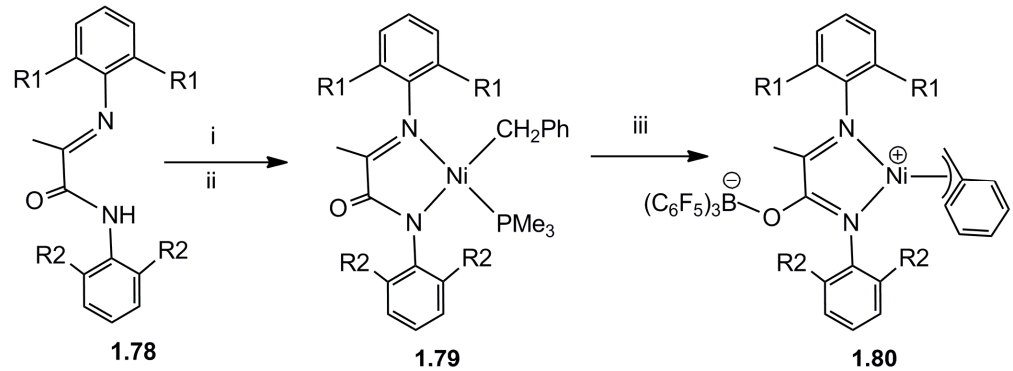

i) KH
ii) Ni(η^3-$CH_2C_6H_5$)Cl(PMe_3)
iii) 2 $B(C_6F_5)_3$

a R1 = R2 = H
b R1 = $CHMe_2$, R2 = H
c R1 = R2 = $CHMe_2$

Figure 1.51. Synthesis of zwitterionic α-iminocarboxamide Ni complexes.

The reaction of the deprotonated carboxamide ligand with Ni(η^3-$CH_2C_6H_5$)Cl(PMe_3) first produces non-zwitterionic complexes. Addition of two equivalents of $B(C_6F_5)_3$ to the non-zwitterionic Ni complexes results in the precipitation of Me_3P-$B(C_6F_5)_3$ and formation of zwitterionic complexes **1.80a-1.80c** (Fig. 1.51). Thus addition of borane results in carbonyl coordination which removes electron density from the nickel center resulting in active catalysts. These zwitterionic complexes mostly produce branched polymer and branching increases with the introduction of bulky ligands.

It is quite surprising that although Brookhart diimine catalysts require bulky aryl substituents for polymerisation activity, Bazan and coworkers[131] found a zwitterionic Ni complex containing the less bulky ligand, 3-(2,6-diisopropylphenylimino)-but-1-en-2-olato is able to polymerise ethylene (Fig. 1.52).

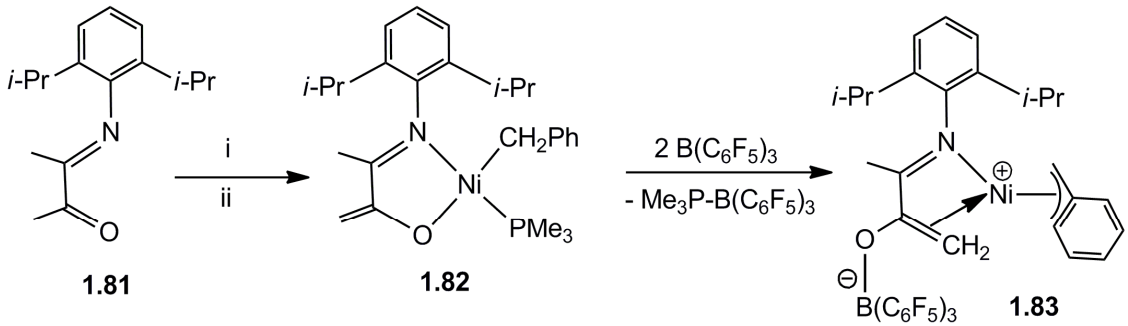

i) NaH
ii) Ni(η^1-$CH_2C_6H_5$)Cl(PMe_3)$_2$

Figure 1.52. Zwitterionic Ni catalyst containing less bulky 3-(arylimino)-but-1-en-2-olato ligand.

The reaction of the sodium salt of the ligand, 3-(2,6-diisopropylphenylimino)-butan-2-one with Ni(PMe_3)$_2$(η^1-$CH_2C_6H_5$)Cl produces the Ni complex, (3-(2,6-diisopropyl-phenylimino)-but-1-en-2-olato)(η^1-benzyl)-(trimethylphosphine)-nickel **1.82** (Fig. 1.52). The addition of 2 equivalents of $B(C_6F_5)_3$ to the Ni complex in toluene results in the precipitation of Me_3P-$B(C_6F_5)_3$ and formation of zwitterionic complex 2-tris(pentafluorophenyl)borate-3-(2,6-diisopropylphenylimino)-but-1-ene(η^3-benzyl)-nickel **1.83.** This zwitterionic complex **1.83** can make polyethylene at 30 ºC and 7

bar without the need of any activator. Moreover, the addition of $B(C_6F_5)_3$ in the catalytic system increases the catalytic activity and also decreases the PDI value. The enhancement in activity upon addition of $B(C_6F_5)_3$ is probably due to the action of $B(C_6F_5)_3$ as a scrubbing agent which removes impurities in the reaction medium that may interfere during propagation.

The catalysis of ethylene/acrylonitrile (AN) copolymerisation by late transition metal compounds still remains a challenge as less success has been achieved with acrylonitrile compared to other polar monomers.[132] Acrylonitrile can bind to the metal via the polar CN group (σ bond) or the olefinic C=C π bond. For polymerisation of the olefin to take place, the π binding mode should be energetically more feasible than the σ bonding of CN to the metal, otherwise poisoning will occur. Thus elimination of the preference for σ-complexation of acrylonitrile is a prerequisite for ethylene/acrylonitrile copolymerisation (Fig. 1.53).

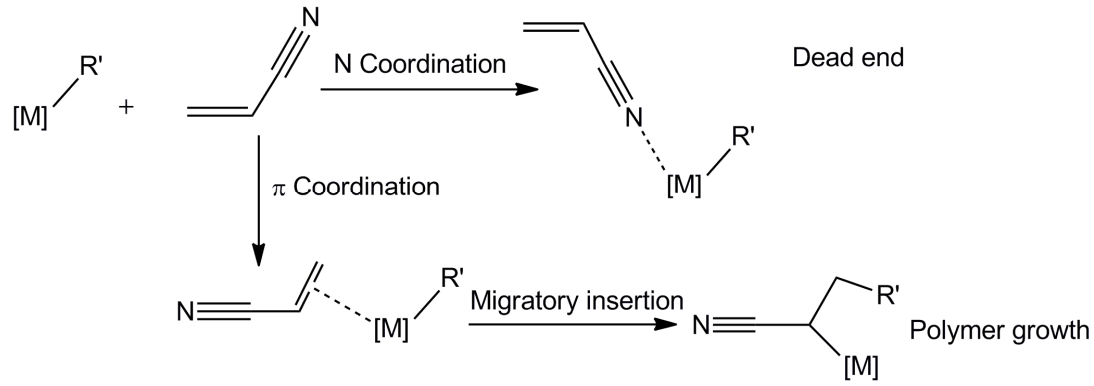

Figure 1.53. π versus N coordination of nitrogen-containing polar monomers with the metal center [M].

The theoretical study by Ziegler[133] indicates that cationic Brookhart catalysts based on both Pd(II) and Ni(II) metal centers prefer σ- bonding to AN and the preference is even more pronounced for Ni(II). The cationic Ni(II) diimine complex exhibits a preference for binding through the CN group of 22.0 kcal mol^{-1}. However, the application of a neutral or anionic environment can promote the π-coordination mode over the σ-mode. In order to make Brookhart catalysts capable of ethylene/acrylonitrile copolymerisation, Ziegler and coworkers[132, 134] have modified the original cationic Brookhart catalyst into its neutral or even anionic version. The

zwitterionic analogues of Brookhart cationic diimine Ni(II) and Pd(II) catalysts have been made by functionalization of the diimine aryl rings (N^N = -NR'C(R1)C(R2)NR' where R' = 2,6-C_6H_3 (*i*-Pr)$_2$ and R1, R2 = Me) by adding one or two anionic groups (BF_3^-, etc) in place of *i*-Pr, or by replacing one Me diimine backbone group (R1) with BH_3^- (Fig. 1.54).

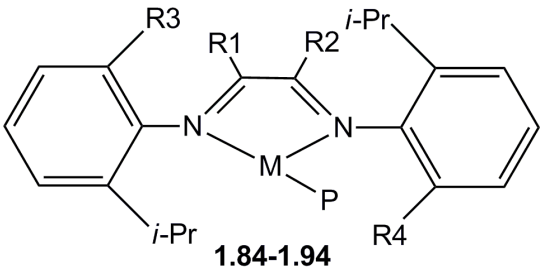

1.84-1.94

No	M	R1	R2	R3	R4
1.84	Ni	Me	Me	*i*-Pr	*i*-Pr
1.85	Ni	Me	Me	BF_3^-	*i*-Pr
1.86	Ni	Me	Me	SO_3^-	*i*-Pr
1.87	Ni	CF_3	CF_3	BF_3^-	*i*-Pr
1.88	Ni	^{t}Bu	^{t}Bu	BF_3^-	*i*-Pr
1.89	Ni	^{t}Bu	^{t}Bu	SO_3^-	*i*-Pr
1.90	Ni	Me	Me	BF_3^-	BF_3^-
1.91	Ni	CF_3	CF_3	BF_3^-	BF_3^-
1.92	Ni	BH_3^-	Me	*i*-Pr	*i*-Pr
1.93	Pd	Me	Me	BF_3^-	*i*-Pr
1.94	Pd	BH_3^-	Me	*i*-Pr	*i*-Pr

Figure 1.54. Zwitterionic Brookhart catalyst: theoretical calculation.

Calculations showed that the introduction of one or two anionic groups (for example, BH_3^-,BF_3^-, SO_3^-, etc.) at the diimine backbone reduces the poisoning by up to 16 kcal mol^{-1}. An even larger reduction in poisoning was found by substituting one or two *i*-Pr groups on the aryl rings. However, substitution on other parts of the ring is less effective. The theoretical study demonstrated that good copolymerisation of ethylene and acrylonitrile catalysts should have a low barrier of insertion, low affinity towards side reactions, such as chelate formation and catalyst oligomer formation after the acrylonitrile insertion. In terms of the relative propagation rate the best catalysts are the complexes **1.85, 1.88, 1.90, 1.91** and **1.92** (Fig. 1.54).[134]

More recently, Bailey and coworkers[135] have developed neutral zwitterionic analogues of Brookhart catalysts by replacing the 1,2-diimine ligand with a 6-aminofulvene-2-aldiminate (AFA) ligand.

The AFA ligand-based zwitterionic catalyst [(Ph_2AFA)PdMe(PPh_3)] was prepared by reacting deprotonated ligand (NaPh_2AFA) with [(COD)PdMeCl] in the presence of the strongly coordinating ligand PPh_3. As shown in Figure 1.55 this complex acts as an active ethylene polymerisation catalyst when activated by $Ni(COD)_2$ as a phosphine scavenger.

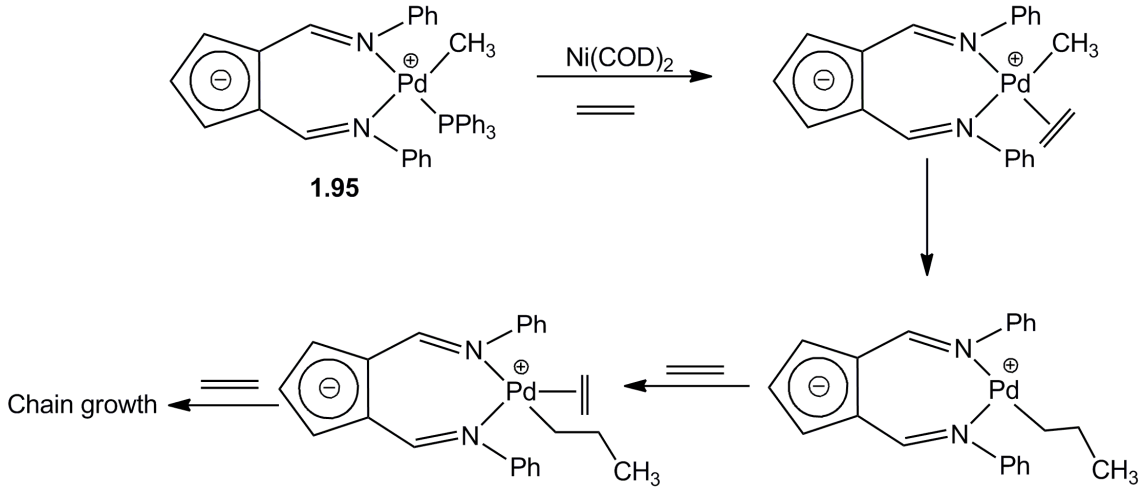

Figure 1.55. Ethylene polymerisation by zwitterionic [(Ph_2AFA)PdMe(PPh_3)] catalyst.

This catalytic system produces linear polyethylene (M_n = 8400, M_w = 140000, PDI = 17) as well as mixtures of oligomers at a pressure of 5 bar and 50 ºC. However, Brookhart cationic Pd α-diimine catalyst produces exclusively branched polymer. The activity of this AFA ligand-based Pd catalyst is extremely low (0.02 Kg of PE mol-1 of Pd h^{-1} bar^{-1} at 50 ºC) and is thought to be due to the poor scavenging effect of $Ni(COD)_2$. The PPh_3 coordinates more strongly to Pd than to Ni which results in a shift towards the left hand side of the activation reaction (Equation 1.1). Thus it provides a lower concentration of the phosphine-free Pd active species. In addition to that the Pd complex of AFA ligand also has substantial lack of axial shielding.

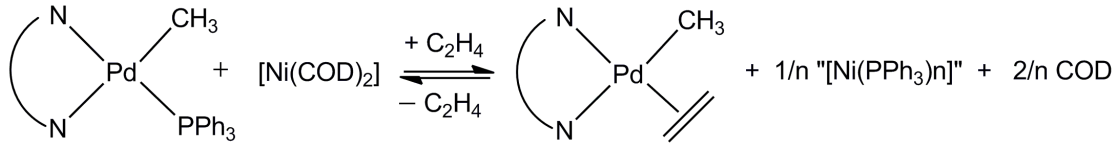

Equation 1.1

1.4 Scope of the thesis

Although the 6-aminofulvene-2-aldiminate (AFA) has been known since the early seventies,[136, 137] little attention has been given to its applicability as a ligand to transition metal complexes and its possible applications in catalysis. The 6-aminofulvene-2-aldiminate (AFA) ligand has the ability to form zwitterionic overall charge-neutral complexes (B), analogues of Brookhart-type cationic alkene polymerisation catalysts (A) (Fig. 1.56).

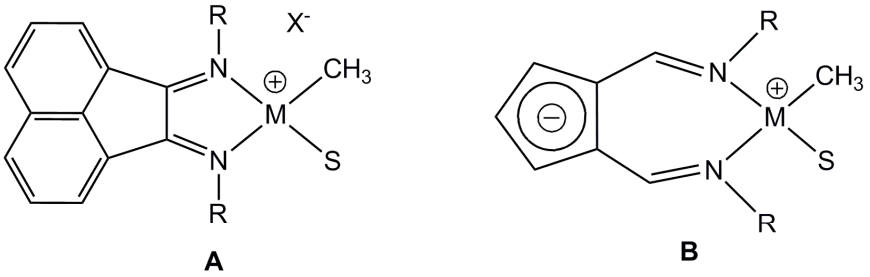

X = anion e.g. BAF^-, CH_3MAO^- etc.

S = ethylene or donor solvent

M = Ni, Pd

Figure 1.56. Brookhart (A) vs. AFA ligand (B) based complex.

In principle, the zwitterionic complexes of the AFA ligand should be preactivated, well-defined single component catalysts which do not require Lewis acid co-catalysts for activation. This will eventually increase productivity as well as reduce production costs.

Due to the preliminary success of AFA ligand based complex in ethylene polymerisation, in this thesis more nitrogen functionalised AFA ligands were synthesised in order to tune steric and/or electronic properties of the metal complexes. Zwitterionic complexes were explored via nitrogen complexation as well as cyclopentadienyl coordiantion of the AFA ligand. The cyclopentadienyl coordination could eventually provide bimetallic cationic complexes which could be used as precusrsors for ethylene polymerisation.

References

1. K. Ziegler, E. Holzkamp, H. Breil and H. Martin, *Angew. Chem*, 1955, **67**, 541.
2. G. Natta, *Angew. Chem*, 1956, **68**, 393.
3. G. Natta, P. Pino, P. Corradini, F. Danusso, E. Mantica, G. Mazzanti and G. Moraglio, *J. Am. Chem. Soc*, 1955, **77**, 1708.
4. J. P. Hogan and R. L. Banks, U.S. Patent 2825721*,* 1958.
5. W. Kaminsky, A. Funck and H. Hähnsen, *Dalton Trans*, 2009, 8803.
6. B. M. Weckhuysen and R. A. Schoonheydt, *Catalysis Today,* 1999, **51**, 215.
7. S. S. Ivanchev, *Russ. Chem. Rev*, 2007, **76**, 617.
8. M. Bochmann, *J. Chem. Soc, Dalton Trans,*1996, 255.
9. G. Wilkinson, P. L. Pauson, J. M. Birmingham and F. A. Cotton, *J. Am. Chem. Soc*, 1953, **75**, 1011.
10. G. Natta, P. Pino, G. Mazzanti and U. Giannini, *J. Am. Chem. Soc*, 1957, **79**, 2975.
11. D. S. Breslow and N. R. Newburg, *J. Am. Chem. Soc*, 1957, **79**, 5072.
12. W. P. Long and D. S. Breslow, *Justus Liebigs Ann. Chem*, 1975, 463.
13. H. Sinn, W. Kaminsky, H.-J. Vollmer and R. Woldt, *Angew. Chem. Int. Ed. Engl*, 1980, **19**, 390.
14. H. Sinn and W. Kaminsky, *Adv. Organometal. Chem*, 1980, **18**, 99.
15. V. Busico, *Dalton Trans*, 2009, 8794.
16. H. G. Alt and A. Köppl, *Chem. Rev*, 2000, **100**, 1205.
17. T. M. J. Anselment, S. I. Vagin and B. Rieger, *Dalton Trans*, 2008, 4537.

18. M. J. Schneider, R. Schäfer and R. Mülhaupt, *Polymer*, 1997, **38**, 2455.
19. A. Nakamura, S. Ito and K. Nozaki, *Chem. Rev*, 2009, **109**, 5215.
20. S. D. Ittel, L. K. Johnson and M. Brookhart, *Chem. Rev*, 2000, **100**, 1169.
21. W. Keim, F. H. Kowaldt, R. Goddard and C. Krüger, *Angew. Chem. Int. Ed. Engl*, 1978, **17**, 466.
22. P. Kuhn, D. Semeril, D. Matt, M. J. Chetcuti and P. Lutz, *Dalton Trans*, 2007, 515.
23. J. Skupinska, *Chem. Rev*, 1991, **91**, 613.
24. W. Keim, R. Appel, S. Gruppe and F. Knoch, *Angew. Chem. Int. Ed. Engl*, 1987, **26**, 1012.
25. G. J. P. Britovsek, V. C. Gibson and D. F. Wass, *Angew. Chem. Int. Ed. Engl*, 1999, **38**, 428.
26. U. Klabunde and S. D. Ittel, *J. Mol. Catal*, 1987, **41**, 123.
27. A. Yamamoto, T. Shimizu and S. Ikeda, *Makromol. Chem*, 1970, **136**, 297.
28. A. Yamamoto, *J. Chem. Soc. Dalton Trans*, 1999, 1027.
29. A. Yamamoto and S. Ikeda, *J. Am. Chem. Soc*, 1967, **89**, 5989.
30. W. Keim, R. Appel, A. Storeck, C. Krüger and R. Goddard, *Angew. Chem. Int. Ed. Engl*, 1981, **20**, 116.
31. V. M. Möhring and G. Fink, *Angew. Chem. Int. Ed. Engl*, 1985, **24**, 1001.
32. L. K. Johnson, C. M. Killian and M. Brookhart, *J. Am. Chem. Soc*, 1995, **117**, 6414.
33. C. Wang, S. Friedrich, T. R. Younkin, R. T. Li, R. H. Grubbs, D. A. Bansleben and M. W. Day, *Organometallics*, 1998, **17**, 3149.
34. T. R. Younkin, E. F. Connor, I. H. Jason, S. K. Friedrich, R. H. Grubbs and D. A. Bansleben, *Science*, 2000, **287**, 460.
35. M. A. Zuideveld, P. Wehrmann, C. Röhr and S. Mecking, *Angew. Chem. Int. Ed. Engl*, 2004, **43**, 869.
36. Z. Guan, *Topics in Organometallic Chemistry, 2009, 26, Metal Catalysts in Olefin Polymerisation, ISBN 978-3-540-87750-9*.
37. D. Takeuchi, *Dalton Trans*, 2010, **39**, 311.
38. V. C. Gibson and E. L. Marshall, *Comprehensive Coordination Chemistry II*, 2004, **9**, 1.

39. M. Svoboda and H. t. Dieck, *J. Organomet. Chem*, 1980, **191**, 321.
40. H. T. Dieck, M. Svoboda and T. Greiser, *Z. Naturforsch*, 1981, **36b**, 823.
41. R. v. Asselt, E. E. C. G. Gielens, R. E. Rulke, K. Vrieze and C. J. Elsevier, *J. Am. Chem. Soc*, 1994, **116**, 977.
42. B. Rieger, L. S. Baugh, S. Kacker and S. Striegler, Late Transition Metal Polymerisation Catalysis, Wiley-VCH, 2003, ISBN 3-527-30435-5.
43. K. Vrieze, *J. Organomet. Chem*, 1986, **300**, 307.
44. N. J. Hill, I. Vargas-Baca and A. H. Cowley, *Dalton Trans*, 2009, 240.
45. E. V. Salo and Z. Guan, *Organometallics*, 2003, **22**, 5033.
46. M. Brookhart, L. K. Johnson, C. M. Killian, S. D. Arthur, J. Feldman, E. F. McCord, S. J. McLain, K. A. Kreutzer, A. M. A. Bennett, E. B. Coughlin, S. D. Ittel, A. Parthasarathy and D. J. Tempel, WO 9623010, 1996.
47. R. van Asselt, E. Rijnberg and C. J. Elsevier, *Organometallics*, 1994, **13**, 706.
48. H. H. Brintzinger, D. Fischer, R. Mülhaupt, B. Rieger and R. M. Waymouth, *Angew. Chem. Int. Ed. Engl*, 1995, **34**, 1143.
49. D. Meinhard, M. Wegner, G. Kipiani, A. Hearley, P. Reuter, S. Fischer, O. Marti and B. Rieger, *J. Am. Chem. Soc*, 2007, **129**, 9182.
50. L. S. Moody, P. B. Mackenzie, C. M. Killian, G. G. Lavoie, J. A. Ponasik, Jr, A. G. Barrett, T. W. Smith and J. C. Pearson, 2000,WO0050470.
51. X. Zeng and K. Zetterberg, *Macromol. Chem. Phys*, 1998, **199**, 2677.
52. D. J. Tempel, L. K. Johnson, R. L. Huff, P. S. White and M. Brookhart, *J. Am. Chem. Soc*, 2000, **122**, 6686.
53. L. K. Johnson, S. Mecking and M. Brookhart, *J. Am. Chem. Soc*, 1996, **118**, 267.
54. P. Jutzi, C. Muller, A. Stammler and H.-G. Stammler, *Organometallics*, 2000, **19**, 1442.
55. D. P. Gates, S. A. Svejda, E. Onate, C. M. Killian, L. K. Johnson, P. S. White and M. Brookhart, *Macromolecules*, 2000, **33**, 2320.
56. C. M. Killian, L. K. Johnson and M. Brookhart, *Organometallics*, 1997, **16**, 2005.
57. S. A. Svejda and M. Brookhart, *Organometallics*, 1999, **18**, 65.

58. L. H. Shultz, D. J. Tempel and M. Brookhart, *J. Am. Chem. Soc*, 2001, **123**, 11539.
59. P. Cossee, *J. Catalysis*, 1964, **3**, 80.
60. Z. Guan, P. M. Cotts, E. F. McCord and S. J. McLain, *Science*, 1999, **283**, 2059.
61. L. Deng, T. K. Woo, L. Cavallo, P. M. Margl and T. Ziegler, *J. Am. Chem. Soc*, 1997, **119**, 6177.
62. L. Deng, P. Margl and T. Ziegler, *J. Am. Chem. Soc*, 1997, **119**, 1094.
63. R. D. J. Froese, D. G. Musaev and K. Morokuma, *J. Am. Chem. Soc*, 1998, **120**, 1581.
64. M. D. Leatherman, S. A. Svejda, L. K. Johnson and M. Brookhart, *J. Am. Chem. Soc*, 2003, **125**, 3068.
65. L. S. Santos and J. O. Metzger, *Angew. Chem. Int. Ed. Engl*, 2006, **45**, 977.
66. P. Chen, *Angew. Chem. Int. Ed. Engl*, 2003, **42**, 2832.
67. C. Hinderling and P. Chen, *Angew. Chem. Int. Ed. Engl*, 1999, **38**, 2253.
68. L. S. Santos and J. O. Metzger, *Rapid Commun. Mass Spectrom*, 2008, **22**, 898.
69. Z. Guan, *Chem. Eur. J*, 2002, **8**, 3087.
70. Z. Guan, *J. Polym. Sci., Part A: Polym. Chem*, 2003, **41**, 3680.
71. C. S. Popeney and Z. Guan, *Macromolecules*, 2010, **43**, 4091.
72. C. Popeney and Z. Guan, *Organometallics*, 2005, **24**, 1145.
73. O. W. Webster, *Science*, 1991, **251**, 887.
74. G. W. Coates, P. D. Hustad and S. Reinartz, *Angew. Chem. Int. Ed. Engl*, 2002, **41**, 2236.
75. G. W. Coates, *J. Chem. Soc., Dalton Trans*, 2002, 467.
76. M. Szwarc, *Nature*, 1956, **178**, 1168.
77. M. Szwarc, M. Levy and R. Milkovich, *J. Am. Chem. Soc*, 1956, **78**, 2656.
78. M. Szwarc, *J. Polym. Sci., Part A: Polym. Chem*, 1998, **36**, IX-XV.
79. G. Bier, *Makromol. Chem*, 1964, **70**, 44.
80. H. Sinn, W. Kaminsky, H.-J. Vollmer and R. Woldt, *Angew. Chem. Int. Ed. Engl*, 1980, **19**, 390.
81. Y. Doi, S. Ueki and T. Keii, *Macromolecules*, 1979, **12**, 814.

82. C. M. Killian, D. J. Tempel, L. K. Johnson and M. Brookhart, *J. Am. Chem. Soc*, 1996, **118**, 11664.
83. A. C. Gottfried and M. Brookhart, *Macromolecules*, 2001, **34**, 1140.
84. A. C. Gottfried and M. Brookhart, *Macromolecules*, 2003, **36**, 3085.
85. G. J. Domski, J. M. Rose, G. W. Coates, A. D. Bolig and M. Brookhart, *Prog. Polym. Sci*, 2007, **32**, 30.
86. A. H. E. Muller and K. Matyjaszewski, Controlled and Living Polymerisations, 2009, Wiley-VCH, ISBN: 978-3-527-32492-7.
87. D. H. Camacho and Z. Guan, *Macromolecules*, 2005, **38**, 2544.
88. E. Y. Tshuva, I. Goldberg, M. Kol and Z. Goldschmidt, *Chem. Commun*, 2001, 2120.
89. M. Mitani, T. Nakano and T. Fujita, *Chem. Eur. J*, 2003, **9**, 2396.
90. G. Wilke, B. Bogdanovic, P. Hardt, P. Heimbach, W. Keim, M. Kröner, W. Oberkirch, K. Tanaka, E. Steinrücke, D. Walter and H. Zimmermann, *Angew. Chem. Int. Ed. Engl*, 1966, **5**, 151.
91. R. F. d. Souza, R. S. Mauler, L. C. Simon, F. F. Nunes, D. V. S. Vescia and A. Cavagnolli, *Macromol. Rapid Commun*, 1997, **18**, 795.
92. G. B. Galland, R. F. de Souza, R. S. Mauler and F. F. Nunes, *Macromolecules*, 1999, **32**, 1620.
93. A. S. Ionkin and W. J. Marshall, *J. Organomet. Chem*, 2004, **689**, 1057.
94. E. F. Connor, T. R. Younkin, J. I. Henderson, A. W. Waltman and R. H. Grubbs, *Chem. Commun*, 2003, 2272.
95. L. S. Boffa and B. M. Novak, *Chem. Rev*, 2000, **100**, 1479.
96. S. Mecking, L. K. Johnson, L. Wang and M. Brookhart, *J. Am. Chem. Soc*, 1998, **120**, 888.
97. L. Johnson, A. Bennett, K. Dobbs, E. Hauptman, A. Ionkin, S. Ittel, E. McCord, S. McClain, C. Radzewich, Z. Yin, L. Wang, Y. Wang and M. Brookhart, *Polym. Mater. Sci. Eng*, 2002, **86**, 319.
98. S. J. McLain, K. J. Sweetman, L. Johnson and E. McCord, *Polym. Mater. Sci. Eng.* , 2002, **86**, 320.
99. C. S. Popeney, D. H. Camacho and Z. Guan, *J. Am. Chem. Soc*, 2007, **129**, 10062.

100. G. G. Hlatky, *Chem. Rev*, 2000, **100**, 1347.
101. H. C. L. Abbenhuis, *Angew. Chem. Int. Ed. Engl*, 1999, **38**, 1058.
102. P. Preishuber-Pflugl and M. Brookhart, *Macromolecules*, 2002, **35**, 6074.
103. H. S. Schrekker, V. Kotov, P. Preishuber-Pflugl, P. White and M. Brookhart, *Macromolecules*, 2006, **39**, 6341.
104. J. R. Severn, J. C. Chadwick and V. Van Axel Castelli, *Macromolecules*, 2004, **37**, 6258.
105. M. Bochmann and S. J. Lancaster, *Organometallics*, 1993, **12**, 633.
106. M. Bochmann, S. J. Lancaster, M. B. Hursthouse and K. M. A. Malik, *Organometallics*, 1994, **13**, 2235.
107. M. Bochmann and A. J. Jaggar, *J. Organomet. Chem*, 1992, **424**, C5-C7.
108. G. G. Hlatky, H. W. Turner and R. R. Eckman, *J. Am. Chem. Soc*, 1989, **111**, 2728.
109. W. E. Piers, *Chem. Eur. J*, 1998, **4**, 13.
110. R. Chauvin, *Eur. J. Inorg. Chem*, 2000, 577.
111. M. Bochmann, *Topics in Catal*, 1999, **7**, 9.
112. W. E. Piers, Y. Sun and L. W. M. Lee, *Topics in Catal*, 1999, **7**, 133.
113. X. Song and M. Bochmann, *J. Organomet. Chem*, 1997, **545-546**, 597.
114. Y. Sun, R. E. v. H. Spence, W. E. Piers, M. Parvez and G. P. A. Yap, *J. Am. Chem. Soc*, 1997, **119**, 5132.
115. G. Erker, *Chem. Commun*, 2003, 1469.
116. J. W. Strauch, G. Erker, G. Kehr and R. Fröhlich, *Angew. Chem. Int. Ed. Engl*, 2002, **41**, 2543.
117. Y. Sun, W. E. Piers and S. J. Rettig, *J. Chem. Soc, Chem. Commun*, 1998, 127.
118. W. E. Piers and T. Chivers, *Chem. Soc. Rev*, 1997, **26**, 345.
119. M. Bochmann, S. J. Lancaster and O. B. Robinson, *J. Chem. Soc., Chem. Commun*, 1995, 2081.
120. H. R. Bigmore, S. R. Dubberley, M. Kranenburg, S. C. Lawrence, A. J. Sealey, J. D. Selby, M. A. Zuideveld, A. R. Cowley and P. Mountford, *Chem. Commun*, 2006, 436.

121. G. J. Pindado, M. Thornton-Pett, M. Bouwkamp, Auke Meetsma, B. Hessen and M. Bochmann, *Angew. Chem. Int. Ed. Engl*, 1997, **36**, 2358.

122. C. C. Lu and J. C. Peters, *J. Am. Chem. Soc*, 2002, **124**, 5272.

123. R. F. Jordan, W. E. Dasher and S. F. Echols, *J. Am. Chem. Soc*, 1986, **108**, 1718.

124. H. van der Heijden, B. Hessen and A. G. Orpen, *J. Am. Chem. Soc*, 1998, **120**, 1112.

125. X. Yang, C. L. Stern and T. J. Marks, *J. Am. Chem. Soc*, 1991, **113**, 3623.

126. B. Temme, G. Erker, J. Karl, H. Luftmann, R. Fröhlich and S. Kotila, *Angew. Chem. Int. Ed. Engl*, 1995, **34**, 1755.

127. J. Karl, G. Erker, R. Fröhlich, F. Zippel, F. Bickelhaupt, M. S. Goedheijt, O. S. Akkerman, P. Binger and J. Stannek, *Angew. Chem. Int. Ed. Engl*, 1997, **36**, 2771.

128. M. Dahlmann, R. Fröhlich and G. Erker, *Eur. J. Inorg. Chem*, 2000, 1789.

129. J. C. M. Sinnema, G. H. B. Fendesak and H. T. Dieck, *J. Organomet. Chem*, 1990, **390**, 237.

130. B. Y. Lee, G. C. Bazan, J. Vela, Z. J. A. Komon and X. Bu, *J. Am. Chem. Soc*, 2001, **123**, 5352.

131. Y. Chen, B. M. Boardman, G. Wu and G. C. Bazan, *J. Organomet. Chem*, 2007, **692**, 4745.

132. M. J. Szabo, N. M. Galea, A. Michalak, S.-Y. Yang, L. F. Groux, W. E. Piers and T. Ziegler, *Organometallics*, 2005, **24**, 2147.

133. M. J. Szabo, R. F. Jordan, A. Michalak, W. E. Piers, T. Weiss, S.-Y. Yang and T. Ziegler, *Organometallics*, 2004, **23**, 5565.

134. M. J. Szabo, N. M. Galea, A. Michalak, S.-Y. Yang, L. F. Groux, W. E. Piers and T. Ziegler, *J. Am. Chem. Soc*, 2005, **127**, 14692.

135. P. J. Bailey, M. Melchionna and S. Parsons, *Organometallics*, 2007, **26**, 128.

136. U. Mueller-Westerhoff, *J. Am. Chem. Soc*, 1970, **92**, 4849.

137. K. Hafner, K. H. Vöpel, G. Ploss and C. König, *Org. Synth*, 1967, **47**, 52.

Chapter 2 Complexes of Palladium and Nickel containing κ^2(N,N)-Aminofulvene-aldiminate Ligands

2.1 Introduction

The 6-aminofulvene-2-aldiminate (AFA) ligand[1-4] has the ability to coordinate to a wide range of metals through either the cyclopentadienyl or imine nitrogen donors, or both at the same time.[5-7] Moreover, a wide range of nitrogen substituents may be introduced to this ligand in order to precisely tune the steric and/or electronic properties.[1] The synthetic route also allows for two different nitrogen substituents to be introduced into the same ligand. The ligand displays facile tautomerism and an intramolecular hydrogen bond (Fig. 2.1).

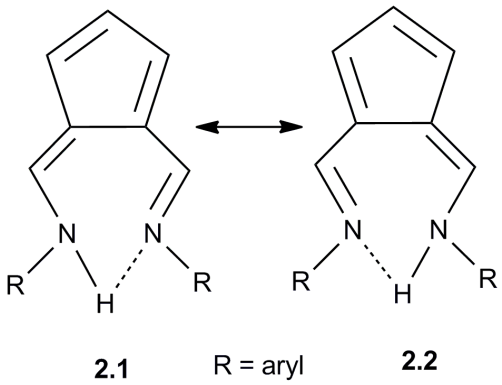

Figure 2.1. Tautomeric forms of the 6-aminofulvene-2-aldimine system.

Once deprotonated, the ligand electronic structure may be represented as two resonance forms (**2.3** and **2.4)** (Fig. 2.2). The characterisation of complexes in which this ligand displays symmetrical η^5-coordination of the cyclopentadienyl ring indicates that substantial negative charge is located here suggesting a predominant contribution from resonance form **2.4** in complexes.[6, 8]

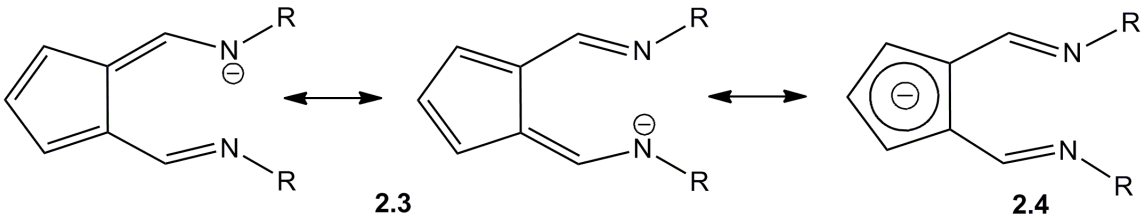

Figure 2.2. Resonance forms for the 6-aminofulvene-2-aldiminate ligand.

This being so, the AFA ligand effectively provides a neutral bis-imine donor set and a negative charge localised in the C_5-ring; neutral metal complexes containing a κ^2-*N*,*N*-AFA ligand will therefore have zwitterionic character and may have significant positive charge at the metal centre **2.5** (Fig. 2.3) which is a significant factor for activity in alkene polymerisation catalysts. Thus the AFA ligand system could in principle form zwitterionic, charge-neutral analogues of Brookhart-type catalyst.

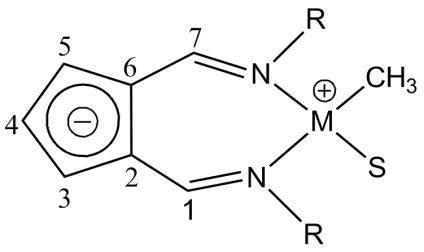

2.5

S = ethylene or donor ligand

M = Ni, Pd

Figure 2.3. The transition metal complexes of AFA ligand and the numbering scheme of C/H atoms used in interpretation of NMR spectra of the AFA ligand and its complexes.

Mitsui Chemicals Inc. has a patent on cobalt complexes (Fig. 2.4) based on a γ-diimine ligand which polymerises ethylene in the presence of methylaluminoxane.[9, 10] In this complex the backbone of the γ-diimine ligand possesses a benzene ring whereas the AFA ligand possesses a C_5 cyclopentadienyl ring.

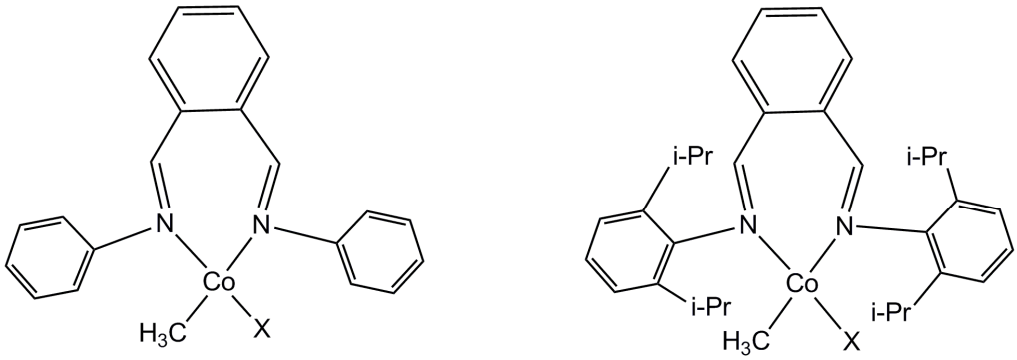

Figure 2.4. Cobalt complexes of γ-diimine ligand for ethylene polymerisation.

Stephan and coworkers[8, 11] developed a 1,2-disubstituted cyclopentadienyl diimine ligand which binds metals through the nitrogen atoms (Fig. 2.5). The extended planar π-systems in this ligand provides some formal charge separation to the metal complex and thus enhances the electrophilic character of the metal center. This bidentate, mono-anionic ligand is closely related to the AFA ligand. The synthesis of the ligand H[1,2-C_5H_3(C(Ph)$NH)_2$] (**2.9**) is straightforward. The reaction of Cp_2Mg with benzonitrile produces a pseudo-tetrahedral (benzonitrile)magnesium complex (1,2-C_5H_3(C(Ph)$NH)_2$)CpMg(NCPh) (**2.8**). In this complex one cyclopentadienyl group remains unaltered and the other is 1,2-disubstituted. Demetallation of **2.8** provides the free ligand, H[1,2-C_5H_3(C(Ph)$NH)_2$] (**2.9**). The reaction of **2.9** with sodamide ($NaNH_2$) and 1 equivalent of $ZrCl_4(THF)_2$ in benzene provides a pseudo-octahedral zirconium complex (1,2-C_5H_3(C(Ph)$NH)_2$)$ZrCl_3$-(THF) (**2.10**) (Fig. 2.5).

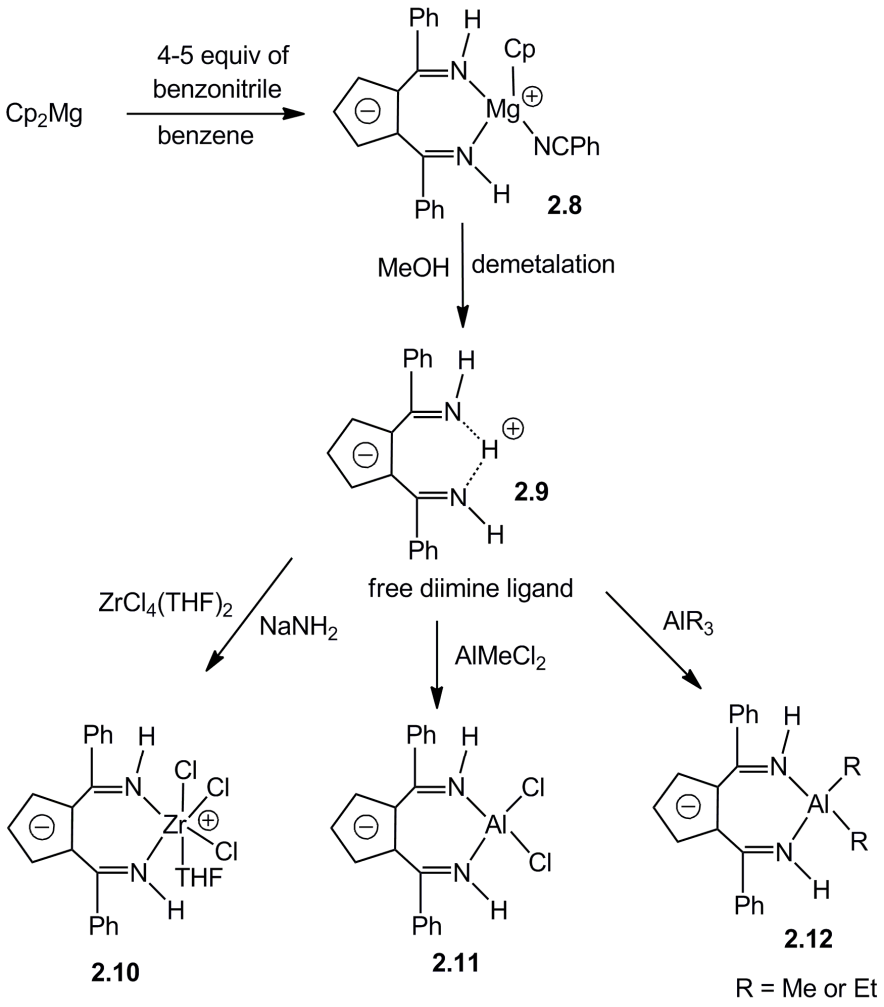

Figure 2.5. The complexes of 1,2-cyclopentadienyl diimine ligand 2.9.

A computational study on (1,2-$C_5H_3(C(H)NH)_2$)$ZrCl_3$(THF) reveals that the HOMO is located on the π-orbitals on the cyclopentadienyl group, and the LUMO is largely a vacant metal-based d-orbital (Fig. 2.6). This bonding mode provides a formal charge separation and thus imparts electrophilic character to the zirconium center.

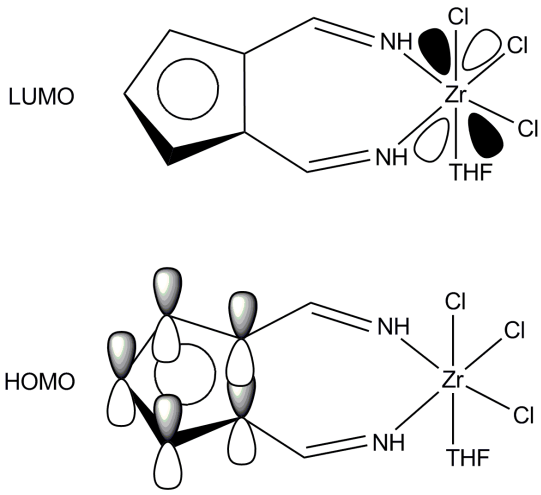

Figure 2.6. LUMO and HOMO of the model compound (1,2-$C_5H_3(C(H)NH)_2)ZrCl_3(THF)$.

The 1,2-cyclopentadienyl diimine ligand H[1,2-$C_5H_3(C(Ph)NH)_2$] (**2.9**) reacts with $MeAlCl_2$ to form a pseudo-tetrahedral aluminum complex [1,2-$C_5H_3(C(Ph)NH)_2]AlCl_2$ (**2.11**). The reaction of the ligand **2.9** with AlR_3 affords [(1,2-$C_5H_3(C(Ph)NH)_2)]AlR_2$ (**2.12**), R = Me, Et. In order to generate Al based zwitterions or cations the complex **2.12** has been reacted with $B(C_6F_5)_3$. However, the reaction provided multiple unknown products.

Bailey and coworkers[5-7] investigated the metal complexes of AFA ligands to develop a zwiterionic alkene polymerisation catalyst. Bailey group synthesised a tetrahedral methyl magnesium complex [(Cy_2AFA)Mg(CH_3)THF] (**2.13**) (Fig. 2.7) by reacting the ligand N,N'-dicyclohexyl-6-aminofulvene-2-aldimine (Cy_2AFAH) with methyllithium followed by methylmagnesium bromide in toluene. The ^{1}H NMR spectrum shows that the complex **2.13** contains a signal at -0.98 ppm for the Mg bound methyl ligand.

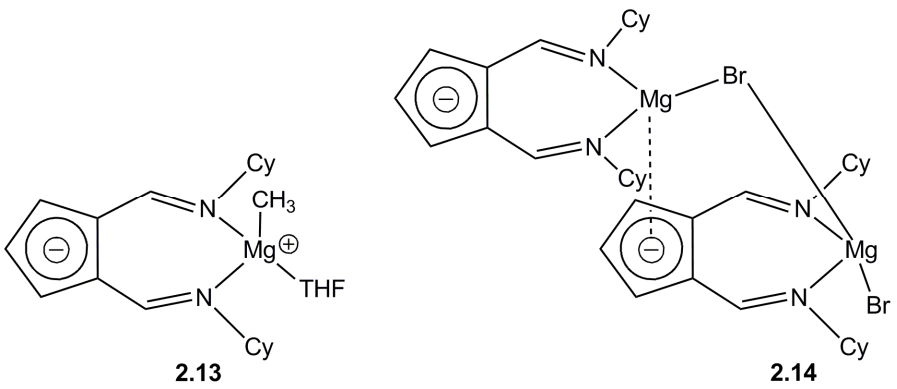

Figure 2.7. Tetrahedral methyl magnesium complex [(Cy_2AFA)Mg(CH_3)THF] and [(Cy_2AFA)$_2$MgBr_2].

The direct reaction of Cy_2AFAH with methylmagnesium bromide without prior lithiation liberates methane and provides [(Cy_2AFA)$_2$MgBr_2] (**2.14**). The magnesium complex **2.14** (Fig. 2.7) provides an example of the ambidentate nature of this AFA ligand. The complex **2.14** shows one magnesium ion is coordinated to the AFA ligand through its two nitrogen donors and the coordination sphere of this magnesium is completed by the symmetrical η^5-coordination of the cyclopentadienyl ring of a second AFA ligand. A bromide ligand bridges the two magnesium centers and the coordination site of the other magnesium is completed by a terminal bromide ligand.

The deprotonation of the AFAH ligand with a base such as NaH, BuLi or CH_3Li provides a metallated ligand which can be reacted with metal precursor to develop transition metal complexes. Scheme 2.1 shows synthetic routes to some complexes of N,N'-diphenyl-6-aminofulvene-2-aldimine (Ph_2AFAH) ligand.

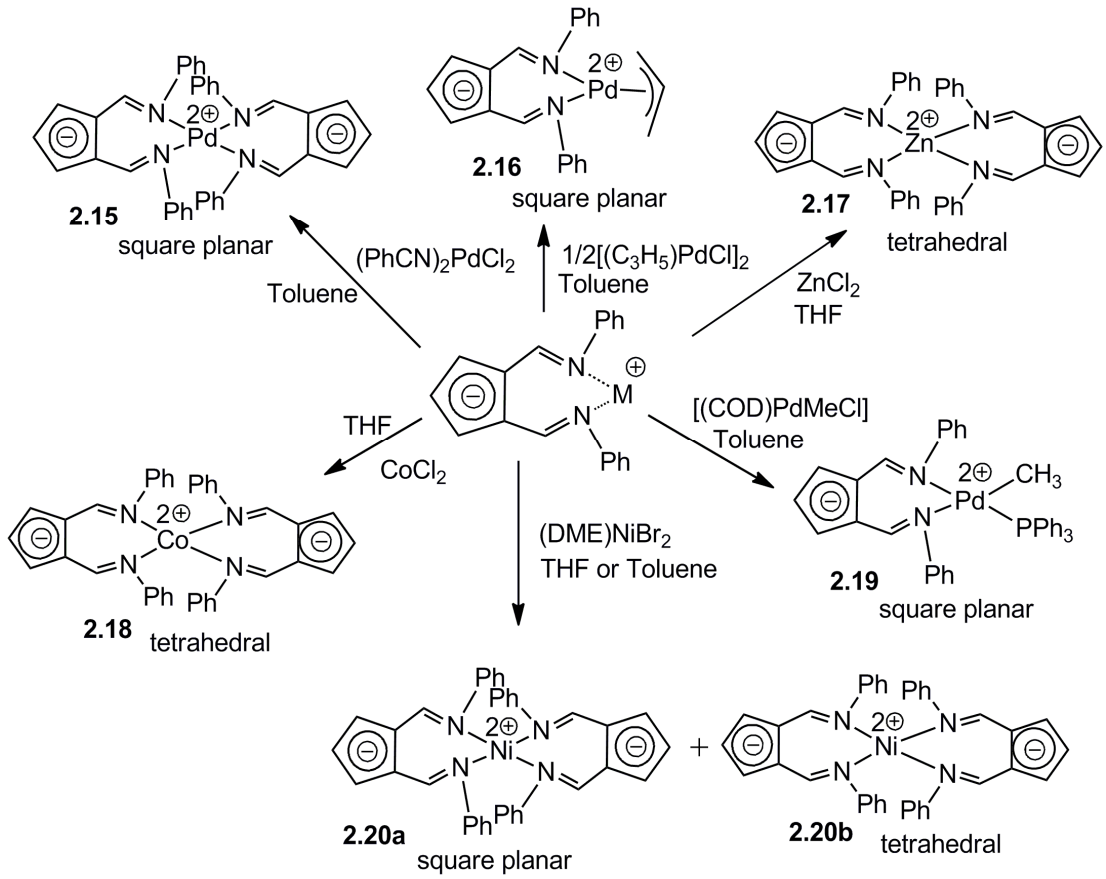

Scheme 2.1. An overview of the metal complexes of AFA ligand.

The deprotonation of Ph_2AFAH ligand with NaH in THF followed by reaction with the anhydrous $ZnCl_2$ (1:1) affords a tetrahedral complex $[Zn(Ph_2AFA)_2]$ (**2.17**) (Scheme 2.1)**.** The square-planar $[Pd(Ph_2AFA)_2]$ (**2.15**) complex is obtained by deprotonation of the Ph_2AFAH ligand with BuLi in toluene followed by reaction with $[(PhCN)_2PdCl_2]$. Similar to the zinc complex **2.17**, a tetrahedral complex $[Co(Ph_2AFA)_2]$ **2.18** is obtained by deprotonation of the Ph_2AFAH in THF with NaH and subsequent addition of anhydrous $CoCl_2$. The d^7 complex **2.18** is paramagnetic, having three unpaired electrons and its ^1H NMR spectrum therefore shows only a broad signal. A mixture of tetrahedral and square-planar nickel complexes $[Ni(Ph_2AFA)_2]$ (**2.20b** and **2.20a** respectively) is formed upon the reaction of the $LiPh_2AFA$ with $[(DME)NiBr_2]$. None of the above bis- chelated complexes are interesting for ethylene polymerisation catalysis. The mono-chelated square-planar complex **2.16** is obtained by reacting the deprotonated ligand (by CH_3Li) in toluene

with ½ equivalent of $[(C_3H_5)PdCl]_2$. Only the complex **2.19** is active in ethylene polymerisation when activated with $Ni(COD)_2$ as phosphine scavenger. The complex $[(Ph_2AFA)Pd(Me)PPh_3]$ (**2.19**) is formed on treatment of [(COD)PdMe(Cl)] with $NaPh_2AFA$ in the presence of PPh_3 (Scheme 2.1).

2.2 Synthesis of the ligands

The synthesis of the ligand is comprised of three steps.

Step 1: Synthesis of 6-(dimethylamino)fulvene

In 1963, Hafner et al. first synthesised 6-(dimethylamino)fulvene.[3] The reaction between dimethylformamide (DMF) and dimethyl sulfate (DMS) first leads to the formation of the N,N'-dimethylformamide-dimethylsulfate complex (Scheme 2.2). The reaction of one equivalent of sodium cyclopentadienide with the N,N'-dimethylformamide-dimethylsulfate produces the 6-(dimethylamino)fulvene (Scheme 2.3). The 6-(dimethylamino)fulvene is light sensitive.

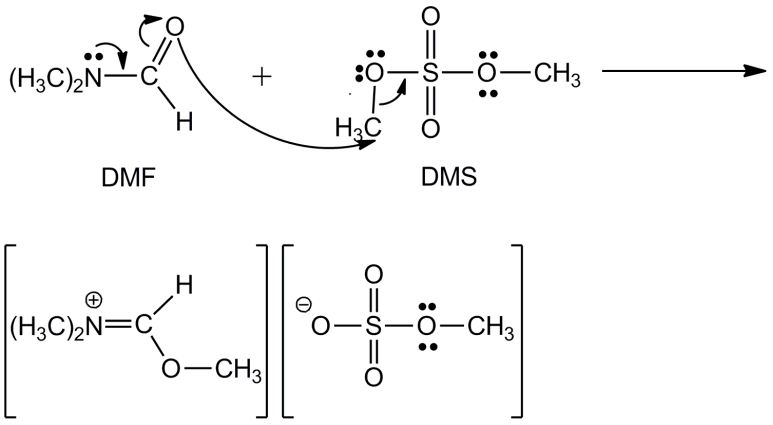

Scheme 2.2. Reaction of N,N'-dimethylformamide with dimethylsulfate.

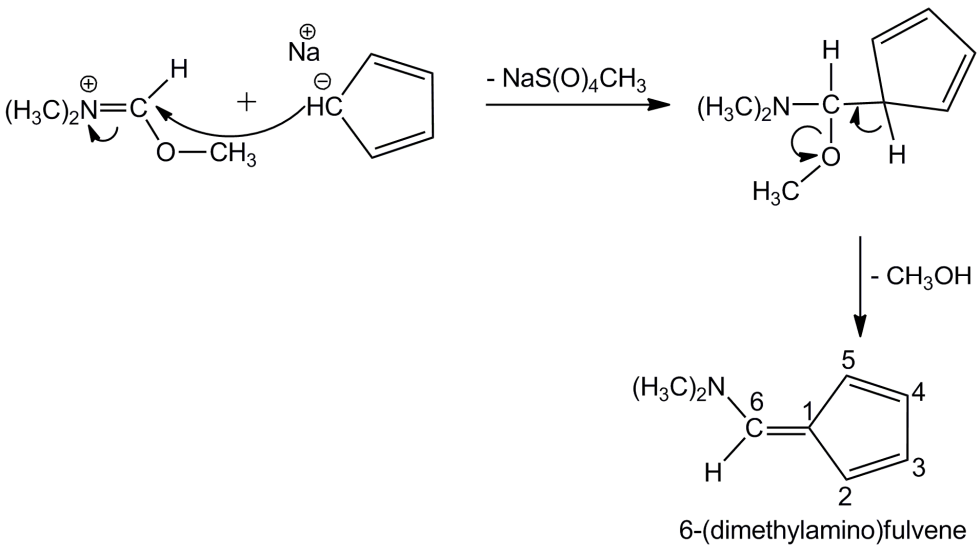

Scheme 2.3. Synthesis of 6-(dimethylamino)fulvene.

Step 2: Synthesis of 6-dimethylaminofulvene-2-N,N'-dimethylaldimonium chloride.

Electrophilic substitution takes place at the 2-position of 6-(dimethylamino)fulvene by the Vilsmeier complex to form the 6-dimethylaminofulvene-2-N,N'-dimethylaldimonium chloride (Scheme 2.4). The Vilsmeier complex is the product of dimethylformamide (DMF) and oxalyl chloride.[1]

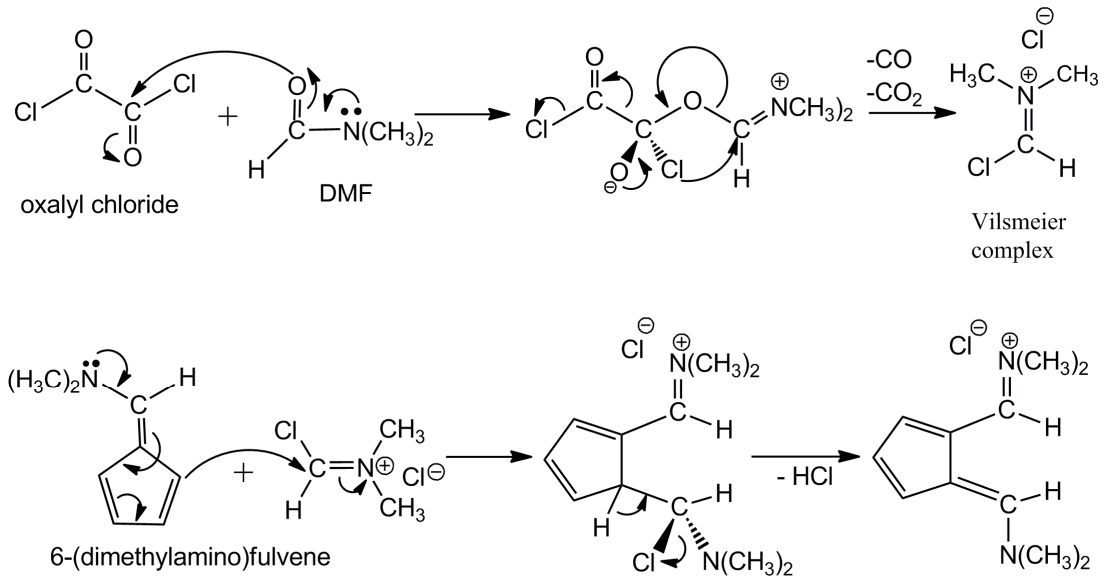

Scheme 2.4. Synthesis of 6-dimethylaminofulvene-2-N,N'-dimethylaldimonium chloride.

Step 3: Synthesis of 6-aminofulvene-2-aldimine

The 6-dimethylaminofulvene-2-N,N'-dimethylaldimonium chloride reacts with ammonia, primary aliphatic or aromatic amines to form the 6-aminofulvene-2-aldimine (Scheme 2.5). This reaction proceeds with the formation of 6-dimethylaminofulvene-2-aldimine intermediate. This intermediate can be isolated if R_1 is an aromatic or larger aliphatic group. Thus, it is possible to obtain "unsymmetrical" ($R_1 \neq R_2$) as well as "symmetrical'' ($R_1 = R_2$) aminoimines. All aminoimines are stable, yellow or red, well-crystallised solids.

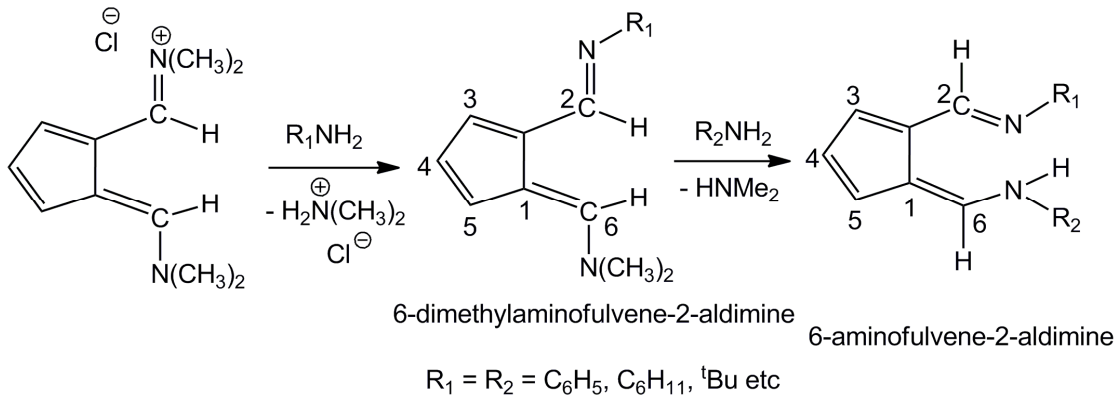

Scheme 2.5. Synthesis of 6-aminofulvene-2-aldimine.

In this thesis a range of different nitrogen-substituted 6-aminofulvene-2-aldimine ligands have been synthesised. These are summarised in the Figure 2.8.

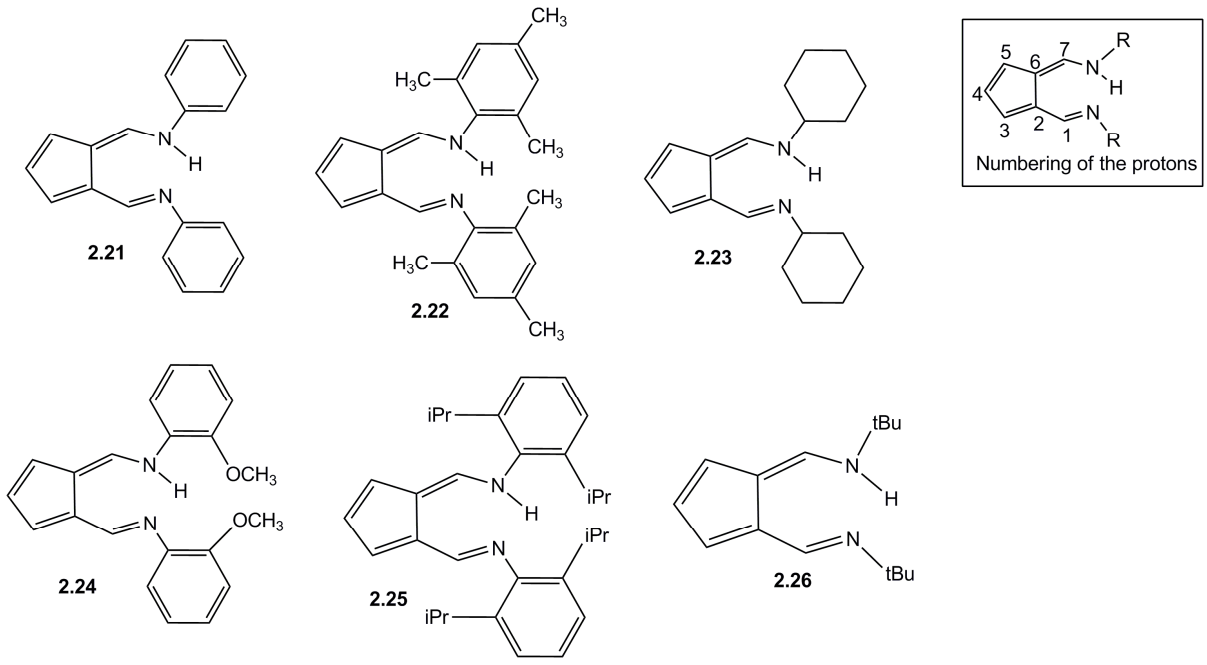

Figure 2.8. Different substituents on nitrogen of the 6-aminofulvene-2-aldimine (AFA) ligands: *N,N′*-diphenyl-6-aminofulvene-2-aldimine **(2.21)**, *N,N′*-di-(2,4,6-trimethylphenyl)-6-aminofulvene-2-aldimine **(2.22)**, *N,N′*-dicyclohexyl-6-aminofulvene-2-aldimine **(2.23)**, *N,N′*-bis(2-methoxyphenyl)-6-aminofulvene-2-aldimine **(2.24)**, ***N,N′***-bis(2,6-diisopropylphenyl)-6-aminofulvene-2-aldimine **(2.25)**, *N,N′*-di^{t}butyl-6-aminofulvene-2-aldimine **(2.26)**.

The ligands **2.21**, **2.22**, **2.23** and **2.26** have been well described by Müller-Westerhoff.[1, 2] In order to tune steric and electronic properties of the AFA ligand based complexes, in this thesis two more new ligands **2.24** and **2.25** have been synthesised and characterised.

2.2.1 N,N'-bis(2,6-diisopropylphenyl)-6-aminofulvene-2-aldimine

The *N*,*N*'-bis(2,6-diisopropylphenyl)-6-aminofulvene-2-aldimine ligand (**2.25**) was synthesised in 37% yield by reacting 6-dimethylaminofulvene-2-*N*,*N*'-dimethylaldimmonium chloride with two molar equivalents of 2,6-diisopropylaniline (Fig. 2.9).

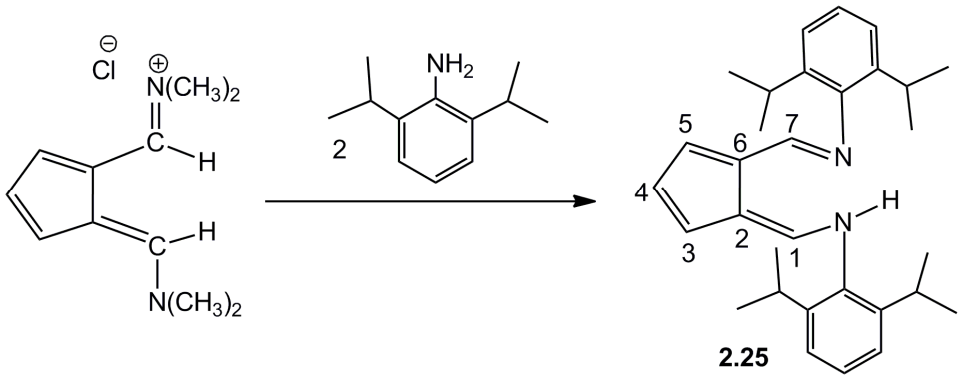

Figure 2.9. *N*,*N*'-bis(2,6-diisopropylphenyl)-6-aminofulvene-2-aldimine (2.25) and the numbering scheme used in interpretation of NMR spectra.

The ^{1}H NMR spectrum of this ligand shows a characteristic triplet at 6.56 ppm for H4 and doublets at 7.97 and 7.13 ppm for H1/H7 and H3/H5 respectively. The presence of the isopropyl groups is indicated by doublet and septet signals at 1.23 and 3.27 ppm respectively. The NH peak appears at 14.55 ppm. Mass spectrometry of **2.25** (EI and +FAB) showed molecular ion peaks at *m*/*z* 440.3 and 439.52 (M - H) consistent with the formulation.

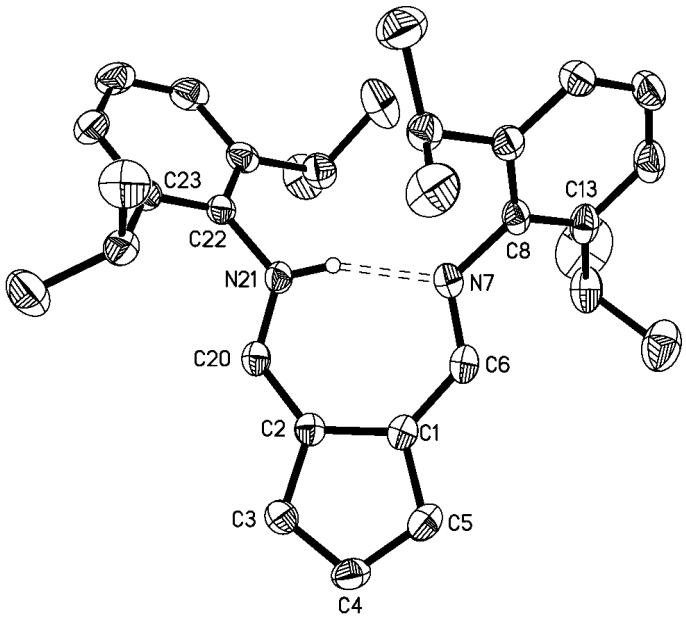

Figure 2.10. Thermal ellipsoid drawing of [(2,6-diipropylphenyl)$_2$AFAH] (2.27) (50% ellipsoids). Hydrogen atoms have been removed for clarity.

The X-ray crystal structure of **2.27** (Fig. 2.10) shows that the plane consisting of C_5 and two imine carbon-nitrogen is planar. However, as expected, the phenyl rings deviate substantially from the above plane (by 56.06º) in order to minimise the steric interaction between the isopropyl groups on each. Also reflecting this are the dihedral angles C13-C8-N7-C6 (58.29º) and C23-C22-N21-C20 (59.34º). The carbon-carbon and carbon-nitrogen distances are intermediate between the usual single and double bonds. The bond angles C1-C6-N7 and C2-C20-N21 are 126.30(16)º and 125.59(16)º respectively, consistent with sp^2 hybridisation at the imine carbon atoms. An N21-H-N7 intramolecular hydrogen bond exists in **2.27**. The hydrogen atom is bonded to N21 atom. The donor (N21)-acceptor (N7) distance is 2.680(2) Å which compares with the value of 2.79 Å in Ph_2AFAH.[1, 2]

Table 2.1. Selected bond lengths (Å) and angles (deg) for [(2,6-diisopropylphenyl)$_2$AFAH].

Bond	Bond length (Å)	Bond	Bond angle (deg)
C(1)-C(2)	1.461(2)	C(1)-C(6)-N(7)	126.30(16)
C(1)-C(5)	1.402(2)	C(2)-C(20)-N(21)	125.59(16)
C(5)-C(4)	1.393(3)	C(6)-N(7)-C(8)	121.41(14)
C(4)-C(3)	1.391(3)	C(20)-N(21)-C(22)	123.03(14)
C(3)-C(2)	1.411(2)	C(2)-C(3)-C(4)	109.55(16)
C(6)-N(7)	1.302(2)		
C(20)-N(21)	1.305(2)		
N(7)-C(8)	1.424(2)		
N(21)-C(22)	1.419(2)		
C(2)-C(20)	1.397(2)		
C(1)-C(6)	1.407(2)		

2.2.2 N,N'-bis(2-methoxyphenyl)-6-aminofulvene-2-aldimine

The ligand *N*,*N*'-bis(2-methoxyphenyl)-6-aminofulvene-2-aldimine (**2.24**) was synthesised in 7% yield by reacting 6-dimethylaminofulvene-2-*N*,*N*'-dimethyl-aldimmonium chloride with two molar equivalents of 2-methoxyaniline (Fig. 2.11). The product is an orange crystalline powder. Several attempts to grow single crystals of **2.24** were unsuccessful.

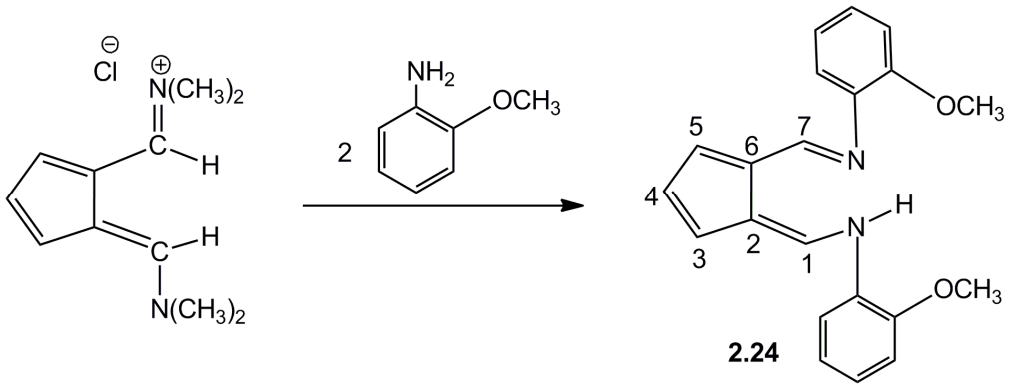

Figure 2.11. *N*,*N*'-bis(2-methoxyphenyl)-6-aminofulvene-2-aldimine (2.24).

The ^{1}H NMR spectrum of **2.24** shows that the NH peak appears at 15.57 ppm. The doublet at 8.28 ppm is attributed to H1/H7 protons. The H1/H7 protons appear as a doublet due to coupling with the NH proton. An intramolecular hydrogen bond and

facile tautomerism exist in this ligand, thus H1 and H7 protons are equivalent. The H3/H5 and H4 protons give a doublet and triplet at 7.02 and 6.43 ppm respectively with J = 3.63 Hz. The six protons of the methoxy groups appear as a singlet at 3.54 ppm, and the eight phenyl protons are in the range of 6.88 – 7.24 ppm. The mass spectrum of **2.24** (EI) showed a molecular ion peak at m/z 332.2 consistent with the molecular structure of the ligand. The chemical shifts observed in the ^{1}H NMR spectrum of **2.24** are consistent with the unsubstituted phenyl group of the Ph_2AFAH ligand (**2.21**). In the NMR spectrum of **2.21**, the NH, H1/H7, H3/H5 and H4 appear at 15.59, 8.29, 7.05 and 6.47 ppm respectively.

2.3 Synthesis of the complexes

In order to assess the effect of replacing the phosphine in [(Ph_2AFA)Pd(Me)PPh_3] with an N-donor, three promising catalyst precursors [(Ph_2AFA)Pd(Me)DMAP] (**2.28**), [(Ph_2AFA)Pd(*N*,*N*-dimethylbenzylamine-2-C,N)] (**2.31**) and [(Ph_2AFA)Ni(η^3-C_3H_5)] (**2.40**) have been synthesised and characterised. Upon Lewis acid activation these complexes may act as catalysts for alkene polymerisation. The ideal phosphine-free catalyst precursor for palladium-based system are the halide-bridged dimers of the form [(R_2AFA)Pd(μ-X)]$_2$, which could be converted into putative active species [(R_2AFA)Pd(Me)C_2H_4] by simple *in situ* alkylation in the presence of ethylene monomer. This chapter describes the efforts towards the synthesis of these dimers.

The numbering scheme of C/H atoms used in interpretation of NMR spectra of the complexes of AFA ligand has been shown in Figure 2.3.

2.3.1 Synthesis and characterisation of [(Ph_2AFA)Pd(Me)(DMAP)]

Driven by the failure of Ni(COD)$_2$ to efficiently activate [(Ph_2AFA)Pd(Me)PPh_3], a complex has been synthesised in which the phosphine is replaced by 4-*N*,*N*'-

dimethylaminopyridine (DMAP). The rationale for using DMAP was that Lewis acid coordination to the uncoordinated dimethylamino group may sufficiently weaken the coordination of the pyridine to allow its substitution by ethylene to provide the potentially catalytically active species [(Ph_2AFA)Pd(Me)C_2H_4].

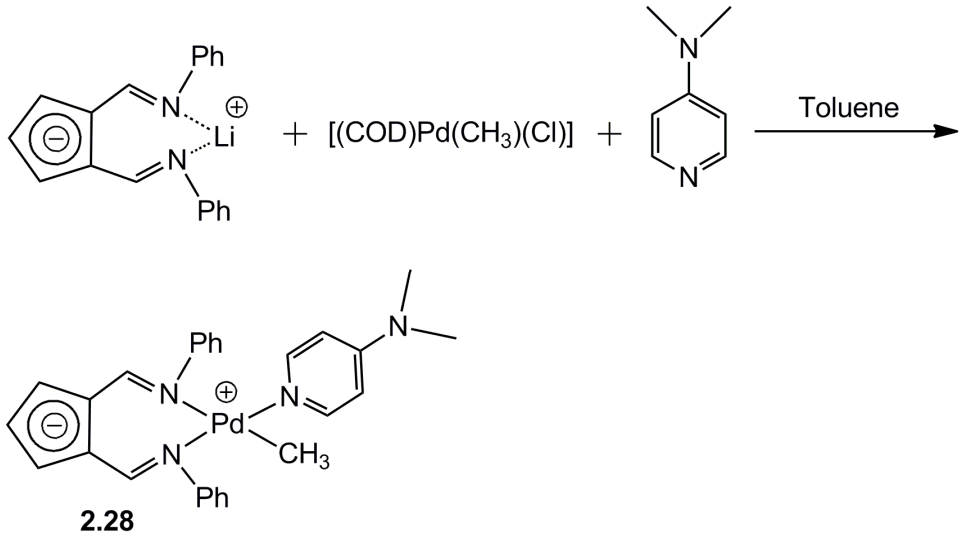

Figure 2.12. Synthesis of [(Ph_2AFA)Pd(Me)DMAP] (2.28).

The complex [(Ph_2AFA)Pd(Me)DMAP] (**2.28**) is prepared by treating [(COD)Pd(CH_3)(Cl)][12] with the lithiated ligand in the presence of DMAP in toluene solution (Fig. 2.12). The ^{1}H NMR spectrum of **2.28** shows the coordination of both the DMAP and AFA ligands to the metal centre. A singlet at -0.1 ppm (3H) confirms the presence of a Pd bound CH_3 ligand. Upon coordination the original doublet due to the proton attached to the imino carbon atoms, H–C=N (H1/H7, **2.21**, Figure 2.8) of the ligand splits into two distinct singlets [8.37 ppm (H1) and 8.29 ppm (H7)] reflecting the absence of mirror-plane symmetry normal to the metal square plane. Upon coordination the H1 proton is shifted to higher frequency; however other ligand protons H3, H4 and H5 and the DMAP protons are shifted to lower frequency. The protons H3/H5 appear as two doublets of doublets due to mutual coupling in addition to coupling to H4. The H7 proton of the free ligand does not shift upon coordination.

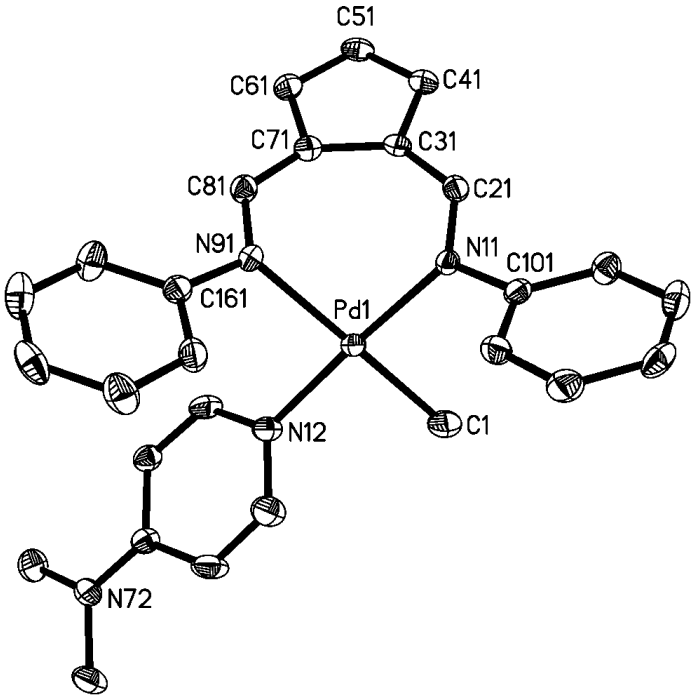

Figure 2.13. Thermal ellipsoid drawing of [(Ph_2AFA)Pd(Me)(DMAP)] (2.29) (50% ellipsoids). Hydrogen atoms have been removed for clarity.

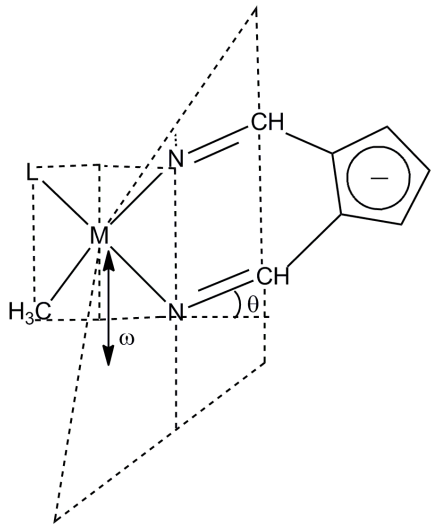

Figure 2.14. Parametrization of the R_2AFA ligand coordination geometry. θ = the acute angle between plane defined by the metal and the two ligand nitrogen atoms and the mean plane defined by the two ligand C=N bonds; ω = the displacement of the metal from this plane.

The X-ray crystal structure of **2.29** (Fig. 2.13) shows that the N–Pd–N angle of 93.41(11)º is close to the ideal square-planar angle. However, the ligand itself is not planar, but greatly distorted. The plane of the C_5-ring is tilted by 61.6º from the metal square plane. The angle between the mean plane of the Pd coordination environment and the plane defined by the two N=C imine bonds (θ, Figure 2.14) is 52.28º and the palladium centre is displaced 1.125 Å from this plane (ω, Figure 2.14). The Pd–N bond *trans*- to the methyl ligand is substantially longer [2.160(3) Å] than that *trans*- to the DMAP ligand [2.041(3) Å], reflecting the greater *trans*-influence of the alkyl ligand. The Pd–N–C angles are close to 120º, consistent with sp^2 hybridisation at N. All the C–C distances in the cyclopentadienyl ring are intermediate between the usual C-C single and double bond values [range 1.393(5)–1.408(5) Å] suggesting electron delocalization in the C_5-ring and a substantial contribution from resonance form **2.4** to the ligand electronic structure. This view is also supported by the similarity of the two C–N bond distances [C81-N91 1.303(4) and C21-N11 1.305(4)] which are consistent with double bonds and the cyclopentadienyl- 1,2-diimine (**2.4**, Fig. 2.2) rather than the 6-aminofulvene-2-aldimine (**2.3**, Fig. 2.2) electronic structure for the coordinated ligand.

Table 2.2. Selected bond lengths (Å) and angles (deg) for [(Ph_2AFA)Pd(Me)(DMAP)] (2.29).

Bond	Bond length (Å)	Bond	Bond angle (deg)
N(11)-Pd(1)	2.041(3)	N(11)-Pd(1)-N(91)	93.42(11)
N(91)-Pd(1)	2.160(3)	C(1)-Pd(1)-N(12)	88.95(15)
C(1)-Pd(1)	2.022(4)	C(21)-N(11)-Pd(1)	121.4(3)
N(12)-Pd(1)	2.051(3)	C(81)-N(91)-Pd(1)	119.4(3)
C(81)-N(91)	1.303(4)		
C(21)-N(11)	1.305(4)		
C(31)-C(71)	1.449(5)		
C(31)-C(41)	1.404(5)		
C(41)-C(51)	1.393(5)		
C(51)-C(61)	1.397(5)		
C(61)-C(71)	1.408(5)		

2.3.2 Synthesis and characterisation of [(Ph_2AFA)(*N*,*N*-dimethylbenzylamine-2-C,N)-Pd(II)]

The cyclometallated complex [(Ph_2AFA)Pd(*N*,*N*-dimethylbenzylamine-2-C,N)] (**2.31**) has been synthesised by reacting the dimer[13] [(*N*,*N*-dimethylbenzylamine-2-C,N)Pd(μ-Cl)]$_2$ (**2.30**) with two equivalents of LiPh_2AFA in THF (Fig. 2.15).

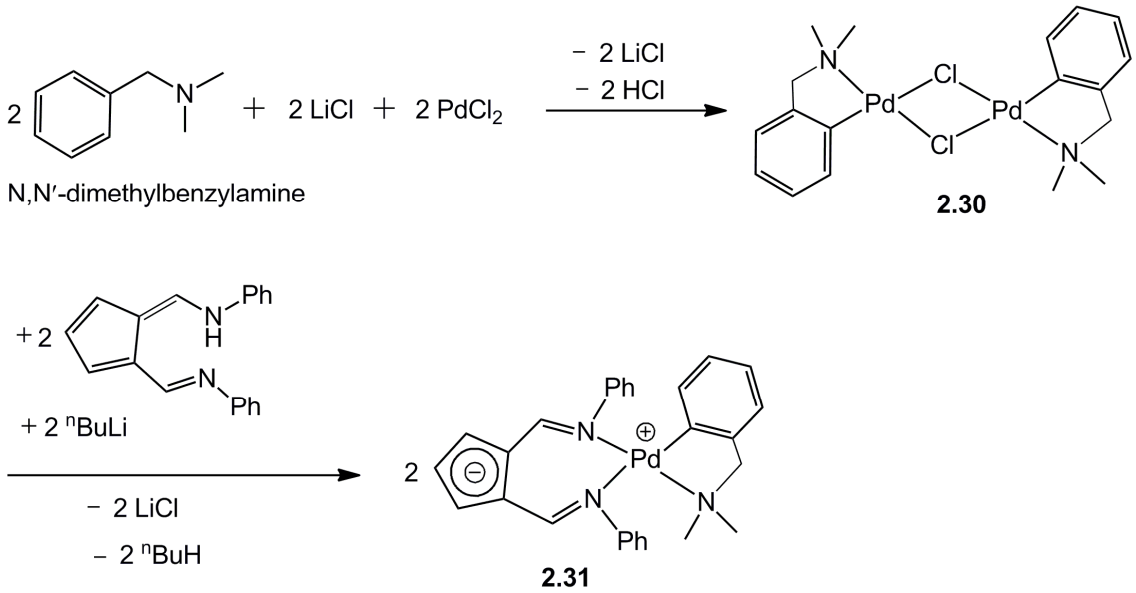

Figure 2.15. Synthesis of [(Ph_2AFA)Pd(*N*,*N*-dimethylbenzylamine-2-C,N)].

The ^{1}H NMR spectrum of **2.31** shows that upon coordination the original doublet at δ 8.29 for the HC=N (H1/H7) protons in the free AFAH ligand (**2.21**) is again split into two distinct singlets [8.65 (H1) and 8.61 ppm (H7)]. The H4 proton appears as a triplet at 6.40 ppm and the H3 and H5 protons of the C_5-ring appear as doublets of doublets at 6.86 and 6.87 ppm respectively. The $N(CH_3)_2$ protons appear as two distinct singlets at 2.30 and 2.53 ppm. The methylene protons appear as two distinct doublets at 3.89 and 3.72 ppm with a geminal coupling constant of 13.54 Hz.

The X-ray crystal structure of **2.32** (Fig. 2.16) shows that the angle at Pd between the two AFA nitrogen donors (N151-Pd1-N71) is 89.01(14)º. The corresponding angle for the cyclometallated dimethylbenzylamine ligand (N82-Pd1-C12) angle is 81.96º reflecting the constrained geometry of the five-membered chelate ring. The angle between the mean plane of the Pd coordination environment and the plane defined by the two N=C imine bonds (θ, Figure 2.14) is 68º and the palladium centre is displaced 1.33 Å from this plane (ω, Figure 2.14). The C_5-ring of the ligand is planar; however, it is tilted by 75.39º to the metal plane. The C(81)-N(71)-Pd angle is 114º which is significantly less than the expected sp^2 hybridisation at nitrogen. As found in **2.29**, all the bond lengths in the C_5-ring of **2.32** are intermediate between those

typical for single and double bonds and the imine C–N bond distances are consistent with double bonds. A distorted square-planar coordination sphere exists around the palladium metal center. The distortion is due the geometrical constraints imposed by chelation. Moreover, the steric hindrance imposed by the two phenyl groups on imine nitrogens and also the steric interaction between the benzyl group and the neighbouring imine phenyl group is responsible for distortion. The deviations of N82 and C12 from the plane containing Pd1, N71 and N151 being 0.311 and 0.242 Å. The five-membered chelate ring and the metal atom is significantly puckered. The C72 is 0.436 Å out of the plane of Pd1, N82, C12 and C62. The displacement of Pd metal to the plane of N71, N151, C12 and N82 is 0.136 Å. The Pd1-N82 bond trans to the N71 atom is longer (2.103 Å) than the Pd1-C12 bond (2.002 Å) trans to the nitrogen atom N151. The predicted Pd1-C12 distance is 2.05 Å. This prediction is from the sum of the Pd-C(sp^2) σ-bonded covalent radii (Pd^{II} 1.31 and C(sp^2 0.74)). The observed Pd1-C12 distance (2.002 Å) is similar to the predicted value.

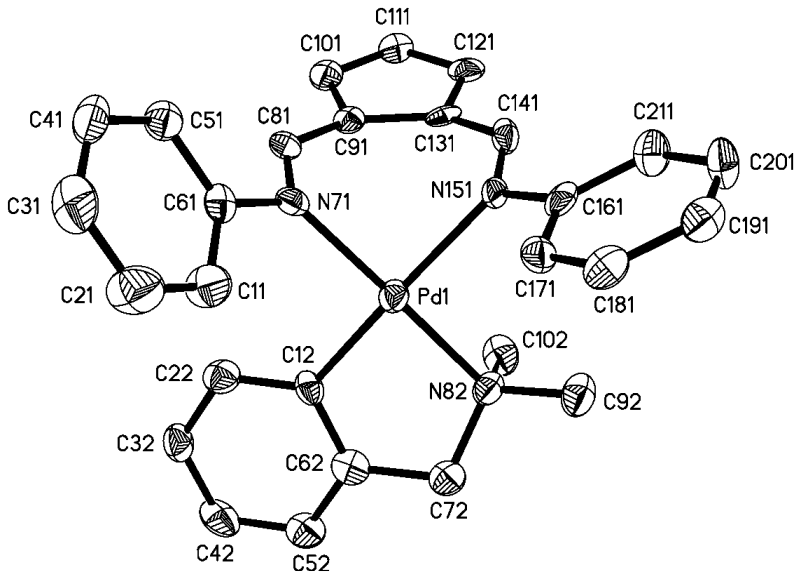

Figure 2.16. Thermal ellipsoid drawing of [(Ph_2AFA)(*N*,*N*-dimethylbenzylamine-2-C,N)-Pd] (2.32) (50% ellipsoids). Hydrogen atoms have been removed for clarity.

Table 2.3. Selected bond lengths (Å) and angles (deg) for [(Ph_2AFA)(*N*,*N*-dimethylbenzylamine-2-C,N)-Pd] (2.32).

Bond	Bond length (Å)	Bond	Bond angle (deg)
C(131)-C(91)	1.454(6)	N(151)-Pd(1)-N(71)	89.01(14)
C(91)-C(101)	1.407(6)	N(82)-Pd(1)-C(12)	81.96(17)
C(101)-C(111)	1.386(6)	C(141)-N(151)-Pd(1)	114.7(3)
C(111)-C(121)	1.394(6)	C(81)-N(71)-Pd(1)	114.9(3)
C(121)-C(131)	1.414(6)	C(72)-N(82)-Pd(1)	108.6(3)
C(141)-N(151)	1.301(5)	N(71)-Pd(1)-C(12)	93.92(17)
C(81)-N(71)	1.272(5)	N(151)-Pd(1)-N(82)	94.13(15)
N(151)-Pd(1)	2.145(4)		
N(71)-Pd(1)	2.045(4)		
Pd(1)-N(82)	2.104(4)		
Pd(1)-C(12)	2.001(4)		

2.3.3 Attempted syntheses of halide-bridged complexes $[(R_2AFA)Pd(\mu\text{-}X)]_2$

In the literature a 1,2-diimine ligand with N-heteroryl substituents is known to form a chloro-bridged dimer complex with nickel.[14] The reaction of ligand **2.33** with one equivalent of (DME)$NiBr_2$ affords the dimer (diimine)$NiBr_2$ (**2.34**) (Fig. 2.17).

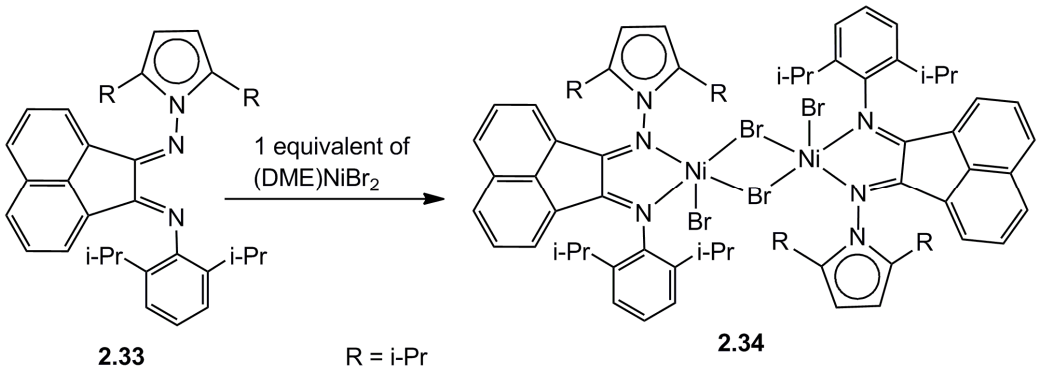

Figure 2.17. Synthesis of the halide bridged dimer (diimine)$NiBr_2$.

In the solid state the complex **2.34** exists as a dimer with an inversion center. The coordination sphere of Ni is essentially square pyramidal. In **2.34**, two 1,2-diimine

ligands are bridged by two bromo ligands and one terminal bromo ligand occupied at the five-coordinated Ni center. The peripheral N-substituents are roughly orthogonal to the Ni-acenaphthonechinone diimine backbone and effectively shield the axial site of Ni atom. The complex **2.34** is paramagnetic.

The pyridylimine-based halide-bridged complexes of Ni and Co (**2.35**) when activated by MAO show ethylene polymerisation activity.[15] Mostly methyl branched polymer is produced in this system. The complex **2.35** resembles the bulky structures of the 1,4-diazabutadiene (i.e. α-diimine) and comprises a chelate consisting of pyridine and 2,6-dialkylphenylimino donors (Fig. 2.18).

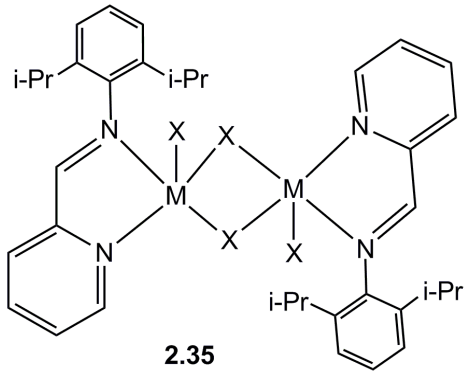

Figure 2.18. Pyridylimine based halide-bridged complex of Ni and Co for ethylene polymerisation.

Moreover, Brookhart and coworkers[16] synthesised chloro-bridged, monocationic dimers of the formula $[(\alpha\text{-diimine})PdMe\text{-}\mu\text{-}Cl]_2BAr'_4$ by reacting $[(\alpha\text{-diimine})PdMeCl]$ with $NaBAr'_4$ in presence of diethyl ether.

Thus ideal catalyst precursors containing AFA ligand could be halide-bridged dimers[15] of the form $[(Ph_2AFA)Pd(\mu\text{-}X)]_2$ (**2.36**) (Fig. 2.19).

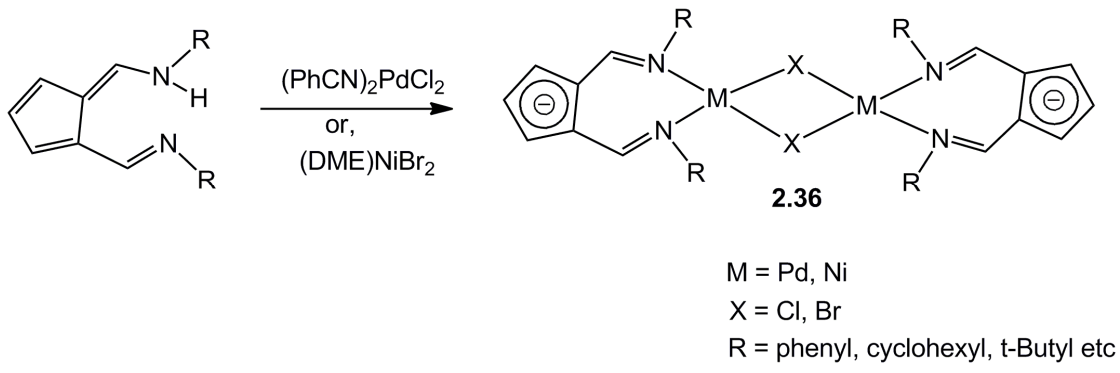

Fig 2.19. Putative halide-bridged dimers containing AFA ligand.

The complex **2.36** could be methylated (MeLi) in presence of a donor solvent (S) to provide [(Ph_2AFA)Pd(Me)S], or potentially [(Ph_2AFA)Pd(Me)C_2H_4] in the presence of ethylene. In an attempt to obtain such species, [$PdCl_2(NCPh)_2$] was treated with $LiPh_2$AFA; however, this reaction resulted in the bis-chelate complex [(Ph_2AFA)$_2$Pd].[6] This observation has lead to introduce more bulky cyclohexyl substituents in the AFA ligand in order to hinder the formation of a complex containing two of the AFA ligands. However, the reaction of $LiCy_2$AFA with [$PdCl_2(NCPh)_2$] again leads to the formation of a bis-chelated complex [(Cy_2AFA)$_2$Pd] (**2.37**) (Scheme 2.6).

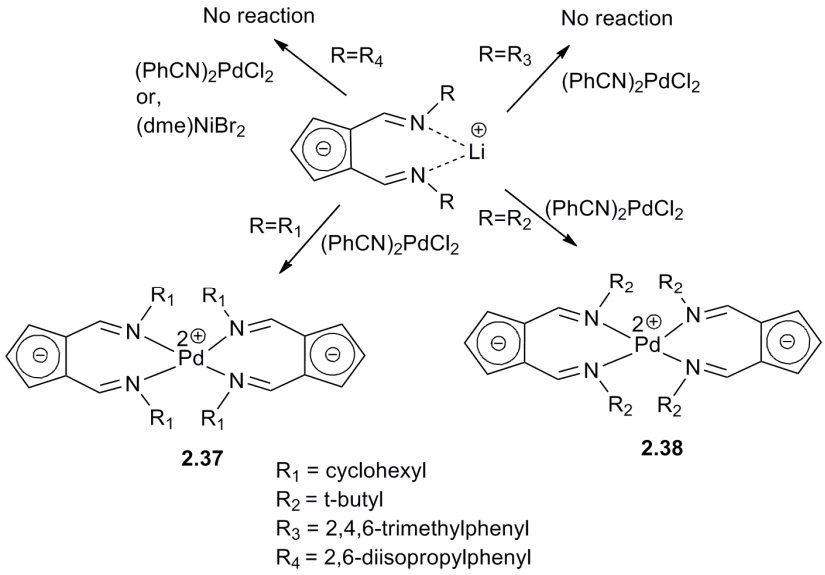

Scheme 2.6. Attempted syntheses of halide-bridged complexes [(R_2AFA)Pd(μ-X)]$_2$.

2.3.4 Synthesis and characterisation of [($Cy_2AFA)_2Pd$]

As shown in Scheme 2.6, the reaction of cyclohexyl substituted AFA ligand (R1 = cyclohexyl) with the palladium precursor provides a bis-chelated complex **2.37**. Metal coordination of the ligand is confirmed by a singlet at 7.71 ppm for H1/H7, which appear as a doublet (δ 7.94, J = 6.6 Hz) in the free ligand Cy_2AFAH due to coupling to the N–H proton. The protons H3 and H5 appear as a doublet at 6.54 ppm and the H4 proton as a triplet at 6.30 ppm.

The X-ray crystal structure of **2.39** (Figure 2.20) shows the complex to be centrosymmetric and the two ligands are therefore equivalent. The geometry of the complex is square-planar with an intraligand N–Pd–N angle of 92.90(7)º. As was observed in the [($Ph_2AFA)_2Pd$] complex,[6] coordination induces the usual distortion of the ligand, with the mean plane of the ligand atoms being tilted toward an axial position relative to the square-planar environment of the metal. The acute angle between the PdN_4 plane and the mean plane defined by the two N=C imine bonds (θ, Figure 2.14) is 50.80º and the displacement of the metal from this plane (ω, Figure 2.14) is 1.091 Å. The corresponding values of θ and ω in [($Ph_2AFA)_2Pd$] are 53.6º and 1.127 Å respectively. Thus it seems that the introduction of cyclohexyl substituents into the ligand surprisingly causes 2.8º less distortion towards an axial position relative to the PdN_4 plane in comparison to the complex containing the Ph_2AFA ligand. This is unexpected as cyclohexyl nitrogen substituents are undoubtedly more sterically demanding than phenyl and yet the distortion observed in **2.39** is less severe than in [($Ph_2AFA)_2Pd$]. This points to an electronic contribution to the distortion observed in these complexes, in addition to the fact that as θ approaches zero the *cis*-nitrogen substituents increasingly occupy the same space.
As expected the Pd–N–C angles in **2.39** are close to 120º consistent with sp^2 hybridisation at N. The C_5-ring of the ligand is planar; however, the imine CH carbon atoms lie 0.249 Å (C12) and 0.262 Å (C9) above this plane, while the nitrogen atoms are 0.153 Å (N13) and 0.161 Å (N2) above this plane. The plane of the C_5-ring is tilted by 55.19º out of the metal square plane.

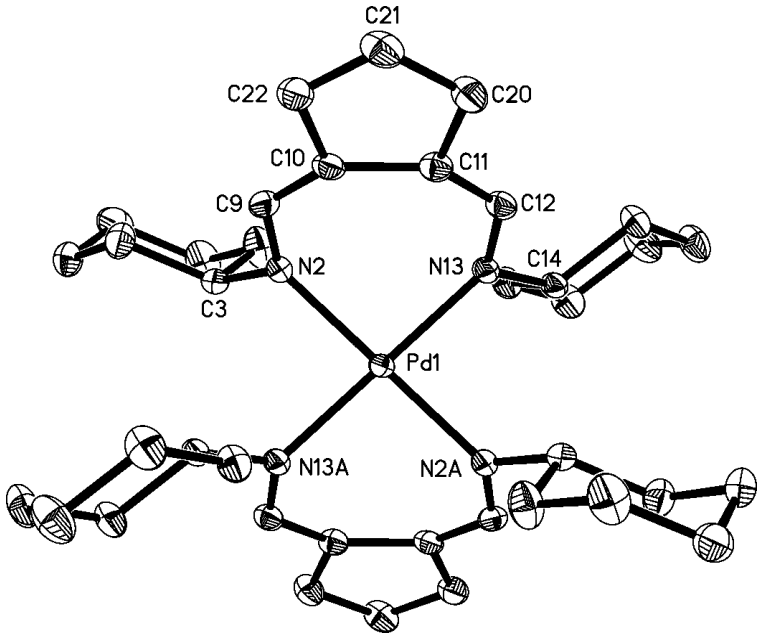

Figure 2.20. Thermal ellipsoid drawing of [($Cy_2AFA)_2Pd$] (2.39) (50% ellipsoids). Hydrogen atoms have been removed for clarity.

Table 2.4. Selected bond lengths (Å) and angles (deg) for [($Cy_2AFA)_2Pd$] (2.39).

Bond	Bond length (Å)	Bond	Bond angle (deg)
Pd(1)-N(2)	2.036(18)	N(2)-Pd(1)-N(13)	92.90(7)
Pd(1)-N(13)	2.049(17)	Pd(1)-N(13)-C(12)	121.49(15)
N(2)-C(9)	1.300(3)	Pd(1)-N(2)-C(9)	121.82(15)
N(13)-C(12)	1.300(3)	N(2)-C(9)-C(10)	129.00(2)
C(10)-C(11)	1.442(3)	N(13)-C(12)-C(11)	128.90(2)
C(10)-C(22)	1.419(3)		
C(22)-C(21)	1.389(3)		
C(21)-C(20)	1.394(3)		
C(20)-C(11)	1.414(3)		

In order to introduce further steric bulk into the AFA ligand *N*,*N*'-bis(2,6-diisopropylphenyl)-6-aminofulvene-2-aldimine (**2.25**) was synthesised. All attempts to synthesise a halide-bridged complex with the ligand **2.25** were unsuccessful. Furthermore, none of the bis-chelated complex, which is formed by treatment of all other AFA ligands with [$PdCl_2(NCPh)_2$], is formed in this case. Only unreacted ligand could be isolated from the reaction mixture. It is therefore clear that the

presence of the 2,6-diisopropylphenyl substituents in **2.27** not only prevents the coordination of two ligands to the same metal, but precludes complexation altogether. It is apparent from the above results that, if there is a steric regime which will permit the formation of our desired species, $[(AFA)Pd(\mu\text{-}Cl)]_2$, by hindering the formation of the apparently preferred bis-chelate complex while still permitting the coordination of one ligand, it lies somewhere between the Cy_2AFA and $(dipp)_2AFA$ ligands. Two further ligands have been prepared to explore this space containing mesityl (**2.22**) and *tert*-butyl (**2.26**) nitrogen substituents.[1] Unfortunately these two ligands lie on either side of the divide with $(mesityl)_2AFA$ failing to coordinate to Pd and $^tBu_2AFA$ forming the bis-chelated complex **2.38** only.

2.3.5 Synthesis and characterisation of [((tert-butyl)$_2$AFA)$_2$Pd]

Instead of forming a halide-bridged dimer, the reaction of Li^tBu_2AFA with $[PdCl_2(NCPh)_2]$ forms a bis-chelated complex $[(^tBu_2AFA)_2Pd]$ (**2.38**) (Scheme 2.6). The ^1H NMR spectrum of **2.38** shows that upon coordination the original doublet at δ 7.95 for the HC=N protons in the free ligand appear as a sharp singlet at δ 7.78 (H1/H7). The protons H3/H5 are also shifted to lower frequency and appear as a doublet at 6.55 ppm. The H4 proton is shifted to higher frequency and appears as a triplet at 6.46 ppm and the methyl protons of the ^{t}Butyl groups appear as a singlet at 1.38 ppm.

2.3.6 Synthesis and characterisation of [(Ph$_2$AFA)Ni(η^3-C$_3$H$_5$)]

The complex **2.40** was obtained in 38% crude yield by the reaction of the deprotonated ligand with ½ equivalent of $[(C_3H_5)NiBr]_2$ (Fig. 2.21).

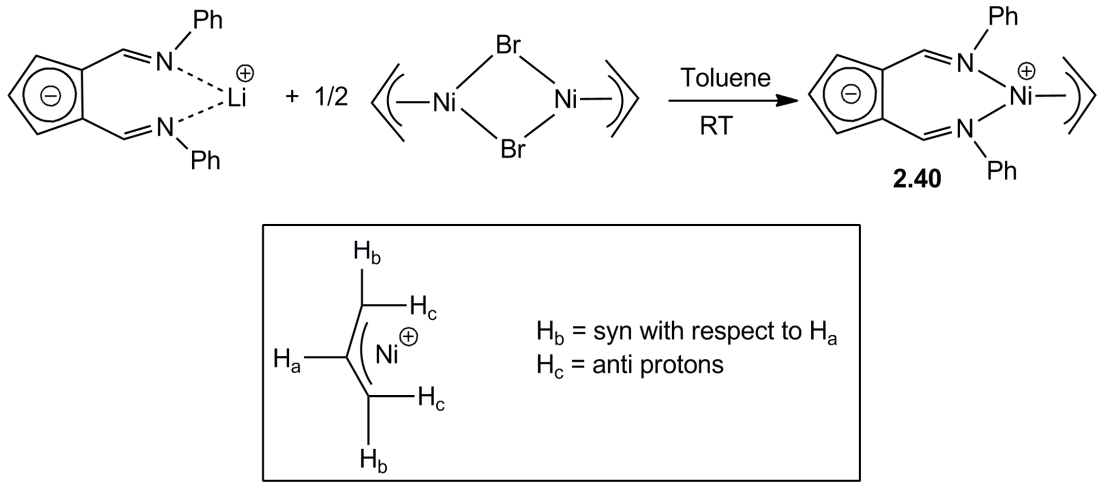

Figure 2.21. Synthesis of [(Ph_2AFA)Ni(η^3-C_3H_5)].

The ^{1}H NMR spectrum of **2.40** shows that upon metallation, the C_5-ring protons of the AFA ligand are shifted upfield. The doublet originating from the two HC=N protons (H1/H7) in the free ligand due to coupling with the NH proton appears as a singlet and is shifted upfield to δ = 8.25. The protons H3/H5 and H4 also shifted to upfield and appear as a doublet at δ = 6.89 and triplet at δ = 6.40 respectively with coupling constant J = 3.63 Hz. The H_b protons (*syn* with respect to H_a) of allyl ligand is less shielded than the H_c protons (*anti* protons), which are more strongly influenced by the transition metal. As expected the protons of the CH_2 groups of allyl ligand appear as two distinct doublets. The H_c protons (anti with respect to H_a) of the allyl ligand appear as a doublet and shifted upfield (δ = 2.21, J = 7.09 Hz) compared to the H_c protons of the starting material, π-allyl nickel bromide (δ = 3.15, J = 6.46 Hz). On the other hand, a small upfield shift for the doublet H_b proton (δ = 1.88, J = 13.40 Hz) has been found compared to the starting nickel reagent (δ = 2.1, J = 13.08 Hz). The CH proton of the allyl is also shifted upfield and appears as triplet of triplets. The high solubility of the complex **2.40** in all polar and non-polar solvents makes it difficult to purify from the unreacted ligand. The complex is sensitive to air and moisture.

2.3.7 Attempted synthesis of [(2-methoxyphenyl)$_2$AFAPd(Cl)]

Hemilabile ligands are polydentate chelates that contain at least two different types of bonding groups; substitutionally inert donor (X) and substitutionally labile donor (Y). The inert donor (X) binds strongly to the metal while the labile donor (Y) is weakly bonding. Therefore coordinating ligands or solvent molecules (Z) can easily displace the labile donor. Thus the labile group (Y) be easily displaced from the metal center, yet it remains available for re-coordination to the metal (Fig. 2.22). Metal complexes containing hemilabile ligands have been found to be catalytically active in a range of reactions, including hydrogenation, carbonylation, hydroformylation of olefins and epoxides, epoxydation, olefin (co)dimerisation and copolymerisation and ring-opening metathesis polymerisation (ROMP).[17, 18]

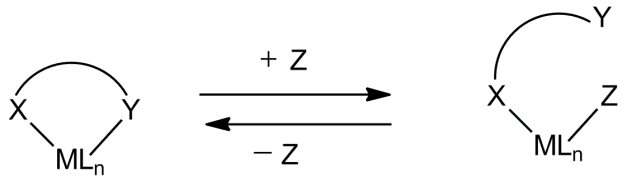

X = substitutionally inert group
Y = substitutionally labile group
Z = ligand or solvent

Figure 2.22. Transition metal complexes of hemilabile ligand having labile (Y) and inert donor (X).

In the late transition metal complexes, the phosphine donor is often chosen as the substitutionally inert group and a group ligating through a heteroatom such as O or N is chosen as the substitutionally labile functionality. The lability of the nitrogen donor is generally lower than that of oxygen donor, dependent on the identity of the metal. Thus metal-oxygen bonds can be cleaved reversibly without separation of the oxygen donors from the complex fragment. Metal-oxygen interaction also increases electron density at the metal center.[19]

In order to exploit the hemilabile property of the metal-oxygen bond, the synthesis of the complex **2.41** was attempted by reacting the deprotonated (2-methoxyphenyl)$_2$AFA ligand with $(PhCN)_2PdCl_2$. Unfortunately, the reaction provides a bis-chelated complex **2.42** (Fig. 2.23).

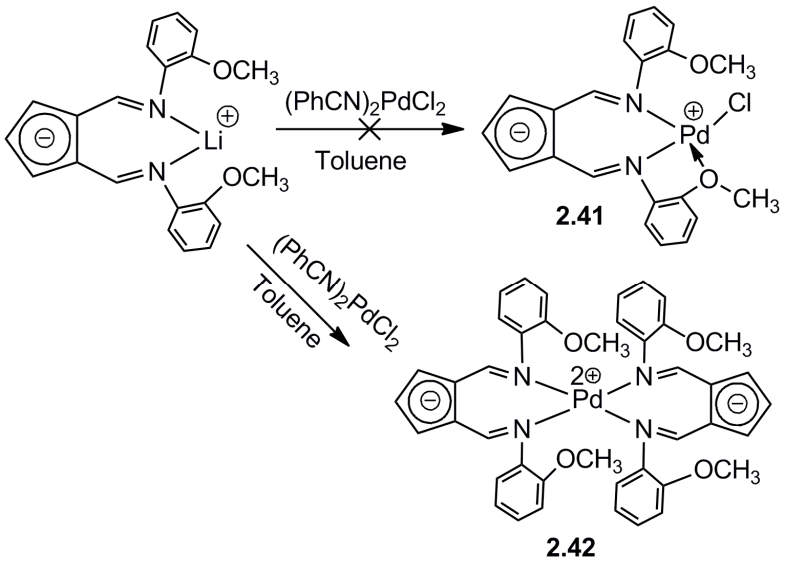

Figure 2.23. Attempted synthesis of [(2-methoxyphenyl)$_2$AFAPd(Cl)].

The ^{1}H NMR spectrum of the complex **2.42** shows that upon metallation all of the C_5-ring protons of the ligand moiety shifted upfield. The doublets at δ 8.28 of the H1/H7 protons in the free ligand (**2.24**) appear as a singlet at δ 7.66 in the complex. The disappearance of the NH peak in **2.42** also indicates metallation of the AFA ligand. The H3/H5 and H4 protons appear as doublet and triplet with coupling constant J = 3.65 Hz. The H3/H5 and H4 protons shifted upfield from the free ligand at δ 7.02 and 6.43 to 6.60 and 6.33 respectively. The methoxy proton appears as a singlet at δ 3.50 whereas in the ligand **2.24**, it appears at δ 3.54. The mass spectrum of **2.42** (+ve FAB) showed a molecular ion peak at m/z 767.6 consistent with the formulation.

2.3.8 Attempted synthesis of [$Cy_2AFAHPdCl_2$]

The complex **2.43** could be a precursor to an ethylene polymerisation catalyst which could be activated by MAO in presence of ethylene.

In an attempt to synthesise **2.43**, the ligand Cy_2AFAH was reacted with bis(acetonitrile)palladium(II)dichloride in THF. Unfortunately, the reaction instead forms the protonated ligand (**2.44**) (Fig. 2.24). The yield of the product is 53%. The brown product **2.44** is insoluble in hexane, toluene and ether but soluble in acetonitrile.

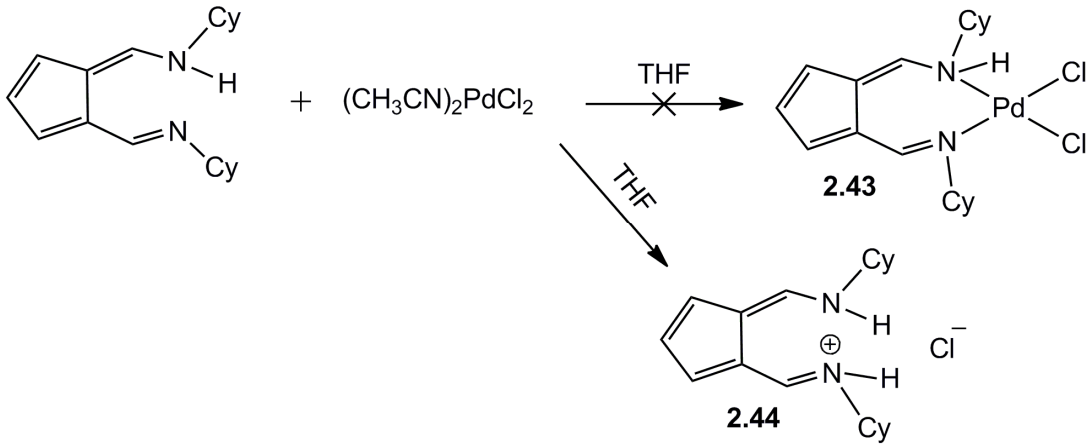

Figure 2.24. Attempted synthesis of [$Cy_2AFAHPdCl_2$].

The ^1H NMR spectrum of **2.44** shows that the NH peak is shifted upfield with respect to the free ligand (NH, δ = 14.04) and appear as a broad peak at δ 8.75. All the other C_5-ring protons of **2.44** are shifted downfield. For example, the H1/H7 proton appear as a doublet at 8.06 ppm with coupling constant J = 15.65 Hz where as in the ligand (**2.23**), it was at 7.94 with coupling constant J = 6.60 Hz. The H3/H5 and H4 protons shifted downfiled with respect to ligand **2.23** and appear at 7.21 and 6.44 ppm respectively. The protons H3/H5 and H4 in the ligand (**2.23**) appear at 6.81 and 6.34 ppm respectively. The mass spectrum of **2.44** (+ve FAB) showed a molecular ion peak at m/z 285 consistent with the formation of the protonated ligand. Addition of trifluoroacetic acid (CF_3-COOH) to the ligand (**2.23**) also provided the protonated ligand (**2.44**) and thus confirmed its formation in the reaction with

$(MeCN)_2PdCl_2$. In order to remove any possible acidic proton present in the bis(acetonitrile)palladium(II)dichloride, the hindered base 2,2,6,6-tetramethyl piperidine was added to a solution of $(CH_3CN)_2PdCl_2$ in toluene followed by addition of a solution of the ligand (**2.23**) in toluene. Unfortunately under these conditions only unreacted ligand was found in the reaction mixture and coordination had therefore failed. It might be possible that upon formation of the desired complex **2.43**, HCl might eliminate from the complex (**2.43**) and act as a source of proton to protonate the ligand (**2.23**).

2.3.9 Attempted synthesis of [Ph_2AFAPd(OAc)]

In order to synthesise the complex **2.45**, the deprotonated ligand was reacted with two equivalents of palladium acetate [$Pd(OAc)_2$]. However, the reaction provides the bis-chelated complex **2.47** (Fig. 2.25). Upon metallation, all the C_5-ring protons of the AFA moiety shifted upfield. Metal coordination of the ligand is confirmed by a singlet at 7.44 ppm for H1/H7, which appear as a doublet in the free ligand Ph_2AFAH due to coupling to the N-H proton. The protons H3/H5 appear as a doublet at 6.72 ppm and the H4 proton as a triplet at 6.42 ppm whereas in the free ligand those protons appear at 7.05 and 6.47 ppm respectively. Mass spectrum of **2.47** (EI) showed a molecular ion peak at m/z 648.1 consistent with the formulation.

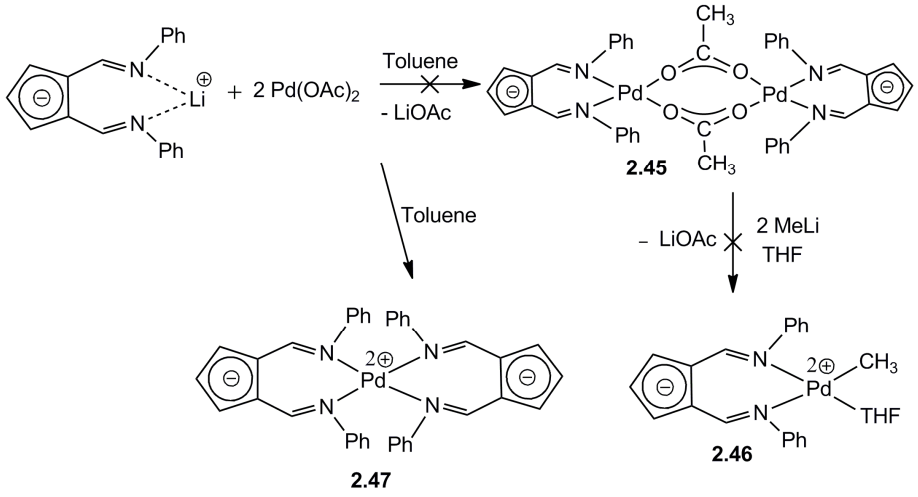

Figure 2.25. Attempted synthesis of [Ph_2AFAPd(OAc)].

2.3.10 Attempted synthesis of [$Ph_2AFAPd(Cl)(CH_3CN)$]

The deprotonated ligand was slowly added to a solution of $(CH_3CN)_2PdCl_2$ in toluene. However, the desired complex **2.48** was not formed. Instead, a bis-chelated complex, $[(Ph_2AFA)_2Pd]$ (**2.47**) was isolated (Fig. 2.26).

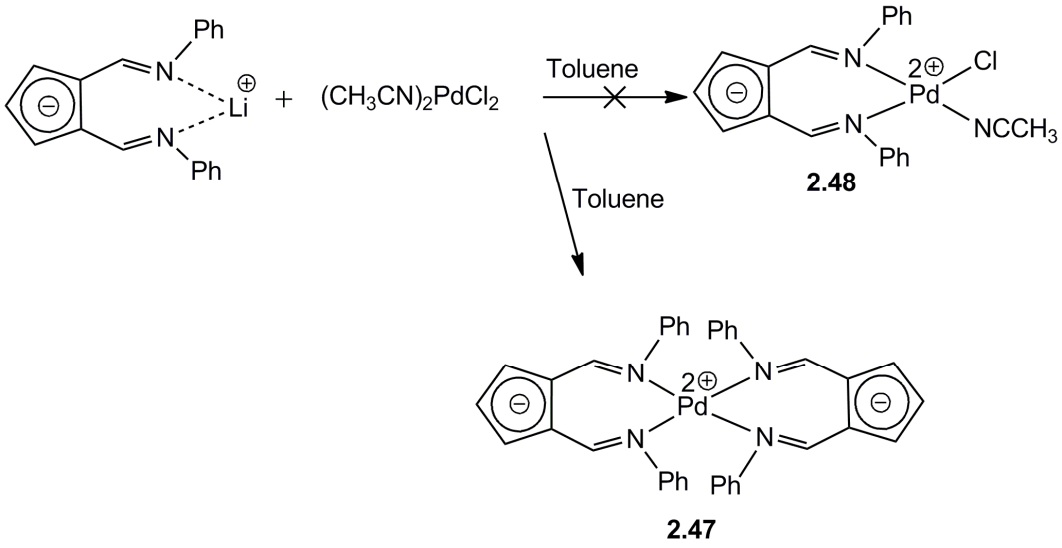

Figure 2.26. Attempted synthesis of [$Ph_2AFAPd(Cl)(CH_3CN)$].

2.3.11 Attempted synthesis of [$(Ph_2AFA)Ni(CH_3)(PMe_3)$]

Several attempts to synthesise **2.49** (Fig. 2.27) were unsuccessful. Only unreacted ligand was found in the reaction mixture. The [trans-$Ni(Cl)(Me)(PMe_3)_2$][20] was prepared by reacting MeLi with a solution of $[(Me_3P)_2NiCl_2]$ in THF.

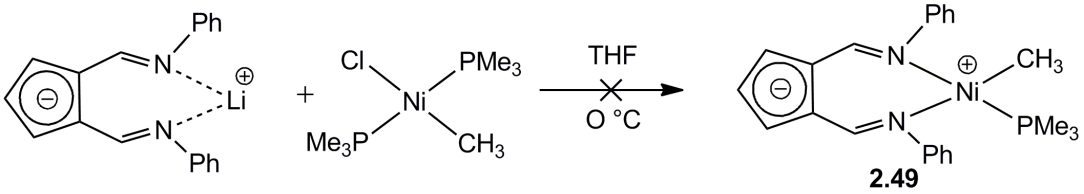

Figure 2.27. Attempted synthesis of [$(Ph_2AFA)Ni(CH_3)(PMe_3)$].

2.3.12 Attempted synthesis of [(Ph_2AFA)Ni(Cl)(PPh_3)]

In an attempt to synthesise **2.50** (Fig. 2.28), $LiPh_2AFA$ in toluene was slowly added to a suspension of $NiCl_2(PPh_3)_2$ in toluene. The $NiCl_2(PPh_3)_2$ is insoluble in toluene and THF. However, the nickel precursor dissolved once the deprotonated ligand was added to it. The ^1H NMR spectrum shows the product is a bis-chelated complex **2.51** instead of **2.50**. The ^1H NMR spectrum in $CDCl_3$ of **2.51** shows a singlet at δ 7.08 for H1/H7 protons. The H3/H5 and H4 protons appear as a doublet at 6.78 ppm and a triplet at 6.56 ppm respectively. Mass spectrum of **2.51** (EI) showed a molecular ion peak at m/z 600.18 consistent with the formulation.

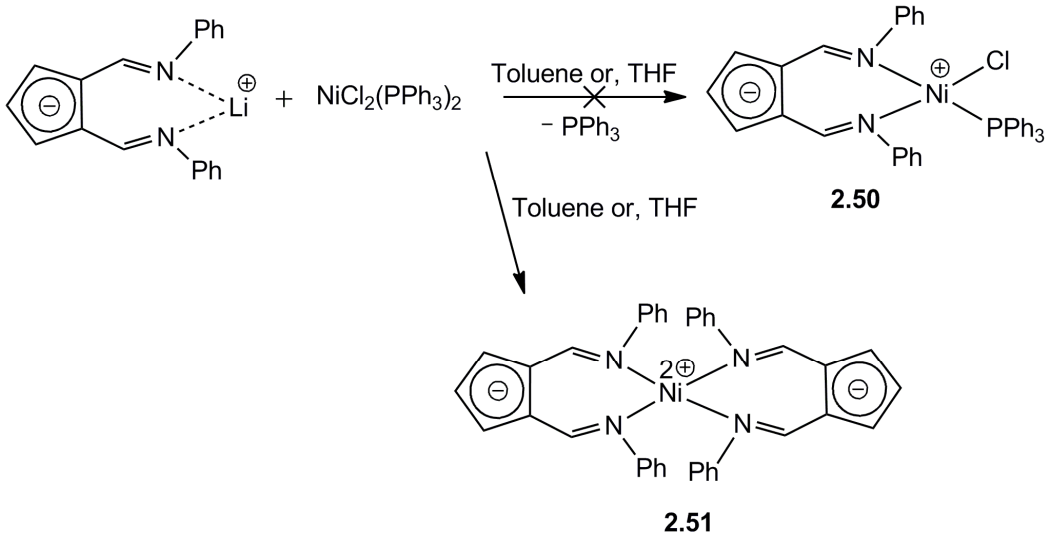

Figure 2.28. Attempted synthesis of [(Ph_2AFA)Ni(Cl)(PPh_3)].

2.3.13 Attempted synthesis of [(Cy_2AFA)Pd(Cl)(NCPh)]

In order to synthesise **2.52** (Fig. 2.29), $LiCy_2AFA$ in toluene was added dropwise to a solution of $(PhCN)_2PdCl_2$ in toluene. Only unreacted ligand was found in the reaction mixture. Conversely, when $(PhCN)_2PdCl_2$ was added to the deprotonated ligand, the bis-chelated complex (**2.37**) was formed.

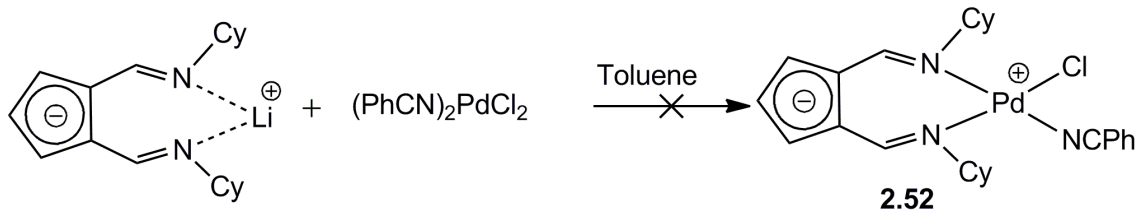

Figure 2.29. Attempted synthesis of [(Cy_2AFA)Pd(Cl)(NCPh)].

2.3.14 Attempted synthesis of [Ph_2AFA($SiMe_3$)]

In an attempt to synthesise **2.53** (Fig. 2.30), chlorotrimethylsilane ($ClSiMe_3$) was added to a solution of $LiPh_2$AFA in toluene. Only unreacted ligand and some undefined species were found in the reaction mixture. Similar results were obtained when THF was used a solvent.

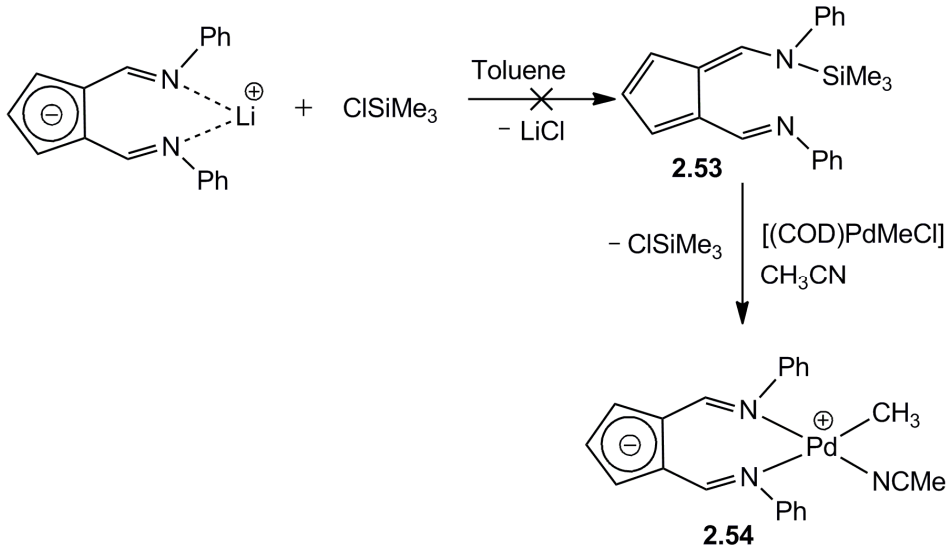

Figure 2.30. Attempted synthesis of [Ph_2AFA($SiMe_3$)].

2.3.15 Attempted synthesis of [(Ph_2AFAAg($NCCH_3$)]

In an attempt to synthesise **2.55** (Fig. 2.31), a solution of [(COD)Pd(Me)Cl] in acetonitrile was added to a mixture of Cy_2AFAH and Ag_2O in acetonitrile. The ^{1}H NMR spectrum shows only unreacted ligand is present in the reaction mixture. The rationale for using Ag_2O in this reaction is that it acts a base to abstract the acidic

proton from the ligand and also acts as a halide abstracting agent. Ag_2O is insoluble in all organic solvents including acetonitrile due to its three-dimensional structure with metal-oxygen bonding; however such a strategy has been shown to be successful in other systems.

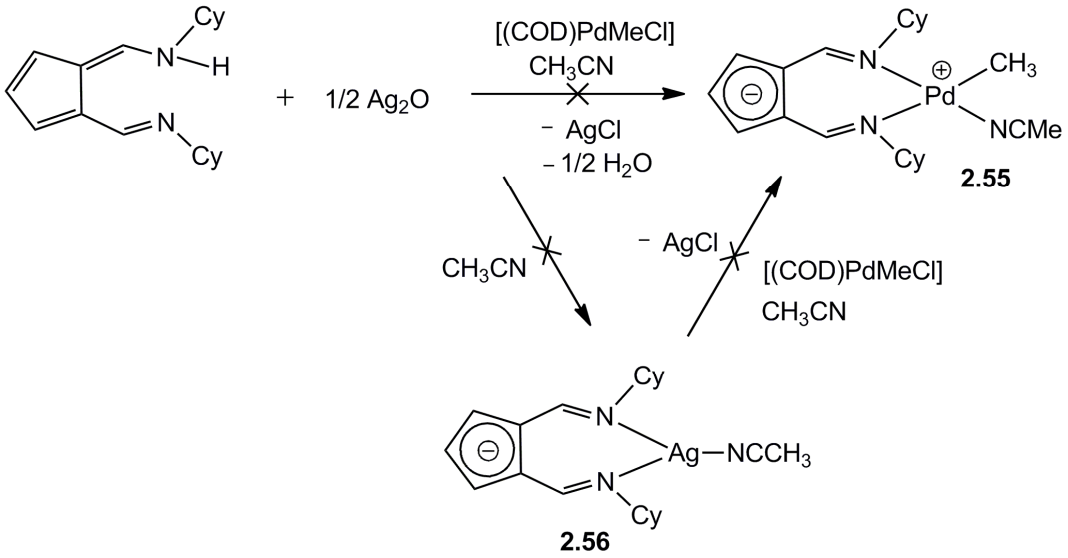

Figure 2.31. Attempted synthesis of [(Ph_2AFAAg(NCCH$_3$)].

2.3.16 Attempted synthesis of [Ph_2AFAHPd(Me)Cl]

In an attempt to synthesise **2.57** (Fig. 2.32), a solution Ph_2AFAH in toluene was reacted with a solution of [(COD)Pd(Me)Cl] in toluene. However, ^{1}H NMR shows only unreacted ligand is present in the mixture. It was then heated at 80 ºC. A thin layer of silvery shining material was seen on the surface of the glass vessel. It seems that during heating palladium metal is formed from the [(COD)Pd(Me)Cl]. The ^{1}H NMR spectrum of this mixture again shows only unreacted ligand.

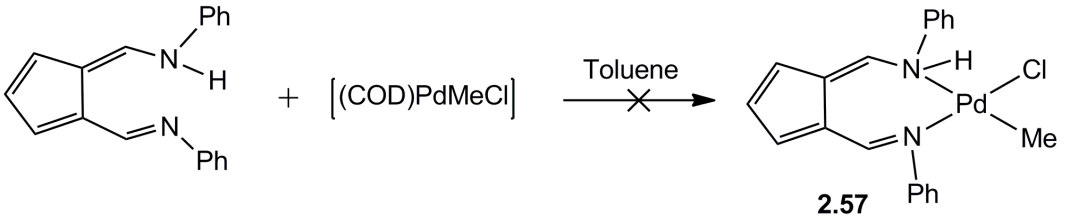

Figure 2.32. Attempted synthesis of [Ph_2AFAHPd(Me)Cl].

2.4 Ethylene polymerisation tests

The complexes [(Ph_2AFA)Pd(Me)(DMAP)] (**2.28**) and [(Ph_2AFA)Pd(N,N-dimethylbenzylamine-2-C,N)] (**2.31**) were tested as catalysts for ethylene polymerisation at 5 bar and 50 ºC. Activation of both complexes with Lewis acids such as BF_3 and $B(C_6F_5)_3$ was also explored. Unfortunately none of the complexes were active for ethylene polymerisation. An aliquot of the mother liquor was also analyzed by EI-MS to detect any formation of oligomers. However, ethylene oligomers were not observed either. The ^{1}H NMR study of the Lewis acid treatment of **2.28** shows that $B(C_6F_5)_3$ abstracts the Pd-bound CH_3 group instead of abstracting DMAP, forming $[CH_3B(C_6F_5)_3]^-$ species (δ_H 1.18, s, br). This is not surprising as $B(C_6F_5)_3$ is known to activate Brookhart type Pd dimethyl complexes [(diimine)$PdMe_2$] and metallocene precatalysts by methyl abstraction.[21-24] The $B(C_6F_5)_3$ has the ability to scavenge PPh_3 and activate ethylene polymerisation catalyst. Activation of the complex [(Ph_2AFA)Pd(CH_3)(PPh_3)] with $B(C_6F_5)_3$ as PPh_3 scavenger at 5 bar and 50 ºC was not successful.

The reaction of LiPh_2AFA with [(COD)PdMeCl] in presence of ethylene at 5 bar and 50 ºC could provide a phosphine free active catalyst (Fig. 2.33). However, this system did not provide any polymer.

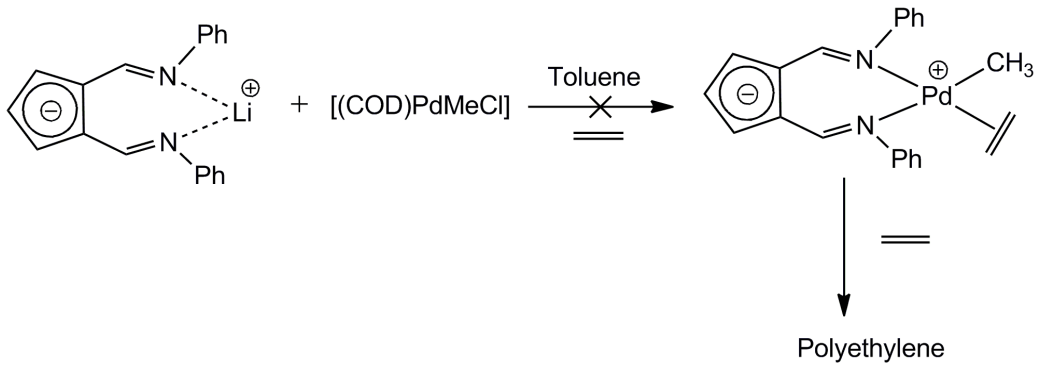

Figure 2.33. Attempted ethylene polymerisation.

2.5 Conclusions

The 6-aminofulvene-2-aldimine ligands (AFA) have been exploited in an attempt to develop Group 10 (Ni and Pd) late transition metal ethylene polymerisation catalysts. A range of complexes of the AFA ligand system have been synthesised and characterised. Three promising zwitterionic square planar complexes **2.28, 2.31** and **2.40** have been synthesised and characterised. Several attempts to activate the complexes **2.28** and **2.31** with Lewis acid (e.g. BF_3 and $B(C_6F_5)_3$) for ethylene polymerisation were not successful. The critical step for the coordination olefin polymerisation catalysis is the activation of the catalyst precursor which generates the active site. The allyl complex $(Ph_2AFA)Ni(\eta^3\text{-}C_3H_5)$ (**2.40**) needs further purification for its application in ethylene polymerisation.

An ideal phosphine-free catalyst precursor would be the halide-bridged dimers of the form $[(R_2AFA)Pd(\mu\text{-}X)]_2$. Although the neutral α-diimine ligands are capable of forming halide-bridged dimers, the synthesis of halide-bridged dimers appears problematic with anionic AFA ligands. Several attempts have been made to develop halide-bridged complexes using the anionic R_2AFA ligands by tailoring the steric properties of the ligand framework. However, introduction of bulky N-substituents in the AFA ligand did not afford any halide-bridged complexes; instead the bis-chelated complexes are formed, *e.g.* $[(Cy_2AFA)_2Pd]$ and $[(^tBu_2AFA)_2Pd]$. It can be concluded that formation of halide-bridged complexes using R_2AFA ligands is not solely

dependent on steric factors, and electronic factors also play an important role. The bis-ligated complexes are not catalytically active as the presence of a cis- oriented metal-carbon bond is a pre-requisite for the olefin insertion catalysis.

Employing R_2AFAH as a neutral ligand and exploiting its lone pair on nitrogen for coordination to Pd to form complexes R_2AFAHPdCl_2 or R_2AFAHPdMeCl was not successful. The reaction of LiPh_2AFA with metal precursors such as Pd$(OAc)_2$, $(Ph_3P)_2NiCl_2$ and $(CH_3CN)_2PdCl_2$ provided bis-chelated complexes (**2.47**, **2.51**, **2.47**). The reaction of the Cy_2AFAH ligand with $(CH_3CN)_2PdCl_2$ provided a protonated ligand (**2.44**) whereas the reaction of the deprotonated ligand LiPh_2AFA with the same metal precursor $(CH_3CN)_2PdCl_2$ provided a bis-chelated complex (**2.47**). It seems that the formation of bis-ligated complexes predominates in the AFA ligand system where precipitation of insoluble inorganic salt e.g, LiCl, NaCl and KBr are the driving force of the reaction. The driving force of **2.47** and **2.51** were the formation of LiCl salt.

Application of organometallic precursors such as (tmeda)$NiMe_2$ (tmeda = N,N,N',N'-tetramethylethylenediamine) would be an ideal metal precursor and this could provide an ideal catalyst of the form [(R_2AFA)Ni(CH_3)(CH_3CN)] employing labile donor acetonitrile.

Development of bimetallic complexes for ethylene polymerisation by exploiting the ambidentate nature of the AFA ligand will be discussed in the next chapter.

References

1. U. Müller-Westerhoff, *J. Am. Chem. Soc*, 1970, **92**, 4849.
2. H. L. Ammon and U. Mueller-Westerhoff, *Tetrahedron*, 1974, **30**, 1437.
3. K. Hafner, K. H. Vöpel, G. Ploss and C. König, *Org. Synth*, 1967, **47**, 52.
4. K. Hafner, K. H. Vöpel, G. Ploss and C. König, *Justus Liebigs Ann. Chem*, 1963, **661**, 52.
5. P. J. Bailey, D. Lorono-Gonzalez and S. Parsons, *Chem. Commun*, 2003, 1426.
6. P. J. Bailey, M. Melchionna and S. Parsons, *Organometallics*, 2007, **26**, 128.
7. P. J. Bailey, A. Collins, P. Haack, S. Parsons, M. Rahman, D. Smith and F. J. White, *Dalton Trans*, 2010, **39**, 1591.
8. N. Etkin, C. M. Ong and D. W. Stephan, *Organometallics*, 1998, **17**, 3656.
9. Y. F. Doi, T. JP Patent 10298225 to Mitsui Chemicals Inc., Japan, priority date April 25, 1997.
10. J. M. Chitanda, D. E. Prokopchuk, J. W. Quail and S. R. Foley, *Organometallics*, 2008, **27**, 2337.
11. C. M. Ong and D. W. Stephan, *Inorg. Chem*, 1999, **38**, 5189.
12. R. E. Rulke, J. M. Ernsting, A. L. Spek, C. J. Elsevier, P. W. N. M. van Leeuwen and K. Vrieze, *Inorg. Chem*, 1993, **32**, 5769.
13. A. C. Cope and E. C. Friedrich, *J. Am. Chem. Soc*, 1968, **90**, 909.
14. B. Rieger, L. S. Baugh, S. Kacker and S. Striegler, Late transition metal polymerisation catalysis, Wiley-VCH, 2003, page. 64.
15. T. V. Laine, K. Lappalainen, J. Liimatta, E. Aitola, B. Lofgren and M.Leskela, *Macromol. Rapid Commun*, 1999, **20**, 487.
16. D. J. Tempel, L. K. Johnson, R. L. Huff, P. S. White and M. Brookhart, *J. Am. Chem. Soc*, 2000, **122**, 6686.
17. C. S. Slone, D. A. Weinberger and C. A. Mirkin, *Prog. Inorg. Chem*, 1999, **48**, 233.
18. P. Braunstein and F. Naud, *Angew. Chem. Int. Ed*, 2001, **40**, 680.
19. E. T. Singewald, C. A. Mirkin, A. D. Levy and C. L. Stern, *Angew. Chem. Int. Ed*, 1994, **33**, 2473.
20. H. F. Klein and H. H. Karsch, *Chem. Ber*, 1972, **105**, 2628.

21. L. K. Johnson, C. M. Killian and M. Brookhart, *J. Am. Chem. Soc*, 1995, **117**, 6414.

22. X. Yang, C. L. Stern and T. J. Marks, *J. Am. Chem. Soc*, 1994, **116**, 10015.

23. X. Yang, C. L. Stern and T. J. Marks, *J. Am. Chem. Soc*, 1991, **113**, 3623.

24. S. D. Ittel, L. K. Johnson and M. Brookhart, *Chem. Rev*, 2000, **100**, 1169.

Chapter 3 Metalloligands of AFA and Corresponding Bimetallic Complexes

3.1 Introduction

The aminofulvene-aldiminate (AFA) is a novel ligand which affords transition metal complexes both via η^5- as well as κ^2-coordination modes. Bailey and co-workers[1] have exploited the ambidentate nature of this fulvene aldimine [N,N]H ligand and synthesised the η^5-coordinated complex [Cp*Ru(η^5-Ph_2AFA)] (**3.2**) (Fig. 3.1). The reaction of the tetrahedral zinc complex [Zn(κ^2-$Ph_2AFA)_2$] (**3.1**) with two equivalents of [Cp*Ru$(MeCN)_3$][BF_4] afforded **3.2**. In the solid state **3.2** is air and moisture stable but in solution it is readily protonated[2] due to its high basicity and forms its conjugate acid [Cp*Ru(η^5-Ph_2AFA)(H)] (**3.3**) (Fig. 3.1). However, Bailey group could not obtain the crystal structure of **3.3**. Presumably, the complex **3.2** might have formed through a Zn/Ru bimetallic or Ru/Zn/Ru trimetallic intermediate which is too unstable and decomposes with the release of **3.2**. Moreover, the electron–rich Cp^*Ru^+ synthon has high affinity towards π-aromatic systems. Thus coordination of Cp*Ru via the C_5 ring of the AFA ligand could also be a probable explanation. The ^{1}H NMR of **3.2** shows the expected upfield shift of the H3/H5 and H4 protons of the C_5 moiety of the AFA ligand as a consequence of the η^5-coordination of the ruthenium metal.

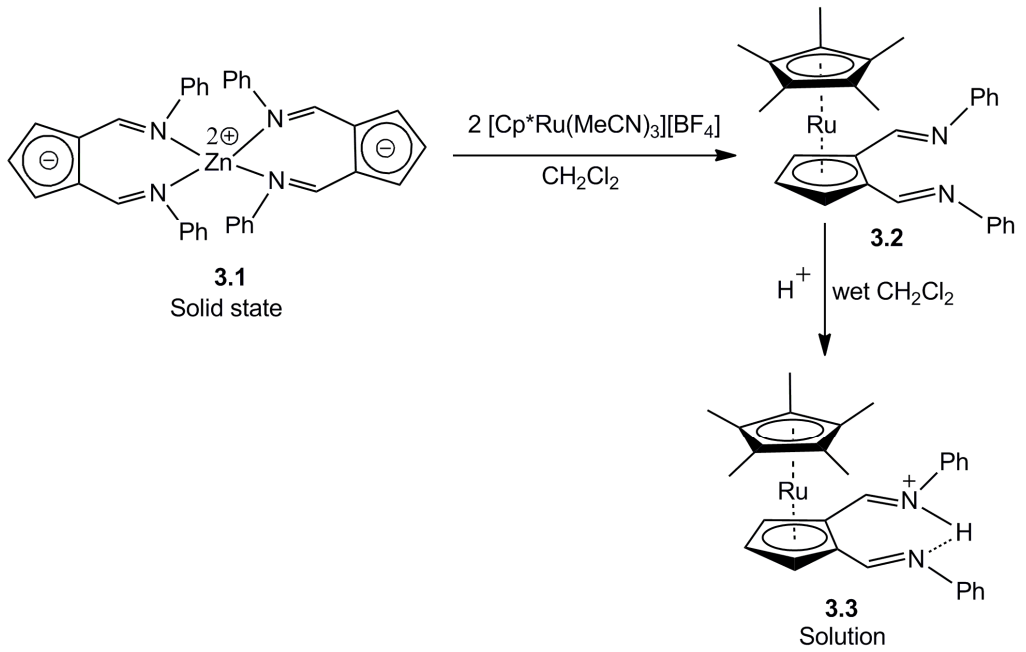

Figure 3.1. Synthesis of [Cp*Ru(η^5-Ph_2AFA)] (3.2).

In an attempt to find an alternate approach of synthesis of **3.2**, and also to establish the fact that coordination via the C_5 moiety is favourable in place of the usual N chelation**,** the Bailey group has reacted $LiPh_2AFA$ with $[Cp^*Ru(MeCN)_3][BF_4]$ (Fig. 3.2). However, the reaction did not afford complex **3.2**.

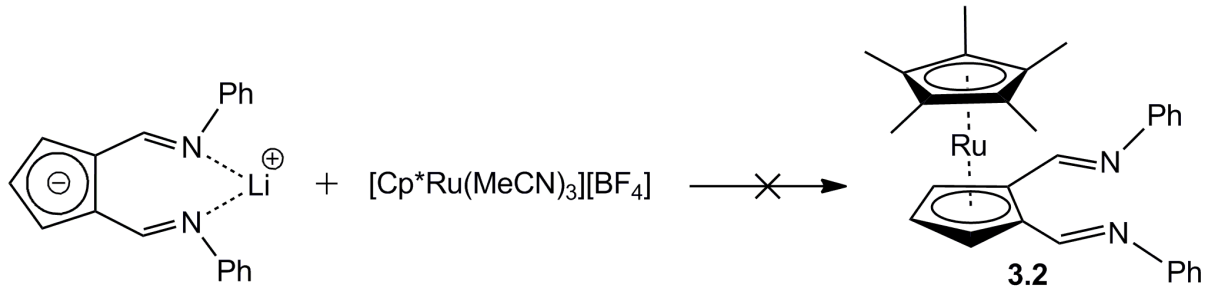

Figure 3.2. Attempted alternative synthesis of 3.2.

Bailey and co-workers[1] also synthesised a trimetallic $PdRu_2$ species (**3.5**). The treatment of $[(Ph_2AFA)_2Pd]$ (**3.4**) with $[Cp^*Ru(NCMe)_3][BF_4]$ in DCM provided the trimetallic complex $[(Cp^*Ru)_2Pd(Ph_2AFA)_2]^{2+}$ (**3.5**) in which both of the cyclopentadienyl rings are coordinated to Ru (Fig. 3.3). The complex **3.5** has an

inversion center at the Pd atom, and both AFA ligands and Ru centers are therefore equivalent.

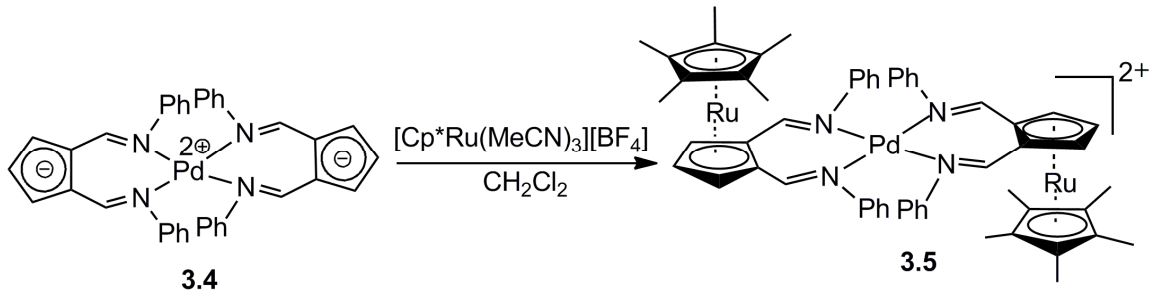

Figure 3.3. Synthesis of trimetallic complex $[(Cp^{*}Ru)_2Pd(Ph_2AFA)_2][BF_4]_2$.

The 6-amino-2-imidoyl-pentafulvene (**3.7-3.9**) (Fig. 3.4) is a structural analogue of the fulvene aldimine [N,N]H ligands. Bildstein and co-workers[3] have recently developed an easy synthetic route for the synthesis of these molecules (**3.7-3.9**) and also synthesised the corresponding cyclopentadienyl coordinated complex, 1,2-bis(imidoyl)pentamethylruthenocene (**3.10, 3.11**) (Fig. 3.5) by reacting the ligands (**3.7-3.9**) with the $Cp^{*}Ru^{+}$-synthon, $[Cp^{*}Ru(CH_3CN)_3]PF_6$.

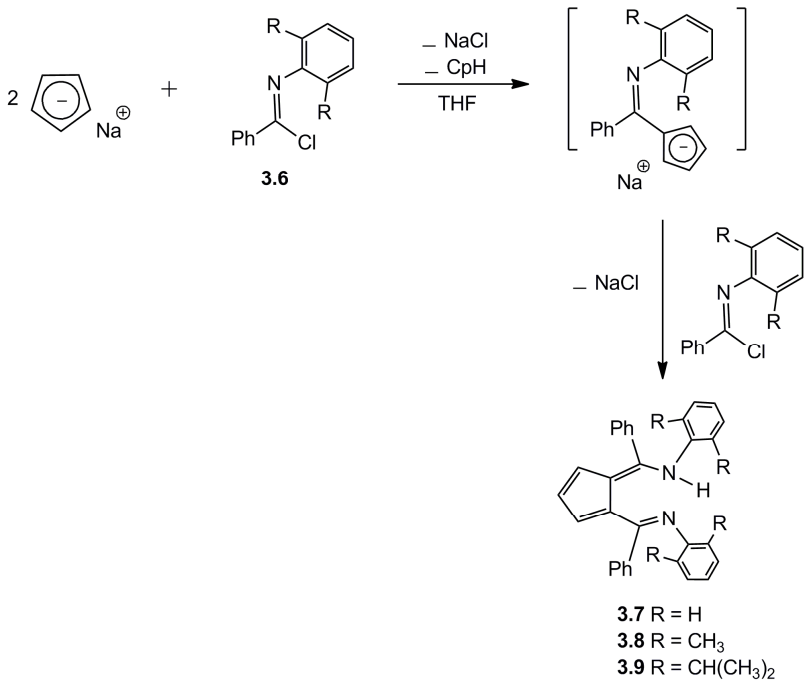

Figure 3.4. Synthesis of 6-amino-2-imidoyl-pentafulvene.

The bright yellow-orange 6-arylamino-2-imidoylpentafulvenes ligands (**3.7-3.9**) have been synthesised in a one-pot reaction by reaction of sodium cyclopentadienide with benzimidoyl chloride as the electrophilic reagents (Figure 3.4). In the first step of the synthesis one equivalent of sodium cyclopentadienide is substituted by a benzimidoyl chloride to give imidoylcyclopentadiene intermediate. In the second step, this intermediate is deprotonated by another equivalent of NaCp to give a sodium imidoylcyclopentadienide. Finally, electrophilic substitution with a second equivalent of imidoylchloride affords 1,2-bis(imidoyl)cyclopentadienes (**3.7-3.9**) (Fig. 3.4). The fulvenes **3.7-3.9** contain intramolecular N-H-N hydrogen bonds. The C-C and C-N bond distances of the enamine/imine part of the fulvenes are alternating between single and double bonds. The 6-arylamino-2-imidoylpentafulvenes (**3.7-3.9**) are ambidentate [N,N]H ligand systems. At low temperature, base such as n-butyllithium or KH in THF can easily deprotonate the 6-arylamino-2-imidoylpentafulvenes (**3.7-3.9**) ligands and can provide κ^2- or η^5-metal complexes depending on the hard/soft character of the metal electrophile. The coordination of a hard metal to **3.7-3.9** could provide κ^2-metal complexes. The reaction of the deprotonated 6-arylamino-2-imidoylpentafulvenes (**3.7-3.9**) ligands with $[Cp^*Ru(CH_3CN)_3]^+PF_6^-$ at room temperature gives new metalloligands 1,2-bis(imidoyl)pentamethylruthenocenes (**3.10, 3.11**) (Fig. 3.5). The air-stable, yellow compounds **3.10** and **3.11** behave as strong Brønsted bases and form seven-membered hydrogen-bridged chelate (conjugate acid, **3.10**$H^+PF_6^-$) upon protonation. Thus acidic conditions should be avoided during the synthesis. The high basicity indicates that **3.10** and **3.11** are highly electron-donating [N,N] ligand system. The electrochemical study of bis(imidoyl)(pentamethyl)ruthenocenes reveal that they are novel redox-active metalloligands.

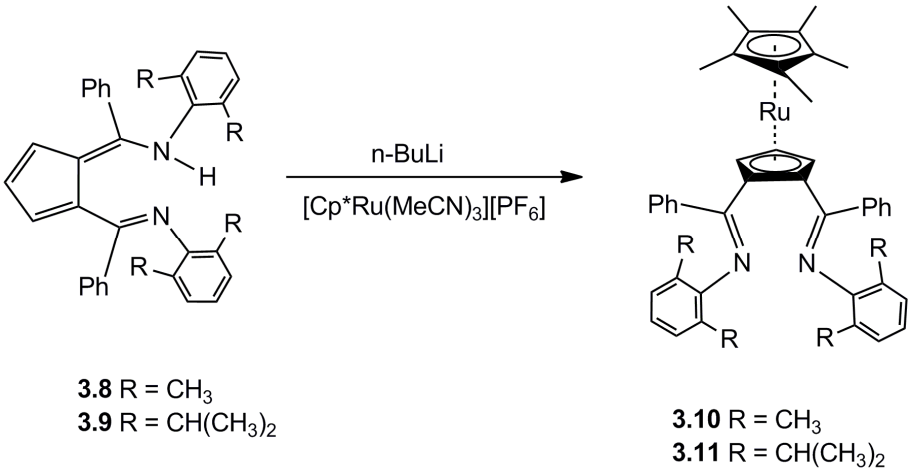

3.8 R = CH_3
3.9 R = $CH(CH_3)_2$

3.10 R = CH_3
3.11 R = $CH(CH_3)_2$

Figure 3.5. Synthesis of bis(imidoyl)(pentamethyl)ruthenocenes.

The amibidenate nature of the AFA ligand could be exploited to develop bimetallic bifunctional catalytic systems employing early and late transition metals (Fig. 3.6).

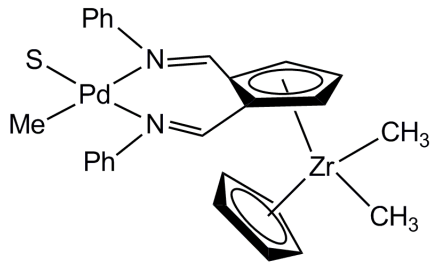

3.12

Figure 3.6. Possible bimetallic bifunctional catalytic system of AFA ligand.

The η^5-coordination of the C_5 moiety of the AFA ligand to group 4 metal (Ti, Zr) and κ^2-coordination by Pd could open a tantalizing prospect of putative complex (**3.12**). This bifunctional catalyst could act as tandem catalysts[4-9] for alkene co-polymerisation. The "Tandem catalysis" involves the cooperative action of two or more catalysts in a single reactor to yield a product that is not accessible by the individual catalysts. In tandem catalysis the first catalyst provides 1-alkene comonomer and the second catalyst uses the 1-alkene feed to copolymerise ethylene with 1-alkene.

For example, catalyst **I** (Fig. 3.7) dimerises ethylene exclusively into 1-butene, whereas catalyst **II** copolymerises 1-butene and ethylene in a tandem polymerisation to high molecular weight poly(ethylene-*co*-butene) materials.[9]

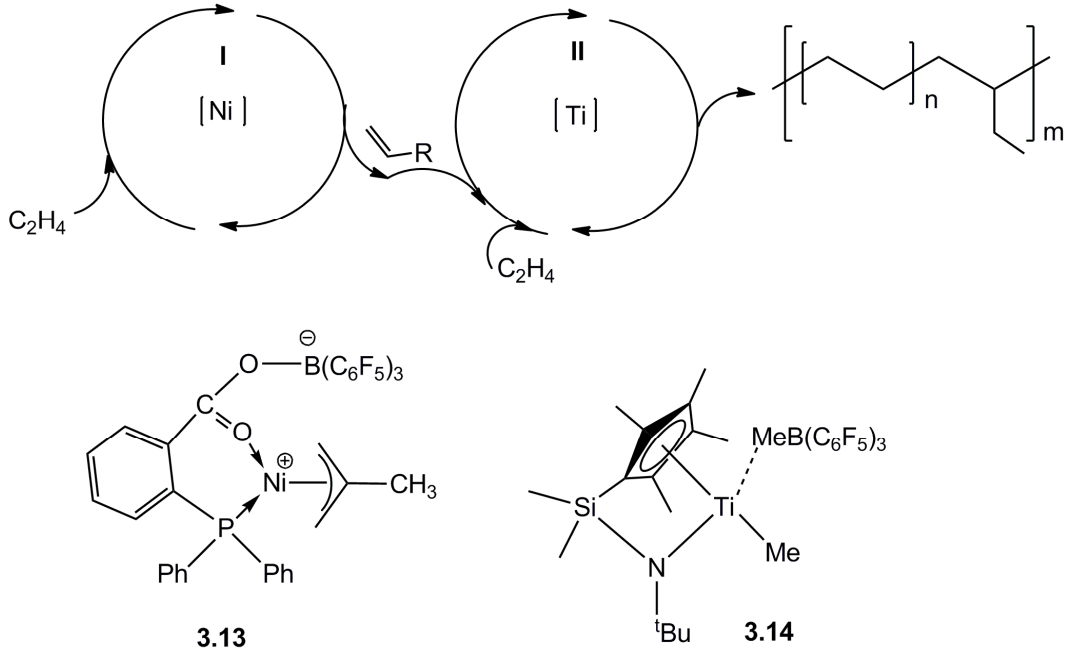

Figure 3.7. An example of tandem catalytic system.

Osakada and co-workers[10] have developed bimetallic early-late transition metal complexes for ethylene polymerisation (Fig 3.8). This system provided branched polymer and the structure and property of the polymer depends on the late transition metal component. The monometallic Pd complex with the iminopyridine ligand **3.16** provides neither polymer nor oligomer of ethylene. Thus polymerisation by **3.19** occurs exclusively at the Zr center and provides linear polymer. On the other hand, Zr-Ni dinuclear complex **3.21** affords branched polymer. Branched α-olefins formed at the Ni center undergo copolymerisation with ethylene at the Zr center. Ethylene polymerisation initiated by bimetallic complexes affords polymer with different micro-structures and properties.

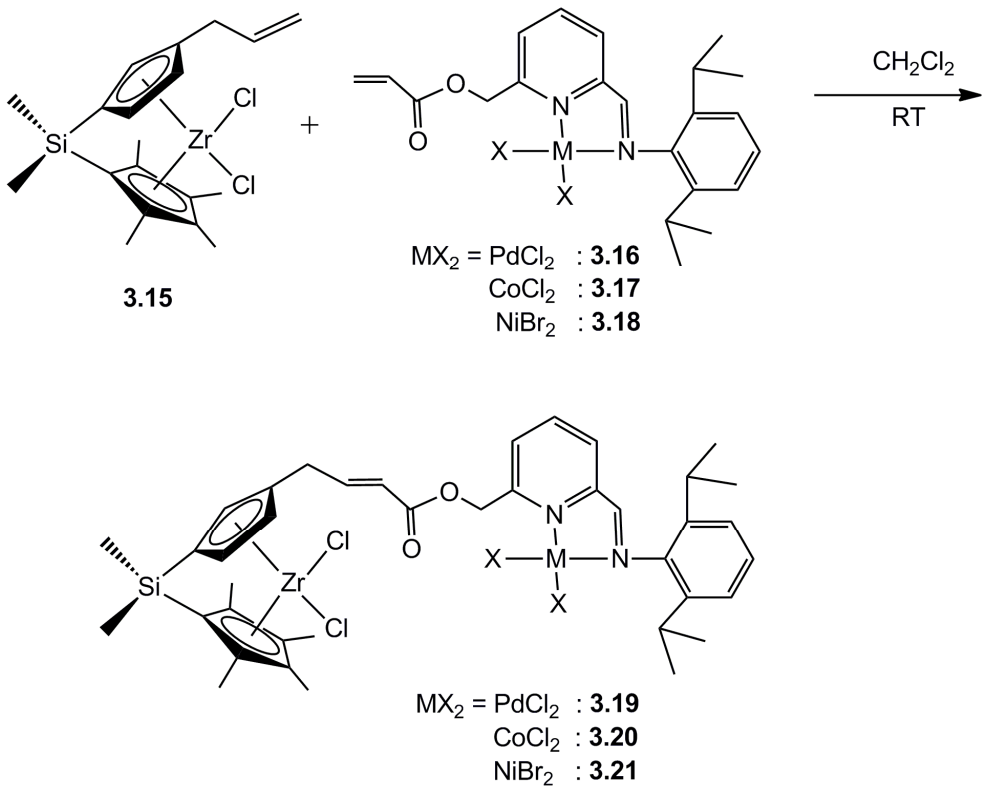

Figure 3.8. Early-late heterobimetallic complexes for ethylene polymerisation.

In this thesis we have independently developed an alternative approach (similar to the approach recently published by Bildstein and co-workers[3]) of the synthesis of **3.22** (Fig. 3.10) and also obtained its crystal structure. This chapter describes an alternate synthetic approach of **3.22** and some other C_5-coordinated complexes of the AFA ligand and the corresponding bimetallic complexes for possible application in alkene polymerisation.

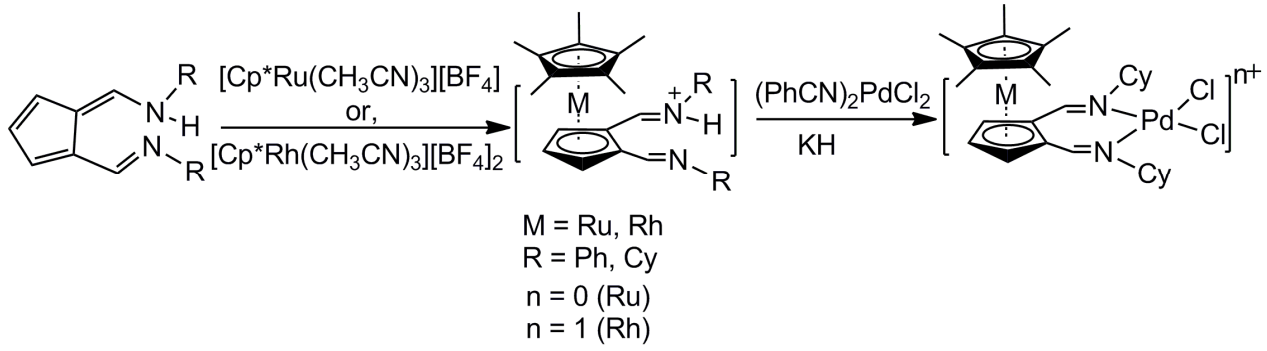

Figure 3.9. Outline of the synthesis of bimetallic complexes of AFA ligand.

The rational of the development of bimetallic catalyst employing AFA ligand is to investigate the charge effect in alkene polymerisation catalysis. Upon activation the monocationic Rh/Pd bimetallic complex would provide a dicationic active species which would in principle be a more highly active catalyst than the Brookhart mono cationic diimine catalysts. In a similar manner, the activation of neutral Ru/Pd bimetallic complex would provide a monocationic active species which would mimic the Brookhart mono cationic catalysts. And thus Rh/Pd bimetallic catalyst would be more active than Ru/Pd bimetallic catalyst.

3.2 Synthesis and characterisation of metalloligands

3.2.1 Synthesis and characterisation of $[Cp^*Ru^{II}(Ph_2AFA)H][BF_4]$

The reaction of Ph_2AFAH ligand with $[Cp^*Ru^{II}(CH_3CN)_3][BF_4]$ in DCM at room temperature gives the metalloligand $[Cp^*Ru^{II}(Ph_2AFA)H][BF_4]$ **(3.22)** (Fig. 3.10). The cationic complex **3.22** is air and moisture stable due to 18 electrons in the valence orbitals of the metal.

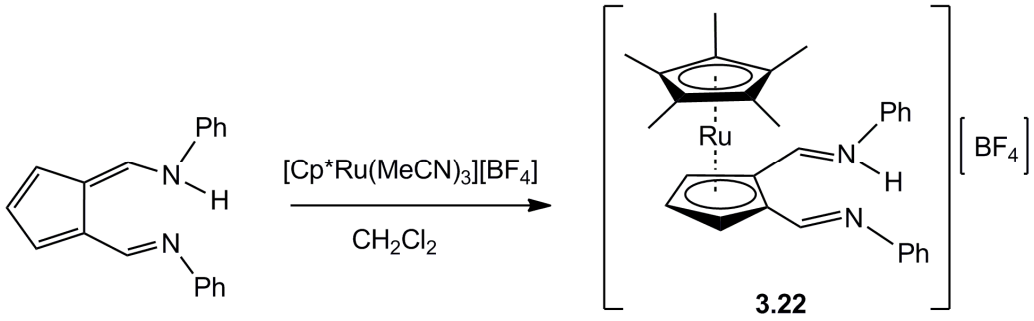

Figure 3.10 Synthesis of $[Cp^*Ru^{II}(Ph_2AFA)H][BF_4]$.

Similar to $[Cp^*Ru^{II}(Ph_2AFA)]$[1], the ^1H NMR study of **3.22** in $CDCl_3$ shows upfield shifts of the C_5 ring protons (H3/H5 and H4) of the AFA due to η^5-coordination to Ru. The N-H peak and H1/H7 of **3.22** is shifted down field (δ 16.51 and 8.93 respectively) compared to the Ph_2AFA ligand (δ 15.59 and 8.29 respectively). The H1/H7 protons appear as a doublet due to coupling with N-H proton with the value

of J = 7.57 Hz. In the Ph_2AFA free ligand the J value due to coupling of H1/H7 protons with the N-H proton is 6.9 Hz. The five magnetically equivalent methyl substituents of the Cp* ligand appear as a singlet at δ_{CH3}1.83 (^1H) and δ_{CH3} 11.58 (^{13}C). The mass spectrum (EI, m/z) also shows the molecular peak at m/z 509 of **3.22**. The η^5-coordination of electron-rich Cp^*Ru^+ synthon to the C_5 ring of the AFA ligand is due to its high affinity for π-aromatic ligands.[11]

The X-ray crystal structure of **3.23** (Fig. 3.11) confirms that the coordination of Cp*Ru(II) has occurred via the C_5 ring of the AFA ligand. The AFA ligand loses its planarity on coordination of Cp*Ru(II) to the C_5 ring. The maximum deviation of non-Ph atoms from the C_5 plane is 0.354 Å (N15A) and is similar to its neutral analogue $[Cp^*Ru(Ph_2AFA)]$[1] which is 0.34 Å. One of the two imine C-N arms is tilted out of the ligand C_5 mean plane and moved towards the Ru metal. As a result, the distance between the Ru center and one of the imine carbon atoms C(14A) is shorter with a value of 2.960 Å, and the distance of the Ru center from the other imine carbon atom C(8A) is greater with a value of 3.234 Å. In the neutral analogue $[Cp^*Ru(Ph_2AFA)]$, the corresponding distance of Ru to imine carbon atoms were 2.972 (C21) and 3.150 Å (C81).[1] An N-H-N intramolecular hydrogen bond exists in **3.23**. The donor (N15A)-acceptor (N7A) distance is 2.69 Å which compares with the value of 2.79 Å in Ph_2AFH.[12] The C-C bond lengths in the C_5 ring are intermediate between typical single and double bond lengths. One of the imine C-N bonds is shorter (C(8A)-N(7A) = 1.276(8) Å) than the other imine C-N bond length (C(14A)-N(15A) = 1.297(8) Å). The distances between Ru and C_5 carbon atoms are in the range of 2.159 to 2.222 Å. The methyl groups in Cp* appear large due to atomistic modeling of free rotation of Cp* ligand which forms a continuous band of electron density. The hydrogen atom of N-H has been placed geometrically.

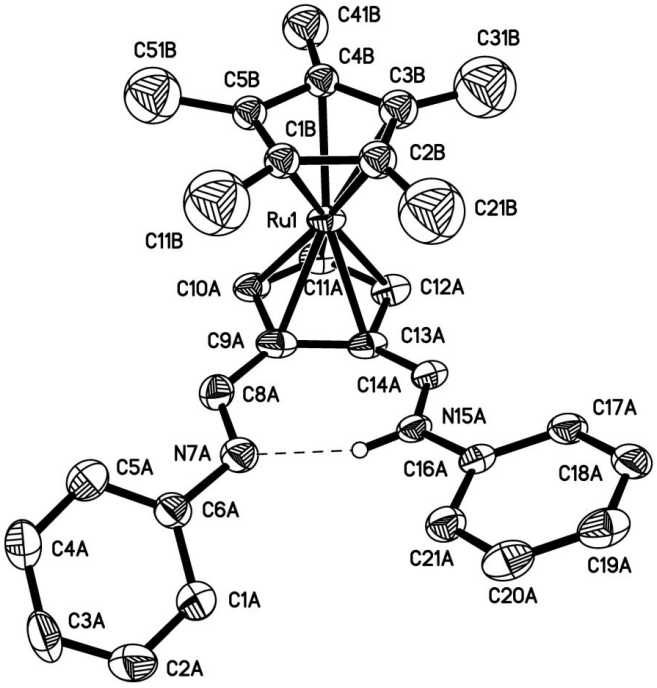

Figure 3.11. Thermal ellipsoid drawing of [Cp*Ru^{II}(Ph$_2$AFA)H][BF$_4$] (3.23) (50% ellipsoids). Hydrogen atoms, BF_4^- and minor disorder components have been removed for clarity.

Table 3.1. Selected bond lengths (Å) and angles (deg) for $[Cp^*Ru^{II}(Ph_2AFA)H][BF_4]$ (3.23).

Bond	Bond length (Å)	Bond	Bond angle (deg)
C(9A)-C(13A)	1.443(9)	C(9A)-C(8A)-N(7A)	122.7(6)
C(9A)-C(10A)	1.450(8)	C(13A)-C(14A)-N(15A)	124.9(6)
C(10A)-C(11A)	1.400(10)	C(14A)-C(13A)-C(9A)	129.6(6)
C(11A)-C(12A)	1.401(9)	C(13A)-C(9A)-C(8A)	130.6(6)
C(12A)-C(13A)	1.439(9)	C(13A)-C(9A)-C(10A)	106.0(6)
C(9A)-C(8A)	1.441(9)	C(9A)-C(10A)-C(11A)	109.2(6)
C(13A)-C(14A)	1.424(8)		
C(8A)-N(7A)	1.276(8)		
C(14A)-N(15A)	1.297(8)		
Ru1-C(11A)	2.222		
Ru1-C(12A)	2.189(6)		
Ru1-C(10A)	2.194(6)		
Ru1-C(9A)	2.170(6)		
Ru1-C(13A)	2.159(6)		

3.2.2 Synthesis and characterisation of $[Cp^*Rh^{III}(Cy_2AFA)H][BF_4]_2$

The rhodium precursor, $[Cp^*Rh^{III}(CH_3CN)_3][BF_4]_2$ was reacted with Cy_2AFAH in CH_2Cl_2 to afford the metalloligand $[Cp^*Rh^{III}(Cy_2AFA)H][BF_4]_2$ **(3.24)** (Fig. 3.12). The dicationic complex **3.24** is stable to air and moisture and is highly soluble in DCM and acetonitrile, but insoluble in hexane and chloroform.

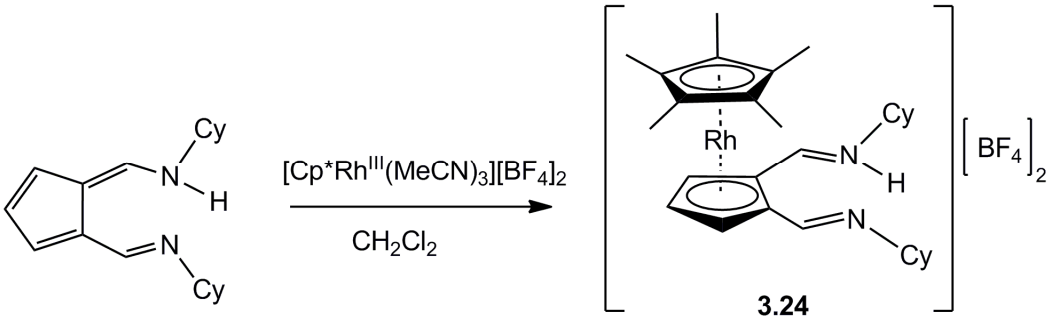

Figure 3.12. Synthesis of $[Cp^*Rh^{III}(Cy_2AFA)H][BF_4]_2$.

The ^{1}H NMR spectrum of **3.24** shows that the Cp*Rh moiety has coordinated to the C_5-ring of the Cy_2AFAH ligand in a η^5-coordination mode. The complex **3.24** is dicationic having Rh in +3 oxidation sate. Upon η^5-coordination of Cp*Rh to the C_5-ring, the H3/H5 protons shift upfield (δ 6.43) with respect to the H3/H5 protons of the free Cy_2AFAH (δ 6.65). Although it is expected that coordination of Cp^*Rh^{2+} to the C_5-ring would shift the H4 protons upfield, the H4 proton is instead shifted slightly downfield having δ = 6.15 with respect to the chemical shift of H4 of the free ligand Cy_2AFAH (δ 6.12). The N-H peak and H1/H7 of **3.24** is shifted downfield (δ 16.80 and 8.55) compared to Cy_2AFAH (δ 13.66 and 7.91 respectively). The H1/H7 protons appear as a doublet with J = 7.25 Hz due to coupling with the N-H proton. The ^{103}Rh is magnetically active and has a spin, I = ½ (abundance 100%). Thus coupling of Rh and ^{1}H as well as Rh and ^{13}C occurs and results a pair of peaks (doublet). Such coupling is also found in the metalloligand **3.24.** The ^{103}Rh couples with C_5-ring protons and thus H3/H5 protons appear as a doublet of doublets (J = 2.64, 0.73 Hz) and H4 proton appears as a doublet of triplets (J = 2.65, 1.0 Hz) due to coupling with Rh and neighbouring protons. In a similar manner, the ^{103}Rh couples with C_5-ring carbon atoms and provides four distinct doublets. The coupling of ^{103}Rh with the quarternary-C of Cp*, C3/C5, C4 and C2/C6 occurs at δ 106.44 (J = 7.72 Hz), 99.06 (J = 5.90 Hz), 96.08 (J = 5.45 Hz) and 94.95 (J = 6.36 Hz) respectively (Fig. 3.13). The five magnetically equivalent methyl substituents of Cp* moiety appear as singlet at δ_{CH3} 2.04 (^{1}H) and δ_{CH3} 11.11 (^{13}C).

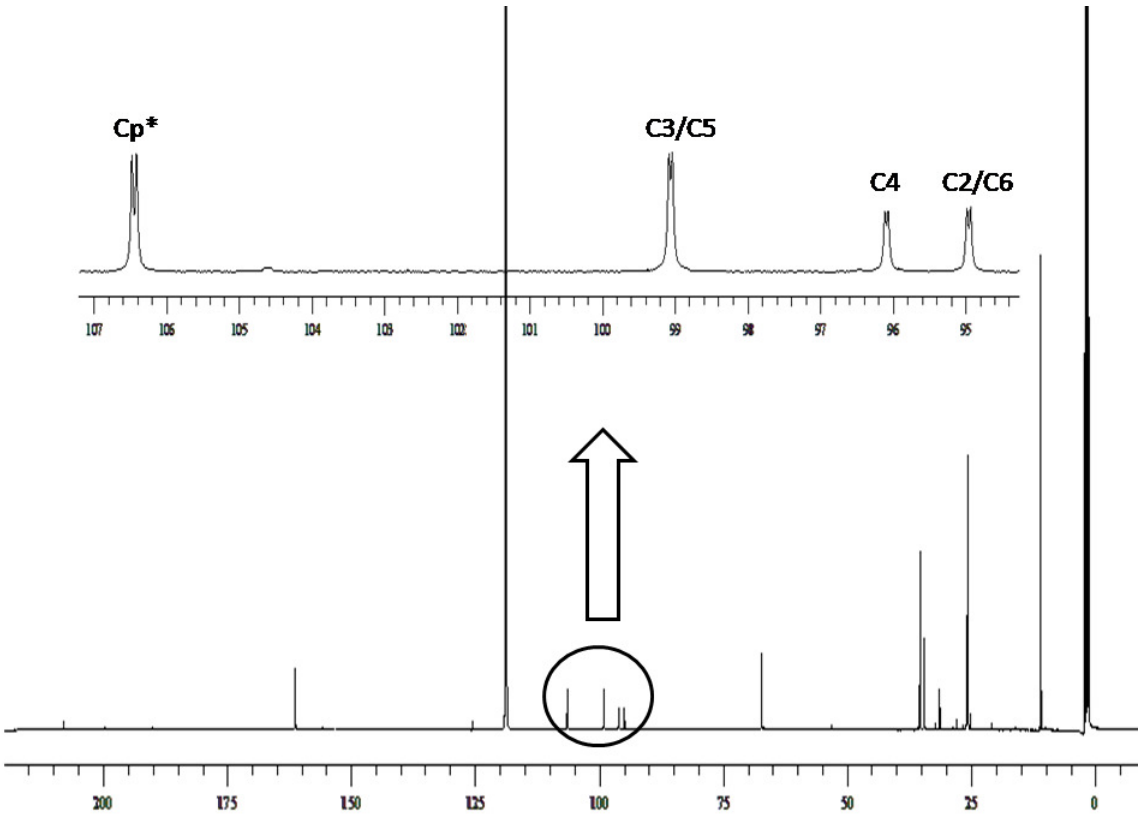

Figure 3.13. ^{13}C NMR spectrum of [Cp*Rh^{III}(Cy_2AFA)H][BF_4]$_2$ (3.24) (acetonitrile-d_3, 500 MHz, 25 °C).

The X-ray crystal structure of **3.25** (Fig. 3.14) shows that Cp*Rh coordinates to AFA ligand via the expected η^5- coordination mode. The C_5-ring of the AFA moiety is planar and the AFA ligand retains its planarity upon η^5-coordination by Cp*Rh^{2+}. The deviation of the imine nitrogen atoms N7A and N15A from the C_5 plane is only 0.127 and 0.059 Å respectively. In contrast to **3.23**, the two imine C-N arms are not tilted towards the Rh metal; the distance between the Rh center and the two imine carbon atoms C14A and C8A are 3.257 and 3.251 Å. However, the Rh-imine carbon distances are larger than the corresponding Ru-imine (**3.23**) carbon distances (2.960 and 3.234 Å). As in **3.23**, an N-H-N intramolecular hydrogen bond exists in **3.25.** The donor (N7A)-acceptor (N15A) distance = 2.687 Å. The distances between Rh and C_5 carbon atoms are in the range of 2.199 to 2.210 Å. These distances are in agreement with the distance between Ru and C_5 carbon atoms.

Although a large difference was observed in the imine C-N bond length in **3.23**, this feature is not evident in **3.25**; the imine C-N bond lengths are identical. The imine C-N bond lengths C(8A)-N(7A) and C(14A)-N(15A) in **3.25** are 1.272(3) and 1.268(3) respectively. The C-C bond lengths in the C_5 ring are intermediate between typical single and double bond lengths. The hydrogen atom of N-H was found in a difference Fourier map and its position allowed to refine.

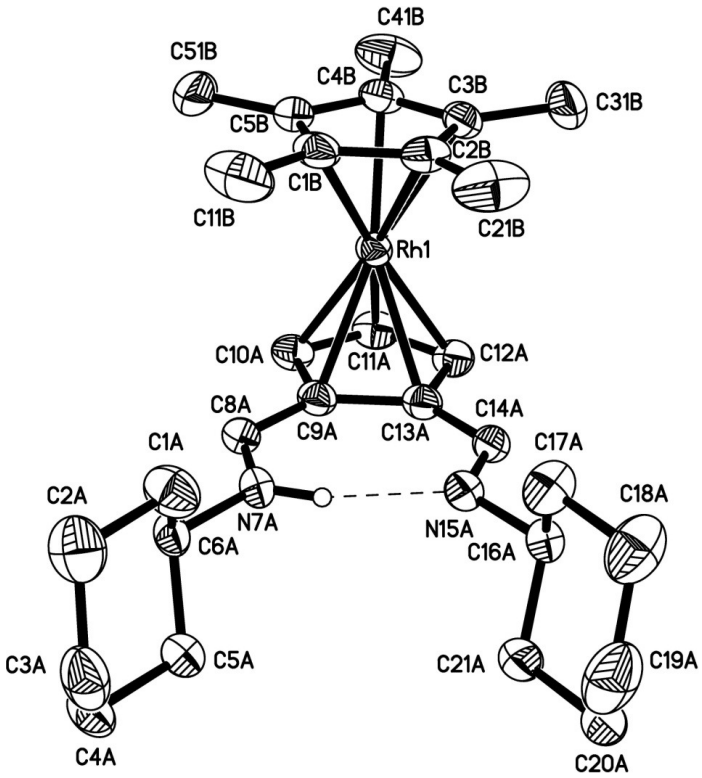

Figure 3.14. Thermal ellipsoid drawing of [Cp*Rh^{III}(Cy$_2$AFA)H][BF$_4$]$_2$ (3.25) (50% ellipsoids). Hydrogen atoms and BF_4^- have been removed for clarity.

Table 3.2. Selected bond lengths (Å) and angles (deg) for $[Cp^*Rh^{III}(Cy_2AFA)H][BF_4]_2$ (3.25).

Bond	Bond length (Å)	Bond	Bond angle (deg)
C(9A)-C(13A)	1.450(3)	C(9A)-C(8A)-N(7A)	124.8(2)
C(13A)-C(12A)	1.432(3)	C(13A)-C(14A)-N(15A)	123.1(2)
C(12A)-C(11A)	1.410(4)	C(13A)-C(9A)-C(10A)	107.84(19)
C(11A)-C(10A)	1.419(3)	C(9A)-C(13A)-C(12A)	106.3(2)
C(10A)-C(9A)	1.430(3)	C(8A)-C(9A)-C(13A)	130.6(2)
C(9A)-C(8A)	1.454(3)	C(9A)-C(13A)-C(14A)	131.10(19)
C(13A)-C(14A)	1.453(3)		
C(8A)-N(7A)	1.272(3)		
C(14A)-N(15A)	1.268(3)		
Rh1-C(11A)	2.210(2)		
Rh1-C(12A)	2.205(2)		
Rh1-C(13A)	2.209(2)		
Rh1-C(10A)	2.197(2)		
Rh1-C(9A)	2.199(2)		

3.2.3 Synthesis and characterisation of $[Cp^*Rh^{III}(Cy_2AFA)][BF_4]$

The reaction of the deprotonated ligand KCy_2AFA with $Cp^*Rh^{III}(CH_3CN)_3][BF_4]_2$ in THF affords $[Cp^*Rh^{III}(Cy_2AFA)][BF_4]$ (**3.26**) as an air and moisture stable product (Fig. 3.15). The basicity of the metalloligand **3.26** is significantly less than that of its Ru analog $[Cp^*Ru(\eta^5\text{-}Ph_2AFA)]$[1] and 1,2-bis(imidoyl)pentamethylruthenocenes,[3] as would be anticipated for a cationic species. The Rh complex **3.26** is found to be less basic and the nitrogen atoms are not protonated even in wet solvents. This is significant as synthesis of bimetallic complexes employing $[Cp^*Rh^{III}(Cy_2AFA)][BF_4]$ (**3.26**) would not require any additional deprotonation step to ligate to the metal precursor. Moreover, as expected in **3.26**, the η^5-coordination is preferred over κ^2-coordination.

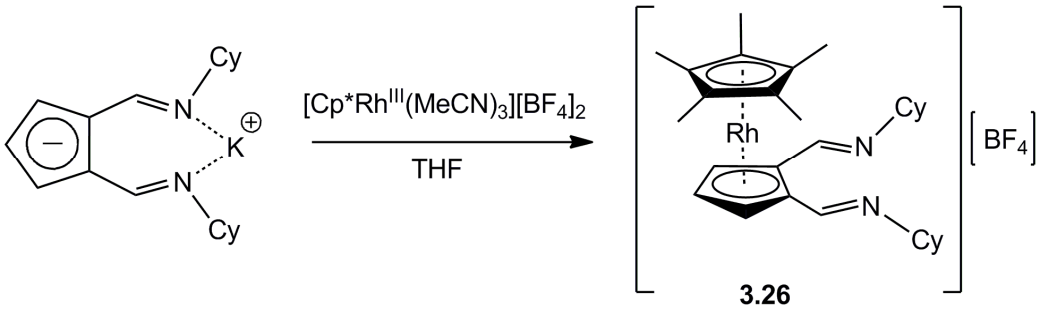

Figure 3.15. Synthesis of [Cp*Rh^{III}(Cy$_2$AFA)][BF$_4$].

The ^{1}H NMR spectrum of **3.26** (Fig. 3.16) shows no N-H peak and the H1/H7 protons appear as a sharp singlet as there is no N-H proton to couple with. Upon η^5-coordination of Cp*Rh^{2+} to the C$_5$-moiety of the AFA ligand, the H1/H7 protons are shifted down-field (δ 8.43) and as expected the H3/H5 and the H4 are shifted upfield (δ 5.93 and 5.68 respectively) from the starting Cy$_2$AFAH ligand. The five magnetically equivalent methyl substituents of Cp* moiety appear as singlet at δ_{CH3} 1.98 (^{1}H) and δ_{CH3} 10.85 (^{13}C).

The ^{103}Rh couples with the C$_5$-ring protons and thus H3/H5 protons appear as a doublet of doublets (J = 2.68, 0.79 Hz) and the H4 proton appears as a doublet of triplets (J = 2.68, 1.1 Hz) due to coupling with Rh and neighbouring protons. As observed in **3.24**, the ^{103}Rh couples with C$_5$-ring carbon atoms and provides four distinct doublets (Fig. 3.17). However, in **3.26** the four carbon doublets are shifted significantly with respect to the metalloligand **3.24**. The coupling of ^{103}Rh with the quarternary-C of Cp*, C3/C5, C4 and C2/C6 occurs at δ 103.46 (J = 8.17 Hz), 90.29 (J = 6.36 Hz), 90.98 (J = 6.81 Hz) and 99.24 (J = 6.36 Hz) respectively.

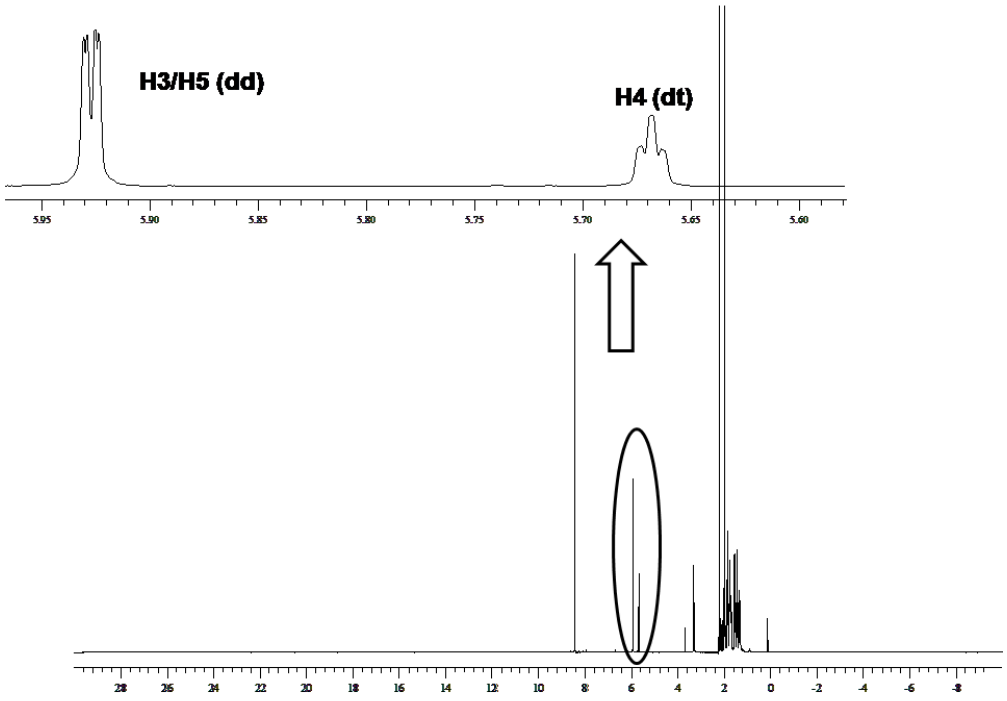

Figure 3.16. ^{1}H NMR spectrum of [Cp*Rh^{III}(Cy$_2$AFA)][BF$_4$] (3.26) (acetonitrile-d$_3$, 500 MHz, 25 °C).

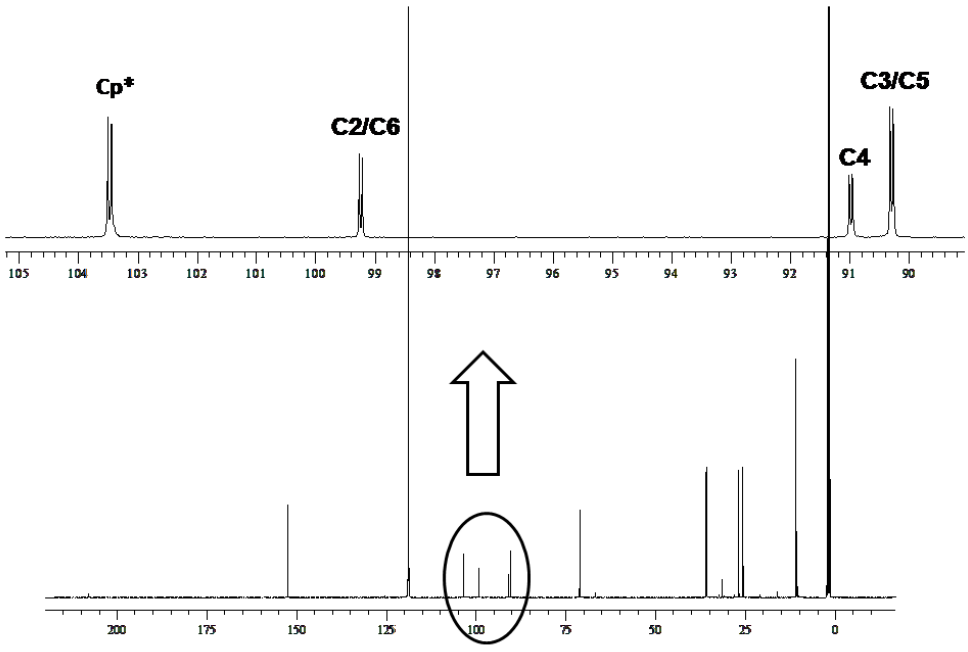

Figure 3.17. ^{13}C NMR spectrum of [Cp*Rh^{III}(Cy$_2$AFA)][BF$_4$] (3.26) (acetonitrile-d$_3$, 500 MHz, 25 °C).

3.2.4 Attempted synthesis of $[CpCo^{III}(Ph_2AFA)](H^+)[OTf]_2$

In an attempt to synthesise the cobalt complex **3.27** (Fig 3.18), Ph_2AFAH was reacted with $[CpCo^{III}(CH_3CN)_3]^{2+}[OTf]_2$ in acetonitrile. Unfortunately the reaction provided only the protonated ligand (**3.28**) (Fig. 3.18). The ^1H NMR spectrum shows a broad N-H peak for two protons at $\delta = 10.52$, shifted upfield compared to the free Ph_2AFAH (N-H, $\delta = 15.59$). Upon protonation all other AFA protons shifted downfield. For example, H1/H7, H3/H5 and H4 protons shifted from 8.29, 7.05 and 6.47 in Ph_2AFAH to 8.68, 7.80 and 6.93 in **3.28**. The coupling constant value of H1H7 proton is quite large (J = 15.65 Hz) and appears as a doublet due to coupling with the N-H proton. The high basicity of Ph_2AFAH could be a reason for the ease of protonation of the ligand. To confirm this reasoning the Ph_2AFAH was reacted with a superacid, triflic acid, TfOH (pKa = -15) in toluene and the reaction provided the above mentioned protonated ligand with spectral features and properties similar to **3.28**.

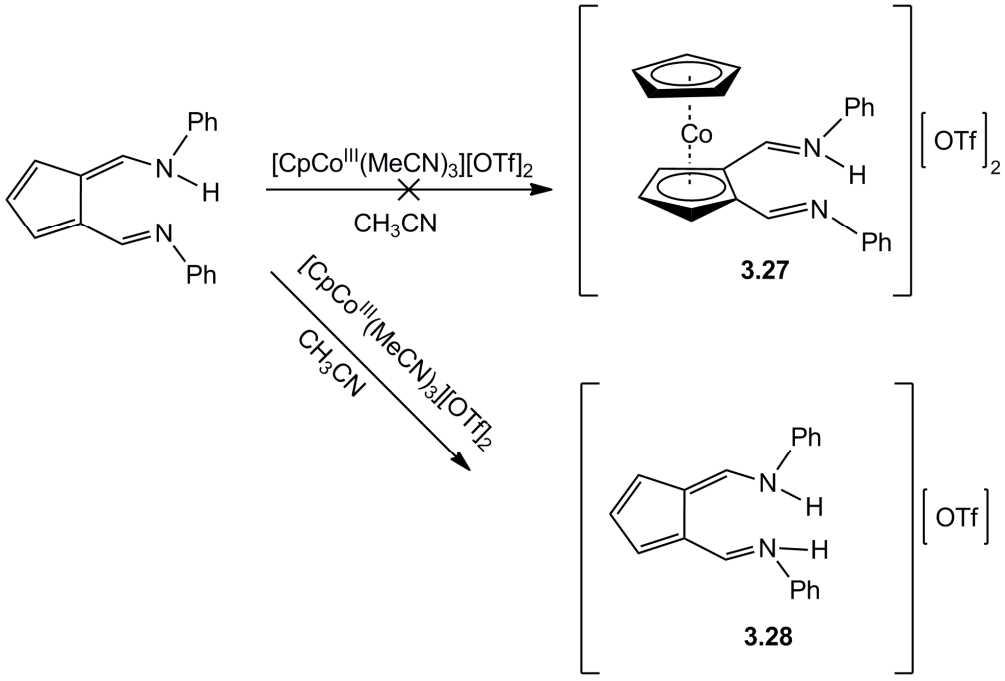

Figure 3.18. Attempted synthesis of $[CpCo^{III}(Ph_2AFA)](H^+)[OTf]_2$

The X-ray crystal structure of **3.28** (Fig. 3.19) shows that indeed one of the imine nitrogens has been protonated and an intermolecular hydrogen bonding exists in **3.28**. One of the donor (N1)-acceptor (O3A) distance is 2.914(3) Å and the other donor (N2)-acceptor (O1) distance is 2.875(3) Å. The AFA moiety is quite planar. The deviation of non-Ph atoms from C_5 plane is only 0.136 (N1) and 0.190 Å (N2). The carbon-carbon and carbon-nitrogen distances are intermediate between the usual single and double bonds. The C2-C1-N1 and C6-C7-N2 angles are 124.0(3)° and 124.8(3)° respectively, consistent with sp^2 hybridization at the imine carbon atoms. The most significant feature of **3.28** is that the imines have a different conformation in comparison to the neutral Ph_2AFAH ligand since there is no internal N-H-N hydrogen bond. The rotation of the C1-C2 and C7-C6 bonds has pointed the N-H protons outwards whereas in the neutral ligand an inward rotation of C-C bonds occurs for the N-H to form a hydrogen bond with the imine nitrogen.

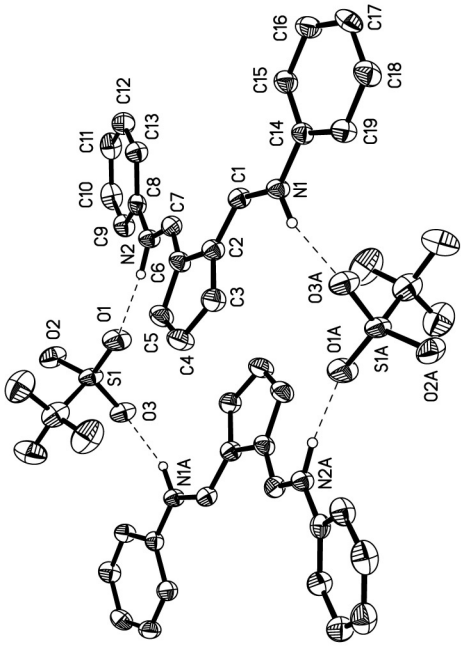

Figure 3.19. Thermal ellipsoid drawing of [Ph_2AFAH(H)][OTf] (3.28) (50% ellipsoids). Hydrogen atoms have been removed for clarity.

Table 3.3. Selected bond lengths (Å) and angles (deg) for [Ph_2AFAH(H)][OTf] (3.29).

Bond	Bond length (Å)	Bond	Bond angle (deg)
C(7)-N(2)	1.324(3)	C(6)-C(7)-N(2)	124.8(3)
C(1)-N(1)	1.324(3)	C(2)-C(1)-N(1)	124.0(3)
C(6)-C(7)	1.388(4)	C(7)-C(6)-C(2)	125.1(2)
C(2)-C(1)	1.393(4)	C(1)-C(2)-C(6)	125.1(3)
C(2)-C(6)	1.469(3)	C(2)-C(6)-C(5)	106.0(2)
C(6)-C(5)	1.412(4)	C(6)-C(2)-C(3)	107.1(2)
C(5)-C(4)	1.389(4)	C(2)-C(3)-C(4)	108.4(3)
C(4)-C(3)	1.396(4)	C(6)-C(5)-C(4)	109.1(2)
C(3)-C(2)	1.408(4)	C(3)-C(4)-C(5)	109.4(3)

3.3 Synthesis and characterisation of bimetallic complexes

3.3.1 Synthesis and characterisation of [Cp*Rh^{III}(Cy_2AFAPdCl_2)][BF_4]

In order to synthesise the bimetallic complex **3.30** (Fig. 3.20) for its application as an ethylene polymerisation catalyst and to understand the effect of charge in catalysis, the metalloligand **3.26** was reacted with metal precursor [$(PhCN)_2PdCl_2$] in acetonitrile. The complex **3.30** is monocationic and is soluble in acetonitrile and DCM, but insoluble in ether and hexane. Hexane was layered on top of a DCM solution of **3.30** but no suitable crystals were obtained for X-ray analysis.

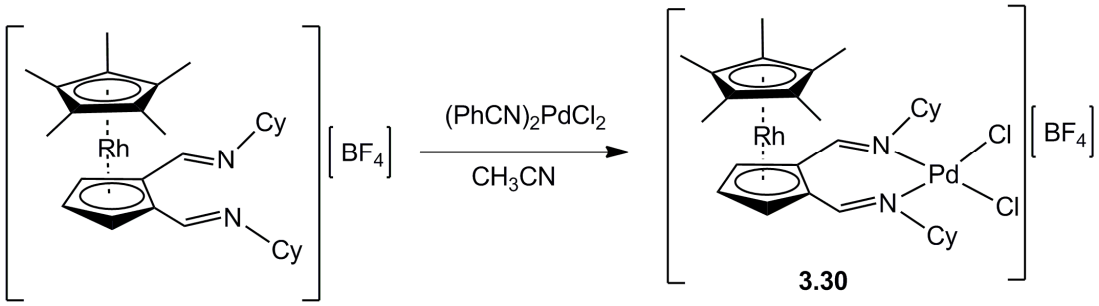

Figure 3.20. Synthesis of [Cp*Rh^{III}(Cy_2AFAPdCl_2)][BF_4].

The ^{1}H NMR spectrum of **3.30** (Fig. 3.21) shows that upon coordination of palladium, the H1/H7 protons are shifted upfield (δ 7.82) and the H3/H5 and H4 protons are shifted downfield (δ 6.31 and 6.18 respectively) compared to the starting complex **3.26** where δ values for H1/H7, H3/H5 and H4 were 8.43, 5.93 and 5.68 respectively. The H1/H7 protons appear as a sharp singlet.

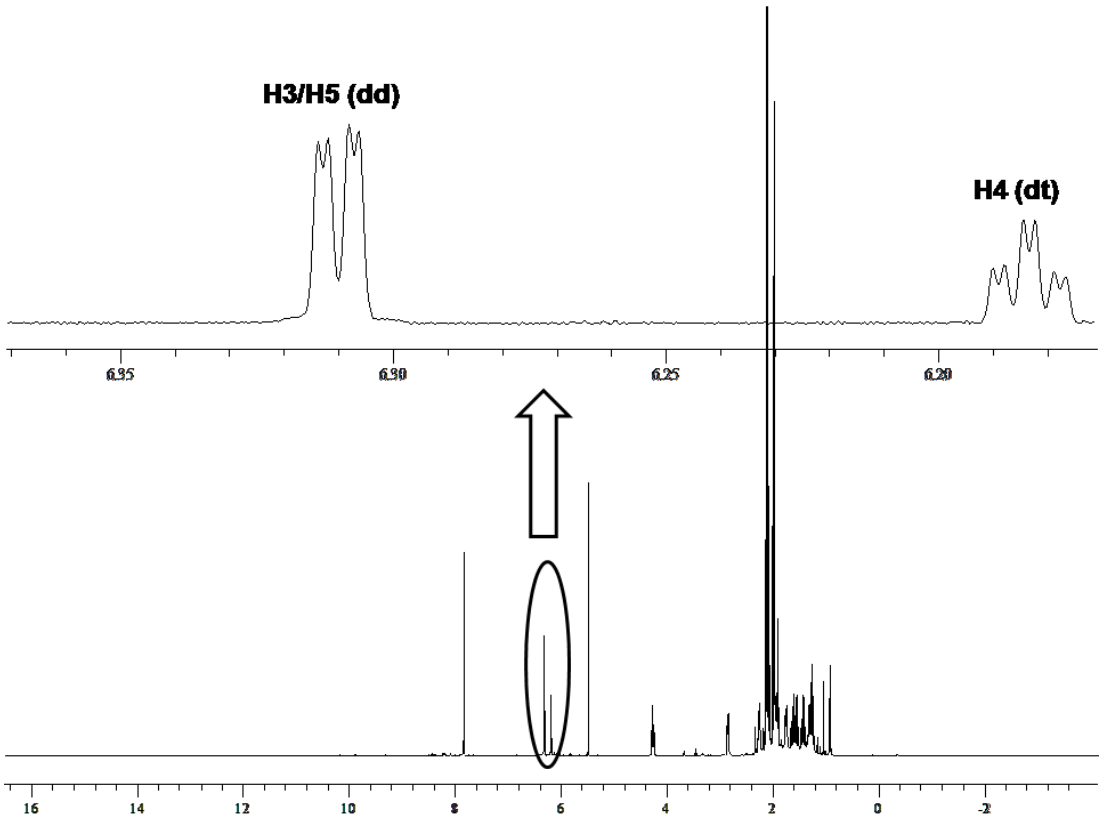

Figure 3.21. ^{1}H NMR spectrum of [Cp*Rh^{III}(Cy$_2$AFAPdCl$_2$)][BF$_4$] (3.30) (acetonitrile-d$_3$, 500 MHz, 25 °C).

The ^{103}Rh couples with C_5-ring protons and thus the H3/H5 protons appear as a doublet of doublets (J = 2.14, 0.92 Hz) and the H4 proton appears as a doublet of triplets (J = 2.70, 0.92 Hz) due to coupling with Rh and neighbouring protons. As observed for **3.26**, the ^{103}Rh couples with the C_5-ring carbon atoms and provides four distinct doublets (Fig. 3.22). However, in **3.30** the four carbon doublets are shifted significantly from those for the staring metalloligand **3.26**. The coupling of ^{103}Rh with the quarternary-C of Cp*, C3/C5, C4 and C2/C6 occurs at δ 105.87 (J = 7.72 Hz), 95.13 (J = 5.90 Hz), 95.01 (J = 5.90 Hz) and 94.69 (J = 6.36 Hz) respectively. The five magnetically equivalent methyl substituents of the Cp* moiety appear as a

singlet at δ_{CH3} 2.08 (^{1}H) and δ_{CH3} 11.42 (^{13}C) and are shifted downfield from the starting complex **3.26** (δ_{CH3} 1.98 (^{1}H) and δ_{CH3} 10.85 (^{13}C) respectively).

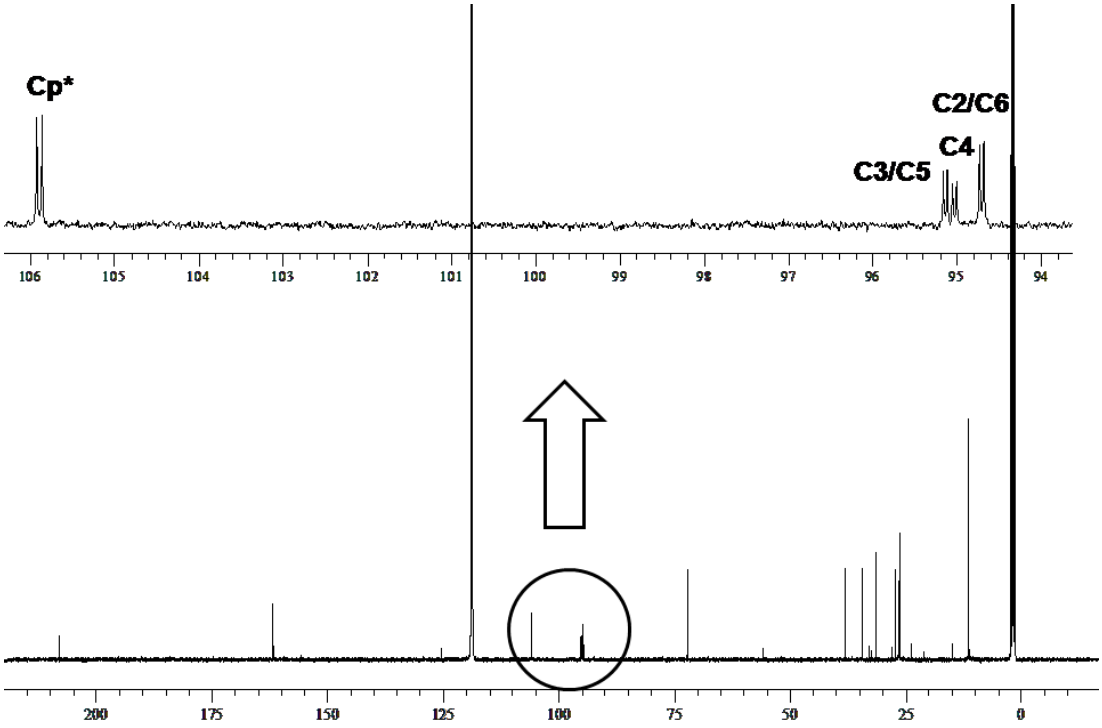

Figure 3.22. ^{13}C NMR of [Cp*Rh^{III}(Cy_2AFAPdCl_2)][BF_4] (3.30) (acetonitrile-d_3, 500 MHz, 25 °C).

3.3.2 Attempted synthesis of [Cp*Ru^{II}(Ph_2AFAPdCl_2)]

The neutral bimetallic complex **3.31** (Fig. 3.23) could be a mimic of a cationic Brookhart palladium catalyst once activated by MAO or other co-catalyst. In an attempt to synthesise **3.31**, the potassium salt of **3.22** was reacted in THF with the palladium complex [$(PhCN)_2PdCl_2$]. The ^{1}H NMR spectrum of **3.31** in $CDCl_3$ shows undefined species. Several synthetic attempts were unsuccessful. The complex [Cp*Ru^{II}((2,4,6-trimethylphenyl)$_2$AFAPdCl_2)] and [Cp*Ru^{II}((2,6-diisopropylphenyl)$_2$AFAPdCl_2)] could be an alternative precursor and could be isolated more easily.

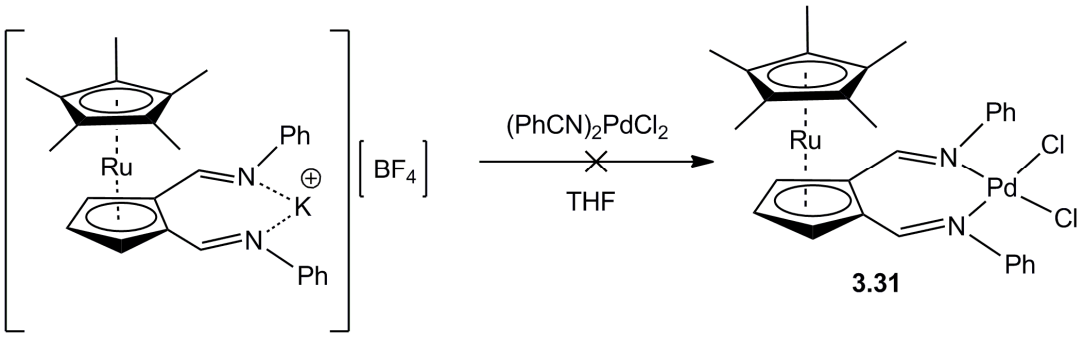

Figure 3.23. Attempted synthesis of [Cp*Ru^{II}(Ph_2AFAPdCl_2)].

3.4 Ethylene polymerisation test by bimetallic complexes

The bimetallic complex [Cp*Rh^{III}(Cy_2AFAPdCl_2)][BF_4] (**3.30**) was tested toward ethylene polymerisation at 5 bar and 0 °C in toluene solution. Methylalumoxane (MAO) was used to activate the catalyst precursor **3.30**. Unfortunately **3.30** was found to be inactive for ethylene polymerisation. An aliquot of the mother liquor was also analysed by EI-MS to detect formation of oligomers, but no ethylene oligomers were observed. It is possible that ethylene dimers (butene) were formed, but these would have been vented off. After quenching the reaction mixture with acidified methanol only $AlCl_3$ was isolated as a white solid which is soluble in water.

3.5 Conclusions

Metalloligands and their corresponding bimetallic complexes based on the AFA ligand have been successfully synthesised and characterised. The Rh/Pd bimetallic complex has been developed in an attempt to investigate the charge effect in alkene polymerisation catalysis.

The bimetallic complex **3.30** has been tested for ethylene polymerisation. Unfortunately, the complex was not found to be active when MAO was used as an activator at 0 °C. The activation process needs to be tested at higher temperature. The basicity of the metalloligand **3.26** is significantly less than that of its Ru analog [Cp*Ru(η^5-Ph_2AFA)] and 1,2-bis(imidoyl)pentamethylruthenocenes and does not

undergo protonation in solution. Thus it opens a potentially easy synthetic route to bimetallic complexes which eliminates the need for a deprotonation step. An alternative cocatalyst Et_2AlCl could be used for activation of **3.30**. The nickel precursor [(DME)$NiBr_2$] could also be employed to develop bimetallic Ni-Ru/Rh complexes for ethylene polymerisation employing the metalloligand **3.26.**

References

1. P. J. Bailey, M. Melchionna and S. Parsons, *Organometallics*, 2007, **26**, 128.
2. R. W. Alder, P. S. Bowman, R. W. S. Sleele and D. R. Winterman, *J. Chem. Soc., Chem. Commun*, 1968, 723.
3. B. Enk, D. Eisenstecken, H. Kopacka, K. Wurst, T. Muller, F. Pevny, R. F. Winter and B. Bildstein, *Organometallics*, 2010, **29**, 3169.
4. R. W. Barnhart and G. C. Bazan, *J. Am. Chem. Soc*, 1998, **120**, 1082.
5. J.-C. Wasilke, S. J. Obrey, R. T. Baker and G. C. Bazan, *Chem. Rev*, 2005, **105**, 1001.
6. Z. J. A. Komon and G. C. Bazan, *Macromol. Rapid. Commun*, 2001, **22**, 467.
7. R. l. Quijada, R. Rojas, G. Bazan, Z. J. A. Komon, R. S. Mauler and G. B. Galland, *Macromolecules*, 2001, **34**, 2411.
8. C. Bianchini, M. Frediani, G. Giambastiani, W. Kaminsky, A. Meli and E. Passaglia, *Macromol. Rapid Commun*, 2005, **26**, 1218.
9. Z. J. A. Komon, X. Bu and G. C. Bazan, *J. Am. Chem. Soc*, 2000, **122**, 1830.
10. J. Kuwabara, D. Takeuchi and K. Osakada, *Chem. Commun*, 2006, 3815.
11. P. J. Fagan, M. D. Ward and J. C. Calabrese, *J. Am. Chem. Soc*, 1989, **111**, 1698.
12. H. L. Ammon and U. Mueller-Westerhoff, *Tetrahedron*, 1974, **30**, 1437.

Chapter 4 Experimental Section

4.1 General procedures

All reactions and manipulations of moisture- and air-sensitive compounds were carried out in an atmosphere of dry nitrogen using Schlenk techniques or in a conventional nitrogen-filled GloveBox (Saffron Scientific), fitted with oxygen and water scavenging columns. Toluene, THF, diethyl ether, DCM, acetonitrile solvents were dried and purified by passage through activated alumina columns (drying column) using a solvent purification system from Glass Contour (www.glasscontour.com).

Hexane was distilled from Na/benzophenone under a nitrogen atmosphere. Dimethyl sulfate (DMS) was dried by refluxing it over $CaCl_2$. Ethanol was dried by refluxing it over magnesium ethoxide. NMR solvents were degassed using freeze-thaw cycles and stored over 4Å molecular sieves. All solvents and reagents were purchased from Sigma-Aldrich, Fischer or Acros and used as received unless otherwise stated. Column chromatography was performed on silica gel (Merck 60, 7-120 mesh).

4.2 Instrumentation

NMR spectra were recorded on Bruker AC 250 MHz, 360 MHz, 400 MHz and 500 MHz spectrometers operating at room temperature (25 ºC). ^{1}H and ^{13}C chemical shifts are reported in ppm relative to $Si(CH_3)_4$ ($\delta = 0$) and were referred internally with respect to the protio solvent impurity or ^{13}C resonances respectively. Elemental analyses were performed using a Perkin Elmer 2400 CHN Elemental Analyzer. Electron impact (EI) mass spectra were obtained either on a Finnigan MAT 4600 quadrupole spectrometer or on a Kratos MS50TC spectrometer. Fast atom bombardment (FAB) mass spectra were obtained on a MS50TC spectrometer.

4.3 Labelling for compounds and ligands

The labeling of all protons and carbon atoms of ligands and complexes for NMR characterisation are referred as shown in the figure below:

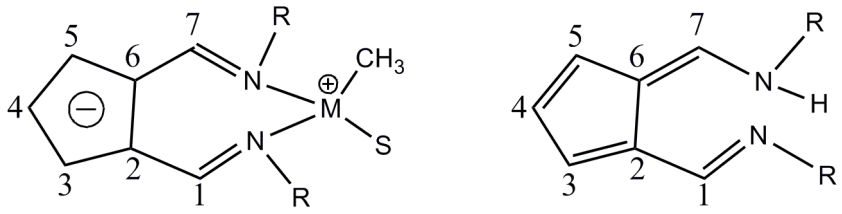

Figure 4.1. Labeling for protons and carbon atoms in the ligands and complexes.

4.4 Synthesis of metal precursors

4.4.1 $[(COD)PdCl_2]$[1]

Palladium (II) chloride (6.0 g, 33.84 mmol) was dissolved in 15 ml of concentrated hydrochloric acid by warming the mixture. The cool red solution was diluted with 360 ml of absolute ethanol and then filtered. To the filtrate 9.0 ml of 1,5-cyclooctadiene was added with stirring. The yellow product precipitated immediately. The solvent was removed and the product was washed with three 30-ml portions of diethyl ether. Yield: 8.97 g (91%).

4.4.2 $[(COD)Pd(CH_3)(Cl)]$[2]

In a Schlenk tube, 4.0 g (14.0 mmol) of $[(COD)PdCl_2]$ was dissolved in 200 ml of DCM. Then 2.67 ml (19.6 mmol) of $[Sn(CH_3)_4]$ was added and stirred at room temperature until the bright yellow color of the precursor had vanished, which normally took *ca.* 1 day. If the yellow color didn't disappear after 1 day stirring, 6.68

ml extra $Sn(CH_3)_4$ (49 mmol) was added to the reaction mixture and stirred at room temperature for two more days. The nearly colorless solution was filtered through celite (kieselguhr) and the solvent was removed under reduced pressure, while the temperature was kept at 0 ºC using an ice bath. The off-white powder was washed with several small portions of diethyl ether in order to remove the $[(CH_3)_3SnCl]$ that is formed during the reaction. Yield: 2.52 g (67%).

4.4.3 $[(PhCN)_2PdCl_2]$[3]

Anhydrous palladium(II) chloride (2.0 g, 11.3 mmol) was loaded into a 200-ml round-bottom flask, equipped with stirring bar. Benzonitrile (60 ml) was added, and the mixture was heated at 100 ºC. Within 3 hours of heating most of the palladium chloride dissolved to give a red-brown solution. The solution was filtered while still hot, and the filtrate was poured into a 500-ml Erlenmeyer flask containing 350 ml of petroleum ether. A precipitate was formed immediately. The yellow-orange product was filtered through a fine frit, washed with 3 portions of 15 ml of petroleum ether and dried *in vacuo*. Yield: 3.38 g (78%).

4.4.4 π–allylnickel bromide[4, 5]

In a Schlenk tube 1.73 g (6.29 mmol) of $Ni(COD)_2$ was suspended in 90 ml diethylether. The temperature of this yellow suspension was lowered to -10 ºC. A solution of allyl bromide (0.59 ml, 6.81 mmol) in 10 ml diethylether was added to the $Ni(COD)_2$ suspension at -10 ºC. The reaction mixture became red and the yellow crystals of $Ni(COD)_2$ started to dissolve. To dissolve $Ni(COD)_2$ completely another extra 0.4 ml allyl bromide (4.62 mmol) was added and the mixture stirred for a further 3h to provide a clear red solution. Ether and COD was removed under vacuum (1.8×10^{-1} mbar) and π-allylnickel bromide was collected as a red powder. Yield: 0.77 g (40%). ^1H NMR ($CDCl_3$, 500 MHz, 25 ºC): δ 5.53 (tt, 1H), 3.15 (d, 2H, J = 6.46 Hz), 2.1 (d, 2H, J = 13.08 Hz); $^{13}C\{^1H\}$ NMR ($CDCl_3$, 125 MHz, 25 ºC): δ 105.69 (C of CH), 56.33 (C of CH_2).

4.4.5 Sodium cyclopentadienide[6]

Freshly cut sodium (10.0 g, 0.43 mol) was added to 400 ml of dicyclopentadiene at room temperature. The reaction mixture was heated at 164 ºC overnight. On heating, a white solid precipitated. When the alkali metal was quantitatively consumed, the dihydrogen evolution stopped. The reaction mixture was filtered using a Schlenk frit and the white solid product was washed with three 50 ml portions of dry hexane and dried *in vacuo*.

Yield: 38.0 g (99%). ^{1}H NMR (d_8-THF, 250 MHz, 25 ºC): δ 5.60 (s, 5H). NaC_p is pyrophoric.

4.4.6 Dibromobis(triphenylphosphine)nickel(II), $[NiBr_2(PPh_3)_2]$[7]

$NiBr_2$ (6.5 g, 0.03 mol) and PPh_3 (18.36 g, 0.07 mol) was heated to reflux in anhydrous ethanol (100 ml). Then the dark green solution was hot filtered, reduced to small volume under vacuum and cooled to initiate crystallisation. The $NiBr_2(PPh_3)_2$ was collected by filtration and dried in vacuum and obtained as bright green solid. Yield: 8.84 g (38%).

4.4.7 Dichlorobis(trimethylphosphine)nickel(II), $[NiCl_2(PMe_3)_2]$[8]

Trimethylphosphine (2.061 ml, 0.02 mol) was added to a green solution of $NiCl_2.6H_2O$ (4.8 g, 0.02 mol) in 32 ml abs. ethanol. After the addition of Me_3P, the solution immediately turned red with the formation of crystalline solids. The mixture was heated gently at 60 ºC for 1h in order to dissolve the crystals which formed instantly. The red solution was cooled in an ice bath to grow crystals. The mother liquor was removed and the red needle crystals were washed with abs. ethanol and dried *in vacuo*. The compound was usually isolated pure, but impure samples could be recrystallised from ethanol. The product is moisture and heat sensitive. Yield: 1.68 g (29%). mp 199-200 ºC.

4.4.8 Bis(trimethylphosphine)methylnickelchloride, [trans-Ni(Cl)(Me)(PMe_3)$_2$][9]

A solution 0.6 M MeLi in ether (6.21 ml, 3.73 mmol) was added dropwise to a solution of [$(Me_3P)_2NiCl_2$] (1.0 g, 3.55 mmol) in thf (20 ml) at -70 ºC and stirred for 2h. Then the temperature of the reaction mixture was increased to 0 ºC. Solvents and volatiles were removed under vacuum and the residue was dissolved in 20 ml toluene and was filtered through celite to remove LiCl. Solvent was removed under vacuum and then 15 ml hexane was added. An orange-yellow solid precipitated. The mother liquor was removed and the orange-yellow product was dried *in vacuo*. Yield: 0.65 g (70%). mp (decomp): 125-126 ºC.

4.4.9 [$(CH_3CN)_2PdCl_2$][10]

2.0 g $PdCl_2$ (0.01 mol) was heated to reflux in 70 ml of acetonitrile until a clear solution was obtained (about 1 h). The solution was filtered hot and reduced to small volume *in vacuo*. The yellow solid product was filtered off, washed with ether, and dried *in vacuo*. The product was recrystalise in acetonitrile.Yield: 1.26 g (44%).

4.4.10 [$Cp^*Ru^{III}Cl_2]_2$][11-13]

All operations were carried out in a 500-ml round-bottomed flask under an inert atmosphere.

To a filtered solution of 8.0 g (31.6 mmol) of $RuCl_3 \cdot 3H_2O$ in 200 ml of CH_3OH was added 11.37 ml (9.6 g, 72 mmol) of C_5Me_5H, and the mixture was refluxed for 4h. The brown solution, which contains part of the product as a microcrystalline precipitate, was chilled to -80 ºC for 12 h and filtered cold through a porous frit. The solid was dried *in vacuo* and was washed twice with 30 ml of pentane in order to remove the decamethylruthenocene. Yield: 5.28 g (56%). As a solid it is stable toward air for shorter periods.

In case the methanolic mother liquor was still green, the reaction had not gone to completion. It can be refluxed for a second time, and more of the product can

be recovered using the above work-up procedure. ^{1}H NMR ($CDCl_3$, 250 MHz, 25 ºC): δ 5.1 (broad singlet). The product is paramagnetic.

4.4.11 $[Cp^*Ru^{II}(\mu_3\text{-}Cl)]_4$[14]

A 100-ml round-bottomed flask was charged with 2.48 g (8.07 mmol) of [Cp^*RuCl_2] and 20 ml of THF. Then 8.07 ml of 1 M lithium triethylborohydride in THF (8.07 mmol) were added all at once to the solution via syringe. The reaction mixture turned to a dark blue-green color initially during the addition, and gas evolution was observed. After 45 minutes of stirring, the crystalline orange precipitate which formed was isolated by filtration and was rinsed twice with small amounts (ca. 2 ml) of THF. It was then dried *in vacuo* to yield 1.19 g (54%) of crystalline orange product. ^{1}H NMR (THF-d_8, 360 MHz, 25 ºC): δ 1.60 (s, Cp*). The product is diamagnetic.

4.4.12 $[Cp^*Ru^{II}(CH_3CN)_3][BF_4]$[14, 15]

An adaptation of the reported synthesis from ref. 14 (above) was used. A Schlenk tube was charged with 1.19 g (1.09 mmol) of [Cp*Ru(μ_3-Cl)]$_4$ and 20 ml of acetonitrile. The mixture was heated to reflux for 1 h and then allowed to cool to room temperature. To the stirred mixture was added a solution of 0.85 g (4.38 mmol) of silver tetrafluoroborate in 15 ml of acetonitrile and the mixture stirred for 1 h. A white precipitate of AgCl was formed. After filtration, the solvent was removed from the filtrate *in vacuo*. Diethyl ether (10 ml) was added to the residue, and the yellow-orange crystalline solid was collected by filtration with a filtered-capped cannula. The product was washed twice with 5 ml of diethyl ether, and dried *in vacuo* to yield 0.88 g (45%) of the desired product. The product is air sensitive. ^{1}H NMR (acetonitrile-d_3, 360 MHz, 25 ºC): δ 1.63 (s, 15H, Cp*), 2 (s, 9H, CH_3CN).

4.4.13 $[Cp^*Ru^{II}(CH_3CN)_3][OTf]$[14]

A Schlenk tube was charged with 2 g (1.84 mmol) of $[Cp^*Ru(\mu_3\text{-}Cl)]_4$ and 40 ml of acetonitrile. The mixture was heated to reflux for 1 h and then allowed to cool to room temperature. To the stirred mixture was added a solution of 1.89 g (7.36 mmol) of silver trifluoromethanesulfonate (AgOTf) in 20 ml of acetonitrile and the mixture stirred for 1 h. A white precipitate of AgCl was formed. After filtration, the solvent was removed from the filtrate *in vacuo*. Diethyl ether (10 ml) was added to the residue, and the yellow-orange crystalline solid was collected by filtration with a filtered-capped cannula. The product was washed twice with 5 ml of diethyl ether, and dried *in vacuo* to yield 2.97 g (79%) of the desired product. The product is air sensitive. ^1H NMR (acetonitrile-d_3, 360 MHz, 25 ºC): δ 1.62 (s, 15H, Cp*), 2 (s, 9H, CH_3CN).

4.4.14 $[Rh^{III}(\eta^5\text{-}C_5Me_5)Cl_2]_2$[16, 17]

Rhodium trichloride trihydrate (2.13 g, 0.01 mol), pentamethylcyclopentadiene (1.61 ml, 0.01 mol), reagent-grade methanol (60 ml) and a magnetic stirring bar were placed in a 250 ml round-bottomed flask fitted with a reflux condenser. A nitrogen bubbler was attached on top of the condenser, the apparatus purged with nitrogen for 5 min, and the mixture then heated to reflux gently under nitrogen for 48h with stirring. The reaction mixture was allowed to cool to room temperature and the dark red precipitate was filtered off through a glass sinter. The red filtrate was reduced in volume to get more products.

The product was dried *in vacuo* to yield 1.65 g (66% based on $RhCl_3.3H_20$) dark red solid. It is pure enough for most purposes. If required, the product may be recrystallised by dissolving in a minimum volume of chloroform, filtering if necessary, and slowly adding twice that volume of hexane. ^1H NMR ($CDCl_3$, 360 MHz, 25 ºC): δ 1.55 (s, 15H, Cp*).

4.4.15 $[Cp^*Rh^{III}(CH_3CN)_3][BF_4]_2$[16, 18]

An adaptation of the reported synthesis from ref. 16 &18 (above) was used. A solution of silver tetrafluoroborate (1.99 g, 10.22 mmol) in 10 ml acetonitrile was added to a solution of $[Rh^{III}(\eta^5\text{-}C_5Me_5)Cl_2]_2$ (1.58 g, 2.56 mmol) in 20 ml acetonitrile. An immediate exothermic reaction occurred with the precipitation of silver chloride. This was filtered and the yellow supernatant solution was freed from any remaining silver salt by filtration through a short column packed with cellulose. The eluate was taken to dryness *in vacuo* and the residue crystallized from acetonitrile-diethyl ether to give crystals of the yellow complex. The complex is insoluble in THF but soluble in acetonitrile. Yield: 1.63 g (60%). ^1H NMR (acetonitrile-d_3, 360 MHz, 25 ºC): δ 1.74 (s, 15H, Cp*), 1.96 (s, 9H, CH_3CN).

4.4.16 $[CpCo^{I}(CO)_2]$[19, 20]

Freshly distilled cyclopentadiene (7.75 ml, 0.09 mol), 60 ml of dried DCM, and octacarbonyldicobalt, $Co_2(CO)_8$ (6.25 g, 0.018 mol) were placed in a 250 ml flask, which was fitted with a reflux condenser. The system was flushed with nitrogen and was covered with aluminum foil to exclude light. The contents were heated to reflux on an oil bath for 2 days, after which time the DCM solvent was distilled leaving 3.91 g (58%) of product as a dark red liquid, bp 75-80 ºC. IR υ(CO) in cyclohexane: 2033 (s) and 1972 (s). The product was stored under nitrogen at -20 ºC in a covered flask.

4.4.17 $[CpCo(CO)I_2]$[21]

A filtered solution of 3.91 g (21.72 mmol) of $[CpCo(CO)_2]$ in 20 ml of anhydrous diethyl ether and 5.59 g (22.02 mmol) of iodine in 100 ml of anhydrous diethyl ether were mixed under nitrogen. Gas evolution and formation of a black precipitate occurred immediately. After stirring 2 days to assure complete reaction, the black crystalline precipitate was filtered, washed with diethyl ether and hexane and dried to

give 4.32 g (47%) of [$CpCo(CO)I_2$]. ^1H NMR ($CDCl_3$, 360 MHz, 25 ºC): δ 5.63 (s, Cp, C_5H_5). IR υ(CO) in KBr pellets: 2045 (s).

4.4.18 $[Co^{III}Cp(CH_3CN)_3][OTf]_2$[22]

An adaptation of the reported synthesis from ref 22 was used. At -20 ºC, a solution of 2.35 g (9.16 mmol) AgOTf in 20 ml acetonitrile was added dropwise to a suspension of 1.86 g (4.58 mmol) of [$CpCo(CO)I_2$] in 10 ml acetonitrile. The reaction mixture was allowed to warm up to room temperature. Solvent was removed *in vacuo* leaving 5 ml of reaction mixture. AgI was filtered using a frit. 15 ml of DCM was added to the filtrate and cool to -40 ºC which gave purple-red crystal. Yield: 1.3 g (52%). ^1H NMR (acetonitrile-d_3, 360 MHz, 25 ºC): δ 6.42 (s, Cp, 5H), 2.01 (s, CH_3CN, 9H). The product is air stable but slightly hygroscopic. It is stable in solid or in acetonitrile solution.

4.4.19 [N, N-dimethylbenzylamine-2-C,N)Pd(μ-Cl)]$_2$[23]

0.096 g (2.26 mmol) lithium chloride and 0.2 g (1.13 mmol) palladium(II) chloride were suspended in 15 ml methanol and stirred for 1 h at room temperature. A solution of 0.32 g (2.40 mmol) of *N,N*-dimethylbenzylamine in 20 ml of methanol was added to the suspension via cannula. After 5 min the color of the initially dark-orange solution became yellow and a yellow-greenish product precipitated. After 20 h stirring, the yellow product was filtered. Recrystallisation from a boiling mixture of toluene (15 ml)/hexane (15 ml) gave di-*μ*-chloro-bis(*N,N*-dimethylbenzylamine-2-C,N)dipalladium(II) as a yellow-greenish fine-powder. Yield: 0.23g (74%). ^1H NMR ($CDCl_3$, 250 MHz, 25 ºC): δ 2.85 (d, 12 H, CH_3, J = 6.5 Hz), 3.93 (s, 4 H, CH_2), 6.80 – 7.21 (m, 8 H, CH_{Ar}).

4.5 Synthesis of the ligands

4.5.1 Synthesis of 6-(dimethylamino)fulvene[24]

All operations were carried out under an inert atmosphere.

Dimethylformamide (30.97 ml, 400 mmol) was placed in a 3-necked flask equipped with mechanical stirrer, dropping funnel and reflux condenser and was heated to 55 ºC. Dimethyl sulphate (37.93 ml, 400 mmol) was added dropwise while stirring during 30 minutes. After the addition was completed, the mixture was stirred for additional 2 hours at 80 ºC. A viscous, colorless ether-insoluble oil of dimethylformamide-dimethylsulphate was obtained.

The DMF-DMS oil (400 mmol) was slowly added to a red solution of sodium cyclopentadienide (200 ml, 2.0 M in THF, 400 mmol) at -10 ºC under a nitrogen atmosphere. When the addition was completed, the mixture was stirred at room temperature over night. The solvent and volatiles were removed *in vacuo.* Activated charcoal and hexane (200 ml) were added and the mixture was heated to reflux for 4 h and filtered while hot. Other 2 portions of 50 ml of hot hexane were added to the solid residue to extract more products. The combined solutions were concentrated under vacuum and stored at -18 ºC to yield 18.53 g (38%) of the 6-(dimethylamino)fulvene as yellow flakes. 6-(dimethylamino)fulvene is light-sensitive. ^{1}H NMR ($CDCl_3$, 250 MHz, 25 ºC): δ 7.15 (s, 1H), 6.62 (m, 1H), 6.56 (m, 1H), 6.44 (m, 1H), 6,35 (m, 1H), 3.29 (s, 6H, CH_3); $^{13}C\{^{1}H\}$ NMR ($CDCl_3$, 62.90 MHz, 25 ºC): δ 148.70, 125.30, 124.50, 119.62, 116.92, 114.00, 30.41 (CH_3); MS (EI, *m*/*z*): 122 (M^+), 107 (M^+- CH_3). Elemental analysis for $C_8H_{11}N$: C, 79.27; H, 9.17; N, 11.56. Found: C, 78.98; H, 9.10; N, 11.46.

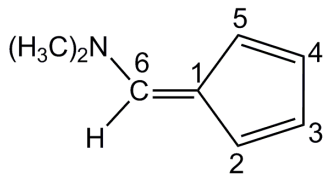

4.5.2 Synthesis of 6-dimethylaminofulvene-2-N,N′-dimethylaldimmonium chloride[25]

In a 3-necked flask equipped with dropping funnel, DMF (13.0 ml, 168.67 mmol) was dissolved in 150 ml of THF. A solution of oxalyl chloride (14.48 ml, 168.67 mmol) in THF (40 ml) was slowly added while keeping the temperature at 0 ºC. After the addition was completed, the white suspension was stirred at room temperature for 1 h. The suspension was slowly added under nitrogen to an orange-yellow solution of 6-dimethylaminofulvene (20.44 g, 168.67 mmol) in THF (200 ml). The temperature was kept below -60 ºC throughout the addition. After the addition, the mixture was stirred overnight at room temperature. The solvent and volatiles were removed *in vacuo* and the crude product washed with 100 ml hexane/ether (50:50) to give 35.0 g (98%) of the product as a pale greenish-yellow solid. The product is sensitive to air and moisture. ^{1}H NMR ($CDCl_3$, 250 MHz, 25 ºC): δ 9.76 (s, 2H, CHN), 7.35 (d, 2H, CpH), 6.78 (t, 1H, CpH), 3.83 (s, 6H, CH_3), 3.42 (s, 6H, CH_3); $^{13}C\{^{1}H\}$ NMR ($CDCl_3$, 62.90 MHz, 25 ºC): δ 160.60, 130.30, 125.81, 119.32, 48.81 (CH_3), 42.13 (CH_3).

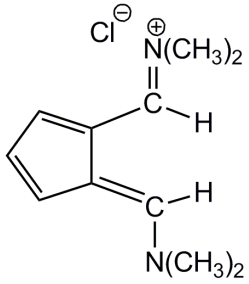

4.5.3 N,N′-diphenyl-6-aminofulvene-2-aldimine[25] (2.21)

A solution of 6-dimethylaminofulvene-2-*N,N′*-dimethylaldimmonium chloride (15.0 g, 70.58 mmol) in 150 ml of ethanol was heated to reflux with aniline (12.86 ml, 141.17 mmol) for overnight. The solvent and volatiles were removed *in vacuo*, activated charcoal was added and the residue heated to reflux in 250 ml of hexane overnight. The mixture was filtered while still hot and 2 portions of 50 ml of hot hexane were used to extract more products from the solid residue. The orange

solutions were combined and the volume reduced to about 1/4. Storage at -20 ºC afforded 4.0 g (20%) of the desired product as orange crystalline powder. ^{1}H NMR ($CDCl_3$, 250 MHz, 25 ºC): δ 15.59 (br, 1H, NH), 8.29 (d, 2H, H1/H7, *J* = 6.9 Hz), 7.38 (m, 4H, C_6H_5), 7.23 (m, 4H, C_6H_5), 7.16 (t, 2H, C_6H_5), 7.05 (d, 2H, H3/H5, *J* = 3.7 Hz), 6.47 (t, 1H, H4, *J* = 3.7 Hz); ^{13}C{^{1}H} NMR ($CDCl_3$, 62.90 MHz, 25 ºC): δ 150.63 (C1/C7), 145.25 (C, *ipso*-Ar), 134.68 (C3/C5), 129.56 (C, Ar), 124.84 (C, Ar), 122.08 (C2/C6), 120.96 (C4), 119.12 (C, Ar); MS (EI, *m/z*): 272 (M^+). Elemental analysis for $C_{19}H_{16}N_2$: C, 83.79; H, 5.92; N, 10.29. Found: C, 83.81; H, 5.87; N, 10.32.

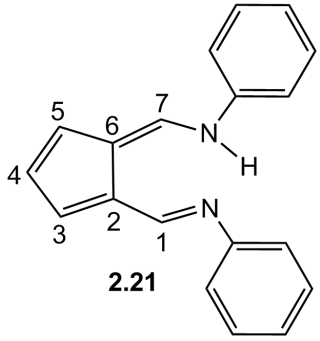

2.21

4.5.4 N,N′-dicyclohexyl-6-aminofulvene-2-aldimine[25] (2.23)

A solution of 6-dimethylaminofulvene-2-*N,N′*-dimethylaldimmonium chloride (15.0 g, 70.58 mmol) in 150 ml of ethanol was heated to reflux with cyclohexylamine (16.09 ml, 141.176 mmol) overnight. The solvent and volatiles were removed *in vacuo*, activated charcoal was added and the residue refluxed in 250 ml of hexane for overnight. The mixture was filtered while still hot and 2 portions of 50 ml of hot hexane were used to extract more products from the solid residue. The solutions were combined and the volume reduced to about 1/4. Storage at -20 ºC afforded 4.32 g (21.71%) of the desired product as red needles. ^{1}H NMR ($CDCl_3$, 250 MHz, 25 ºC): δ 14.04 (br, 1H, NH), 7.94 (d, 2H, H1/H7, *J* = 6.6 Hz), 6.81 (d, 2H, H3/H5, *J* = 3.5 Hz), 6.34 (t, 1H, H4, *J* = 3.5 Hz), 3.25 (m, 2H, *ipso*-CyH), 1.20-2.01 (m, 20H, CyH); ^{1}H NMR (acetonitrile-d_3, 500 MHz, 25 ºC): δ 13.66 (br, 1H, NH), 7.91 (d, 2H, H1/H7, *J* = 6.31 Hz), 6.65 (d, 2H, H3/H5, *J* = 3.57 Hz), 6.12 (t, 1H, H4, *J* = 3.57 Hz), 3.23 (m, 2H, *ipso*-CyH), 1.90-1.18 (m, 20H, CyH); ^{13}C{^{1}H} NMR ($CDCl_3$, 62.90 MHz, 25 ºC): δ 154.78 (C1/C7), 129.86 (C3/C5), 120.08 (C2/C6), 117.65

(C4), 64.19 (*ipso*-C, Cy), 35.39 (C, Cy), 26.00 (C, Cy), 25.49 (C, Cy); MS (FAB, *m/z*): 284 (M^+). Elemental analysis for $C_{19}H_{28}N_2$: C, 80.23; H, 9.92; N, 9.85. Found: C, 80.19; H, 9.95; N, 9.86.

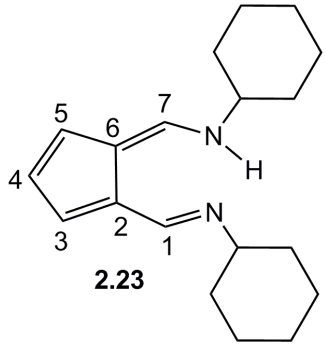

2.23

4.5.5 N,N′-di-(2,4,6-trimethylphenyl)-6-aminofulvene-2-aldimine (2.22)

A solution of 6-dimethylaminofulvene-2-*N,N′*-dimethylaldimmonium chloride (5.72 g, 26.90 mmol) in absolute ethanol (150 ml) was heated to reflux with an excess of 2,4,6-trimethylaniline (11.33 ml, 80.70 mmol) for 4 days. The solvent and volatiles were removed *in vacuo*, activated charcoal was added and the product refluxed in hexane (200 ml) overnight. The solution was filtered while still hot and the solid residue extracted with another 3x30 ml portions of hot hexane. The combined solutions were concentrated and stored at -20 ºC for 1 day to produce the final product as a yellow crystalline solid, which was separated and dried *in vacuo*. Yield: 2.0 g (21.57%). ^{1}H NMR ($CDCl_3$, 250 MHz, 25 ºC): δ 14.96 (br, 1H, NH), 7.89 (d, 2H, H1/H7, *J* = 7.0 Hz), 7.00 (d, 2H, H3/H5, *J* = 3.7 Hz), 6.88 (s, 4H, Ar-H), 6.44 (t, 1H, H4, *J* = 3.7 Hz), 2.27 (s, 6H, *p*-CH_3), 2.16 (s, 12H, Ar-CH_3); ^{13}C{^{1}H} NMR ($CDCl_3$, 62.90 MHz, 25 ºC): δ 156.81 (C1/C7), 141.68 (C, *ipso*-Ar), 134.65 (*o*-C, Ar), 132.71 (C3/C5), 130.73 (*p*-C, Ar), 129.91 (*m*-C, Ar), 120.85 (C2/C6), 119.14 (C4), 20.65 (*p*-CH_3, Ar), 18.44 (*o*-CH_3, Ar); MS (EI, *m/z*): 356 (M^+). Elemental analysis for $C_{25}H_{28}N_2$: C, 84.23; H, 7.92; N, 7.86. Found: C, 84.21; H, 7.95; N, 7.84.

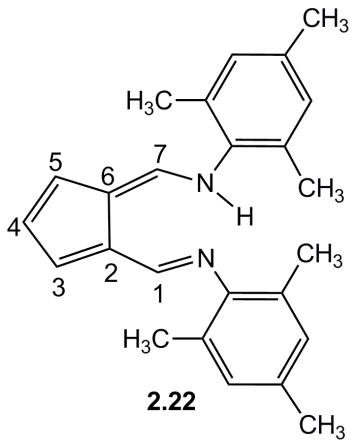

2.22

4.5.6 N,N′-di^{t}butyl-6-aminofulvene-2-aldimine[25] (2.26)

A solution of 6-dimethylaminofulvene-2-N, N'-dimethylaldimonium chloride (10.0 g, 47.06 mmol) in 150 ml dry ethanol was heated to reflux overnight with ^{t}butylamine (9.93 ml, 94.12 mmol). The mixture was cooled and the solvent and volatiles were removed *in vacuo*. The solid residue was refluxed with activated charcoal in 200 ml hexane. The mixture was filtered while still hot and washed with two portions of 50 ml hexane. The solvent was removed under vacuum and the product was crystallised from pentane to produce yellow-orange needles. Yield: 0.28 g (2.56%). ^{1}H NMR ($CDCl_3$, 500 MHz, 25 ºC): δ 13.82 (br, 1H, NH), 7.95 (2H, H1/H7), 6.78 (d, 2H, H3/H5, *J* = 3.53 Hz), 6.29 (t, 1H, H4, *J* = 3.53 Hz), 1.38 (s, 18H, ^{t}Butyl-CH_3). ^{13}C{^{1}H} NMR ($CDCl_3$, 125 MHz, 25 ºC): δ 151.43 (C1/C7), 129.88 (C3/C5), 119.80 (C2/C6), 117.24 (C4), 55.01 (quarternery-C, ^{t}Butyl), 30.32 (CH_3-C, ^{t}Butyl); MS (EI, FAB *m/z*): 232.2 (M^+). Elemental analysis for $C_{15}H_{24}N_2$: C, 77.53; H, 10.41; N, 12.06. Found: C, 77.57; H, 10.46; N, 12.08.

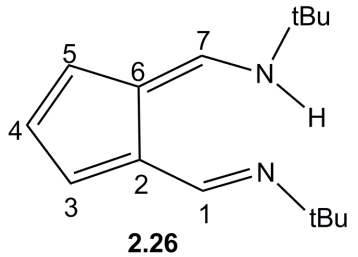

2.26

4.5.7 N,N′-bis(2,6-diisopropylphenyl)-6-aminofulvene-2-aldimine[26] (2.25)

A solution of 6-dimethylaminofulvene-2-*N,N′*-dimethylaldimmonium chloride (2.01 g, 9.45 mmol) in dry ethanol (35 ml) was heated to reflux with 2,6-diisopropylaniline (3.54 ml, 18.80 mmol) for 12 h. The solvent and volatiles were removed *in vacuo*. The resulting solid was then refluxed in hexane (150 ml) with activated charcoal (5.0 g) for 1.5 h. The mixture was filtered through celite while still hot and 3 portions of hot hexane (15 ml) were used to extract more products from the solid residue. The solutions were combined and the volume was reduced. The product was purified by column chromotography on silica using hexane and ethyl acetate (20:1) as an eluent. Crystals suitable for X-ray analysis were obtained on cooling at -30 ºC in hexane. Yield: 1.548 g (37%). ^{1}H NMR ($CDCl_3$, 360 MHz, 25 ºC): δ 14.55 (br, NH), 7.97 (d, 2H, H1/H7, *J* = 6.78 Hz), 7.18-7.34 (m, 6H, C_6H_5), 7.13 (d, 2H, H3/H5, *J* = 3.65 Hz), 6.56 (t, 1H, H4, *J* = 3.65 Hz), 3.27 (sept, 4H, ^{i}PrCH, *J* = 6.78 Hz), 1.23 (d, 24H, ^{i}PrCH$_3$, *J* = 6.78 Hz); ^{13}C{^{1}H} NMR ($CDCl_3$, 90.6 MHz, 25 ºC) 157.42 (C1/C7), 142.15 (C, *ipso*-Ar), 142.09 (*o*-C, Ar), 133.40 (C3/C5), 126.28 (C4), 123.44 (*m*-C, Ar), 120.80 (C2/C6), 119.43 (*p*-C, Ar), 28.19 (C, ^{i}Pr-CH), 23.94 (C, ^{i}Pr-CH$_3$); MS (EI, m/z): 440.3 (M+). Anal. Calcd for $C_{31}H_{40}N_2$: C, 84.49; H, 9.15; N, 6.36. Found: C, 84.40; H, 9.21; N 6.56.

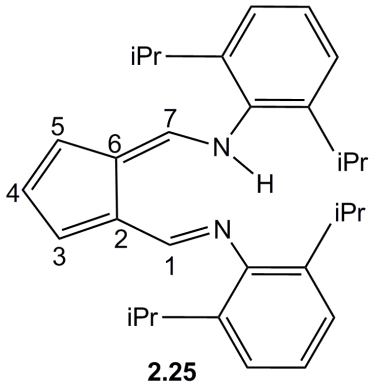

2.25

4.5.8 N,N′-bis(2-methoxyphenyl)-6-aminofulvene-2-aldimine (2.24)

A solution of 6-dimethylaminofulvene-2-*N,N′*-dimethylaldimmonium chloride (2.0 g, 9.41 mmol) in dry ethanol (50 ml) with 2-methoxyaniline (2.13 ml, 18.82 mmol) was heated to reflux overnight. The solvent and volatiles were removed *in vacuo*. The resulting solid was then refluxed in hexane (50 ml) for 3 h. The reaction mixture was concentrated and was kept in the fridge at -20 ºC. The unreacted 2-methoxyaniline precipitated and the mother liquor was transferred to another round-bottom flux. The mother liquor was concentrated and was kept in the fridge at -20 ºC. An orange solid precipitated. The orange solid melted at room temperature. It was washed three times with hexane and was recrystalised in hexane to get pure orange solid product. Yield: 0.22 g (7 %). ^{1}H NMR ($CDCl_3$, 500 MHz, 25 ºC): δ 15.57 (t, 1H, NH), 8.28 (d, 2H, H1/H7, *J* = 6.94 Hz), 7.24-7.22 (m, 2H, Ar), 7.14-7.10 (m, 2H, Ar), 7.02 (d, 2H, H3/H5, *J* = 3.63 Hz), 7.0-6.97 (m, 2H, Ar), 6.90-6.88 (m, 2H, Ar), 6.43 (t, 1H, H4, *J* = 3.63 Hz), 3.54 (s, 6H, OCH_3); ^{13}C{^{1}H} NMR ($CDCl_3$, 125 MHz, 25 ºC): δ 151.83 (C1/C7), 151.70 (quarternery-C, Ar), 135.62 (*ipso*-C, Ar), 133.69 (C3/C5), 125.33 (C, Ar), 122.44 (C2/C6), 120.90 (C, Ar), 120.15 (C4), 119.49 (C, Ar), 111.22 (C, Ar), 55.43 (C, OCH_3); MS (EI, *m/z*): 332.2 (M+). Anal. Calcd for $C_{21}H_{20}O_2N_2$: C, 75.88; H, 6.06; N, 8.43. Found: C, 74.92; H, 6.02; N, 8.20.

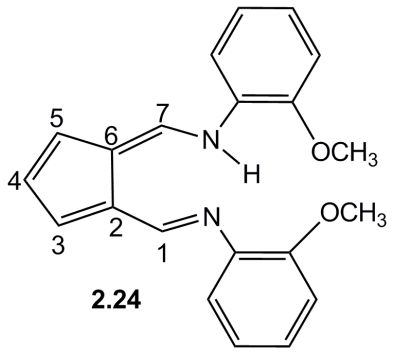

2.24

4.6 Synthesis of the complexes

4.6.1 [(Ph_2AFA)Pd(CH_3)(DMAP)][26] (2.28)

To a solution of Ph_2AFAH (0.538 g, 1.98 mmol) in toluene (40 ml), 1.24 ml (1.98 mmol) of ^{n}BuLi (1.6 M in hexane) were added and the mixture was stirred for 1 h. To a solution of [(COD)Pd(CH_3)(Cl)] (0.524 g, 1.98 mmol) in toluene (20 ml), DMAP (0.241 g, 1.98 mmol) was added and the resulting brown suspension was transferred into the solution of the deprotonated ligand. The colour of the reaction mixture immediately became dark red. The mixture was stirred overnight at room temperature. After filtration through celite, the volume of the solvent was reduced to *ca.* 2/3 under vacuum. Upon storage at -10 ºC, the red product precipitated. Suitable crystals for X-ray analysis were obtained by slow diffusion of hexane into a dichloromethane solution of the product. Yield: 0.30 g (44%). ^{1}H NMR ($CDCl_3$, 250 MHz, 25 ºC): δ 8.37 (s, 1H, H1), 8.29 (s, 1H, H7), 7.81 (d, 2H, DMAP, *J* = 7 Hz), 7.66-6.89 (m, 10H, C_6H_5), 6.83 (dd, 1H, H5, *J* = 5.28, 2.31 Hz), 6.80 (dd, 1H, H3, *J* = 5.6, 2.31 Hz), 6.35 (t, 1H, H4, *J* = 3.63 Hz), 6.12 (d, 2H, DMAP, *J* = 7.26 Hz), 2.92 (s, 6H, DMAP), -0.1 (s, 3H, CH_3–Pd); ^{13}C{^{1}H} NMR ($CDCl_3$, 62.90 MHz, 25 ºC): δ 163.74 (C1), 160.34 (C7), 154.06, 153.92, 152.87, 150.95 (C, DMAP), 133.02, 132.62, 128.79, 128.68, 124.78, 124.15, 123.94, 122.55, 117.98, 117.81, 117.54, 107.21 (C, DMAP), 39.40 (*N*-CH_3), 1.37 (CH_3-Pd); MS (FAB, *m/z*): 515 (M+). Anal. Calcd for $C_{27}H_{28}N_4Pd$: C, 62.97; H, 5.48; N, 10.88. Found: C, 63.54; H, 5.56; N, 10.52.

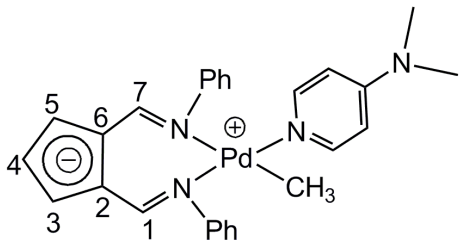

2.28

4.6.2 Synthesis of [(Ph_2AFA)(N,N′-dimethylbenzylamine-2-C,N)-Pd(II)][26] (2.31)

To a solution of Ph_2AFAH (0.224 g, 0.822 mmol) in THF (15 ml) was added ^{n}BuLi (0.56 ml, 1.6M in hexane, 0.91 mmol) at -78 ºC. The mixture was stirred for 1.5 h, and then allowed to warm to -40 ºC. The colour of the solution turned from yellow-orange to dark orange. A solution of di-μ-chloro-bis(*N*,*N*-dimethylbenzylamine-2-C,N)dipalladium (0.227 g, 0.411 mmol) in THF (15 ml) was added at -40 ºC. The color of the reaction mixture turned to dark red. The mixture was stirred overnight at room temperature. The solvent was removed *in vacuo* and the crude product was washed with a solvent mixture of toluene–hexane (2: 1) and the residue was subsequently dissolved in a CH_2Cl_2 hexane mixture (8: 1) and filtered through celite to remove LiCl. The solvent was removed *in vacuo* and the resulting residue washed with hexane which yielded pure product. Yield: 0.012 g (3%). Crystals suitable for X-ray analysis were obtained from slow diffusion of hexane into a concentrated solution of the product in CH_2Cl_2. ^{1}H NMR ($CDCl_3$, 250 MHz, 25 ºC): δ 2.30 (s, 3H, CH_3), 2.53 (s, 3H, CH_3), 3.72 (d, 1H, *J* = 13.54 Hz), 3.89 (d, 1H, *J* = 13.54 Hz), 6.40 (t, 1H, H4, *J* = 3.63 Hz), 6.58-6.85 & 6.89-7.87 (m, 14H, Ar), 6.86 (dd, 1H, H3, *J* = 3.63, 1.65 Hz), 6.87 (dd, 1H, H5, *J* = 3.30, 1.32 Hz), 8.61 (s, 1H, H7), 8.65 (s, 1H, H1); ^{13}C{1H} NMR ($CDCl_3$, 62.90 MHz, 25 ºC): δ 158.83 (C1), 158.40 (C7), 149.82, 148.54, 146.88, 146.55, 134.67, 132.47, 131.96, 129.30, 128.79, 124.79, 124.72, 124.60, 123.99, 123.72, 121.55, 121.51, 121.06, 119.37, 119.06 (C4), 73.66 (C, CH_2), 52.13 (C, NCH_3), 51.42 (C, NCH_3); MS (EI, *m/z*): 511(M+). Anal. Calcd for $C_{28}H_{27}PdN_3$: C, 65.69; H, 5.32; N, 8.21 Found: C, 65.29; H, 5.41; N, 8.31.

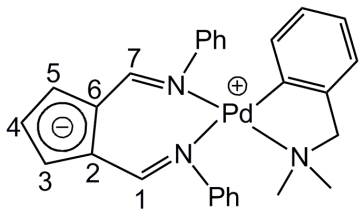

2.31

4.6.3 Synthesis of $[(Cy_2AFA)_2Pd]^{26}$ (2.37)

To a red solution of Cy_2AFAH (0.311 g, 1.097 mmol) in toluene (25 ml), 0.822 ml (1.316 mmol) of CH_3Li (1.6M in diethyl ether) were added and the mixture was stirred at RT for 1 h. A pale red solution of $(PhCN)_2PdCl_2$ (0.421 g, 1.097 mmol) in toluene (50 ml) was stirred at 50 ºC for 1 h and then transferred to the deprotonated ligand. The dark red reaction mixture was stirred at room temperature over night. After filtration through celite, the volume of the solvent was reduced to *ca.* 2/3 under vacuum and then acetonitrile was added to precipitate the product from the unreacted ligand. The solution was decanted and the solid orange product was dried under vacuum. Crystals suitable for X-ray analysis were obtained by slow evaporation of a solution in a mixture of toluene and acetonitrile solvents under nitrogen. Yield: 0.07 g (10%). ^{1}HNMR ($CDCl_3$, 250 MHz, 25 ºC): δ 7.71 (s, 2H, H1/H7), 6.54 (d, 2H, H3/H5, *J* = 3.30 Hz), 6.3 (t, 1H, H4, *J* = 3.30 Hz), 3.11 (2H, *ipso*-CyH), 0.96-1.81(m, 20H, CyH); ^{13}C{1H} NMR ($CDCl_3$, 62.90 MHz, 25 ºC): δ 160.97 (C1/C7), 127.27 (C3/C5), 116.89 (C4), 115.54 (C2/C6), 65.31 (*ipso*-C, Cy), 37.02 (C, Cy), 32.79 (C, Cy), 26.24 (C, Cy); MS (EI, *m*/*z*): 672.4 (M+). Anal. Calcd for $C_{38}H_{54}N_4Pd$: C, 67.79; H, 8.08; N, 8.32. Found: C, 67.09; H, 7.98; N, 8.11.

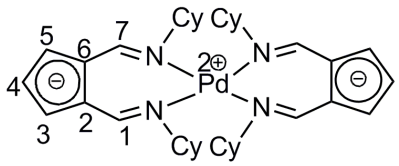

2.37

4.6.4 Synthesis of $[(^tBu_2AFA)_2Pd]^{26}$ (2.38)

To a yellow solution of $^tBu_2AFAH$ (0.10 g, 0.43 mmol) in toluene (15 ml), 0.4 ml (0.64 mmol) of CH_3Li (1.6 M in diethyl ether) were added and the mixture was stirred at RT for 1 h. A pale red solution of $(PhCN)_2PdCl_2$ (0.165 g, 0.43 mmol) in toluene (30 ml) was stirred at 50 ºC for 1 h and then slowly transferred to the deprotonated ligand. The brown reaction mixture was stirred at room temperature over night. After filtration through celite, the solvent was removed under vacuum

and the unreacted ligand was partly removed by washing with hexane. The brown solid product contains traces amount of ligand. Yield: 0.10 g (41%). Suitable crystals for X-ray analysis were not obtained. Slow diffusion of hexane into a toluene solution of the product yielded only brown powder. ^{1}HNMR ($CDCl_3$, 360 MHz, 25 ºC): δ 7.78 (s, 2H, H1/H7), 6.55 (d, 2H, H3/H5, *J* = 3.30 Hz), 6.46 (t, 1H, H4, *J* = 3.30 Hz), 1.38 (s, 18H, ^{t}Bu-CH_3); ^{13}C{1H} NMR ($CDCl_3$, 90.6 MHz, 25 ºC) δ 164.83 (C1/C7), 151.74 (C2/C6), 124.15 (C3/C5), 118.38 (C4), 59.95 (quaternary-C, ^{t}Bu), 32.66 (C, ^{t}Bu-CH_3); MS(EI, *m/z*): 568.2. NMR (^{1}H and ^{13}C) spectra showed the presence of small amounts of the free ligand which resulted in elemental analysis results being unsatisfactory.

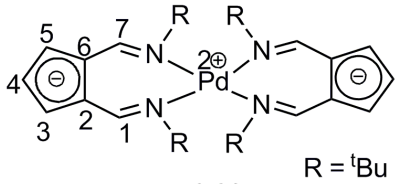

2.38

4.6.5 [{(2-methoxyphenyl)$_2$AFA}Pd] (2.42)

To a solution of (2-methoxyphenyl)$_2$AFAH (0.02 g, 0.06 mmol) in toluene (30 ml), 0.05 ml (0.08 mmol) of CH_3Li (1.6M in diethyl ether) were added and the mixture was stirred at RT for 1 h. A solution of $(PhCN)_2PdCl_2$ (0.023 g, 0.06 mmol) in toluene (30 ml) was stirred at 50 ºC for 1 h and then transferred to the deprotonated ligand. The reaction mixture was stirred at room temperature over night. After filtration through celite, the solvent was removed *in vacuo* and the reaction mixture was washed with hexane to remove the unreacted ligand. The product was dissolved in hot hexane and kept in the fridge at – 20 ºC. The product precipitated as brown solid. Yield: 0.025 g (54%). ^{1}H NMR ($CDCl_3$, 500 MHz, 25 ºC): δ 7.66 (s, 2H, H1/H7), 7.67 (d, 1H, Ar, *J* = 1.44 Hz), 7.64 (d, 1H, Ar, *J* = 1.70 Hz), 7.11 - 7.03 (m, 2H, Ar), 6.85 – 6.75 (m, 4H, Ar), 6.60 (d, 2H, H3/H5, *J* = 3.65 Hz), 6.33 (t, 1H, H4, *J* = 3.65 Hz), 3.50 (s, 6H, OCH_3); ^{13}C{1H} NMR ($CDCl_3$, 125 MHz, 25 ºC): δ 165.46 (C1/C7), 153.85 (quarternery-C, Ar), 139.41 (*ipso*-C, Ar), 133.64 (C3/C5), 127.76 (C, Ar), 126.33 (C, Ar), 121.03 (C, Ar), 119.79 (C4), 118.60 (C2/C6), 112.51 (C, Ar), 56.23 (C, OCH_3); MS (+ve FAB, *m/z*): 767.6 (M+). Anal. Calcd for $C_{42}H_{38}O_4N_4Pd$: C, 65.58; H, 4.98; N, 7.28. Found: C, 65.62; H, 5.01; N, 7.29.

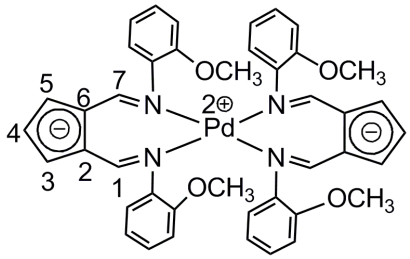

2.42

4.6.6 [(Ph_2AFA)Ni(η^3-C_3H_5)] (2.40)

To a solution of Ph_2AFAH (0.135 g, 0.496 mmol) in toluene (15 ml), 0.31 ml (0.496 mmol) CH_3Li (1.6 M in diethyl ether) were added and the mixture stirred for 1h. A red solution of π-allyl nickel bromide (0.074 g, 0.248 mmol) in toluene (15 ml) was added via a cannula to the deprotonated ligand and the red color mixture stirred for overnight. After filtration through celite, the solvent was removed. The product contains unreacted ligand. In an attempt to purify the product, the reaction mixture was dissolved in hexane (5ml) and cooled to -64 ºC in freezer. Some solid was precipitated. The mother liquor was decanted and ^{1}H NMR sprectrum of the solid and the mother liquor were recorded which showed the presence of unreacted ligand in both the solid precipitate and the mother liquor. Both the ligand and the complex are highly soluble in toluene, DCM, Ether, Hexane, THF and acetonitrile. The product is air and moisture sensitive. ^{1}H NMR ($CDCl_3$, 500 MHz, 25 ºC): δ 8.25 (s, 2H, H1/H7), 7.15-7.59 (m, 10H, C_6H_5), 6.89 (d, 2H, H3/H5, *J* = 3.63 Hz), 6.40 (t, 1H, H4, *J* = 3.63 Hz), 5.43 (tt, 1H, Allyl CH, *J* = 7.17 Hz), 2.21 (d, 2H, Allyl CHH, *J* = 7.09 Hz), 1.88 (d, 2H, Allyl CHH, *J* = 13.40 Hz); ^{13}C{1H} NMR ($CDCl_3$, 125 MHz, 25 ºC): δ 161.66 (C1/C7), 154.74 (*ipso*-C of Ar), 132.68 (C3/C5), 129.14 (C-Ar), 124.84 (C-Ar), 122.05 (C-Ar), 118.71 (C4), 117.41 (C2/C6), 111.56 (CH of allyl), 56.72 (CH_2 of allyl). NMR (^{1}H and ^{13}C) spectra showed the presence of small amounts of the free ligand which resulted in elemental analysis results being unsatisfactory.

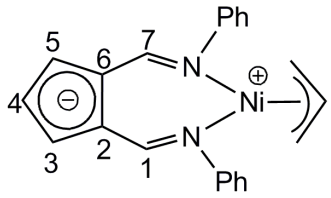

2.40

4.6.7 [Cp*Ru^{II}(Ph$_2$AFA)H][BF$_4$] (3.22)

An orange-yellowish solution of Ph_2AFAH (0.37 g, 1.37 mmol) in 25 ml DCM was added via cannula to a yellow solution of [Cp*Ru^{II}(CH_3CN)$_3$][BF_4] (0.61 g, 1.37 mmol) in 30 ml DCM. The reaction mixture immediately turned to red. After stirring overnight at room temperature, the solvent was removed *in vacuo*. To remove unreacted ligand, the reaction mixture was dissolved in 20 ml acetonitrile and hexane (20 ml) was added and was shake vigorously. The unreacted ligand dissolved in hexane and stayed on top of acetonitrile solution. The top layer (hexane containing free ligand) was decanted and the bottom layer of acetonitrile solution was collected. Acetonitrile was removed *in vacuo* and the product was washed with hexane (3 x 10 ml). Crystals suitable for X-ray analysis were obtained by layering hexane on DCM solution of the complex. Yield: 0.70 g (86.40%). The complex is stable in air and moisture and highly soluble in DCM and acetonitrile but insoluble in hexane. ^{1}H NMR ($CDCl_3$, 400 MHz, 25 ºC): δ 16.51 (t, 1H, NH), 8.93 (d, 2H, H1/H7, *J* = 7.57 Hz), 7.51-7.35 (m, 10H, C_6H_5), 5.66 (d, 2H, H3/H5, *J* = 2.65 Hz), 5.17 (t, 1H, H4, *J* = 2.77 Hz), 1.83 (s, 15H, $CpCH_3$); ^{13}C{1H} NMR ($CDCl_3$, 100 MHz, 25 ºC) δ 161.73 (C1/C7), 142.53 (*ipso*-C, Ar), 130.53 (C, Ar), 128.27 (C, Ar), 119.78 (C, Ar), 92.30 (C2/C6), 85.73 (C3/C5), 84.70 (C4), 79.37 (C_5Me_5), 11.58 (C_5Me_5); MS(EI, *m/z*): 509.1 (M+). Anal. Calcd for $C_{29}H_{31}BF_4N_2Ru$: C, 58.50; H, 5.25; N, 4.70. Found: C, 58.53; H, 5.27; N, 4.74.

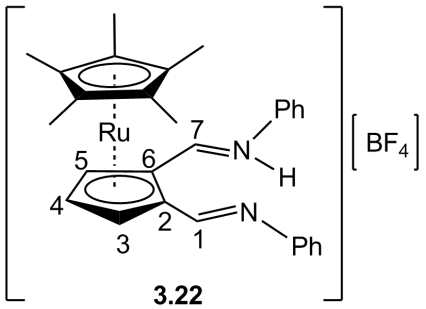

3.22

4.6.8 $[Cp^*Rh^{III}(Cy_2AFA)H][BF_4]_2$ (3.24)

An orange-yellowish solution of Cy_2AFAH (0.10 g, 0.351 mmol) in 10 ml DCM was added via cannula to a yellow solution of $[Cp^*Rh^{III}(CH_3CN)_3][BF_4]_2$ (0.187 g, 0.351 mmol). The reaction mixture immediately turned to red. After stirring overnight at room temperature, the solvent was removed *in vacuo* and pure product was obtained. Yield: 0.2 g (81.70%). Orange block crystals suitable for X-ray analysis were obtained by layering ether on top of an acetonitrile solution of the complex. The complex is stable in air and moisture and highly soluble in DCM and acetonitrile but insoluble in hexane and chloroform. ^{1}H NMR (acetonitrile-d_3, 500 MHz, 25 ºC): δ 16.80 (t, 1H, NH), 8.55 (d, 2H, H1/H7, *J* = 7.25 Hz), 6.43 (dd, 2H, H3/H5, *J* = 2.64 Hz, *J* = 0.73 Hz), 6.15 (dt, 1H, H4, *J* = 2.65 Hz, *J* = 1.0 Hz), 3.80 (m, 2H, *ipso*-CyH), 2.04 (s, 15H, Cp*), 1.96-1.27 (m, 20H, CyH); ^{13}C{^{1}H} NMR (acetonitrile-d_3, 125 MHz, 25 ºC): δ 161.27 (s, C1/C7), 106.44 (d, quaternary-C of Cp*, *J* = 7.72 Hz), 99.06 (d, C3/C5, *J* = 5.90 Hz), 96.08 (d, C4, *J* = 5.45 Hz), 94.95 (d, C2/C6, *J* = 6.36 Hz), 67.27 (s, *ipso*-C, Cy), 26.0 (C, Cy), 25.82 (C, Cy), 25.70 (C, Cy), 11.11 (s, Cp*); MS(EI, *m*/*z*): 520.2 (M^+ - 2H). Anal. Calcd for $C_{29}H_{43}N_2RhB_2F_8$: C, 50.03 ; H, 6.23; N, 4.02. Found: C, 50.25; H, 6.38; N, 4.05.

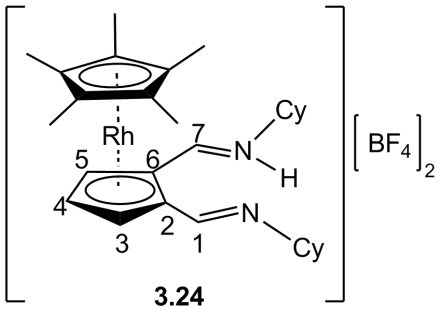

3.24

4.6.9 [Cp*Rh^{III}(Cy_2AFA)][BF_4] (3.26)

To a solution of Cy_2AFAH (0.30 g, 1.05 mmol) in THF (15 ml) at -70 ºC , KH (0.04 g, 1.05 mmol) in 15 ml THF was added drop wise via cannula. The mixture was stirred for 1h at room temperature. [Cp*Rh^{III}(CH_3CN)$_3$][BF_4]$_2$ (0.56 g, 1.05 mmol) was added as solid to the deprotonated ligand. The reaction mixture was heated at 70 ºC for 2h and then stirred at room temperature for over night. Some yellowish-brown precipitate was formed. The reaction mixture was filtered and the yellowish-brown precipitate was dried *in vacuo* to get pure product. Yiled: 0.19 g (29%). ^{1}H NMR (acetonitrile-d_3, 500 MHz, 25 ºC): δ 8.43 (s, 2H, H1/H7), 5.93 (dd, 2H, H3/H5, *J* = 2.68 Hz, *J* = 0.79 Hz), 5.68 (dt, 1H, H4, *J* = 2.68 Hz, *J* = 1.1 Hz), 3.30 (m, 2H, *ipso*-CyH), 1.98 (s, 15H, Cp*), 1.8-1.3 (m, 20H, CyH); ^{13}C{^{1}H} NMR (acetonitrile-d_3, 125 MHz, 25 ºC): δ 152.34 (s, C1/C7), 103.46 (d, quaternary-C of Cp*, *J* = 8.17 Hz), 99.24 (d, C2/C6, *J* = 6.36 Hz), 90.98 (d, C4, *J* = 6.81 Hz), 90.29 (d, C3/C5, *J* = 6.36 Hz), 71.13 (s, *ipso*-C, Cy), 35.91 (C, Cy), 35.77 (C, Cy), 25.64 (C, Cy), 10.85 (s, Cp*); MS(EI, *m*/*z*): 521.2 (M^+). Anal. Calcd for $C_{29}H_{42}RhN_2BF_4$: C, 57.25; H, 6.96; N, 4.60. Found: C, 57.36; H, 7.0; N, 4.53.

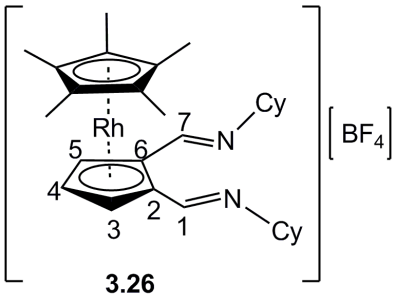

3.26

4.6.10 [Cp*Rh^{III}(Cy_2AFAPdCl_2)][BF_4] (3.30)

A solution of [(PhCN)$_2$PdCl_2] (0.03 g, 0.08 mmol) in acetonitrile (15 ml) was transferred via cannula to a solution of [Cp*Rh^{III}(Cy_2AFA)][BF_4] (0.05 g, 0.08 mmol) in acetonitrile (15 ml). The reaction mixture was heated at 70 ºC for 2h and then stirred over night at room temperature. The solvent was removed *in vacuo* and the residue was washed with ether to remove remaining benzonitrile. Hexane was

layered on top of a DCM solution of the complex but no suitable crystals were formed for X-ray analysis. Yiled: 0.03 g (38%). ^{1}H NMR (acetonitrile-d_3, 500 MHz, 25 ºC): δ 7.82 (s, 2H, H1/H7), 6.31 (dd, 2H, H3/H5, *J* = 2.14 Hz, *J* = 0.92 Hz), 6.18 (dt, 1H, H4, *J* = 2.70 Hz, *J* = 0.92 Hz), 4.26 (m, 2H, *ipso*-CyH), 2.08 (s, 15H, Cp*), 1.78 – 1.20 (m, 20H, CyH); ^{13}C{^{1}H} NMR (acetonitrile-d_3, 125 MHz, 25 ºC): δ 161.76 (s, C1/C7), 105.87 (d, quaternary-C of Cp*, *J* = 7.72 Hz), 95.13 (d, C3/C5, *J* = 5.90 Hz), 95.01 (d, C4, *J* = 5.90 Hz), 94.69 (d, C2/C6, *J* = 6.36 Hz), 72.19 (s, *ipso*-C, Cy), 38.10 (C, Cy), 34.43 (C, Cy), 27.17 (C, Cy), 11.42 (s, Cp*); MS(EI, *m*/*z*): 521.1 (M^+ - $PdCl_2$). Anal. Calcd for $C_{29}H_{42}RhN_2PdCl_2BF_4$: C, 44.33 ; H, 5.39; N, 3.57. Found: C, 44.13; H, 5.05; N, 3.77.

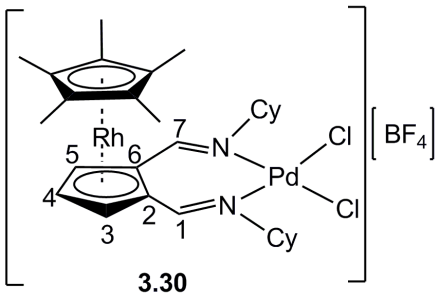

3.30

4.6.11 Attempted synthesis of [CpCo^{III}(Ph$_2$AFA)](H$^+$)[OTf]$_2$, resulting in synthesis of [Ph$_2$AFAH(H)][OTf] (3.28)

An orange solution of Ph_2AFAH (0.045 g, 0.165 mmol) in 10 ml acetonitrile was added via cannula to a light blue solution of $[CpCo^{III}(CH_3CN)_3][OTf]_2$ (0.089 g, 0.165 mmol) in 20 ml acetonitrile. The reaction mixture immediately turned to red. After stirring 1h at room temperature, the reaction mixture was filtered and the solvent was removed *in vacuo*. Crystals suitable for X-ray analysis were obtained by diffusion of chloroform into acetonitrile solution of the product. Yield: 0.06 g (85%). The obtained protonated ligand is insoluble in hexane, chloroform, toluene, diethylether, DCM but soluble in acetonitrile and acetone. ^{1}H NMR (acetonitrile-d_3, 500 MHz, 25 ºC): δ 10.52 (br, 2H, NH), 8.68 (d, 2H, H1/H7, *J* = 15.09 Hz), 7.80 (d, 2H, H3/H5, *J* = 3.84 Hz), 7.65 - 7.55 (m, 8H, Ph), 7.44 – 7.40 (m, 2H, Ph), 6.93 (t, 1H, H4, *J* = 3.84 Hz); ^{13}C{^{1}H} NMR (acetonitrile-d_3, 125 MHz, 25 ºC): δ 148.32 (C1/C7), 138.34 (C2/C6), 131.74 (C3/C5), 128.80 (C4), 124.60 (*ipso*-C, Ar), 127.65

(C, Ar), 129.93 (C, Ar), 119.06 (C, Ar); MS(+ve FAB, *m/z*): 273.3. Anal. Calcd for $C_{20}H_{17}N_2F_3SO_3$: C, 56.87; H, 4.06; N, 6.63. Found: C, 56.93; H, 4.10; N, 6.69.

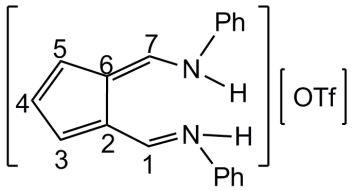

3.28

4.6.12 Attempted synthesis of [Cy_2AFAHPdCl_2], resulting in synthesis of [Cy_2AFAH(H)][Cl] (2.44)

A solution of Cy_2AFAH (0.05 g, 0.176 mmol) in 20 ml THF was added via cannula to a pale orange solution of [$(CH_3CN)_2PdCl_2$] (0.045 g, 0.176 mmol) in 10 ml THF. The reaction mixture immediately turned to dark brown. After stirring over night at room temperature, some brown solid precipitated. Hexane was added to the concentrated reaction mixture and more solid precipitated. The mother liquor was removed and the solid product was dissolved in acetonitrile and filtered and solvent was removed *in vacuo* and the solid was washed with hexane to remove unreacted ligand. The solid product is insoluble in hexane, toluene, ether but soluble in acetonitrile and partially soluble in THF. Yield: 0.03 g (53%). ^{1}H NMR (acetonitrile-d_3, 360 MHz, 25 ºC): δ 8.75 (br, 2H, NH), 8.06 (d, 2H, H1/H7, *J* = 15.65 Hz), 7.21 (d, 2H, H3/H5, *J* = 3.86 Hz), 6.44 (t, 1H, H4, *J* = 3.86 Hz), 3.56 (m, 2H, *ipso*-CyH), 1.75 – 1.04 (m, 20H, CyH); MS (+ve FAB, *m/z*): 285 (M+).

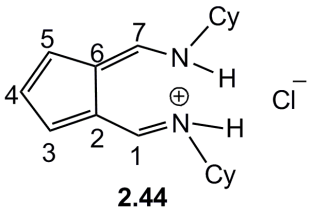

2.44

4.6.13 Attempted synthesis of [Ph_2AFAPd(OAc)], resulting in synthesis of [(Ph_2AFA)$_2$Pd] (2.47)

To a solution of Ph_2AFAH (0.1 g, 0.367 mmol) in toluene (10 ml), 0.23 ml (0.367 mmol) of CH_3Li (1.6 M in diethyl ether) was added and the mixture was stirred at RT for 2 h. The deprotonated ligand was then transferred via cannula to an orange-yellow solution of $Pd(OAc)_2$ (0.08 g, 0.367 mmol) in toluene (10 ml). The reaction mixture immediately became red. After stirring overnight, the reaction mixture was filtered through celite and the solvent was removed *in vacuo*. To remove the unreacted ligand, 20 ml hexane was added to the reaction mixture and was heated at 80 ºC and the mother liquor was decanted and the solid product dried *in vacuo*. Yield: 0.15 g (62%). ^{1}H NMR ($CDCl_3$, 500 MHz, 25 ºC): δ 7.44 (s, 2H, H1/H7), 7.40 – 7.12 (m, 10H, Ph), 6.72 (d, 2H, H3/H5, J = 3.65 Hz), 6.42 (t, 1H, H4, J = 3.65 Hz); ^{13}C{^{1}H} NMR ($CDCl_3$, 125 MHz, 25 ºC): δ 160.74 (C1/C7), 149.28 (*ipso*-C, Ph), 135.33 (C3/C5), 128.87 (C, Ar), 125.65 (C, Ar), 123.18 (C, Ar), 120.78 (C4), 117.65 (C2/C6); MS(EI, *m*/*z*): 648.1. Anal. Calcd for $C_{38}H_{30}N_4Pd$: C, 70.31 ; H, 4.66; N, 8.63. Found: C, 70.37; H, 4.71; N, 8.67.

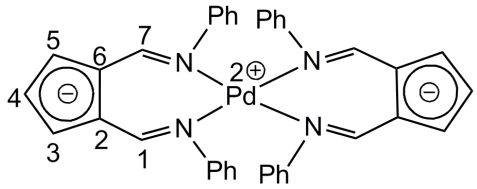

2.47

4.6.14 Attempted synthesis of [Ph_2AFAPd(Cl)(CH_3CN)], resulting in synthesis of [(Ph_2AFA)$_2$Pd] (2.47)

To a solution of Ph_2AFAH (0.05 g, 0.183 mmol) in toluene (15 ml), 0.14 ml (0.22 mmol) of CH_3Li (1.6 M in diethyl ether) was added and the mixture was stirred at RT for 1 h. The deprotonated ligand was then transferred via cannula to a yellow solution of $(CH_3CN)_2PdCl_2$ (0.047 g, 0.18 mmol) in toluene (15 ml). The reaction mixture became brown. After stirring over night, the reaction mixture was filtered

through celite and the solvent was removed *in vacuo*. The reaction mixture was washed with ether. In order to remove the unreacted ligand, 5 ml hexane and 15 ml ether was added to the reaction mixture and was kept at -20 ºC. Dark brown product precipitated which was dried *in vacuo*. The product is insoluble in ether but highly soluble in acetonitrile, THF and partially soluble in hexane. Yield: 0.06 g (50%). ^{1}H NMR ($CDCl_3$, 500 MHz, 25 ºC): δ 7.44 (s, 2H, H1/H7), 7.40 – 7.12 (m, 10H, Ph), 6.72 (d, 2H, H3/H5, *J* = 3.65 Hz), 6.42 (t, 1H, H4, *J* = 3.65 Hz); ^{13}C{^{1}H} NMR ($CDCl_3$, 125 MHz, 25 ºC): δ 160.74 (C1/C7), 149.28 (*ipso*-C, Ar), 135.33 (C3/C5), 128.87 (C, Ar), 125.65 (C, Ar), 123.18 (C, Ar), 120.78 (C4), 117.65 (C2/C6); MS(EI, *m*/*z*): 648.1. Anal. Calcd for $C_{38}H_{30}N_4Pd$: C, 70.31 ; H, 4.66; N, 8.63. Found: C, 70.37; H, 4.71; N, 8.67.

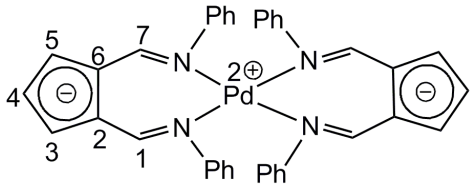

2.47

4.6.15 Attempted synthesis of [Ph_2AFA($SiMe_3$)] (2.53)

To a solution of Ph_2AFAH (0.06 g, 0.22 mmol) in toluene (30 ml), 0.15 ml (0.23 mmol) of CH_3Li (1.6 M in diethyl ether) was added and the mixture was stirred at RT for 1 h. Then chlorotrimethylsilane 0.03 ml (0.22 mmol) was added to the deprotonated ligand via syringe. The reaction mixture became brown. After stirring over night, the reaction mixture was filtered and the solvent was removed *in vacuo*. ^{1}H NMR ($CDCl_3$, 360 MHz, 25 ºC) shows unreacted ligand and some undefined species in the reaction mixture.

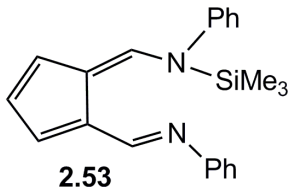

2.53

4.6.16 Attempted synthesis of [(Ph_2AFA)Ag($NCCH_3$)] (2.56)

Cy_2AFAH (0.1g, 0.35 mmol) and Ag_2O (0.04 g, 0.176 mmol) were mixed in a Schlenk tube and 30 ml acetonitrile was added to it. The Cy_2AFAH ligand was soluble in acetonitrile but Ag_2O remained insoluble and didn't react to the Cy_2AFAH ligand. A solution of [(COD)Pd(Me)(Cl)] (0.09 g, 0.35 mmol) in 20 ml acetonitrile was added to the Cy_2AFAH and Ag_2O mixture and stirred overnight and some precipitate was found. The reaction mixture was filtered and NMR was taken of the filtrate. ^{1}H NMR ($CDCl_3$, 360 MHz, 25 ºC) shows presence of only unreacted ligand in the filtrate.

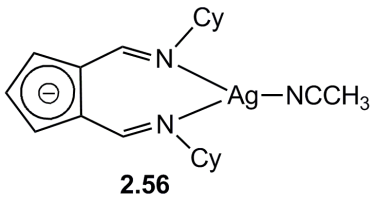

2.56

4.7 Ethylene polymerisation test

4.7.1 Procedure of ethylene polymerisation test of [(Ph_2AFA)Pd(CH_3)(DMAP)] (2.28) and [(Ph_2AFA)(N,N′-dimethylbenzylamine-2-C,N)-Pd(II)] (2.31)

A 100 ml Büchi glass autoclave was heated at 80 ºC under vacuum for 3 h and then cooled to room temperature under an ethylene pressure. The autoclave was charged with 20 ml of toluene and the ethylene pressure and temperature was set to 5 bar and 50 ºC respectively. After releasing the pressure, a solution of [(Ph_2AFA)Pd(CH_3)(DMAP)] or [(Ph_2AFA)(N,N′-dimethylbenzylamine-2-C,N)-Pd(II)] (75 mmol in 5 ml of toluene) and tris(pentaflurophenyl)borane, $B(C_6F_5)_3$ or borontrifluoride, BF_3 (150 mmol in 5 ml of toluene) were added *via* syringe. The reactor was sealed and pressurised with ethylene to 5 bar. The reaction mixture was stirred under constant pressure for 6 h, after which time the pressure was released

and acidified (HCl) methanol was added to quench the catalyst. An aliquot of the mother liquor was also analyzed by EI-MS to detect formation of oligomers.

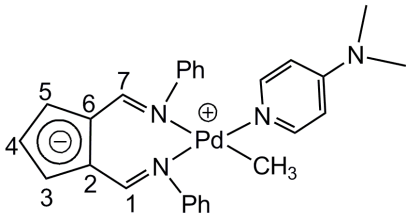

2.28

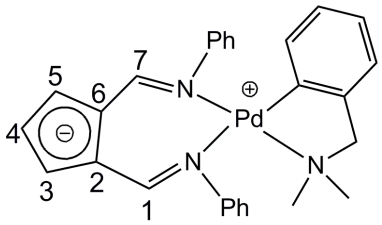

2.31

4.7.2 Procedure of ethylene polymerisation test of $[Cp^*Rh^{III}(Cy_2AFAPdCl_2)][BF_4]$ (3.30)

A 100 ml Büchi glass autoclave was heated at 80 ºC under vacuum for 3 h and then cooled to room temperature under an ethylene pressure. The autoclave was charged with 20 ml of toluene and the ethylene pressure and temperature was set to 5 bar and 0 ºC respectively. After releasing the pressure, a solution of $[Cp^*Rh^{III}(Cy_2AFAPdCl_2)][BF_4]$ (0.02 g, 2.54 x 10^{-5} mol) in 10 ml toluene was added via syringe. Then MAO (10 wt% toluene solution from Sigma Aldrich) (8.41 ml, 0.013 mol, catalyst: MAO = 1:500) was added via syringe. The reactor was sealed and pressurised with ethylene to 5 bar. The reaction mixture was stirred under constant pressure for 1h, after which time the pressure was released and acidified methanol (HCl) was added to quench the catalyst. An aliquot of the mother liquor was also analyzed by EI-MS to detect formation of oligomers.

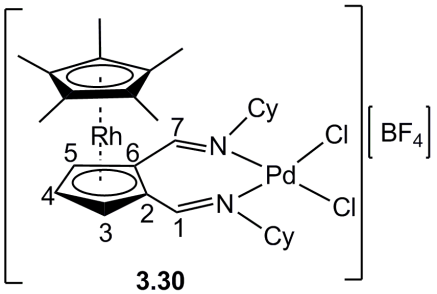

3.30

4.8 Crystallographic details

	2.27
Crystal data of [N,N'-bis(2,6-diisopropylphenyl)-6-aminofulvene-2-aldimine]	
Chemical formula	$C_{31}H_{40}N_2$
M_r	440.67
Crystal system, space group	Triclinic, $P\bar{1}$
Temperature (K)	150
a, b, c (Å)	10.4988 (2), 13.5676 (3), 19.0281 (4)
α, β, γ (°)	89.809 (1), 83.736 (1), 87.957 (1)
V (Å^3)	2692.53 (10)
Z	4
Radiation type	Mo $K\alpha$
μ (mm^{-1})	0.06
Crystal size (mm)	0.45 × 0.26 × 0.25
Data collection	
Diffractometer	Area diffractometer
Absorption correction	Multi-scan *SADABS* (Siemens, 1996)
T_{min}, T_{max}	0.84, 0.98
No. of measured, independent and observed [$I > 2.0\sigma(I)$] reflections	52192, 15537, 9712
R_{int}	0.047
Refinement	
$R[F^2 > 2\sigma(F^2)]$, $wR(F^2)$, S	0.069, 0.178, 0.94
No. of reflections	15536
No. of parameters	614
No. of restraints	13
H-atom treatment	H-atom parameters constrained
$\Delta\rangle_{max}$, $\Delta\rangle_{min}$ (e Å^{-3})	0.52, -0.40

	2.29
Crystal data of [Ph_2AFAPd(DMAP)]	
Chemical formula	$C_{27}H_{28}N_4Pd$
M_r	514.95
Crystal system, space group	Monoclinic, $P2_1/n$
Temperature (K)	150
a, b, c (Å)	10.5970 (3), 16.3536 (5), 13.4978 (4)
β (°)	94.160 (2)
V (Å^3)	2332.99 (12)
Z	4
Radiation type	Mo $K\alpha$
μ (mm^{-1})	0.82
Crystal size (mm)	0.26 × 0.12 × 0.05
Data collection	
Diffractometer	Bruker *SMART* diffractometer
Absorption correction	Multi-scan *SADABS* (Siemens, 1996)
T_{min}, T_{max}	0.51, 0.96
No. of measured, independent and observed [$I > 2.0\sigma(I)$] reflections	19154, 6128, 4650
R_{int}	0.053
Refinement	
$R[F^2 > 2\sigma(F^2)]$, $wR(F^2)$, S	0.048, 0.100, 0.90
No. of reflections	6128
No. of parameters	318
No. of restraints	27
H-atom treatment	H atoms treated by a mixture of independent and constrained refinement
$\Delta\rangle_{max}$, $\Delta\rangle_{min}$ (e Å^{-3})	0.93, -0.88

	2.32
Crystal data of [(Ph_2AFA)(NN'-dimethylbenzylamine-2-C,N)-Pd(II)]	
Chemical formula	$C_{28}H_{27}N_3Pd$
M_r	511.93
Crystal system, space group	Triclinic, $P\bar{1}$
Temperature (K)	150
a, b, c (Å)	11.2909 (6), 13.9873 (8), 15.0483 (8)
α, β, γ (°)	87.193 (4), 87.521 (4), 76.180 (4)
V (Å^3)	2303.8 (2)
Z	4
Radiation type	Mo $K\alpha$
μ (mm^{-1})	0.83
Crystal size (mm)	0.24 × 0.11 × 0.09
Data collection	
Diffractometer	Bruker Smart Apex CCD diffractometer
Absorption correction	Multi-scan TWINABS version 1.05
T_{min}, T_{max}	0.43, 0.93
No. of measured, independent and observed [$I > 2\sigma(I)$] reflections	13456, 13456, 5654
R_{int}	0.075
Refinement	
$R[F^2 > 2\sigma(F^2)]$, $wR(F^2)$, S	0.047, 0.080, 0.68
No. of reflections	13456
No. of parameters	578
No. of restraints	0
H-atom treatment	Riding
$\Delta\rangle_{max}$, $\Delta\rangle_{min}$ (e Å^{-3})	1.36, -1.07

	2.39
Crystal data of $[(Cy_2AFA)_2Pd]$	
Chemical formula	$C_{38}H_{54}N_4Pd$
M_r	673.27
Crystal system, space group	Monoclinic, $P2_1/c$
Temperature (K)	150
a, b, c (Å)	9.4867 (2), 16.9336 (3), 10.6112 (2)
β (°)	101.690 (1)
V (Å^3)	1669.27 (6)
Z	2
Radiation type	Mo $K\alpha$
μ (mm^{-1})	0.59
Crystal size (mm)	0.29 × 0.14 × 0.10
Data collection	
Diffractometer	Area diffractometer
Absorption correction	Multi-scan *SADABS* (Siemens, 1996)
T_{min}, T_{max}	0.52, 0.94
No. of measured, independent and observed [$I > 2.0\sigma(I)$] reflections	21684, 4918, 3757
R_{int}	0.042
Refinement	
$R[F^2 > 2\sigma(F^2)]$, $wR(F^2)$, S	0.035, 0.079, 0.87
No. of reflections	4918
No. of parameters	196
No. of restraints	0
H-atom treatment	H-atom parameters constrained
$\Delta\rangle_{max}$, $\Delta\rangle_{min}$ (e Å^{-3})	0.72, -0.61

	3.23
Crystal data of [Cp*Ru^{II}(Ph$_2$AFA)H][BF$_4$]	
Chemical formula	$C_{29}H_{31}N_2Ru\cdot BF_4$
M_r	595.44
Crystal system, space group	Monoclinic, $P2_1/c$
Temperature (K)	150
a, b, c (Å)	8.4632 (2), 22.8818 (6), 13.7328 (4)
β (°)	91.7806 (13)
V (Å^3)	2658.12 (12)
Z	4
Radiation type	Mo $K\alpha$
μ (mm^{-1})	0.64
Crystal size (mm)	0.36 × 0.18 × 0.13
Data collection	
Diffractometer	Bruker Smart Apex CCD diffractometer
Absorption correction	Multi-scan *SADABS* 2007/2
T_{min}, T_{max}	0.806, 0.924
No. of measured, independent and observed [$I > 2\sigma(I)$] reflections	21093, 5447, 4742
R_{int}	0.039
Refinement	
$R[F^2 > 2\sigma(F^2)]$, $wR(F^2)$, S	0.082, 0.180, 1.17
No. of reflections	5447
No. of parameters	325
No. of restraints	25
H-atom treatment	H-atom parameters constrained
	$w = 1/[\sigma^2(F_o^2) + (0.0457P)^2 + 18.4846P]$ where $P = (F_o^2 + 2F_c^2)/3$
$\Delta\rangle_{max}$, $\Delta\rangle_{min}$ (e Å^{-3})	2.37, -1.00

	3.25
Crystal data of $[Cp^*Rh^{III}(Cy_2AFA)H][BF_4]_2$	
Chemical formula	$C_{29}H_{43}N_2Rh \cdot 2(BF_4)$
M_r	696.18
Crystal system, space group	Monoclinic, $P2_1/n$
Temperature (K)	150
a, b, c (Å)	15.1769 (10), 13.6304 (9), 15.9647 (11)
β (°)	109.470 (1)
V (Å^3)	3113.7 (4)
Z	4
Radiation type	Mo $K\alpha$
μ (mm^{-1})	0.62
Crystal size (mm)	0.43 × 0.38 × 0.23
Data collection	
Diffractometer	Bruker Smart Apex CCD diffractometer
Absorption correction	Multi-scan *SADABS* 2007/2
T_{min}, T_{max}	0.747, 0.865
No. of measured, independent and observed [$I > 2\sigma(I)$] reflections	18536, 6361, 5679
R_{int}	0.032
Refinement	
$R[F^2 > 2\sigma(F^2)]$, $wR(F^2)$, S	0.032, 0.081, 1.04
No. of reflections	6361
No. of parameters	424
No. of restraints	10
H-atom treatment	H atoms treated by a mixture of independent and constrained refinement
$\Delta\rangle_{max}$, $\Delta\rangle_{min}$ (e Å^{-3})	0.57, -0.36

	3.28
Crystal data of [Ph_2AFAH(H)][OTf]	
Chemical formula	$C_{20}H_{17}F_3N_2O_3S$
M_r	422.43
Crystal system, space group	Monoclinic, $P2_1/n$
Temperature (K)	150
a, b, c (Å)	10.6175 (5), 16.2766 (9), 11.6321 (6)
β (°)	109.216 (3)
V (Å^3)	1898.22 (17)
Z	4
Radiation type	Mo $K\alpha$
μ (mm^{-1})	0.22
Crystal size (mm)	55.00 × 0.37 × 0.25
Data collection	
Diffractometer	Area diffractometer
Absorption correction	Multi-scan *SADABS* (Siemens, 1996)
T_{min}, T_{max}	0.71, 0.95
No. of measured, independent and observed [$I > 2.0\sigma(I)$] reflections	16727, 4982, 2842
R_{int}	0.070
Refinement	
$R[F^2 > 2\sigma(F^2)]$, $wR(F^2)$, S	0.060, 0.179, 0.74
No. of reflections	4982
No. of parameters	262
No. of restraints	0
H-atom treatment	H-atom parameters not refined
$\Delta\rangle_{max}$, $\Delta\rangle_{min}$ (e Å^{-3})	0.77, -0.88

References

1. D. Drew and J. R. Doyle, *Inorg. Synth*, 1990, **28**, 346.
2. R. E. Rulke, J. M. Ernsting, A. L. Spek, C. J. Elsevier, P. W. N. M. V. Leeuwen and K. Vrieze, *Inorg. Chem*, 1993, **32**, 5769.
3. G. K. Anderson and M. Lin, *Inorg. Synth*, 1990, **28**, 60.
4. S. Kohle, *German Published Patent Application*, 1963, 1194417.
5. G. Wilke, B. Bogdanovic, P. Hardt, P. Heimbach, W. Keim, M. Kröner, W. Oberkirch, K. Tanaka, E. Steinrücke, D. Walter and H. Zimmermann, *Angew. Chem. Internat. Edit*, 1966, **5**, 151.
6. T. K. Panda, M. T. Gamer and P. W. Roesky, *Organometallics*, 2003, **22**, 877.
7. J. Zhang, Z. Ke, F. Bao, J. Long, H. Gao, F. Zhu and Q.Wu, *J. Mol. Catal. A: Chem,* 2006, **249**, 31.
8. O. Dahl, *Acta. Chem. Scand*, 1969, **23**, 2342.
9. H. F. Klein and H. H. Karsch, *Chem. Ber*, 1972, **105**, 2628.
10. F. R. Hartley, S. G. Murray and C. A. McAuliffe, *Inorg. Chem*, 1979, **18**, 1394.
11. U. Koelle and J. Kossakowski, *Inorg. Synth*, 1992, **29**, 225.
12. N. Oshima, H. Suzuki and Y. Moro-Oka, *Chem. Lett*, 1984, 1161.
13. T. D. Tilley, R. H. Grubbs and J. E. Bercaw, *Organometallics*, 1984, **3**, 274.
14. P. J. Fagan, M. D. Ward and J. C. Calabrese, *J. Am. Chem. Soc*, 1989, **111**, 1698.
15. J. L. Schrenk, A. M. McNair, F. B. McCormick and K. R. Mann, *Inorg. Chem*, 1986, **25**, 3501.
16. C. White, A. Yates, P. M. Maitlis and D. M. Heinekey, *Inorg. Synth*, 1992, **29**, 228.
17. J. W. Kang, K. Moseley and P. M. Maitlis, *J. Am. Chem. Soc*, 1969, **91**, 5970.
18. C. White, S. J. Thompson and P. M. Maitlis, *J. C. S. Dalton Trans*, 1977, 1654.
19. M. D. Rausch and R. A. Genetti, *J. Org. Chem*, 1970, **35**, 3888.
20. R. B. King and M. B. Bisnette, *J. Organometal. Chem*, 1967, **8**, 287.

21. R. B. King, *Inorg. Chem*, 1966, **5**, 82.
22. U. Koelle, *J. Organomet. Chem*, 1980, **184**, 379.
23. A. C. Cope and E. C. Friedrich, *J. Am. Chem. Soc*, 1968, **90**, 909.
24. K. Hafner, K. H. Vöpel, G. Ploss and C. König, *Org. Synth*, 1967, **47**, 52.
25. U. Mueller-Westerhoff, *J. Am. Chem. Soc*, 1970, **92**, 4849.
26. P. J. Bailey, A. Collins, P. Haack, S. Parsons, M. Rahman, D. Smith and F. J. White, *Dalton Trans*, 2010, **39**, 1591.